The impact of advanced maternal age on endometrial differentiation and placental development

Laura Woods

The Babraham Institute
Sidney Sussex College
University of Cambridge

This dissertation is submitted for the degree of Doctor of Philosophy
April 2018

Declaration

This dissertation is the result of my own work and includes nothing which is the outcome of work done in collaboration except where specifically indicated in the text. Neither this dissertation, nor the work presented herein, has been submitted for any other qualification at the University of Cambridge or any other institution. The research presented in this dissertation was carried out between October 2014 and April 2018 under the supervision of Dr Myriam Hemberger at the Babraham Institute, Cambridge.

This dissertation does not exceed the limit of 60 000 words imposed by the Cambridge University Faculty of Biology Degree Committee.

Laura Woods

April 2018

Acknowledgements

The completion of my PhD, and this thesis, would not have been possible without a number of truly brilliant people who I have the pleasure of calling my family, friends, and colleagues.

Firstly, I would like to thank my supervisor Dr Myriam Hemberger, whose guidance and mentorship I have valued greatly. The amount of support and understanding she has shown me over the last three and a half years has been truly remarkable, and I appreciate it more than I can say. The members of the Hemberger lab have been wonderful to work with, I've learnt a great deal from you all. Vicen, from the first day you arrived at Babraham the lab was a brighter place. Thank you for being my collaborator and friend, working with you built my confidence so much, my time at Babraham and this thesis wouldn't be the same without you. Claire, you've been a great role model, showing me the kind of person, and scientist I want to be. Thank you Elena for the great support you've given me and allowing me to try and do the same for you. Ruslan, thank you for being my mentor. I know you always say you didn't teach me anything, but I've learnt from your quiet self-confidence and stoicism, not to mention that you always share your chocolate with me. Georgia, it's been wonderful having you in the lab, I can tell you're going to achieve some great things in the next few years. Alex, Stephanie, and Dominika, thank you for your welcoming natures, smiles, and willingness to help. Natasha, thank you for being a such a great support, always so willing to share your expertise and time with me. You're one of the best friends I have ever known, listening to my many complaints, always being there to lean on, and always finding something exciting to do. I know we'll stay friends wherever in the world we are. I couldn't have got through this without you.

Imy, who's been my best friend for so many years now, hanging out with you always makes my day and without you the world would be a lot more boring. I hope you know how important you are to me. Tash and Tom, I hope we can always sit together for hours playing Catan, one of these days I might even win.

To my family. Mum and Adi, thank you for always supporting me, giving me a place of refuge, and showing me I could do it if I just kept on trying. Dad, Judie, and Lottie of course, thank you for all the support and encouragement you've given me, this wouldn't have been possible without you. To my surrogate family Charlie, Jane, and Beccy, thank you for always welcoming me into your family. The support and kindness you show me is overwhelming, and I appreciate it so much. Last but not least, thank you Chris for being my favourite person in the world. For sharing my excitement, happiness, silliness, ambition, and love. For standing by me when I wanted to give up, for lifting me up when I

needed your help, and bringing me back down to earth. I wouldn't have got through the last few years without your love and patience, and I can't wait to see what comes next.

Assistance to be acknowledged

Initial training in techniques, laboratory practice and subsequent mentoring:

Myriam Hemberger (M.H., supervisor), Alex Murray (lab member), Michelle King (colleague), Claire Senner (lab member), Vicente Perez-Garcia (V.P-G., lab member).

Data obtained from a technical service provider:

Next-generation sequencing of mRNA, ChIP, MeDIP, and BS libraries was carried out at the Babraham Next Generation Sequencing Facility by Kristina Tabbada and Clare Murnane (The Babraham Institute). Next-generation sequencing data was processed and aligned by Felix Krueger and Simon Andrews in the Bioinformatics group at The Babraham Institute. Animal husbandry and embryo transfer experiments were performed by the Biological Services Unit at the Babraham Institute.

Data produced jointly:

Dissection of mouse embryos, placentas, and uteri, and isolation of mouse uterine stromal cells was performed jointly with M.H. (supervisor) and V.P-G. (lab member). Western blotting for H3K4me3 was performed jointly with V.P-G.

Isolation of decidual leukocytes was performed by Jens Kieckbusch (J.K.; Colucci lab, Cambridge) with the help of Laura Woods and V.P-G. J.K. performed the flow cytometry, and analysed flow cytometry data.

Data provided by someone else:

Deciduoma assay and Esr1 immunohistochemical (IHC) stainings were performed by Xiaoqui Wang (DeMayo lab, USA), microarray data was provided by Dr Francesco DeMayo (DeMayo lab, USA). V.P-G. performed the proliferation assay, and western blots for Bmp2, (p)Stat3, and Pgr. IHC for 5mC/5hmC was performed by Natasha Morgan (lab member). Statistical analysis of embryo developmental variability and uterine stromal cell proliferation was performed by Anne Segonds-Pichon in the Bioinformatics group at The Babraham Institute.

Summary

Maternal age is a significant risk factor for adverse pregnancy outcomes and is strongly associated with an increased risk of aneuploidy of the conceptus, as well as a significantly higher frequency of serious pregnancy complications known as the “Great Obstetrical Syndromes”, including miscarriage, pre-eclampsia and fetal growth restriction. In the last 40 years average maternal age has increased considerably in many wealthy countries, and in the UK the number of babies born to women aged 35 and over is set to surpass those born to women under 25. The high incidence of aneuploidy in older mothers can be attributed to abnormalities in the oocyte and embryo, however the “Great Obstetrical Syndromes” do not appear to be related to the oocyte and may instead be linked to abnormal development of the placenta.

In this thesis, I show that advanced maternal age in the mouse is associated with a drastically increased variability of developmental progression *in utero*, including developmental delays and growth restriction, severe embryonic abnormalities and higher resorption rates. I find that these embryonic defects are always accompanied by gross morphological and transcriptomic abnormalities in the placenta. Notably, I show that the increased risk of these complications can be rescued by transfer of embryos from aged females to a young surrogate mother, thus implicating the aged maternal uterus as the basis for embryonic and placental defects. Transcriptomic analysis of the decidua compartment in placentas from aged pregnancies revealed abnormal expression of genes involved in the decidualization process, which occurs during early pregnancy and facilitates implantation and development of the conceptus. I show that these defects are already obvious in the peri-implantation window, with endometrial stromal cells from aged females being unable to mount an adequate decidualization response due to a decline in their ability to respond to pregnancy hormones. This blunted decidualization reaction in turn may lead to abnormal development of the placenta. These age-associated decidualization defects are cell-intrinsic and can be recapitulated *in vitro.* The detected insufficient activation levels and abnormal intracellular distribution of phospho-STAT3, combined with highly variable progesterone receptor expression, may be possible causes of these defects.

In addition, I examined the possible effects of ageing on the epigenome as a potential contributor to the decline in endometrial function. My results indicate that ageing of the

uterus displays some of the common epigenetic hallmarks of tissue ageing. However, more importantly, decidual cells of aged females exhibit abnormal distributions of the histone modification H3K4me3, and are refractory to the profound DNA methylation remodelling that I find takes place during pregnancy. These age-related changes in the epigenome may underpin, or contribute to, the observed decline in uterine function during pregnancy.

Understanding the mechanism underlying these epigenomic and functional changes in the ageing reproductive tract may pave the way for new therapeutic strategies to improve maternal and fetal outcomes of pregnancy in older mothers.

Abbreviations

5hmC	5-hydroxymethylcytosine
5mC	5-methylcytosine
A->Y	Embryo transfer from aged donor to young recipient
Aa	Grossly abnormal conceptus from an aged female
An	Grossly normal conceptus from an aged female
B6	C57BL/6 mouse
BS-seq	Next-generation sequencing of bisulphite converted DNA
CGI	CpG island
ChIP-seq	Chromatin immunoprecipitation followed by next-generation sequencing
CM	Conditioned medium
DBA	Dolichos Biflorus Agglutinin
DC	Dendritic cell
DMR	Differentially methylated region
DNMT	DNA methyltransferase
E	Embryonic day
E2	Estrogen
EPC	Ectoplacental cone
Fgf	Fibroblast growth factor
GE	Glandular epithelium
GO	Gene ontology
H&E	Haematoxylin and eosin
H3K4me3	Trimethylation of lysine 4 of histone 3
ICM	Inner cell mass
IHC	Immunohistochemistry
KO	Knock-out
LE	Luminal epithelium
MeDIP-seq	Methylated DNA immunoprecipitation followed by next-generation sequencing
MEF	Mouse embryonic fibroblast
OVX	Ovariectomized

P4	Progesterone
PCA	Principal component analysis
PDZ	Primary decidual zone
RNA-seq	Next-generation RNA sequencing
RT-qPCR	Quantitative reverse transcription PCR
SDZ	Secondary decidual zone
SpT	Spongiotrophoblast
SynT	Syncytiotrophoblast
TE	Trophectoderm
TF	Transcription factor
TGC	Trophoblast giant cell
TS cell	Trophoblast stem cell
uNK	Uterine natural killer cell
USC	Uterine stromal cell
Y->Y	Embryo transfer from young donor to young recipient

Table of Contents

Chapter I
Introduction

1.1 Reproductive decline with advanced maternal age

1.1.1 Trends in the timing of childbearing

Pregnancy in women of advanced age has become increasingly common in high income countries, in recent decades. In the UK, the number of live births to women ≥35 years of age has increased steadily from the late 1970's (Fig 1.1), culminating in average maternal age reaching 30 years for the first time, in 2013 (Statistics, 2014). In 2013 the largest group of babies were born to mothers aged between 25-34. However, in the near future the number of babies born to the 35 years and over group looks set to surpass those born to women >25 (Fig 1.1). Surveys in other countries have reported a similar pattern of increasing average age at first birth, with the greatest increases in the 35-39 year old group (ABS, 2008; Breart et al., 2003; Martin et al., 2010; Ventura et al., 2009).

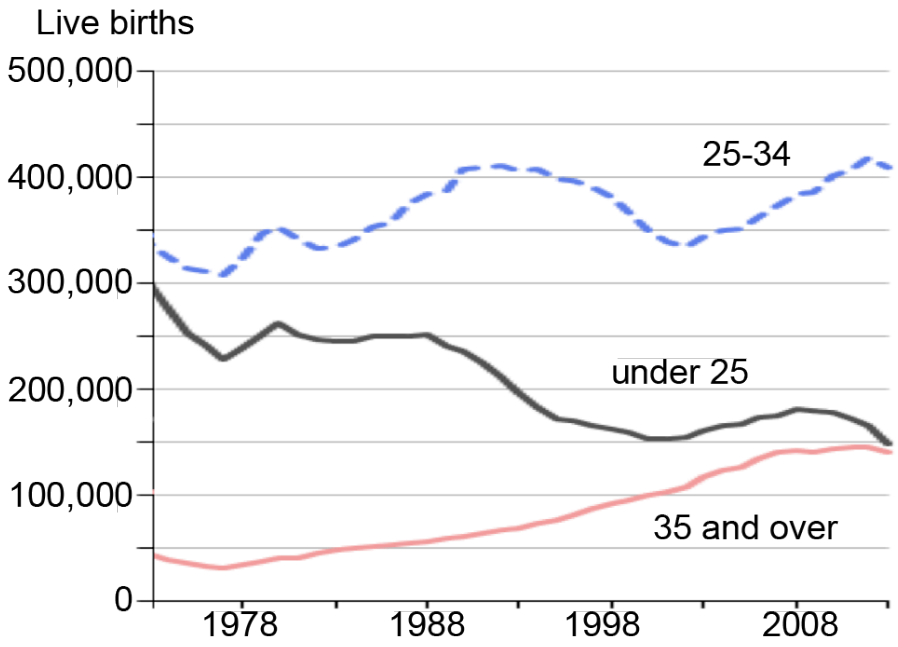

Figure 1.1 - Live births by age group of the mother in England and Wales 1938-2013. Black line indicates number of live births to women <25 years old, blue dashed line to women aged 25-24, and the red line to women aged 35 and over. Adapted from (Statistics, 2014).

1.1.2 Oocyte ageing

Advanced maternal age is associated with a rapid decline in reproductive success in women (Baird et al., 2005; Broekmans et al., 2007; te Velde and Pearson, 2002), most commonly due to a decline in the number and quality of oocytes available. As a result, older women experience reduced fertility and an increased risk of early miscarriage due to reduced oocyte availability and poor oocyte quality, respectively (Block, 1952; Faddy et al., 1992). Oocyte development begins during embryonic life, when the primordial follicle pool is established – at approximately 18 weeks of gestation in humans, and embryonic day 13.5 (E13.5) in the mouse (Baker, 1963; Borum, 1961; Fulton et al., 2005; Motta et al., 1997; Pepling, 2012). At this time, primordial germ cells which give rise to the oocyte begin to enter meiosis, and become arrested in prophase of meiosis I. Prophase arrest persists until meiotic resumption is stimulated by ovulation, and the oocyte can be fertilised and lead to pregnancy.

It is widely believed that the full complement of primordial follicles is established in fetal life, and no new follicles are produced postnatally (Findlay et al., 2015; Kerr et al., 2013), thereby rendering the oocyte particularly vulnerable to the effects of ageing.

1.1.2.1 Aneuploidy

Oocyte ageing has been studied extensively and is associated with the development of chromosomal abnormalities such as aneuploidy. Aneuploidy describes deviations from the normal chromosome complement of the diploid nucleus, i.e. the presence of 2 copies of each autosome. Aneuploidy can affect one or multiple chromosomes, and manifests as trisomy where there are three copies of a chromosome, monosomy where there is only one copy, or nullisomy when a chromosome is completely absent.

In humans, most aneuploidies are incompatible with development to term. Aneuploid pregnancies commonly fail either because the embryo is pre-implantation lethal and will not even implant, or it does implant but leads to miscarriage during the first trimester of pregnancy (Hardy and Hardy, 2015; Macklon et al., 2002). These outcomes stem from chromosomal aberrations either inherited from the oocyte, or acquired during the early mitotic divisions (van Echten-Arends et al., 2011), although mitotic errors during preimplantation development are not affected by maternal ageing (McCoy et al., 2015). Implantation failure in aneuploid pregnancies occurs as a result of developmental arrest and

degeneration in the early cleavage stages of embryogenesis (Maurer et al., 2015). This occurs during the preclinical stage of pregnancy when the mother will be unaware she is pregnant. Therefore, implantation failure due to aneuploidy manifests as a reduction in pregnancy rates amongst older women (Heffner, 2004; Joseph et al., 2005; Menken et al., 1986; Munne, 2002). Pregnancy rates in older women can be improved in IVF cycles by the use of karyotypically normal oocytes from young donors (Cohen et al., 1999; Munne, 2002; Wang et al., 2012), or after excluding aneuploid embryos upon karyotyping by pre-implantation genetic diagnosis (Harton et al., 2013). This suggests that chromosomal aberrations are a major cause of infertility and early embryonic demise in older mothers.

Even when an aneuploid embryo is able to implant successfully, the result is often miscarriage in the first trimester of pregnancy, or less commonly live birth with congenital abnormalities in the offspring (Beckman and Brent, 1984; Farfalli et al., 2007; Hardy and Hardy, 2015). As a result, the dramatic increase in aneuploidy in older mothers is reflected in the significantly increased rates of miscarriage in this group (Dai et al., 2017; Khalil et al., 2013; Kroon et al., 2011; Mills and Lavender, 2011).

Reflecting the prevalence of aneuploidies in older women, the incidence of those aneuploidies that are able to lead to live birth is also significantly increased, including Down's Syndrome - caused by trisomy of chromosome 21 - which rises from 1 in 1500 births in women at 25 years of age, to 1 in 16 at 40 years (Nelson et al., 2013). The correlation between aneuploidy and increasing maternal age has been shown to stem from the increased risk of chromosomal non-disjunction in the oocyte with age, although the precise mechanism leading to this increase is not well understood (Hassold and Hunt, 2001).

The majority of aneuploidies in the ageing oocyte arise as a result of chromosomal non-disjunction during meiosis I (McCoy et al., 2015). In meiosis I, homologous chromosomes are replicated and undergo meiotic recombination, leading to the generation of chiasmata which physically connect the homologous chromosomes, keeping them together. Chiasmata are maintained by cohesion between the sister chromatids, mediated by the cohesin complex (Nasmyth and Haering, 2009). The oocyte remains arrested in this state until meiotic resumption is triggered at ovulation, allowing progression into metaphase I. In metaphase I the homologous chromosomes remain firmly attached at chiasmata and

align at the metaphase plate, where they are connected to opposing metaphase spindles at their centromeres. In anaphase, cohesion between the homologous chromosomes is released allowing them to segregate to opposite spindle poles. One set of chromosomes becomes the haploid complement of the oocyte, whereas the other is extruded as the first polar body. The maintenance of chiasmata in metaphase oocytes is crucial to ensure

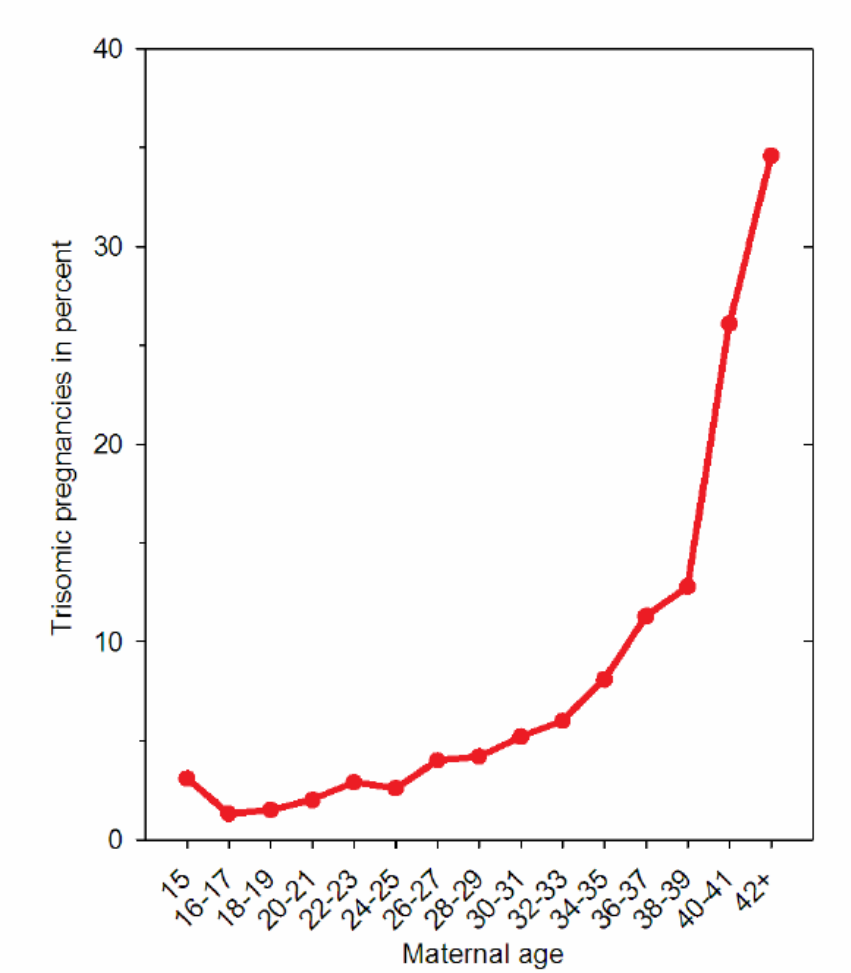

Figure 1.2 - The incidence of trisomic pregnancies rises exponentially with increasing age of the mother. Figure taken from (Stindl, 2011), data from (Hassold and Chiu, 1985).

balanced chromosome segregation (MacLennan et al., 2015). Failure of these attachments results in chromosomal non-disjunction, generating an aneuploid oocyte with an inappropriate complement of chromosomes (Herbert et al., 2015).

The period between prophase I arrest and meiotic resumption spans the lifetime of the individual. As such an oocyte can be arrested in prophase for more than 40 years, rendering it susceptible to perturbation by maternal ageing (Nagaoka et al., 2012). Studies of naturally ageing mice and humans show that cohesion between homologous chromosomes

decreases with age. This enhances the likelihood that chromosome attachments at the chiasmata will fail during meiosis, leading to increased levels of unbalanced chromosome segregations, and the generation of aneuploid oocytes (MacLennan et al., 2015). As such, chromosomal aberrations and aneuploidies in the oocyte become increasingly common with age. 50% of the oocytes to women over 35 years, and 80% to women over 40 years show defects in spindle formation and chromosomal alignment at the first meiotic division (Battaglia et al., 1996; Volarcik et al., 1998). Thus, the incidence of trisomy increases, from less than 5% in women under 25, to nearly 40% in women over 40 (Fig 1.2) (Hassold and Chiu, 1985).

1.1.2.2. Mitochondrial dysfunction

During the very early cell divisions of embryo development, the conceptus does not produce its own proteins, RNA, metabolites, or organelles. Therefore, the metabolic and macromolecular needs of the conceptus must be met by the oocyte, and as such the ooplasm supplies all the factors necessary for the first cell divisions of the embryo. The quality of the ooplasm deteriorates with maternal ageing, leading to biochemical changes which affect oocyte competence and embryo quality (Qiao et al., 2014). Of particular interest is the contribution of mitochondrial dysfunction to age-related decline in oocyte function, as the mitochondria and mitochondrial DNA are inherited solely from the ooplasm, with no contribution of paternal mitochondria (Sato and Sato, 2013).

In general, mitochondrial function deteriorates with ageing in terms of their capacity to produce energy, their involvement in various signalling pathways, and the stability of mitochondrial DNA (Bratic and Larsson, 2013; Corral-Debrinski et al., 1992; Eichenlaub-Ritter, 2012; Tilly and Sinclair, 2013). Specifically in the oocyte, ageing is associated with mitochondrial swelling and alterations in structure of the cristae (Kushnir et al., 2012; Simsek-Duran et al., 2013), as well as alterations to mitochondrial membrane potential (Ben-Meir et al., 2015) and a reduction in their capacity to generate ATP (Selesniemi et al., 2011). Ageing of the oocyte mitochondria directly affects early embryonic cellular function, leading to premature biogenesis of mitochondria in the embryo, affecting embryo quality (May-Panloup et al., 2016). These defects in mitochondrial function may be mechanistically associated with chromosome segregation defects (Eichenlaub-Ritter, 1998; Schon et al., 2000), and may be one mechanism by which the frequency of aneuploidy increases in

oocytes from older women (Zhang et al., 2006). Mitochondrial ageing has been shown to impact on chromosome segregation during the early cleavage stages. This is associated with decreased embryo implantation potential, probably due to growth arrest and degeneration of aneuploid embryos during preimplantation development (Diez-Juan et al., 2015; Farfalli et al., 2007; Wells et al., 2014).

1.1.3 Uterine ageing

Advanced maternal age is associated with an increased risk of poor fetal outcomes and obstetric complications in the mother. This includes early miscarriages and birth defects caused by chromosomal abnormalities in the oocyte, as discussed above. However, poor outcomes are also significantly increased in euploid pregnancies in women over the age of 35. Pregnancy in advanced maternal age carries an increased risk of non-chromosomal abnormalities in the offspring, including - for example - congenital heart defects, club foot, and diaphragmatic hernia (Hollier et al., 2000; Miller et al., 2011). It is also a risk factor for the "Great Obstetrical Syndromes", which include pre-eclampsia, intrauterine growth restriction, miscarriage, and stillbirth (Brosens et al., 2011; Carolan and Frankowska, 2011; Huang et al., 2008; Jacobsson et al., 2004; Mills and Lavender, 2011; Ozalp et al., 2003). For example, the rate of stillbirth increases from 1:1000 in women <35 years to 1:440 in women >35 (Fretts and Usher, 1997), and continues to increase in women >40 years of age (Huang et al., 2008; Nybo Andersen et al., 2000). The risk of preeclampsia increases by almost 50% in women over the age of 35 (Lamminpaa et al., 2012), and one study found an almost 2-fold increase in the risk of preterm birth and low birth weight in older mothers (Nelson and Lawlor, 2011). Importantly, these outcomes occur independently of karyotypic abnormalities in the embryo, and may instead be attributed to poor placental function caused by ageing of the uterus.

The "Great Obstetrical Syndromes" are disorders of deep placentation, which come about as a result of insufficient remodelling of the maternal spiral arteries in the placental bed. These defects occur as a consequence of abnormal communication between the maternal decidua and fetal trophoblast during the first trimester of pregnancy (Brosens et al., 2011). The prevalence of these conditions during pregnancy in older women suggests that communication between embryonic and maternal tissues may become abnormal in advanced age, leading to defective placental development, and consequently, abnormal

embryonic development. The prevalence of congenital heart malformations (Hollier et al., 2000; Schulkey et al., 2015) in the offspring of aged pregnancies provides further evidence for this link between maternal age and uteroplacental function, as they can result from placental insufficiency as a result of defects in placentation (Linask, 2013; Llurba et al., 2013; Matthiesen et al., 2016).

This evidence is in line with the hypothesis that adverse pregnancy outcomes with advanced maternal age - which are independent of chromosomal abnormalities - may be caused by age-related placental insufficiency (Lean et al., 2017), as a result of poor performance of the ageing uterus (Main et al., 2000). In support of this, studies looking at older women undergoing IVF show improved implantation and pregnancy rates when using donor oocytes from younger women, compared to using their own "old" oocytes. However, the subsequent rates of miscarriage, preterm birth, and fetal growth restriction remain significantly increased in older compared to younger women (Cano et al., 1995; Soares et al., 2005), thus implicating age-related dysfunction of the endometrium as the root cause.

This evidence in humans is supported by early work in ageing rodents. Uteri from old mice and rats exhibit a diminished artificial decidualization response after mechanical stimulation or intraluminal oil injection of the hormonally primed endometrium (Finn, 1966; Holinka and Finch, 1977; Ohta, 1987; Shapiro and Talbert, 1974), indicative of a lesser capacity of the older uterus to support pregnancy. Decidualization failure could be a consequence of an abnormal hormonal milieu, as the rodent estrous cycle becomes irregular after 10-12 months of age, with fluctuating levels of steroid hormones (LeFevre and McClintock, 1988; Lu et al., 1979; Nelson et al., 1982). However, the artificial decidualization response is still significantly decreased in aged mice, even after hormonal supplementation (Holinka and Finch, 1977). In addition, a study by Holinka and colleagues in 1979 found that plasma levels of progesterone do show a small, but significant decrease on day 4 of gestation in older females, however this did not correlate with fetal viability or resorption at mid-gestation, suggesting that altered levels of progesterone *per se* do not cause abnormal development or pregnancy loss (Holinka et al., 1979). Histological examination of the ageing rodent uterus shows age-related structural changes, such as the accumulation of collagen fibres in the stromal compartment - although this in itself is not thought to be responsible for the decline in uterine function (Hsueh et al., 1979; Loeb et al., 1938; Ohta, 1987). Altered morphology of the endometrial luminal epithelium during pregnancy, and accumulation of

lipofuscin deposits in uterine stromal cells have also been noted in aged females (Craig, 1981; Kong et al., 2012; Martin et al., 1970). Taken together, these studies implicate age-related changes to uterine morphology and physiology that may impact on reproductive performance independent of subtle alterations in hormone levels in older females.

1.1.5 The maternal ageing phenotype and placentation

As mentioned earlier, pregnancies in advanced maternal age are at increased risk of what have been termed the "Great Obstetrical Syndromes", encompassing pre-eclampsia, fetal growth restriction, preterm birth, and stillbirth. These disorders are associated with abnormal placental development, where the perturbation of deep placentation and spiral artery remodelling leads to such complications due to restriction of the size of the placental bed and the reduced supply of maternal blood that is achieved (Brosens et al., 2011). In addition to the "Great Obstetrical Syndromes", advanced maternal age is also associated with an increased risk of congenital heart malformations in the offspring (Hollier et al., 2000; Miller et al., 2011).

The origins of the susceptibility of the developing heart to maternal ageing have recently been teased apart in an elegant study by Schulkey and colleagues (Schulkey et al., 2015). These authors assessed the effect of maternal ageing on congenital heart defects in mice carrying a heterozygous mutation of the Nkx2-5 gene, which have an increased risk of ventricular septal defects (VSDs) in the offspring with increasing maternal age. By reciprocal ovarian transplantation between young and old females, the authors showed that the risk of VSDs in the offspring resides within the uterine environment of the older mother, and not the older oocyte. Interestingly, this risk was independent of maternal diet and obesity, and could be mitigated by maternal exercise begun either in early or later life, suggesting such interventions aimed at the mother could reduce the risk of maternal age-related cardiac malformations in the offspring.

The fetal heart and placenta develop in parallel and are linked by common signalling pathways and the continuous fetal blood circulation (Linask, 2013). Thus, abnormal vascular development in the placenta can affect fetal heart development. This is in particular the case because the blood pressure of the fetal circulation is set by the placental microvasculature, which in turn is required for normal heart tube formation. In mice, deletion of *p38α MAP*

kinase leads to cardiac defects (and malformation of blood vessels in the head region), which are secondary to placental insufficiency (Adams et al., 2000). Similar examples are provided by the *Map3k3* and *PPAR-gamma* mutations in which heart defects occur solely due to deficiencies in the placental trophoblast lineage (Barak et al., 1999; Yang et al., 2000). A recent study by Perez-Garcia, Fineberg et al showed that even in a systematic screen of genes required for embryonic survival, placental defects correlated strongly with abnormalities in the brain, heart, and vasculature (Perez-Garcia et al., 2018). Thus, it is tempting to speculate that the increase in heart defects depending on maternal uterine age found by Schulkey et al. originate in placental abnormalities, a possibility also hinted at in the News & Views article that accompanied this paper (Hitz and Andelfinger, 2015).

1.2 Gestation in the mouse: Key events in pregnancy and development

Successful implantation and the immediately following steps of extra-embryonic development, which ultimately lay the foundations for normal placentation, requires highly orchestrated communication between the embryo at the blastocyst stage and the receptive uterus (Cha and Dey, 2014). Therefore, abnormal uterine function can alter this tightly regulated dialogue, implicating uterine ageing in the genesis of disorders of placentation including the “Great Obstetrical Syndromes”, and embryonic defects as a consequence.

1.2.1 Structure of the mouse uterus

The mouse uterus has a bicornate structure consisting of 2 horns which connect and open into a single vagina. Each horn of the uterus is a hollow tube consisting of an outer muscular layer called the myometrium, and an inner layer called the endometrium. The endometrium is comprised of a basal layer of uterine stromal cells (USCs), overlaid by luminal epithelial (LE) cells, which line the lumen of the uterus (Fig 1.3). The luminal epithelium becomes highly invaginated in parts, extending into the uterine stroma (Goad et al., 2017). This forms the glandular epithelium (GE), composed of secretory epithelial cells that form the uterine glands (Fig 1.3).

1.2.2 Early pregnancy in the mouse

The successful achievement of pregnancy requires that formation of the mature blastocyst is synchronised with the acquisition of uterine receptivity, which in turn is achieved by the tightly controlled action of ovarian hormones. Disruption of this synchronicity can lead to adverse ripple effects in development, the consequences of which can manifest through the remaining course of pregnancy (Cha and Dey, 2014; Song et al., 2002).

1.2.2.1 Implantation

The main events of early pregnancy are the acquisition of uterine receptivity and concomitant implantation of a competent blastocyst. The acquisition of uterine receptivity occurs as a result of priming of the uterus under the influence of ovarian hormones. In the first 2 days of pregnancy - with E0.5 the appearance of the vaginal plug - the uterus is predominantly regulated by ovarian estrogen (E2) acting through the estrogen receptor (*Esr1*). This drives proliferation of the LE and GE. On E2.5, E2 levels begin to decline while progesterone (P4) increases due to secretion from the newly formed corpora lutea. The action of P4, superimposed on an E2 primed uterus, causes proliferation to cease in the LE and GE cells that instead start to differentiate. In contrast to the LE and GE, P4 promotes proliferation in the stromal compartment from E2.5 onwards (Dey et al., 2004). This transition from epithelial to stromal proliferation, mediated by P4, is critical for implantation (Large and DeMayo, 2012). Uterine receptivity is achieved on E4 of pregnancy and persists only until E5 (Paria et al., 2002), during which time blastocyst competency must be achieved for successful implantation.

In a receptive uterus, embryo implantation proceeds in 3 main stages of apposition, attachment, and invasion (Fig 1.3) (Enders, 1967). Firstly, in the mouse, the blastocyst trophectoderm (TE) becomes closely apposed to the anti-mesometrial LE of the receptive uterus (note: in humans, apposition occurs at the polar TE). This is followed by the attachment reaction (Fig 1.3), when contacts between the TE and LE are strengthened by the expression of cell adhesion molecules such as L-selectins (Achache and Revel, 2006; Cha et al., 2012). Once this has occurred the blastocyst can no longer be dislodged by uterine flushing (Enders, 1967). The attachment reaction coincides with increased vascular permeability at the site of attachment, which can be visualised by intravenous injection of Chicago blue dye into the tail vein (Psychoyos, 1973). Following attachment, the blastocyst

begins to penetrate the uterine wall by invasion of the TE into the LE (Fig 1.3). Mechanisms of TE penetration through the LE are species specific; in the mouse LE cells contacting the TE undergo apoptosis, thereby allowing invasion of the TE into the underlying uterine stroma, whereas in primates the syncytiotrophoblast intrudes between LE cells to penetrate the basal lamina (Wang and Dey, 2006). Invasion of the TE into the underlying uterine stroma is thought to be facilitated by matrix metalloproteinases, most notably Mmp9 (Fig 1.3) (Zhu et al., 2012).

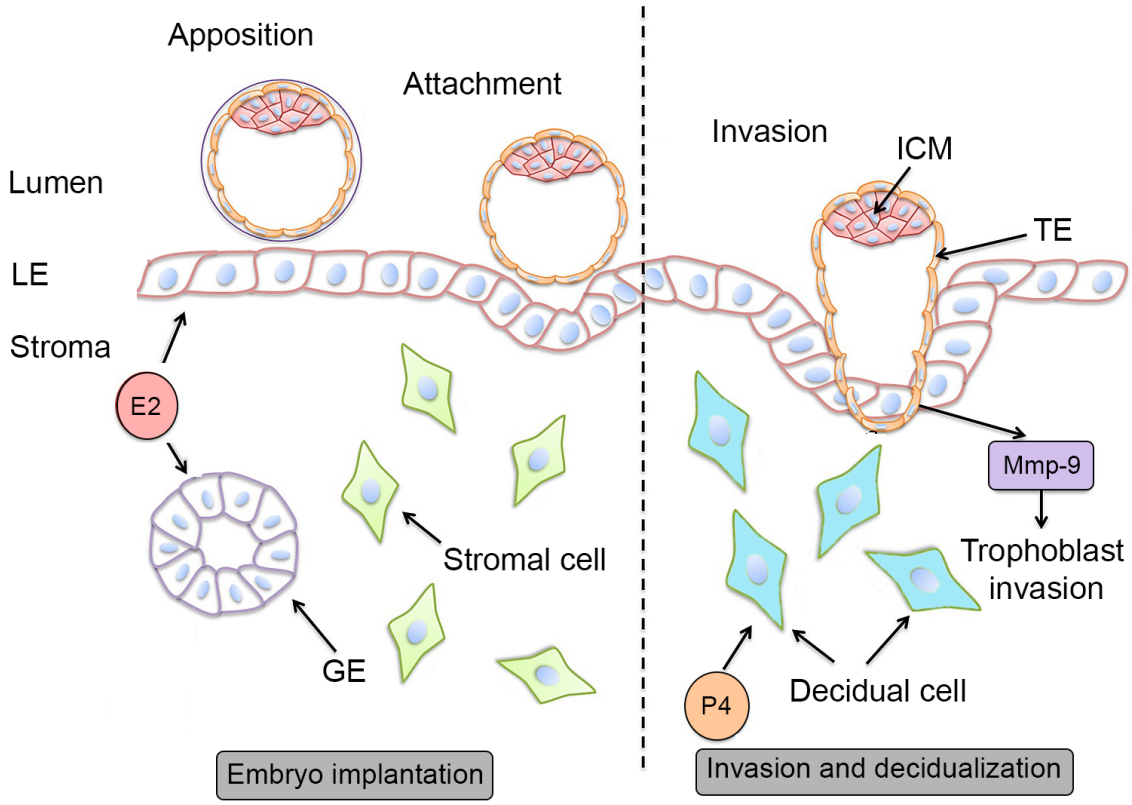

Figure 1.3 - The mouse uterus in early pregnancy. Implantation of the blastocyst into the uterine wall proceeds in 3 main stages. Apposition of the blastocyst to the receptive luminal epithelium (LE) is dependent on priming with estrogen (E2). The embryo attaches more strongly to the LE in the attachment phase, and then starts to invade through the LE into the underlying stroma. Invasion occurs under the control of Mmp9, and triggers decidualization of uterine stromal cells, under the control of progesterone (P4). ICM, inner cell mass. TE, trophectoderm. GE, glandular epithelium. Adapted from (Qi et al., 2014).

1.2.2.2 Decidualization

The processes of blastocyst attachment and invasion of the TE into the stromal compartment trigger the surrounding uterine stromal cells to undergo the decidualization reaction (Fig 1.3, 1.4). Decidualization facilitates further invasion and allows the blastocyst to embed itself completely into the uterine stromal bed. In mice, decidualization during pregnancy is dependent on the presence of the blastocyst, however a decidualization response can be stimulated artificially by intraluminal injection of oil, application of a mechanical stimulus, or the introduction of Sepharose beads into a hormonally primed uterus (Herington et al., 2009). The resulting growth is termed a deciduoma.

Decidualization involves the extensive proliferation and differentiation of the fibroblastic uterine stromal cells into large decidual cells with a unique secretory phenotype. During decidualization the uterine stromal compartment undergoes proliferation and differentiation to form the decidua, which constitutes the maternally derived portion of the placenta. The decidua performs a variety of functions, including regulation of trophoblast invasion, the production of growth factors and cytokines which influence embryo development, and synthesis of E2. In addition, the decidua acts as the interface between fetus and mother with the accompanying immuno-regulatory challenges (Alam et al., 2008; Das et al., 2009; Dudley et al., 1992; Oreshkova et al., 2012; Sharma et al., 2016; Singh et al., 2011). The decidua also acts to regulate the invasiveness of the trophoblast, allowing trophoblast invasion to occur in order to anchor the placenta to the uterus and allow remodelling of the maternal spiral arteries. Disruption of this process can lead to disorders such as placental abruption and pre-eclampsia, when invasion is too shallow, whereas excessive invasion leads to placenta accreta and choriocarcinoma (Goldman-Wohl and Yagel, 2002; Sharma et al., 2016). Decidual cells also play a pro-angiogenic role, supporting maternal blood vessel formation which is necessary for perfusion of the placenta and nourishment of the developing embryo (Lima et al., 2014; Ma et al., 2001). As decidualization progresses, cells in the secondary decidual zone at the anti-mesometrial pole of the implantation site undergo successive rounds of DNA replication without cell division and become polyploid (Fig 1.4) (Cha et al., 2012; Sroga et al., 2012). This is thought to enable the synthesis and secretion of large volumes of signalling factors, and may limit the life-span of decidual cells to enable regression of the decidua later in pregnancy, and allows expansion of the placenta (Ogle et al., 1999; Ogle et al., 1998)

1.2.2.3 Hormonal regulation of decidualization

Decidualization is under the control of the steroid hormones E2 and P4. The actions of E2 and P4 are mediated by their receptors, estrogen receptor (*Esr1/2*) and progesterone receptor (*Pgr*), respectively. Each controls a large and context specific repertoire of downstream signalling factors necessary for successful pregnancy. The Pgr and Esr1/2 are both nuclear receptors. In their inactive form they reside in the cytoplasm, but upon binding of their respective ligands they homo-dimerise and translocate to the nucleus (Sever and Glass, 2013). On nuclear translocation, Pgr and Esr1/2 bind to specific genomic regions, to regulate the transcription of target genes. In the case of Pgr, when inactive it is bound by a complex of heat shock proteins and the immunophilins Fkbp4 and Fkbp5, which act to maintain the structure and competence of the Pgr in preparation for hormone binding and transcriptional regulation (Pratt and Toft, 1997; Renoir et al., 1990). Disruption of this complex by deletion of *Fkbp4* leads to female infertility with complete failure of implantation and decidualization due to impaired transcriptional activation of *Pgr* target genes (Tranguch et al., 2005; Yang et al., 2006).

Evidence from mouse KO models shows that the action of E2 and P4 is a requirement for successful establishment of pregnancy. *Esr1* knockout (KO) females are infertile, with hypoplastic uteri and ovaries that do not respond to E2 (Lubahn et al., 1993). These mice fail to undergo artificial decidualization (Pawar et al., 2015), suggesting the action of E2 is necessary for the decidualization response. Furthermore, KO mice which lack *Esr1* in the LE and GE but retain expression in the stroma are also unable to decidualize. This study showed that epithelial *Esr1* is required for decidualization of the underlying stromal compartment, suggesting that paracrine signals from the LE are essential for stromal cell decidualization (Pawar et al., 2015). *Esr1* also induces the expression of *Pgr* in the endometrium, suggesting it is also involved in regulating the capacity of the uterus to respond to P4.

Pgr KO mice are infertile and exhibit defects in all female reproductive tissues, including abnormal mammary gland development, failure of ovulation and decidualization, and hyperplasia of the LE due to the unopposed action of E2 (Dey et al., 2004; Lydon et al., 1995). Subsequent studies showed that uterine receptivity and stromal decidualization are mediated primarily by the progesterone receptor A (*PgrA*) isoform in mice (Conneely et al., 2001) and in humans (Brosens et al., 1999; Wang et al., 1998).

Collectively, these studies established that E2 primarily regulates the window of receptivity and is required to prime the stroma to enable it to decidualize in response to P4,

whereas P4 is the predominant regulator of decidualization itself, stimulating the proliferation and differentiation of USCs (Franco et al., 2008; Lee and DeMayo, 2004).

1.2.2.4 Molecular mechanisms of decidualization

E2 and P4 control the events of early pregnancy through the regulation of numerous target genes, including the Epidermal Growth Factor Receptor (*Egfr*), Bone Morphogenetic Protein 2 (*Bmp2*), and Wingless-Type MMTV Integration Site Family, Member 4 (*Wnt4*) (Fig 1.4). *Bmp2* is a P4 regulated gene induced in uterine stromal cells during decidualization (Lee et al., 2007; Li et al., 2007; Paria et al., 2001). It is expressed in the uterine stroma underlying the implantation site in early pregnancy (Ying and Zhao, 2000), and in stromal cells surrounding the embryo once implantation has occurred (Lee et al., 2007). *Bmp2* KO mice are unable to decidualize in response to an artificial stimulus with defects in proliferation and differentiation of uterine stromal cells. This can be partially rescued by supplementation with recombinant human BMP2, showing its necessity in decidualization (Lee et al., 2007). In addition, *Bmp2* is itself able to accelerate decidualization *in vitro* (Li et al., 2007). The induction of decidualization by *Bmp2* is mediated by *Wnt4*, also implicating the Wnt pathway in decidualization (Fig 1.4). A more recent study found that *Bmp2* and *Wnt4* also play distinct roles in decidualization, both of which are regulated by the upstream activity of *Egfr*, which is itself necessary for decidualization (Large et al., 2014) (Fig 1.4). Interestingly, *Egfr* mediated decidualization of uterine stromal cells is regulated by secretion of the paracrine signalling factor Indian hedgehog (*Ihh*) by the luminal epithelium (Fig 1.4) (Franco et al., 2010; Lee et al., 2006). *Pgr* works synergistically with *Lif* secreted from the uterine glands in response to E2 to induce *Ihh* production (Fig 1.4) (Pawar et al., 2015). *Ihh* from the LE triggers decidualization in the uterine stroma through its receptor Patched-1 (*Ptch1*), which is expressed by uterine stromal cells. Thus, factors produced by the LE and GE mediate a cross-talk to induce stromal cell decidualization and signalling from both compartments is indispensable for this process. This may be the mechanism which necessitates epithelial *Esr1* in the stromal decidualization response.

Implantation and decidualization are vital events in early pregnancy, which must be tightly regulated in order for successful development of the placenta to occur. Aberrant signalling through *Pgr* and *Esr1*, and consequent effects on the regulation of their target genes, can lead to defects in implantation, decidualization and placentation (Cha and Dey, 2014). They are also implicated in disorders of pregnancy such as recurrent pregnancy loss

(Carranza-Lira et al., 2000; Itsekson et al., 2007; Su et al., 2011), and human endometrial disorders such as endometriosis and endometrial cancer (Ishikawa et al., 2010; Patel et al., 2015; Ramathal et al., 2010)

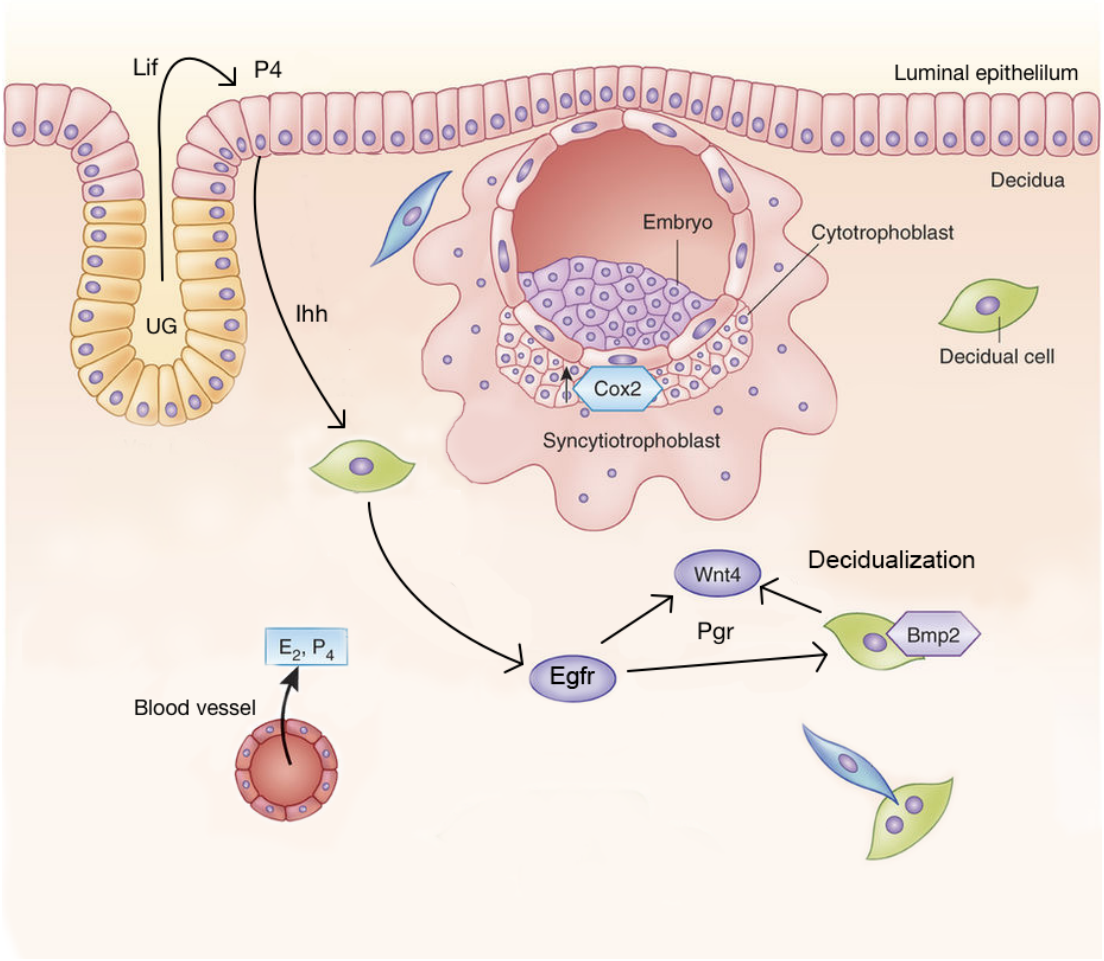

Figure 1.4 - Molecular control of decidualization. Implantation of the blastocyst into the uterine wall triggers decidualization of the uterine stroma. This requires paracrine secretion of Indian Hedgehog (*Ihh*) from the LE to the stroma under the control of P4 and *Lif*. This paracrine signal, along with *Pgr* actvity, triggers decidualization via downstream effectors including *Egfr, Bmp2*, and *Wnt4*. Adapted from Cha and Dey 2012.

1.2.1 Placental development in the mouse

The blastocyst is composed of two distinct groups of cells: the inner cell mass (ICM) from which epiblast cells emerge and give rise to the embryo proper, and an outer layer of trophectoderm (TE) cells that give rise to placental lineages (Fig 1.5). Once the blastocyst has implanted into the uterine wall, the polar TE (i.e. the cells overlying the ICM) proliferates in response to *Fgf4* secreted by the ICM, whilst cells of the mural TE cease to proliferate and instead start to differentiate into trophoblast giant cells (TGCs). It is these mural TE cells that

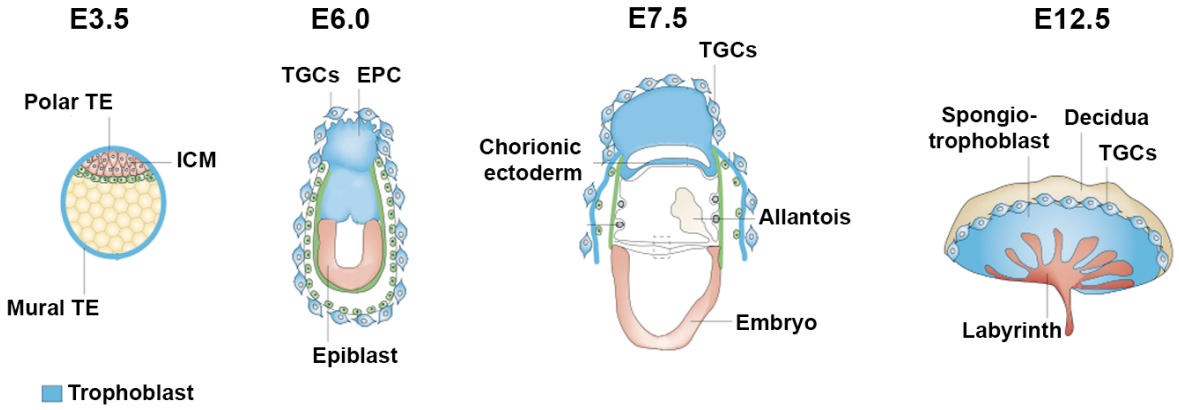

Figure 1.5 - Placental development in the mouse. Early development of the mouse embryo and placenta between E3.5-E12.5. ICM, inner cell mass. TE, trophectoderm. EPC, ectoplacental cone. TGCs, trophoblast giant cells. Adapted from (Rossant and Cross, 2001).

initiate the early penetration into the receptive uterus. Within the next 2-3 days following implantation, the continued proliferation of the polar TE leads to the formation of the extraembryonic ectoderm (ExE) and ectoplacental cone (EPC), bounded by a layer of mural TE-derived TGCs which surrounds the conceptus at E6 (Fig 1.5) (Rossant and Cross, 2001; Senner and Hemberger, 2010). By E7.5, morphogenetic events that occur as a consequence of gastrulation give rise to extra-embryonic mesoderm cells. Through these events, cells of the extra-embryonic ectoderm and mesoderm form the chorion, while mesodermal cells at the posterior end of the primitive streak form the allantois (Fig 1.5). Continued migration and proliferation cause the allantois to expand until it makes contact with the chorion, triggering these two layers to undergo chorio-allantoic fusion at around E8. This process is critical to generate the site at which fetal blood vessels, derived from the allantoic mesoderm, start to invaginate into the chorionic ectoderm to form the fetal vasculature of the emerging placenta. Chorio-allantoic fusion is vital for placental development, and its failure results in mid-gestational lethality (Downs, 2002; Rossant and Cross, 2001).

At E9.5 the chorio-allantois undergoes extensive branching morphogenesis to form the placental labyrinth. When formed, the labyrinth consists of an intricate network of fetal blood vessels that are in close contact with the maternal blood circulation. This architecture enables the efficient exchange of gases and nutrients between the maternal and fetal blood circulations. Unlike the fetal vessels, maternal blood percolates into lacunae that are established by one fenestrated layer of sinusoidal TGCs and two layers of syncytiotrophoblast. The layer closest to the maternal blood is commonly referred to as syncytiotrophoblast layer I (SynT-I), which is apposed to SynT-II, followed by the fetal endothelial cells and then the fetal blood (Georgiades et al., 2002). Fetal blood enters and flows through the labyrinth through a highly branched network of fetal vasculature, and as such the labyrinth contains a population of endothelial cells and supporting pericytes, which originate from the allantois. The proper development and function of these cell layers is vital for ensuring adequate nourishment of the conceptus.

Separating the labyrinth compartment from the maternal side is a layer of spongiotrophoblast (SpT) (Fig 1.5). The function of the SpT is poorly understood, but may provide structural support as well as additional hormonal supply, growth factor production (e.g. Igf2), and glycogen stores (Cross et al., 2002; Iwatsuki et al., 2000), and is characterised by the expression of *Ascl2* and *Tpbpa* (Fig 1.6). In direct contact with the remaining maternal decidual layer is a thin layer of parietal trophoblast giant cells (Fig 1.5). This, the mature placenta consists of the three main layers: (i) the labyrinth, (ii) the SpT and TGC layer, the combination of which is sometimes termed the junctional zone, and (iii) the maternal decidua.

1.2.3.1 Trophoblast differentiation

Not only does the placenta form the feto-maternal interface for the exchange of gases and nutrients between mother and conceptus, it also produces large quantities of hormones, angiogenic factors, and tissue remodelling factors (Rossant and Cross, 2001), which are vital for successful pregnancy and fetal development. As such, it consists of multiple cell types which are specialised for performing these various functions, including SynT, SpT, and TGCs. These differentiate during the first half of gestation from a trophoblast stem cell-like precursor cell pool that ultimately arises from the polar TE. Indeed, the stem cell potential can be maintained in trophoblast stem (TS) cells *in vitro*. TS cells can be derived from the TE of blastocyst stage embryos, and from the ExE and chorion up to E8.5 (Tanaka et al., 1998;

Uy et al., 2002), and cultured *in vitro* to investigate their self-renewal capacity, and differentiation to the various trophoblast lineages. TS cells represent the progenitor

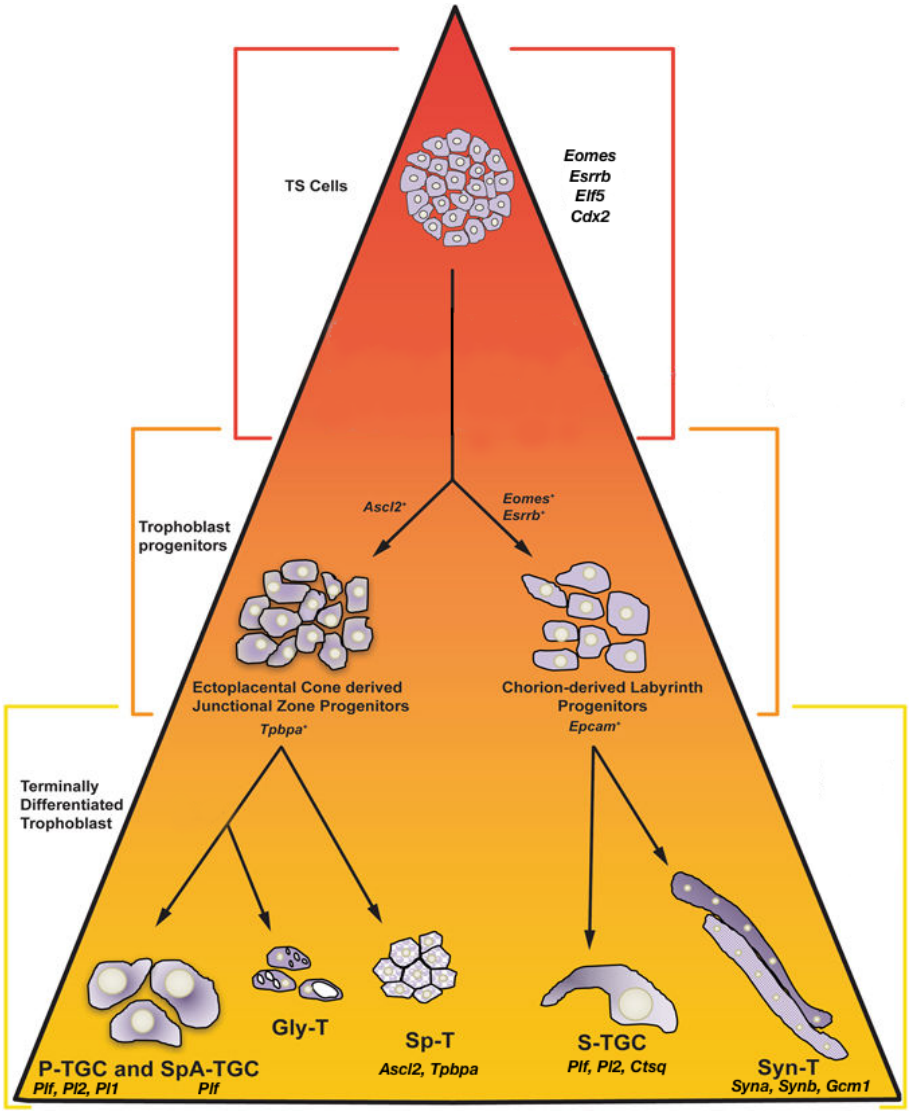

Figure 1.6 - Model of TS cell differentiation showing marker genes expressed at each stage of differentiation. TS cells, trophoblast stem cells. P-TGC, parietal trophoblast giant cells. SpA-TGC, spiral artery trophoblast giant cells. GlyT, glycogen trophoblast. SpT, spongiotrophoblast. S-TGC, sinusoidal trophoblast. SynT, syncytiotrophoblast. Adapted from (Natale et al., 2017).

population of the early placenta, and as such are able to give rise to all trophoblast cell lineages *in vitro* and in chimeras *in vivo* (Tanaka et al., 1998). The TS cell state is specified and maintained by a complex transcriptional network consisting of a number of transcription factors, including *Cdx2, Eomes, Elf5,* and *Esrrb* (Fig 1.6). *Cdx2* is essential for maintenance of TS cell identity and is also required for the specification of TE fate during early lineage

commitment. *Cdx2* restricts the expression of the embryonic stem cell pluripotency factors *Oct4* and *Nanog*, which specify the embryonic fate (Senner and Hemberger, 2010; Strumpf et al., 2005). The transcription factors *Eomes* and *Elf5* are not required for specification of the TS cell fate, but rather are important for the establishment and maintenance of the multipotent state, and expansion of the trophoblast stem or progenitor cell niche in early placental tissues (Latos and Hemberger 2014; Senner and Hemberger 2010).

The TS cell state is dependent on activation of the Fgf signalling pathway. TS cells can be maintained *in vitro* when cultured with Fgf and heparin in the presence of mouse embryonic fibroblast (MEF) conditioned medium, and withdrawal of these factors promotes differentiation (Tanaka, 2006). TS cells have the capacity to differentiate into all major trophoblast lineages. On differentiation stem cell factors are down-regulated, and differentiation progresses along two main routes (Fig 1.6). The major route is generally referred to as the "TGC pathway". This occurs via intermediate stages when cells are still diploid and express markers such as *Ascl2* and *Tpbpa*; hence this "intermediate trophoblast" is reminiscent of cells of the EPC (Carney et al., 1993; Cierna et al., 2016; Guillemot et al., 1994; Simmons et al., 2007). Apart from various TGC subtypes that differentiate as the main component (parietal TGCs, spiral-artery-associated TGCs), these cells also give rise to terminally differentiated cells in the junctional zone, consisting of SpT and glycogen trophoblast cells (Fig 1.6) (Mould et al., 2012; Simmons et al., 2007) . The second prominent route is the "SynT pathway". These cells are believed to originate from the basal part of the extraembryonic ectoderm, i.e. the part closer to the epiblast. This region contains *Esrrb*+ and *Eomes*+ TS-like cells, which give rise to *Epcam*+ progenitors that are routed towards the labyrinth fate (Fig 1.6) (Simmons et al., 2007; Simmons et al., 2008; Ueno et al., 2013; Uy et al., 2002). These progenitors differentiate further to form the SynT as well as sinusoidal TGCs which together make up the labyrinth trophoblast (Fig 1.6).

In vitro, TS cells differentiate most readily down the TGC route, as TS cell self-renewal factors in the culture medium actively suppress TGC formation, and their removal allows rapid differentiation to the TGC lineage (Erlebacher et al., 2004; Guzman-Ayala et al., 2004; Hughes et al., 2004; Tanaka et al., 1998). Thus, TS cells give rise to terminally differentiated TGCs, that undergo multiple rounds of DNA synthesis in the absence of cytokinesis to produce large, polyploid cells (Gardner and Davies, 1993; MacAuley et al., 1998), which are characterised by the expression of members of the prolactin family of hormones (Fig 1.6) (Simmons et al., 2007). *In vivo,* TGCs mediate the invasion of trophoblast into the

endometrial stroma, a feature first exhibited by the TE and later by the parietal and spiral artery-associated TGCs differentiating at the margins of the ectoplacental cone (Cross, 2000; Simmons et al., 2007). TGCs also produce large quantities of steroid hormones and paracrine factors, which promote adaptation of the maternal vasculature to pregnancy (Carney et al., 1993; Cross et al., 2002; Hu and Cross, 2010; Simmons and Cross, 2005).

The SynT cells characteristic of the labyrinth are defined by expression of Syncytins A and B (*Syna, Synb*) (Fig 1.6), with *Syna* being specific for the SynT-I layer and *Synb* for SynT-II (Dupressoir et al., 2009; Dupressoir et al., 2011). SynT precursors in the chorionic plate initially express *Gcm1,* defining the sites where branching morphogenesis is initiated (Anson-Cartwright et al., 2000). *Gcm1* expression is then restricted as precursors exit the cell cycle and fuse to form a syncytium, in a process that is currently not well understood (Simmons and Cross, 2005).

Trophoblast differentiation is essential for the successful development of the placenta and embryo. Perturbations to this tightly regulated differentiation programme often results in abnormalities in the formation of these trophoblast cell types and placental layers. This can result, for example, in disproportionate compartment sizes between labyrinth and SpT, or a general under-development of the intricate vascular organization of the labyrinth, leading to defects in fetal growth and development (Perez-Garcia et al., 2018). Many of these events continue to be influenced by the cross-talk between the trophoblast and maternal decidual compartment. As mentioned, the remodelling of maternal spiral arteries is chiefly mediated by invasive TGCs and later aided by glycogen cells, trophoblast cells secrete pro-angiogenic and vasodilatory factors to promote blood flow into the developing placenta, and at the same time the decidua generally limits trophoblast invasion and controls these tightly coordinated events.

1.3 Comparison of mouse and human reproductive biology

The mouse is the most commonly used model of human pregnancy due to the relative similarities in mouse and human reproduction. There are however important structural and functional differences between the two systems which may impact on the translational impact of mouse studies.

1.3.1 Structure and function of the uterus and endometrium

The most striking differences between pregnancy in the mouse and human are the number of progeny per birth and length of gestation. Mice give birth to litters consisting of 6-8 pups on average after a short gestation time of 19.5 days, whereas the vast majority of human pregnancies produce one baby with a much longer gestation period of about 40 weeks. The structure of the mouse uterus is well adapted to polytocous pregnancy, consisting of two uterine horns which join to form a single vagina. After conception multiple embryos implant simultaneously in both uterine horns, generating multiple implantation sites each containing an individual conceptus. In contrast, the human uterus is pyriform, and is comprised of a single chamber into which a single embryo (most commonly) implants. Multiple pregnancy in humans occurs in only 1-3% of all cases with the vast majority of those being twin pregnancies, and, in stark comparison with mouse pregnancy, presents significant risks to mother and baby. Obstetric complications including pre-term birth, fetal growth restriction, fetal demise, gestational diabetes and pre-eclampsia occur in 80% of multiple pregnancies compared to 25% of singleton pregnancies (Norwitz et al., 2005).

The mouse and human uterus are both lined by an inner layer of hormonally responsive endometrium into which the embryo must implant for successful pregnancy. The female mouse and human undergo a regular reproductive cycle, regulated primarily by the secretion of luteinising hormone and follicle stimulating hormone from the pituitary gland. These act on the ovarian follicles to regulate oocyte maturation ovulation, and on the endometrium to regulate its growth and differentiation. The mouse estrous cycle is 4-7 days long whereas the human menstrual cycle lasts for 28 days on average, but despite this significant difference in length the pattern of hormone secretion is relatively comparable between humans and rodents (Staley and Scharfman, 2005). There are however some subtle differences; during mouse pregnancy, the window of implantation is initiated by a nidatory surge of estrogen whereas this is not the case in the human, probably reflecting the need for synchronised implantation of multiple embryos in the mouse which is not necessary in human pregnancy (de Ziegler et al., 1992). During human pregnancy P4 is initially produced by the corpus luteum, but this is subsequently taken over by the placenta (luteo-placental shift), whereas in the mouse the corpora lutea are responsible for P4 production for the duration of pregnancy (Ratajczak and Muglia, 2008). The most striking difference between the mouse and human reproductive cycles is the cyclical shedding of the endometrium which occurs at the end of each menstrual cycle in humans, termed menstruation.

Menstruation does not occur in the vast majority of mammals, including the mouse and may be a result of the spontaneous decidualization which occurs during every human menstrual cycle, but is not present in the mouse. Recent evidence suggests that this cyclical shedding of the endometrium may allow for endometrial remodelling, thus potentially altering the cellular composition of the endometrium between cycles (Brighton et al., 2017).

In both species the endometrium consists of an upper layer of luminal epithelial cells, and the underlying uterine stroma containing uterine stromal cells and uterine glands. Both the mouse and human undergo endometrial decidualization during early pregnancy, in response to the action of E2 and P4 which act as critical regulators of endometrial growth and decidualization during the reproductive cycle. As in the mouse, human endometrial decidualization is regulated by signalling pathways including the ESR, PGR, BMP2 and WNT pathways (Kaya Okur et al., 2016; Li et al., 2007; Ramathal et al., 2010; Sonderegger et al., 2010), suggesting that the underlying molecular pathways are somewhat conserved and that findings from studies performed in mouse may be translated to the human condition. However, a major difference between the human and mouse is the timing of onset of decidualization. The mouse endometrium undergoes decidualization only in response to the implanting blastocyst, whereas the human endometrium initially undergoes spontaneous decidualization during the secretory phase of each menstrual cycle, immediately following ovulation (Gellersen and Brosens, 2014; Ramathal et al., 2010). While some clear differences exist between the reproductive cycles of the mouse and human, there appears to be significant conservation of the molecular regulation of implantation and decidualization, and the mouse remains the most widely used, well defined model of human endometrial function.

1.3.2 Comparison of the mouse and human placenta

Mammalian placentation is functionally convergent, however placental morphology can vary significantly between species. Both mouse and human placenta are discoid in shape, and exhibit a haemochorial type of placentation, where the fetal trophoblast cells are in direct contact with maternal blood. The placenta is a heterogeneous tissue consisting of multiple cell types with various functions. Some analogous cell types can be identified in mouse and human, through overlapping patterns of gene expression as well as similar cellular morphology and function, however in some cases a direct comparison is not

straightforward. In the mouse and human the structures responsible for gas and nutrient exchange between the fetal and maternal circulation are the labyrinth and the placental villi respectively. Both structures share a similar syncytial cell-type which is directly bathed in maternal blood. However, in humans there is only one syncytial layer overlying a layer of cytotrophoblast which are thought to continuously fuse with and replenish the syncytium throughout pregnancy, whereas the mouse exhibits a trilaminar structure with two adjacent layers of syncytium and a single fenestrated layer of TGCs. Despite these structural differences between the mouse and human exchange surfaces, the development of the mouse labyrinth and human villi may be regulated by some common factors. For example, GCM1, a marker of labyrinth progenitors required for branching morphogenesis in the mouse placenta (Anson-Cartwright et al., 2000), is similarly expressed by the syncytio- and cytotrophoblast of the human placental villi (Nait-Oumesmar et al., 2000).

Although there are significant morphological and functional similarities between the mouse labyrinth and human placental villi, a direct equivalent of the mouse junctional zone is less clear cut. The closest comparison that can be made is with the human cytotrophoblast cell column, which anchor the placenta to the uterine wall. They consist of tightly packed cytotrophoblast cells which are highly proliferative at the base of the column, thus contributing to its growth. At its distal tip the column cytotrophoblast in contact with the maternal decidua undergoes an epithelial-mesenchymal transition and differentiates into an invasive cell type called extravillous trophoblast (EVT) (DaSilva-Arnold et al., 2015; E. Davies et al., 2016). EVT cells invade deeply into the decidua, migrating to erode the vasoactive lining of the maternal spiral arteries and also becoming polyploid in a similar way to the mouse TGCs, although to a lesser extent. As such, the cytotrophoblast cell column shows some similarities with the mouse junctional zone in terms of the invasive characteristics of the EVT, and its remodelling of the maternal vasculature which is instrumental in regulating the flow of maternal blood to the placenta, as is seen with mouse TGCs (Pijnenborg et al., 2011).

1.4 Preliminary data

A study from Lopes and colleagues in 2009 showed that pregnancy during advanced maternal age in C57BL/6 (B6) mice results in a higher frequency of abnormal development in the offspring (Fig 1.7a). In the litters that were studied, they reported developmental abnormalities including enlargement of the heart, hindbrain defects, and embryo resorption (Fig 1.7a). As discussed earlier, these particular defects suggest abnormalities of the placenta. In line with this, gross histological examination performed in that study indicated that the placentas from older B6 mothers exhibited developmental defects in the trophoblast compartment (Fig 1.7b).

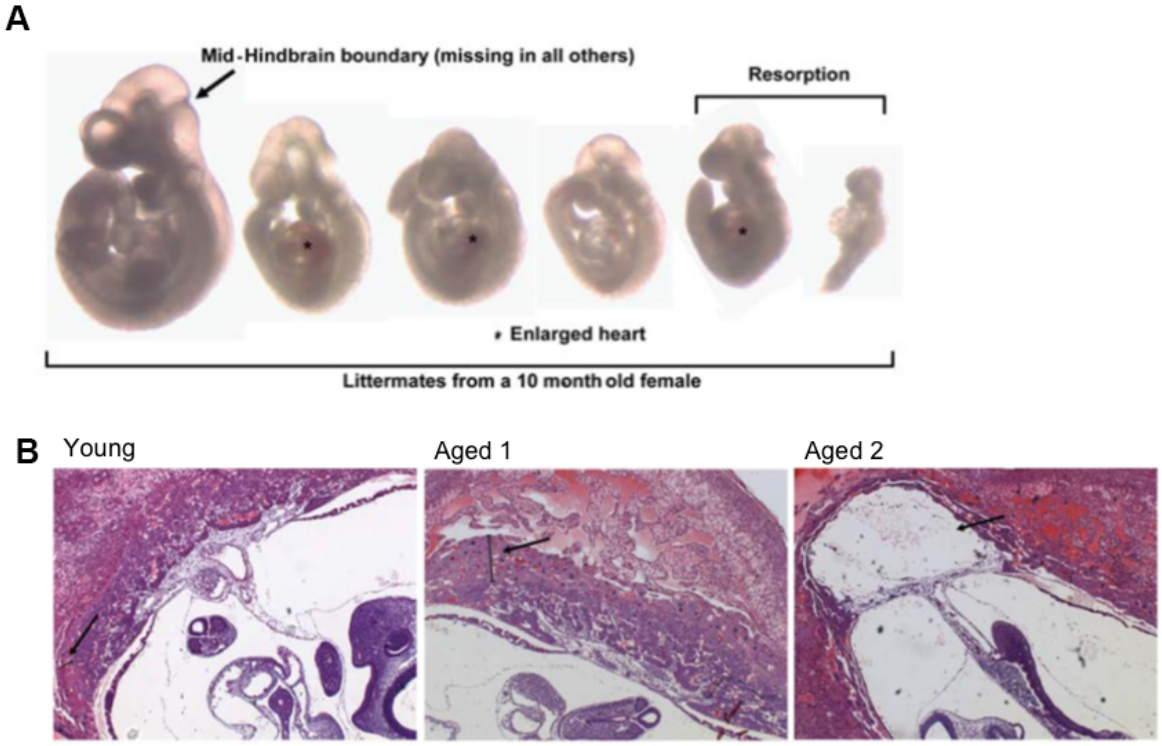

Figure 1.7 - Effects of maternal age on embryonic and placental development at E12.5, showing a) the variability of embryonic development, and the incidence of heart and brain defects, and resorption, b) normal placentation at one implantation site from a young mother, and two sites from an aged mother. Black bar and arrow in Young and Aged 1 show thickness of the TGC layer. Arrow in Aged 2 points to abnormal labyrinth development. Taken from (Lopes et al., 2009).

This study suggested that placentation is adversely affected by maternal ageing. However, only a limited number of pregnancies in aged females were studied (n=3), leaving open questions about the penetrance and reproducibility of this phenotype. Importantly the authors noted that these defects could arise due to a) poor quality of the aged oocyte, or b)

alterations in the uterine environment of aged females, however, this question has remained open and the origin of placental defects remains unknown.

It has previously been suggested that maternal ageing impairs the ability of the uterus to successfully achieve and maintain pregnancy, leading to defects in placentation, however there is so far no direct evidence to support this. If placental defects do originate from the aged maternal environment and not the embryo, they may arise from perturbations to the molecular cross-talk between the blastocyst and endometrium in early pregnancy.

Most of these data are from very early studies and/or have remained at an observational level lacking molecular insights, including the above-mentioned study by Lopes et al. in aged B6 females. Thus, the aim of my project was to use the B6 model to systematically analyse the effect of advanced maternal age on embryonic and placental development, and investigate the molecular basis of the reproductive decline in ageing females.

1.5 Hypotheses and aims

There is a significant body of work investigating the relationship between advanced maternal age and decline in the size and quality of the oocyte pool, however research into the contribution of uterine ageing and placental dysfunction to reproductive decline in advanced maternal age has been largely neglected.

My primary hypothesis is that a significant proportion of the developmental abnormalities in offspring from older B6 mothers occur as a result of defective placentation. My secondary hypothesis is that maternal age-related placentation defects are rooted in ageing of the maternal uterus, and do not reside with the oocyte. The aim of this project is to delineate the causes and consequences of reproductive decline with advanced maternal age, with a view to gain a better understanding of the mechanisms of reproductive ageing.

The sub-aims of this project are:

- To systematically characterise defects in embryonic and placental development in the offspring of older mothers.

- To establish whether the underlying basis for embryonic and placental defects resides with the aged oocyte, or uterus.
- To assess the functional capability of endometrial cells to respond to pregnancy hormones in young versus aged females.
- To identify the potential mechanism that underlies abnormal uterine function and placental development in advanced maternal age.

Chapter II
Methods

2.1 Mice

C57BL/6*Babr* mice were used throughout this study. Virgin females were housed in groups of up to 5 per cage until reaching the desired age as indicated for each experiment. All animal experiments were conducted in full compliance with UK Home Office regulation and with approval of the local animal welfare committee (AWERB) at The Babraham Institute, with relevant project and personal licences in place. Where "young" females were used, they were between 8-12 weeks of age. Timed matings were set up with 8-16 week old C57BL/6*Babr* stud males, with the morning of the vaginal plug designated as E0.5. Where "aged" males were used, they were 1 year old. Pregnancy was confirmed by presence of the plug, and subsequently females were dissected at the gestational age indicated in each experiment. Dissected tissue was processed for histology, RNA isolation, or uterine stromal cell isolation as indicated.

2.2 Deciduoma assay

Mice were maintained in the designated animal care facility at Baylor College of Medicine according to the institutional guidelines for the care and use of laboratory animals. The artificial decidual response has been previously described (Finn, 1966). Briefly, ovariectomized mice were injected 3 times a day with 100 ng of estradiol (E2) per mouse. After 2 days of rest, mice were then injected daily with 1 mg of progesterone (P4) and 6.7 ng of E2 per mouse for 3 days, subcutaneously. One uterine horn was subjected to an intraluminal injection of 50µl of sesame oil 6 h after the final P4 and E2 injection. The other horn was not subjected to sesame oil injection and served as a control. Mice were given daily subcutaneous injections of 1 mg of P4 and 6.7 ng of E2 per mouse each day after the trauma. Mice were sacrificed 2 days after the trauma by cervical dislocation while under anaesthetic, Avertin (2,2-tribromoethyl alcohol; Sigma-Aldrich, St. Louis, MO), and uteri dissected out.

2.3 Histology

Dissected tissues for histology were fixed overnight in 4% paraformaldehyde, before being embedded in paraffin wax and cut into 7µm thick sections on a Leica paraffin microtome. For haematoxylin and eosin (H&E) staining, sections were deparaffinised and incubated in Mayer's Haematoxylin (Sigma #51275) for 10 minutes, before washing briefly in tap water.

Staining was differentiated by incubating in 70% acid alcohol (70% ethanol, 1% hydrochloric acid) for 10 seconds, and then in cold tap water for 10 minutes. Eosin staining (alcoholic Eosin, Sigma HT110116) was performed for 30 seconds, followed by dehydration, and mounting of sections with Eukitt quick-hardening mounting medium (Sigma #03989). For immunohistochemistry slides were deparaffinised in xylene and rehydrated in an ethanol series. Antigen retrieval was performed by microwave boiling of sections in 10mM Na-citrate pH 6.0, or 10mM Tris pH9.5, 1mM EDTA for 30 minutes, and washed 3 times in 50mM Tris pH7.8, 330mM NaCl, 0.1% NP-40. Slides were then blocked in PBS, 0.5% BSA, 0.01% Tween-20 for 30 minutes, before incubation with primary antibody diluted in PBS, 0.5% BSA, 0.01% Tween-20 overnight at 4^{o}C, in the dark. Antibodies used were Ki67 (Abcam ab15580, 1:200), Pgr (DAKO A0098, 1:1000), pStat3 (Cell Signaling 9138S, 1:200), Esr1 (Santa Cruz sc-543, 1:200), pEsr1 (Santa Cruz sc-101675, 1:200), 5-methylcitidine (Eurogentec BI-MECY-0100), and 5-hydroxymethylcytosine (Active motif 39769). Secondary antibodies were either the appropriate AlexaFluor or horseradish-peroxidase (HRP) conjugated antibodies at 1:500 and 1:100 respectively. uNK staining was performed using HRP-conjugated *Dolichus biflorus agglutinin* (Sigma #L1287) at 1:75 dilution, after boiling in 10mM Na-citrate buffer pH 6.0. Sections were counterstained with DAPI for immunofluorescence and haematoxylin for immunohistochemistry. For RNA *in situ* hybridization, slides were deparaffinised and rehydrated as described above. Linearised plasmids containing cDNA inserts from *Plf* cDNA were used to generate digoxigenin (DIG) labelled probes, using the DIG RNA-labelling kit according to the manufacturer's instructions (Roche 11277073910). In situ hybridisation was performed overnight at 52^{o}C using, and signals were detected using an anti-DIG-alkaline phosphatase conjugated antibody (Roche). Staining was carried out overnight using NBT and BCIP reagants (Promega S3771). Sections were counterstained with nuclear fast red (Sigma N3020).

2.4 DNA and RNA isolation

RNA and DNA from tissues were isolated simultaneously using the Allprep DNA/RNA Mini Kit (Qiagen 80204), following the manufacturer's instructions. DNA and RNA concentration was measured on a Nanodrop and run on a 2% agarose gel to determine quality. RNA from cells was isolated using Tri reagent (Sigma T9424), following the manufacturer's instructions.

2.5 RT-qPCR expression analysis

0.5µg of purified RNA from the decidua and trophoblast portion of each placenta was pooled to make 1µg of RNA. RNA was reverse transcribed using a mixture of random hexamer (Thermo Scientific EP0451), and oligodT_{18} primers (Fermentas S0132) at 0.2 and 0.5µg/ml respectively, incubated for 5 mins at 70°C, followed by cDNA synthesis at 42°C for 90 mins, resulting cDNA was diluted 1:30 in H_20. RT-qPCR was performed using SYBR green Jump Start Taq Ready mix (Sigma 4438) and run on a Bio-Rad CFX96 or CFX384 thermocycler, using gene-specific intron-flanking primers. Gene expression analysis was performed on samples in triplicate, and Ct values normalised to *Sdha* as a housekeeping gene. Where appropriate, student's t-test was performed to calculate statistical significance of differential gene expression ($p<0.05$).

2.6 RNA sequencing

For RNA-seq of E11.5 trophoblast and decidua, and E3.5 uteri, the mRNA fraction was isolated form 350ng total RNA using the Dynabeads mRNA purification kit (Life Technologies 61006). Indexed, strand specific libraries were generated using the ScriptSeq V2 RNA-Library preparation kit (Epicentre SSV21106) per manufacturer's instructions, and purified using Agencourt AMPure XP beads (Beckman Coulter A63881).

For RNA-seq of uterine stromal cells, the mRNA fraction was isolated from 350ng total RNA, and indexed, strand specific libraries were generated using the Agilent SureSelect Strand Specific RNA Library kit (Agilent G9691A) per manufacturer's instructions, and purified using Agencourt AMPure XP beads (Beckman Coulter A63881).

Libraries were quantified and assessed for quality using both the BioAnalyzer 2100 System (Agilent), and KAPA Library Quantification Kit (KAPA Biosystems KK4824). Indexed libraries were pooled and sequenced on an Illumina HiSeq2500 sequencer, using a 100bp single-end protocol. Raw fastq data were mapped to the *Mus musculus* GRCm38 genome assembly using TopHat v2.0.12.

2.7 Methylated DNA immunoprecipitation sequencing

DNA was purified using Allprep DNA/RNA Mini Kit (Qiagen 80204). 3µg of DNA was sonicated into fragments between 200-700bp using a BioRuptor (Diagenode), and quantified on a

Nanodrop before running on a 1% agarose gel to confirm fragment size. DNA libraries were prepared using the NEBNext DNA Library Prep Master Mix Set for Illumina (New England BioLabs E6040L), following the manufacturer's instructions with some modifications. Briefly, 1.5µg of sonicated DNA was used in the end repair reaction and incubated at 20°C for 30 mins, before purification with Agencourt AMPure XP beads (Beckman Coulter A63881), without elution of DNA from the beads. End repair was followed by the dA-tailing reaction, incubated at 37 °C for 30 mins. 20% PEG 8000 in 1.35M NaCl was then added to bind DNA to the beads, before washing with 80% ethanol. Adaptor ligation was then performed for 15 mins at 20 °C using Illumina paired-end adaptors at a final concentration of 1.5µM. Again, PEG 8000 was added to the beads to allow washing, before eluting in warm EB.

Methylated DNA immunoprecipitation (MeDIP) was performed on the resulting DNA libraries to isolate only methylated DNA fragments. Three immunoprecipitations (IPs) were performed per sample, each using 500ng of library DNA, plus an input sample of 500ng. IP samples were denatured at 99 °C before incubation with 1.25µl of 5mC antibody (Eurogentec BI-MECY-0100) for 2 hours at 4 °C, and then for a further 2 hours with pre-blocked Dynabeads M-280 Sheep anti-mouse IgG (Invitrogen 112-01D). Beads were washed 3x and treated with proteinase K for 30 mins, and the 3 IP samples were pooled before purification with MinElute PCR purification kit (Qiagen 28004). IP efficiency was analysed by qPCR of known methylated and unmethylated regions. Purified, immunoprecipitated library DNA was amplified according to the NEBNext DNA Library Prep Kit instructions, using PE PCR primer 1.0, and an iPCR tag primer both at 10nM, to generate indexed MeDIP-sequencing libraries. Libraries were purified using QIAquick PCR Purification kit (Qiagen 28104) before size selection either by gel extraction or using AMPure beads. For gel extraction, MeDIP libraries were run on a 2% agarose gel and cutting a band between 200-500bp before purifying using QIAquickGel Extraction kit (Qiagen 28704). For AMPure bead double size selection, libraries were incubated for 10 minutes with 0.6x volume of beads, and the supernatant retained and incubated with 0.45x total volume of beads for 10 minutes, before washing with 80% EtOH and eluting in nuclease free H_2O (Qiagen 129114). Libraries were quantified and assessed for quality using both the BioAnalyzer 2100 System (Agilent), and KAPA Library Quantification Kit (KAPA Biosystems KK4824). Indexed libraries were pooled and sequenced on an Illumina HiSeq2500 sequencer, using a 50bp paired-end protocol. Raw fastq data were mapped to the *Mus musculus* GRCm38 genome assembly using Bowtie2.

2.8 Native histone chromatin immunoprecipitation sequencing (ChIP)

2.8.1 Chromatin isolation and digestion

Histone ChIP was performed pellets of 200,00 uterine stromal cells isolated from E3.5 uteri from young (n=3) and aged (n=3) mice as described in section 2.11, and snap frozen in passage 3-4. Frozen pellets were resuspended in 10mM Tris pH7.5, 10mM NaCl, 3mM $MgCl_2$, 1mM $CaCl_2$, 0.4% NP-40, before separating into 3 equal fractions. All buffers were treated with protease inhibitors (Roche 5056489001) to prevent the degradation of histones. Chromatin was digested with MNase (Sigma N5386-200UN) at 1x, 1/2x and 1/4x concentration, for 8 minutes at 37°C. The digest was quenched on ice with EDTA to a final concentration of 10mM, before centrifuging at 2,500g at 4 °C. The supernatant (S1) was isolated, and the pellet resuspended in 10mM Tris pH7.5, 10mM NaCl, 3mM $MgCl_2$, 0.25mM EDTA, 0.4% NP-40, and incubated on ice for 15 minutes. The resuspended pellet was passed 4 times through a 20 gauge needle and 4 times through a 25 gauge needle, before centrifuging at 10,000g for 10 minutes a 4°C, and combining the supernatant (S2) with S1. NaCl concentration was raised to 150mM before incubating on ice for 20 minutes and centrifuging at 10,000g for 15 minutes and retaining the supernatant. 20µl of chromatin was taken and DNA was purified using the Qiaquick PCR purification kit (Qiagen 28106) and run on the Agilent BioAnalyzer 2500 to confirm the extent of chromatin digestion. Chromatin from digests at 1x, 1/2x, and 1/4x concentration were pooled at this point.

2.8.2 ChIP

The digested chromatin was diluted to a final volume of 800µl per ChIP. 20µl of Dynabeads Protein A for Immunoprecipitation beads (Dynabeads 10001D) per ChIP were washed 3x with 10mM Tris pH7.4, 50mM NaCl, 5mM EDTA, and 10µl of beads were added to 800µl of chromatin and 1µg of rabbit IgG (Santa Cruz Biotechnology sc-2027X) and rotated for 2 hours at 4°C to preclear chromatin. Beads were discarded and 10% of chromatin was taken for input, before adding 0.25µg of H3K4me3 (Abcam ab1791) or rabbit IgG (Santa Cruz Biotechnology sc-2027X) to precleared chromatin, and rotating overnight at 4°c. 10µl of prewashed Protein A beads were added to each ChIP, and rotated for 4 hours at 4°C. After 4 hours beads were washed 5 times in ice cold NChIP buffer, then resuspended in NChIP + 1% SDS at room temperature for 15 minutes, and treated with TE buffer pH6.5 and proteinase K for 30 minutes at 45°C. Input and ChIP samples were purified using the Qiaquick PCR

purification kit. qPCR was performed for regions known to be enriched or depleted for H3K4me3 and K3K9me3 to check efficiency of the pull down.

2.8.3 ChIP-seq library preparation

DNA libraries were generated from H3K4me3, H3K9me3, and input DNA, using the NEBNext Ultra II DNA library prep kit (Illumina E7645), following the manufacturer's instructions. Libraries were purified, and double size selected in the same way as MeDIP libraries using Agencourt AMPure XP beads (Beckman Coulter A63881). Size selected libraries were amplified using NEBNext Ultra II kit, and Sanger 8 base pair indexed oligos: 10µM PE1.0 primer and 10µM iPCR tag, using the programme 98°C for 30s, 12-15 cycles of 98°C for 10s, 65°C for 75s, followed by final extension at 65°C for 5 minutes. ChIP libraries were purified with AMPure XP beads. Libraries were quantified and assessed for quality using both the BioAnalyzer 2100 System (Agilent), and KAPA Library Quantification Kit (KAPA Biosystems KK4824). Indexed libraries were pooled and sequenced on an Illumina HiSeq2500 sequencer, using a 50bp paired-end protocol. Raw fastq data were mapped to the *Mus musculus* GRCm38 genome assembly using Bowtie 2.

2.9 Sequencing of amplicon targets from bisulphite treated DNA

1µg of DNA was bisulphite treated using the EpiTect Bisulphite Kit (Qiagen 59104) according to the manufacturer's instructions. Primers were designed to differentially methylated regions identified by MeDIP-seq, and used to amplify 30ng BS treated DNA with HiFi HotStart Uracil+ Readymix (Kapa Biosystems KK2801). PCR products were purified with Agencourt AMPure XP beads (Beckman Coulter A63881). Multiple products pooled together for each sample, and amplified a second time using a Sanger 8 base pair indexed oligos, and HiFi Hotstart Readymix (Kapa Biosystems KK2601). Libraries were quantified and assessed for quality using both the BioAnalyzer 2100 System (Agilent), and KAPA Library Quantification Kit (KAPA Biosystems KK4824). Indexed libraries were pooled and sequenced on an Illumina MiSeq sequencer, using a 150bp paired-end protocol. Raw fastq data was mapped to the *Mus musuclus* GRCm38 genome assembly and methylation calls generated using the Bismark tool (Babraham Bioinformatics).

2.10 Bioinformatic analysis

Raw next generation sequencing data was processed and mapped by the Bioinformatics facility at The Babraham Institute.

2.10.1 RNA-seq analysis

RNA-seq data was visualised and quantitated at the mRNA level using the RNA-seq quantitation pipeline in SeqMonk software (http://www.bioinformatics.babraham.ac.uk), and normalised according to total read count (reads per kilobase of transcript per million mapped reads, RPKM), and 75% distribution if necessary. Differential expression was calculated using DESeq2 (Love et al., 2014) and the intensity difference filter in SeqMonk, with a *p* value threshold of 0.05 and adjusted for multiple testing correction using the Benjamini-Hochberg method. Gene lists used for analysis were either stringent with the gene called by both methods, or less stringent with differential expressed called by either or both methods.

Heatmaps were generated using Heatmap.2 in R. Principal component analysis was performed using DESeq2 rlog-normalised RNA-seq data on read counts using the top 500 most variable genes, before plotting the principal component analysis using prcomp in R.

For the analysis of gene proximity to *Pgr* and *Esr1* binding elements, I first determined the cohort of differentially expressed genes between young and aged deciduas using DESeq2 and intensity difference in SeqMonk. Proximity of these genes to *Pgr* and *Esr1* binding sites was determined using published data, available in NCBI GEO dataset accession numbers GSE34927 and GSE36455 in bed format, using a distance cut-off of 10 kb. Differentially expressed genes were split into up-regulated and down-regulated genes, which were analysed separately. Statistical significance of the overlap was calculated by Fisher's exact test in R.

2.10.2 MeDIP-seq analysis

MeDIP-seq data was visualised using Seqmonk software. Differential methylation was determined using the MEDIPS package in R (Lienhard 2014), with a window size of 200bp, and a bonferroni adjusted p value cut-off of 0.5 for comparisons between young and aged, and 0.01 for comparison between E3.5 and E11.5. Enrichment of 5mC in different genomic features was determined by calculating the percentage of reads from each library in each

feature and dividing it by the percentage of the genome occupied by that feature. This figure was log2 transformed to find the log2 relative enrichment, and plotted using ggplot2 in R.

2.10.3 ChIP-seq analysis

Peaks were called on bam files from H3K4me3 ChIP-seq libraries using the MACS2 command line tool (Feng et al., 2012; Zhang et al., 2008) in broad peak mode with an FDR cutoff of 0.05, using data from the input library of one young sample as the reference input for all samples. ChIP-seq peak data was analysed using the R package DiffBind (Stark and Brown, 2011) to examine the correlation between samples, and generate consensus peak lists containing either peaks present in all young samples (n=3), peaks present in all aged samples (n=3), or peaks present in all young and/or all aged samples. H3K4me3 ChIP-seq data was visualised in Seqmonk, and reads under MACS2 peaks were quantified and normalised according to total read count (reads per kilobase of transcript per million mapped reads, RPKM). Peaks containing significantly different levels of H3K4me3 were found using DESeq2 $p<0.05$. Further normalisation at the 20th and 90th percentiles in Seqmonk was required to correct for variation in the efficiency of H3K4me3 immunoprecipitation, informed by measurement of total protein levels of H3K4me3 by Western blot. For analysis of H3K4me3 peak breadth, peaks overlapping between the young and aged consensus peak lists were found using the intersect function in the BEDtools Suite (Quinlan and Hall, 2010). The difference in breadth between matched peaks present in young and aged was calculated and plotted in R.

2.10.4 Amplicon bisulphite-seq analysis

Percentage methylation at each CpG site analysed was extracted in R from coverage files produced by the Bismark aligner (https://www.bioinformatics.babraham.ac.uk/projects/bismark/). Only CpGs located in the MEDIPS window tested for were included. Average DNA methylation at each CpG was calculated by finding the mean % methylation, and plotted using ggplot2 in R.

2.10.5 Heatmap generation

Median centred heatmaps were generated in R using the Heatmap.2 package.

2.10.6 Gene ontology and enrichment analysis

For identification of enriched terms in RNA-seq data, enrichment was calculated using The Database for Annotation Visualisation and Integrated Discovery (DAVID) (Huang da et al., 2009) (https://david.ncifcrf.gov/), using all genes containing more than 10 reads in the tissue of interest as a background. For analysis of regions of interest in bed format including ChIP-seq and MeDIP-seq data, the Genomic Regions Enrichment of Annotations Tool (GREAT) (McLean et al., 2010) (http://great.stanford.edu/public/html/) was used, with the mm10 genome as a background. In both cases, terms with a Bonferroni adjusted p value > 0.05 were considered significantly enriched.

2.10.7 Principal component analysis

Principal component analysis was performed using DESeq2 rlog-normalised RNA-seq data on read counts using the top 500 most variable genes, before plotting the principal component analysis using prcomp in R.

2.10.8 Generation of cell-type specific gene expression signatures

Gene expression signatures specific to luminal epithelial (LE) cells and uterine stromal cells (USCs) were generated using publicly available RNA-seq data from the GEO database, generated from LE isolated by laser capture microdissection on day 4 of pregnancy (GSE57680), and RNA-seq data from USCs generated as described in sections 2.11 and 2.6. LE fastq data was downloaded from the sequence read archive and remapped to the GRCm38 genome using Hisat2, for visualisation and analysis in Seqmonk. RNA-seq data was normalised to the 75th percentile, and genes specific to the LE were found by differential expression (DE) analysis with DESeq2 $p<0.05$. Genes DE between LE and USCs with a difference >4 were selected. These were filtered further by removing any genes in the LE list with >10 reads in USC libraries, and removing genes in the USC list with >10 reads in LE libraries.

2.10.9 Microarray analysis

Acquisition and analysis of microarray data was kindly performed in Dr Francesco DeMayo's lab, USA. Microarrays of uterine RNA samples from conditional ablation of *Bmp2*, *Wnt4*, *Egfr2* and their respective control groups were performed by Genomic and RNA profiling Core of Baylor College of Medicine as described previously (Large et al., 2014). Two-tailed *t* test and fold changes were used to define differentially expressed probes. To obtain a non-

redundant list of significantly altered genes, multiple probe sets for a given gene (when present) were averaged. Genes with an absolute fold change of ≥1.4 and a *p* value of ≤0.01 were considered for further analysis.

The overlap between *Pgr*, *Bmp2, Wnt4*, and *Egfr2* regulated genes identified by microarray, and genes dys-regulated in aged E3.5 uteri was calculated. The significance of the pairwise overlap between the datasets was then determined by Fisher's exact test, against a background of all genes detected in both RNA-seq and microarray datasets.

2.10.10 Analysis of motif enrichment

Enrichment of transcription factor binding motifs in differentially methylated regions (DMRs) was determined using the Analysis of Motif Enrichment (AME) tool (McLeay and Bailey, 2010) in MEME Suite (http://meme-suite.org/). Fasta sequences were extracted from DMRs in bed format, using the UCSC Table Browser (https://genome.ucsc.edu/cgi-bin/hgTables), masking repeats to N. Repeat masked sequences were run through AME using the HOCOMOCO v11 full motif database, with shuffled versions of the input sequences as a control.

2.11 Uterine stromal cell isolation and culture

Uterine stromal cells were isolated as previously described (Afonso et al., 2002), with a few modifications. Briefly, uteri from pregnant mice were dissected at E3.5 and slit longitudinally. Uteri were incubated with 2.5% pancreatin (Sigma P3293) and 0.5% trypsin type III (Sigma T4799) in Hank's basic salt solution (HBSS)-calcium/magnesium free (Life Technologies 55021C) for 1.5h on ice, and vortexed and washed twice in HBSS to remove luminal epithelial cells. Uterine stromal cells were isolated by digestion for 20 mins at 37^{o}C, with HBSS containing 0.007% collagenase (ThermoFischer Scientific 17104-019), 0.02% DNaseI (Roche 10104159001), and 0.008% protease (Sigma P8811), vortexing every 10 minutes. Dissociated tissues were triturated and passed through a 70µm cell strainer (BD Biosciences) and spun at 1000g for 5 mins at 4^{o}C. Cell pellets were resuspended and cultured in phenol-red free Dulbecco's modified Eagle's medium: Nutrient Mixture F-12 (DMEM/F-12) (ThermoFisher Scientific 21041-025) plus 10% foetal bovine serum, 1mM sodium pyruvate (ThermoFisher Scientific 11360-039), 1X antimycotic/antibiotic (ThermoFisher Scientific #15240-062) and 50 µM 2-mercaptoethanol (ThermoFisher Scientific #31350-010).

2.1.1 Proliferation assay

For analysis of cell proliferation rates, 10,000 uterine stromal cells from young and aged mice were plated in either complete DMEM/F12 medium or complete medium containing the decidualisation-inducing cocktail (E2 + P4 + cAMP) and collected every 24 h over 4 days. After trypsinisation the number of viable cells was counted using the Muse Count & Viability Assay Kit (Merck Millipore MCH100102) and run on the Muse cell analyser (Merck Millipore), according to manufacturer's instructions. Statistical analysis was performed using ANOVA followed by Holm-Sidak's post-hoc test.

2.11.2 In vitro decidualization

Decidualisation of cultured uterine stromal cells was induced by incubating the cells with complete DMEM/F-12 medium plus 10nM β-estradiol (Sigma #E2758), 1µM medroxyprogesterone 17-acetate (Sigma #M1629) and 10 µM 8-bromoadenosine 3',5'-cyclic monophosphate (Sigma #B5386) (E2 + P4 + cAMP). The culture medium was changed every 2 or 3 days with continuous supplementation with these treatments.

2.11.3 Generation of USC conditioned media and trophoblast stem (TS) cell differentiation

Conditioned medium (CM) was generated by plating mouse embryonic fibroblasts or uterine stromal cells from young or aged mice in a 6cm dish, and culturing for 3 days in TS base medium. USCs were supplemented with 10nM β-estradiol (Sigma #E2758), 1µM medroxyprogesterone 17-acetate (Sigma #M1629) and 10 µM 8-bromoadenosine 3',5'-cyclic monophosphate (Sigma #B5386) (E2 + P4 + cAMP), to induce decidualization. CM was collected after 3 days and filtered through a filter unit to remove any cells (Thermo Scientific 122-0045). For TS cell culture under stem cells conditions, Rosa26 TS cells in passage 70 were plated in a 12 well plate, and cultured in complete TS medium, consisting of 3/10 TS base and 7/10 CM plus 37.5ng/ml bFgf (Stem Cell Institute) and 1µg/ml heparin (Sigma Aldrich H3149). After 2 days RNA was collected from TS cells at sub-confluence using Tri reagent as described in section 2.4. For TS differentiation, Rosa26 TS cells in a 12 well plate were cultured in TS medium consisting of 3/10 TS base and 7/10 CM, without bFgf and Heparin, for 3 days and 5 days. TS cells at sub-confluence were then isolated using Tri reagent.

2.12 Western blotting

Total cell extracts from deciduas were prepared in radioimmunoprecipitation assay buffer (20 mM Tris-HCl, pH 8.0, 137 mM NaCl, 1 mM $MgCl_2$, 1 mM $CaCl_2$, 10% glycerol, 1% NP-40, 0.5% sodium deoxycholate, 0.1% sodium dodecyl sulphate), or in the case of uterine stromal cells, cells were lysed in a detergent buffer (10 mM Tris-HCl, pH 7.4, 150 mM NaCl, 10 mM KCl, 0.5% Nonidet P-40) containing a protease inhibitor cocktail (Sigma P2714), and incubated at 4°C for 1 h, followed by centrifugation (9300 × *g*, 10 min). For H3K4me3, total cells or tissues were lysed in 50mM Tris pH6.8, 100mM DTT, 2% SDS, 0.1% bromophenol blue, 10% glycerol, and quantified by eye. Western blotting was performed following a standard protocol. Blots were probed with the following antibodies: anti-pStat3 (Tyr705) (Cell Signaling Technology #9138S), anti-Stat3 (Cell Signaling Technology #12640S), anti-Pgr (Dako #A0098), anti-beta-actin (Abcam ab6276), anti-Bmp2 (Peprotech #500-P195), anti-H3K4me3 (Abcam ab1791), anti-H3 (Abcam ab1791). Horseradish peroxidase-conjugated secondary antibodies were from Bio-Rad. Detection was carried out with enhanced chemiluminescence reaction (GE Healthcare RPN2209) using standard X-ray films. Band intensities were quantified using ImageJ software.

2.13 Leukocyte flow cytometry analysis

Preparation of single cell suspensions and FACS analysis were performed by Jens Kieckbusch (Colucci lab, Cambridge) as per established protocols. Briefly, mesometrial poles of E10.5 implantation sites were dissected, pooled and minced and tissue homogenates digested with Liberase TM (Sigma 05401119001). Cells were typed with fluorochrome-conjugated antibodies for CD45 (30-F11), NK1.1 (PK138), CD11b (M1/70), CD49a (HMα1), CD49b (DX5), I-A/I-E (M5/114.15.2), Gr-1 (RB6-8C5), F4/80 (BM8), CD11c (N418), CD3ε (145-2C11), NKp46 (29A1.4) and Eomes (Dan11mag) purchased from BD PharMingen, BioLegend or eBioscience. For intracellular and intra-nuclear antigens, Fix & Perm and Foxp3 staining buffer set (both eBioscience) were used, respectively. Cells were acquired on an LSRFortessa.

2.14 Statistical analysis

Statistical analyses including ANOVA and student's t-test were carried out using Graphpad Prism software, unless otherwise stated. Coefficient of variation data was analysed by one way ANOVA followed by Tukey's post-hoc test (performed by AS-P). QPCR and 5mC

distribution experiments were analysed by one-way ANOVA followed by Tukey's post-hoc test when more than 2 groups were compared, and by two-tailed t-test when only 2 groups were compared (performed by LW). Deciduoma assay was analysed by two-tailed t-test (performed by XW). Proliferation assays were analysed by two-way ANOVA followed by Holm-Sidak's multiple comparisons test (performed by AS-P). Western blot data was analysed by one-way ANOVA followed by Holm-Bonferroni's post-hoc test (performed by AS-P). The significance of overlaps between RNA-seq and microarray data, and between ChIP-seq and *Pgr*/*Esr1* binding site data were determined by Fisher's exact test in R. P-value is denoted as follows: $p<0.05$ (*), $p<0.01$ (**), $p<0.001$ (***).

Chapter III
Developmental consequences of pregnancy in advanced maternal age

3.1 Introduction

Advanced maternal age in humans is associated with infertility, an increase in fetal developmental abnormalities including fetal growth restriction, and increased risk of a spectrum of pregnancy complications known as the "Great Obstetrical Syndromes". The same pattern has been previously described in ageing mice, where maternal age correlates with reduced litter size and decreased post-implantation fetal viability (Holinka et al., 1979; Talbert, 1971). Embryos from older mothers are also at a significantly increased risk of developmental abnormalities including fetal growth restriction, heart and brain malformations, and of undergoing fetal resorption (Holinka et al., 1979; Kidd et al., 1993; Lean et al., 2017; Lopes et al., 2009). Therefore, ageing mice reflect similar aspects of the effects of maternal age on reproductive outcome as those observed in humans. As such they seem an adequate model system in which to investigate the fetal developmental abnormalities that arise in pregnancies complicated by advanced maternal age, despite the known differences in endometrial cycle between both species.

The reproductive life-span of C57BL/6 (B6) female mice begins at 5-6 weeks of age, when they reach sexual maturity (B. Anne Croy, 2013) and enter the mouse reproductive cycle, termed the estrous cycle. The B6 estrous cycle is 4-5 days in length, and consists of 4 stages; proestrus, estrus, metestrus, and diestrus. Estrous cycles tend to become unpredictable and less frequent, and to increase in length after 12 months of age (Nelson et al., 1982). The B6 reproductive life span is relatively long, and females can often enter estrous and achieve pregnancy beyond 12-15 months of age, however the number of viable pups per litter decreases as maternal age increases (Patel et al., 2017; Talbert, 1971).

As mentioned earlier, maternal age-related abnormalities in embryonic development and embryo resorption, could be caused either by age-related defects in the maternal oocyte, or the uterus. Oocytes obtained from the ovaries of older mice have a significantly higher incidence of aneuploidy which reduces the success of blastocyst formation (Merriman et al., 2012; Pan et al., 2008). For example, one study found that the proportion of super-ovulated oocytes which were aneuploid increased from 2.9% in 1 month old mice, to 37.5% in 12 month old mice (Merriman et al., 2012). It is however unlikely that developmental defects in the offspring of aged mice are entirely caused by aneuploidy in the oocyte, as most aneuploidies are not viable and lead to embryonic death and resorption in the early stages of pregnancy. The particular developmental defects associated with advanced

maternal age - fetal growth restriction, and cardiac and vascular defects - have also been linked to abnormal development and function of the placenta (Linask, 2013; Perez-Garcia et al., 2018; Salafia et al., 2006). In line with this, a study in 2009 showed that advanced maternal age was accompanied by both embryonic defects – cardiac malformations and growth restriction – and abnormal placentation (Lopes et al., 2009). In this study, Lopes et al analysed the gross morphology of a small number of implantation sites at mid-gestation by Haematoxylin and Eosin staining (H&E), reporting that advanced maternal age was associated with increased thickness of the TGC layer, and, in a few cases, impaired labyrinth formation. This study remained largely superficial, looking only at gross morphological defects of the embryo and placenta in a small number of aged pregnancies. Taking this as further evidence of the link between advanced maternal age and placental abnormalities, I endeavoured in this PhD project to investigate in depth the effect of maternal ageing on placental development, and the mechanism giving rise to pregnancy defects.

3.2 Results

3.2.1 Advanced maternal age is associated with abnormal embryo development

It has long been known that advanced maternal age is accompanied by a decline in fertility (Speroff, 1994), however the precise underlying reasons for this have not been elucidated. Oocyte numbers stay unaffected up until at least 1 year of age in the mouse, thus not contributing to fewer offspring numbers. Therefore, we set out to systematically investigate the reproductive decline that is observed in C57BL/6 (B6) females with advanced age. A total of 40 pregnancies were assessed in B6 females ranging from 42-52 weeks of age (Fig 3.1a) (Table 1) at E11.5. This time point was chosen because mid-gestation (i.e. ~E10.5) is a bottleneck for developmental progression in the mouse due to the necessary switch from yolk sac nutrition to requiring a functional placenta by this time point. Thus, E11.5 litters would reveal the detrimental effects of placental failure.

The average number of implantation sites at E11.5 (including resorptions) was not affected by maternal age (Fig 3.1b), however, significantly more embryos were developmentally abnormal in E11.5 litters from aged mothers (“aged litters”) than in those from young mothers (“young litters”) (Fig 3.1a, c).

While young litters were relatively homogeneous, we observed significant variability in terms of developmental progression in aged litters. We also observed frequent developmental abnormalities including growth restriction, cardiac edema, vascular defects, and brain and neural tube closure defects (Fig 3.1a). To quantify the developmental variability, we used crown-rump length measurements as a proxy. This confirmed that aged litters are significantly more variable in their development than young litters (Fig 3.1d).

Table 1 – Developmental outcomes of embryos derived from young females (8-12 weeks), aged females (42-52 weeks). Figures in brackets are total number of embryos in each category.

	Young Female	Aged Female
n	97	185
normal	93.8% (91)	41.6% (77)
abnormal	2.1% (2)	37.8% (70)
resorption	4.1% (4)	20.5% (38)

While some embryos were normal in size and comparable to the developmental stage of embryos from young litters, there was an increase in the number of growth-retarded embryos, and embryos undergoing resorption in aged litters (Fig 3.1c). On average, aged litters contained fewer normal embryos, with a concomitant increase in embryos which were abnormal or undergoing resorption (Fig 3.1c). 93.8% of embryos from young litters were normal, compared to only 41.6% of those from aged litters. Only 2.1% of embryos from young litters displayed gross abnormalities, whereas 37.8% from aged litters were abnormal, and the incidence of resorption increased from 4.1% in young litters to 20.5% in aged litters (Fig 3.1c, Table 1).

Whilst developmentally abnormal embryos and resorption sites were commonly seen in matings between aged mothers and young stud males; these defects were extremely uncommon when young females were mated either with young males, or old males at 52 weeks of age (Fig 3.1a). This demonstrates that the root of the developmental abnormalities in these embryos can be attributed to the aged maternal reproductive system, whereas the aged paternal system does not have a clear effect on gross development of the embryo.

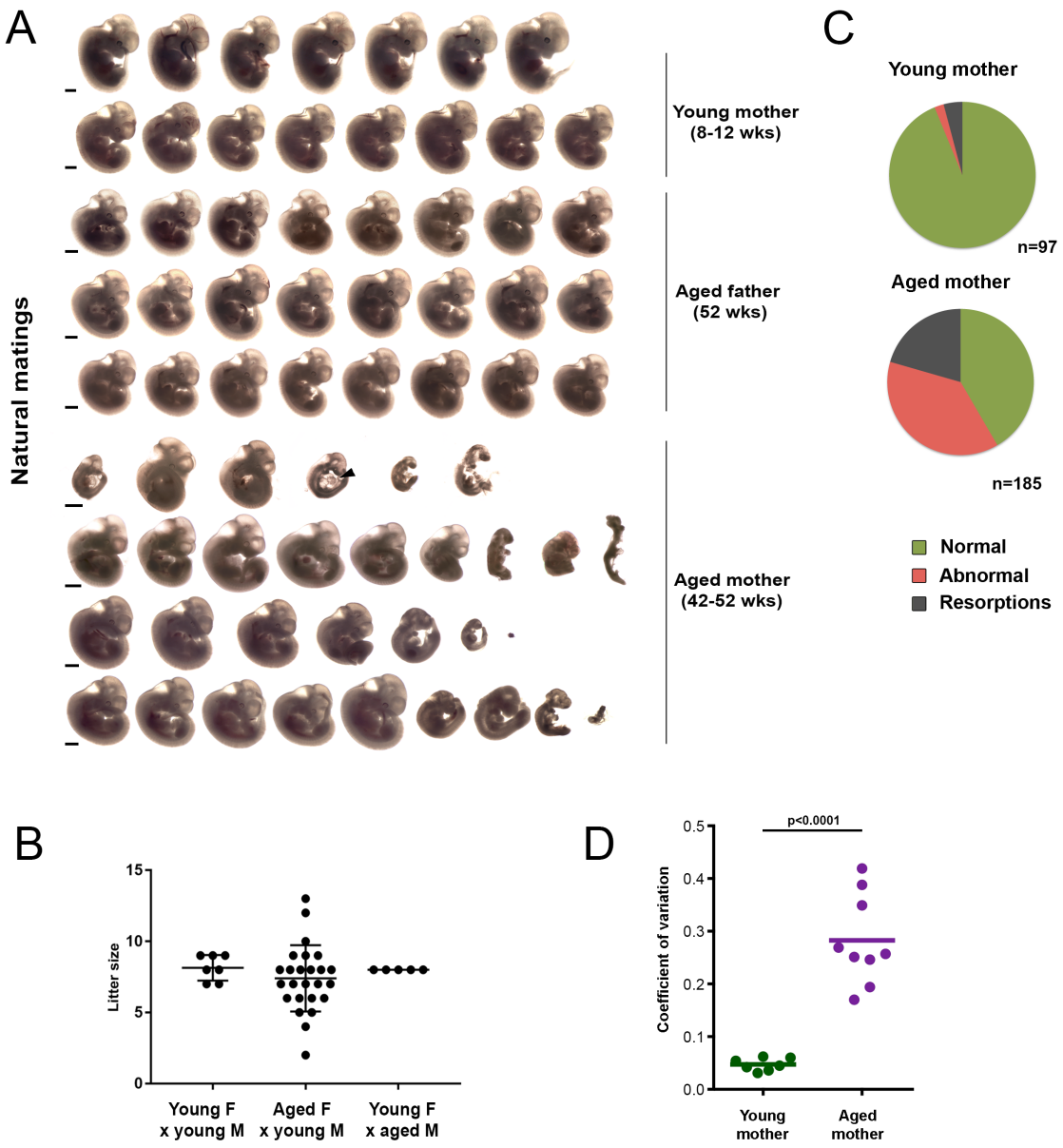

Figure 3.1 - Congenital abnormalities in litters from old mothers

a) Gross morphology of embryos at E11.5 of pregnancy in matings between young females (8-12 weeks) and young males, young females mated with aged males (52 weeks), and aged females (42-52 weeks) with young males. Each row represents one litter. Arrowhead points to cardiac malformation in the embryo. Scale bars 1mm. (Matings performed by BSU, dissection performed by MH).

b) Number of implantation sites present at E11.5 in litters from matings between young females (F) and young males (M), aged females and young males, and young females and aged males, including resorptions. Each point represents one litter. Mean +/- S.E.M..

c) Pie charts showing the mean percentage of embryos in litters from young mothers and aged mothers which are morphologically normal, abnormal, or undergoing resorption at E11.5 of pregnancy.

d) Dot plot showing developmental variability within litters from young and aged mothers at, displayed as coefficient of variation. Fully resorbed sites were omitted. Coefficient of variation was calculated from crown-rump length measurements of each embryo in a litter at E11.5, each point represents the coefficient of variation in one entire litter. Statistical analysis was by ANOVA followed by Tukey's multiple comparisons post-hoc test, performed by AS-P.

3.2.2 Advanced maternal age is accompanied by abnormal placentation and trophoblast differentiation

Interestingly, many of the developmental abnormalities that were associated with advanced maternal age, such as fetal growth restriction, developmental retardation and heart and brain defects have been shown to be linked to defects in placentation (Linask, 2013; Perez-Garcia et al., 2018; Salafia et al., 2006). Therefore, we analysed the morphology of each placenta from 3 entire aged litters alongside their accompanying embryos, by haematoxylin and eosin (H&E) staining (Fig 3.2a), to investigate whether developmental abnormalities of the embryo proper correlated with defects in placental development. In every case assessed we found that an abnormal embryo was associated with an abnormal placenta, whereas embryos that appeared morphologically normal also had grossly normal placentas (Fig 3.2a).

The extent of placental abnormality appeared to correlate with the severity of the embryonic defect. Embryos which were only slightly growth restricted, or presented with minor heart or brain defects had placentas with minor abnormalities in size, shape, or orientation of the placenta, or a reduced labyrinth compartment. By contrast, those embryos which were severely growth restricted or undergoing resorption exhibited a dramatically abnormal placental morphology, in particular a severely reduced expansion, or complete lack of the labyrinth layer (Fig 3.2a). *In situ* hybridisation for the TGC marker *Prl2c2* (*Plf*) was used to demarcate the boundary between fetal trophoblast and the maternal decidua (Fig 3.2a). This staining highlighted the variability in size reduction of the fetal labyrinth compartment in conceptuses of varying abnormality, as well as indicating a disproportionate overabundance of TGCs in relation to the remaining trophoblast

compartment in severely abnormal conceptuses. These age-related defects in trophoblast development prompted me to further characterise the progression of differentiation of the various trophoblast cell types in the aged placenta by RT-qPCR. Placentas were designated as young (Y, n=3), aged normal (An, n=3), or aged abnormal (Aa, n=3), determined by the gross morphology of the placenta and associated embryo, and were separated into these groups for analysis. Aa placentas showed significantly increased expression of the trophoblast stem (TS) cell marker *Eomes*. *Esrrb*, and *Elf5* were also increased, but did not reach significance (Fig 3.2b). This was accompanied by downregulation of the intermediate trophoblast/spongiotrophoblast (SpT) and syncytiotrophoblast (SynT) markers *Tpbpa* and *Synb*. The expression of TGC marker *Prl2c2* (*Plf*) was increased with age although this did not reach significance. Overall, the expression of TGC markers was increased and more variable in Aa trophoblast (Fig 3.2b). Interestingly, An trophoblast also exhibited differences in trophoblast marker expression, albeit to a lesser extent than trophoblast from Aa conceptuses (Fig 3.2b). This suggests that all placentas from aged mothers experience some level of de-regulated trophoblast differentiation, even if trophoblast abnormalities were not overtly obvious by gross morphological appearance.

As discussed in Chapter 1 (Fig 1.6), trophoblast differentiation can progress down two major routes, allowing TS cells to become either SynT which makes up the majority of the labyrinth, or towards the SpT and TGC lineages. Differentiation down these routes behaves antagonistically. In the case of aged females, preferential differentiation down the TGC route comes at the expense of the alternative SynT pathway (Fig 3.2c). This failure of SynT differentiation reflects the morphologically clear deficit in labyrinth formation with advanced maternal age. Failing labyrinth development likely underpins the observed embryonic developmental defects, particularly fetal growth restriction, as the labyrinth layer is responsible for all nutrient and gas exchange at the feto-maternal interface.

Not only were lineage markers differentially expressed in trophoblast from aged pregnancies, some were also considerably more variable, indicating that the morphological variability in placental development is reflected at the molecular level (Fig 3.2a, b). Interestingly, the TS cell markers *Eomes*, *Esrrb*, and *Elf5* were up-regulated, while another TS marker *Cdx2* tended to be down-regulated in Aa trophoblast (Fig 3.2b). Cells expressing these markers are unlikely to be true TS cells at this time, as TS cells can only

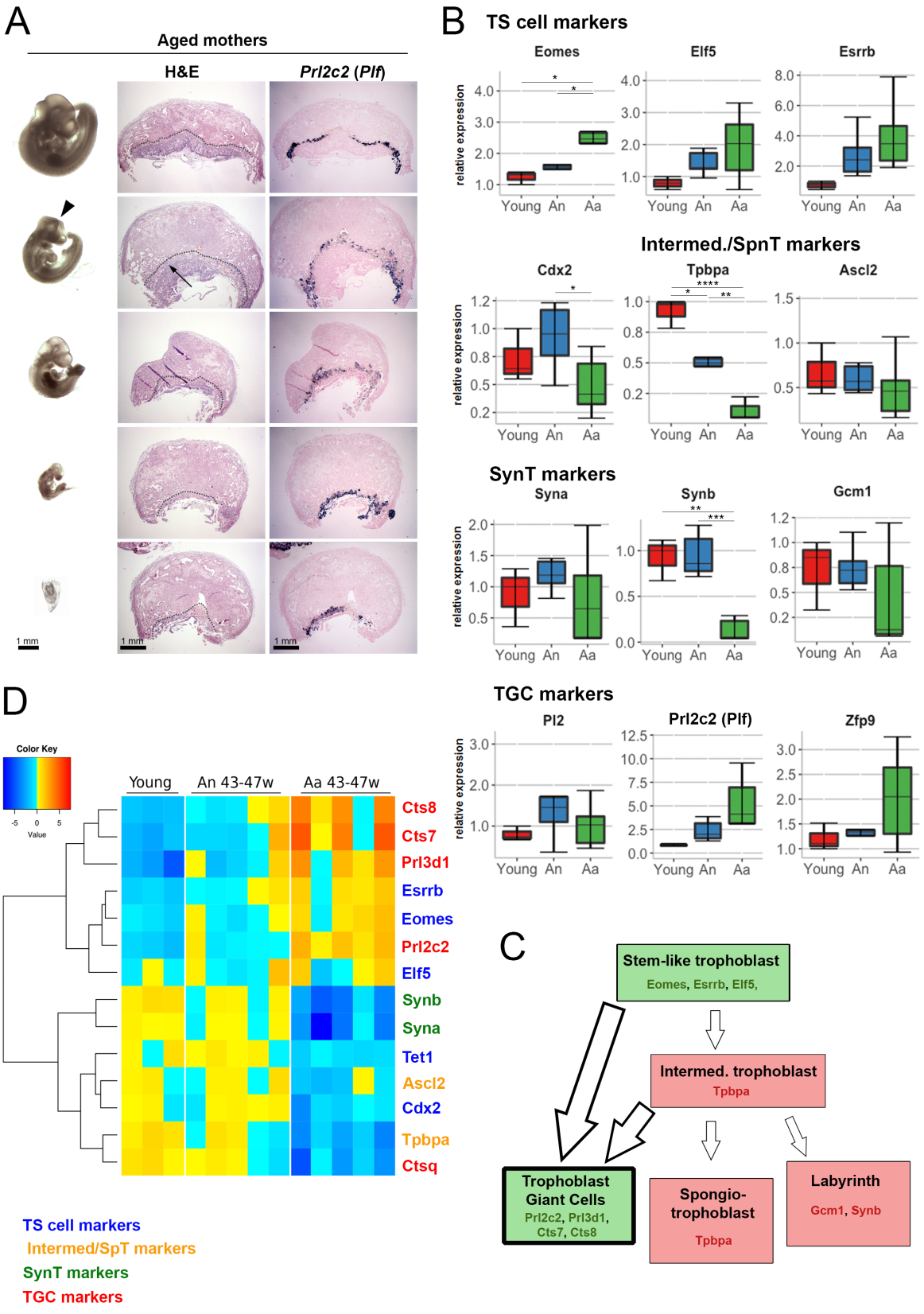
A
Aged mothers
H&E
Prl2c2 (Plf)
1 mm
B
TS cell markers
Eomes
Elf5
Esrrb
relative expression
Young An Aa
Intermed./SpnT markers
Cdx2
Tpbpa
Ascl2
SynT markers
Syna
Synb
Gcm1
TGC markers
Pl2
Prl2c2 (Plf)
Zfp9
C
Stem-like trophoblast
Eomes, Esrrb, Elf5,
Intermed. trophoblast
Tpbpa
Trophoblast Giant Cells
Prl2c2, Prl3d1, Cts7, Cts8
Spongio-trophoblast
Tpbpa
Labyrinth
Gcm1, Synb
D
Color Key
Value
Young
An 43-47w
Aa 43-47w
Cts8
Cts7
Prl3d1
Esrrb
Eomes
Prl2c2
Elf5
Synb
Syna
Tet1
Ascl2
Cdx2
Tpbpa
Ctsq
TS cell markers
Intermed/SpT markers
SynT markers
TGC markers

Figure 3.2 - Placental abnormalities in litters from old mothers

a) Gross morphology of embryos and their accompanying placentas in one entire litter from an aged mother at E11.5. Placentas in the LH column were stained with Haemotoxylin and Eosin, dotted line demarcates the junction between trophoblast and decidua. Placentas in the RH column were stained by immunohistochemistry for *Prl2c2 (Plf)* mRNA. Arrowhead indicates defect in forebrain development. Arrow indicates skewed direction of implantation. (Matings performed by BSU, dissection and histology performed by MH, and LW).

b) Boxplots showing relative expression of trophoblast lineage markers in trophoblast from young mothers (n=3), aged mothers where the embryo was grossly normal (An, n=6) or abnormal (Aa, n=6) (all mated to young males). *p<0.05, **p<0.01, *** p<0.001. Statistical analysis was by one-way ANOVA, followed by Tukey's multiple comparisons post-hoc test. Error bars are S.E.M.

c) Model of trophoblast differentiation defects in aged pregnancies. Colour of boxes indicates the direction of gene dysregulation as found by RT-qPCR or RNA-seq, green = up-regulated in aged, red = downregulated in aged.

d) Heatmap showing expression of trophoblast lineage markers in E11.5 trophoblast from young, aged normal (An), and aged abnormal (Aa) pregnancies. Colour of gene name

be derived from extra-embryonic tissues up to E8.5 of development (Tanaka et al., 1998; Uy et al., 2002). However, Eomes-positive cell clusters are retained in the placenta until post-mid-gestation (Wu et al., 2003). Hence it is possible that the up-regulation of markers commonly regarded as "stem cell" genes reflects a failure of trophoblast progenitor cells to differentiate at normal rates and in the correct temporal dynamics.

I confirmed the dysregulation of trophoblast marker expression in aged placentas by RNA-sequencing (RNA-seq) analysis, showing upregulation of TS cell and TGC markers, accompanied by downregulation of SpT and SynT markers (Fig 3.2d). There were slight differences in expression patterns between the 2 methods, which may be due to differences in sample preparation. RNA-seq was performed on RNA extracted from the fetal part of the placenta only, with the decidua dissected away, whereas RT-qPCRs were performed on RNA from whole placentas consisting of both fetal and maternal portions.

The RNA-seq data also portrayed a global picture of the trophoblast transcriptome at E11.5. Young control trophoblast samples were obtained from 8 week old mothers (n=3). In

order to capture the differences between morphologically normal and abnormal conceptuses, pairs of samples were taken from 5 pregnancies in 43-47 week old mothers, where one littermate was morphologically normal (An, n = 5), and the other abnormal (Aa, n = 5). Principal component analysis (PCA) showed that the samples cluster into 2 main groups, with young and An trophoblast clustering closely together, while Aa samples lie considerably removed along PC1 which represents the largest proportion of the variation between the datasets (Fig 3.3a).

DESeq2 and the intensity difference filter in SeqMonk were applied to identify genes which were strongly and consistently differentially expressed in Aa trophoblast. I focussed on the differences between young and Aa samples, as PCA analysis suggested that this is where the most striking differences would be found. This stringent approach identified 42 genes that were differentially expressed with age, 21 of which were up-regulated and 21 down-regulated in trophoblast from aged females (Fig 3.3b) (Appendix, Supplementary table 1). Notably, this list included a number of placenta specific genes, including those in the prolactin family, as well as pregnancy-specific glycoproteins (*Psg*), carcinoembryonic antigen-related cell adhesion molecules (*Ceacam*), and cathepsins (*Cts*) (Fig 3.3b). Syncytin b (*Synb)* was significantly down-regulated in trophoblast from aged mothers, confirming the RT-qPCR results (Fig 3.3b, Fig 3.2b). Gene ontology (GO) analysis performed on all differentially expressed genes (i.e. differentially expressed by either DESeq2 $p<0.05$, or intensity difference $p<0.05$) showed that maternal age-related genes were enriched for terms relating generally to pregnancy, and hormones, as well as several functions and properties of TGCs, such as collagen degradation, focal adhesions, and positive regulation of angiogenesis (Fig 3.3c) (Hemberger et al., 2003; Katz, 1995; Parast et al., 2001). This list was also significantly enriched for genes involved in positive regulation of the Erk signalling pathway, which maintains the expression of key transcription factors in TS cells (Latos et al., 2015) (Fig 3.3c). These results add weight to the finding that trophoblast development is perturbed in aged pregnancies, characterised by abnormal gross morphology of the trophoblast, and abnormal maintenance of TS marker expression. This is coupled with preferential differentiation of the remaining cells to the TGC lineage at the expense of SynT,

confirming maternal age-related restriction of the labyrinth on a morphological and molecular level (Fig 3.2c).

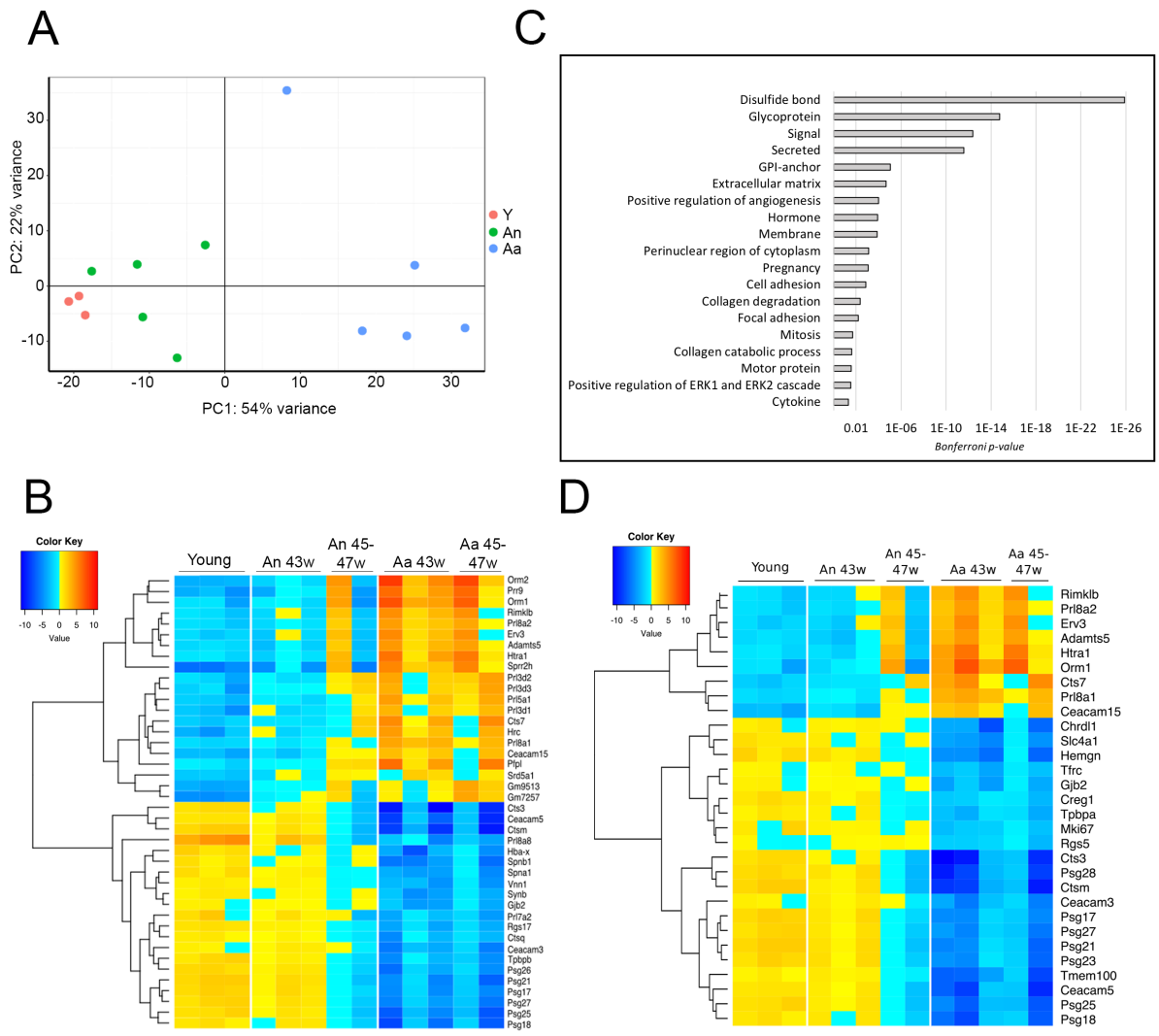

Fig 3.3 - RNA-seq analysis of E11.5 trophoblast from young and aged pregnancies

a) Principal component analysis (PCA) of RNA-seq data from E11.5 trophoblast in young (Y), aged normal (An) and aged abnormal (Aa) pregnancies. Each point represents one samples.

b) Heatmap showing expression of 42 genes which are significantly differentially expressed between young and Aa trophoblast. Differentially expressed genes were identified by both DESeq2 ($p<0.05$) and intensity difference ($p<0.05$).

c) Gene ontology annotations enriched in genes differentially expressed between young and Aa trophoblast (*Bonferroni* $p<0.05$). Differentially expressed genes were identified by either DESeq2 ($p<0.05$) and intensity difference ($p<0.05$).

d) Heatmap showing genes significantly differentially expressed between An and Aa trophoblast. Differentially expressed genes were identified by both DESeq2 ($p<0.05$) and intensity difference ($p<0.05$).

Genes which were differentially expressed between young and Aa trophoblast were also dys-regulated - albeit to a lesser extent - in An placentas, despite their grossly normal appearance on the morphological level (Fig 3.3b). Interestingly this subtle transcriptional de-regulation was only seen in trophoblast from mothers aged 45 weeks or more, and not in those aged 43 weeks. This suggests that the impact of advanced maternal age on trophoblast gene expression in normal conceptuses changes rather dramatically between 43-45 weeks of age.

This observation indicates that in pregnancies with females aged 45 weeks and over, all conceptuses exhibit perturbations in trophoblast gene expression. However, this only leads to developmental abnormalities of the embryo and placenta in a subset of cases when analysed by H&E staining and *in situ hybridisation* for the TGC marker *Prl2c2* (Fig 3.2a). It may be that some conceptuses are able compensate for the effects of advanced maternal age and are therefore less susceptible to developmental abnormalities. Alternatively, it is also possible that more subtle defects are present which cannot be detected by gross morphological analysis alone, or that embryos which are normal at E11.5 will go on to develop abnormalities later in gestation. I next compared An versus Aa trophoblast in order to identify differentially expressed genes which may reflect adaptations of the trophoblast to pregnancy in advanced maternal age in An trophoblast. This identified 29 differentially expressed genes which were dys-regulated in An trophoblast from 45-47 week old mothers, compared to young (Fig 3.3d). However, all the genes which were differentially expressed between young and An trophoblast were also dys-regulated in Aa samples (Fig 3.3d), suggesting these genes are differentially expressed as a result of abnormal trophoblast development and not due to adaptations which promote normal development in An conceptuses.

3.2.3 The aged maternal environment underlies reproductive decline in advanced maternal age

The above results suggested that high levels of developmental abnormalities, growth restriction, and resorptions in aged pregnancies are related to defects in placental development. As mentioned previously these defects could occur as a result of age-related deterioration of either the oocyte, or the maternal reproductive tract. Although most studies have focused on oocyte related defects such as aneuploidy and mitochondrial function, some have suggested that the ageing uterus may also play a role (Talbert and Krohn, 1966).

In mice, most chromosomal aberrations are incompatible with development to term and conceptuses die during early pregnancy. Therefore, aneuploid embryos tend to be resorbed in the early stages of pregnancy. In aged pregnancies there were relatively few empty implantation sites resulting from early embryonic demise compared to the number of more developed embryos, suggesting that the majority of conceptuses from aged litters developed beyond this period of early pregnancy (Fig 3.1a). Therefore, it is unlikely that the gross morphological defects observed in litters from aged females result from age-related karyotypic defects in the oocyte and may instead be attributed to the aged uterine environment. To confirm the absence of aneuploidies in the conceptuses analysed in section 3.2.2, I performed an e-karyotyping analysis as described by (Weissbein et al., 2016) on the trophoblast RNA-seq data. This technique is able to detect whole chromosome monosomy and trisomy which are commonly observed in aged pregnancies. This suggested that all conceptuses analysed from aged pregnancies were karyotypically normal, and therefore any observed defects were not due to large scale chromosomal aberrations in the oocyte. This analysis may not however detect small scale chromosomal abnormalities, genetic mutations, or DNA damage which may affect the offspring of older mothers.

We then performed embryo transfer experiments in order to delineate whether the maternal age-related defects in embryo and placental development were intrinsic to the oocyte, or related to the ability of the aged uterus to support pregnancy. Preimplantation blastocysts were isolated from aged mothers at E2.5 and transferred to pseudo pregnant 8-10 week old ‘young’ recipients (A->Y). Embryos from young mothers were transferred into young recipients in parallel, as a control (Y->Y). The A->Y transfer rescued a large proportion of the maternal age associated embryonic defects (Fig 3.4a), with striking reductions in the

incidence of embryonic defects from 37.8% to 12.2%, and embryo resorption from 20.5% to 14.6% (Fig 3.4b, Table 2). Placental development also largely returned to normal in A->Y transfer conceptuses when compared with the clear variability and gross abnormalities observed in those which developed in the uterine environment of aged mothers (Fig 3.4c, 3.2a). In line with this visual appearance of developmental rescue, the variability in crown-rump length within each litter was significantly reduced in A->Y transfers compared to aged litters, and indeed was not significantly different from Y->Y transfers or young controls (Fig 3.4d).

Table 2 – Developmental outcomes of embryos derived from young females (8-12 weeks), aged females (42-52 weeks), and embryo transfers. Y->Y, embryos derived from young females and transferred to young surrogates. A->Y, embryos derived from aged females and transferred to young surrogates. Figures in brackets are total number of embryos in each

	Young Female	Aged Female	Transfer Y->Y	Transfer A->Y
n	97	185	42	41
normal	93.8% (91)	41.6% (77)	83.3% (35)	73.2% (30)
abnormal	2.1% (2)	37.8% (70)	9.5% (4)	12.2% (5)
resorption	4.1% (4)	20.5% (38)	7.1% (3)	14.6% (6)

In 1966, Talbert and Krohn performed similar experiments, transferring embryos derived from aged mothers into young recipients, and in line with our findings saw that embryos from aged donors were able to successfully develop in a young host uterus. However, this study did not analyse placental development in the resulting conceptuses. It also failed to take into account the effect of parity, which can impact on embryo survival, and fetal and placental weight (Gosden, 1979; Hetherington, 1972), as a number of donor and recipient mice had undergone previous pregnancies. The results I have presented build on this study, confirming that advanced age of the donor does not preclude successful development of the embryo in a young primiparous recipient. My findings provide evidence that placental abnormalities in litters from aged mothers are induced by an age-related decline of the maternal uterus and not the oocyte.

Talbert and Krohn also performed the reciprocal experiment transferring young donor embryos into aged recipients (Y->A) and found that this induced embryonic defects in the resulting litters (Talbert and Krohn, 1966). We did not perform Y->A transfers, as the

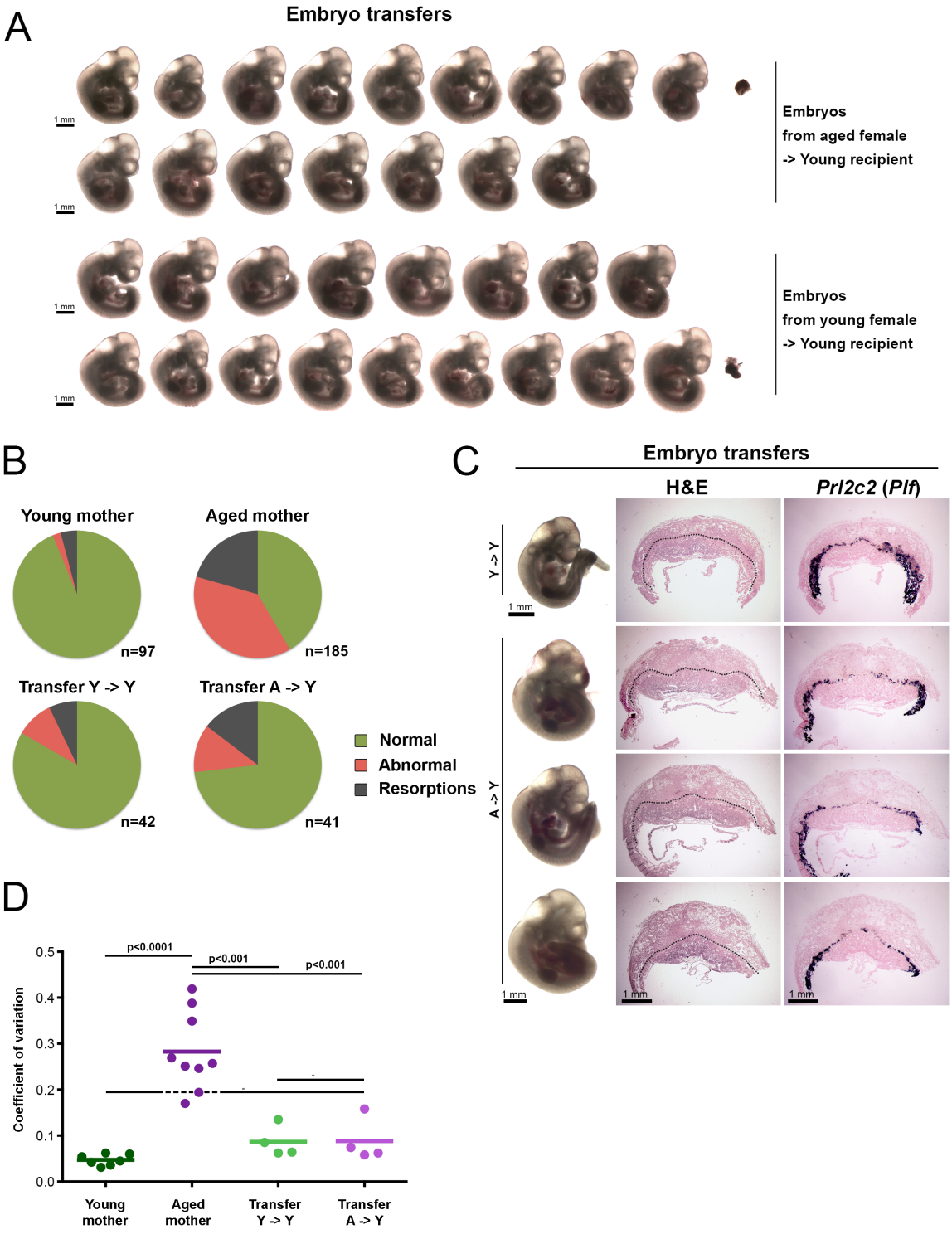

Figure 3.4 - Embryo transfer to a young surrogate rescues embryonic and placental defects of embryos from aged mothers.

a) Gross morphology of embryos at E10.5 after embryo transfer. Embryos were either isolated from a young mother and transferred to a young surrogate,or isolated from an aged mother and transferred to a young surrogate. Each row represents one litter. (Embryo transfer performed by BSU, dissection performed by MH).

b) Pie charts showing the mean proportion of embryos in litters from Y->Y and A->Y transfer pregnancies which are morphologically normal, abnormal, or undergoing resorption at E10.5 of pregnancy.

c) Gross morphology of embryos and their accompanying placentas from Y->Y and A->Y transfer pregnancies. Placentas in the LH column were stained with Haemotoxylin and Eosin, dotted line indicates the junction between trophoblast and decidua. Placentas in the RH column were stained by IHC for *Prl2c2 (Plf)* mRNA. (Dissection and histology performed by MH and LW).

d) Dot plot showing developmental variability within litters from young and aged mothers, and Y->Y and A->Y transfer pregnancies, fully resorbed sites were omitted. Coefficient of variation was calculated from crown-rump length measurements of each embryo in a litter at E11.5, each point represents the coefficient of variation in one entire litter. Statistical analysis was by ANOVA followed by Tukey's multiple comparisons post-hoc test, performed by AS-P. n.s. = not significant.

timing of mating and hence formation of the vaginal plug is extremely unpredictable in aged females. Therefore, it is difficult to successfully induce pseudopregnancy in a sufficient number of aged females on a given day, which needs to be synchronised with young pregnant females, in order to perform embryo transfers. Due to this significant technical difficulty, the number of animals required to obtain an appropriate sample size was deemed too large to justify this experiment, in light of the principles of the 3Rs (Prescott and Lidster, 2017). A more recent study by Schulkey et al in 2015 showed convincing evidence that transplant of ovarian tissue from young donors to aged recipients led to cardiac malformations in the offspring. As mentioned previously, such cardiac defects may in fact be secondary to abnormal placental development. This adds further weight to the hypothesis that these defects are caused by uterine ageing and not defects in the oocyte (Schulkey et al., 2015).

In addition to rescuing embryonic development, placental development was also grossly normal in conceptuses from A->Y transfer pregnancies (Fig 3.4c). When analysed by RT-qPCR and RNA-seq, the trophoblast compartment of A->Y transfers was transcriptomically indistinguishable from Y->Y transfers (Fig 3.5a, b). The 42 genes that were identified by RNA-seq as dys-regulated in aged trophoblast were not differentially expressed between A->Y and Y->Y trophoblast (Fig 3.5c, d).

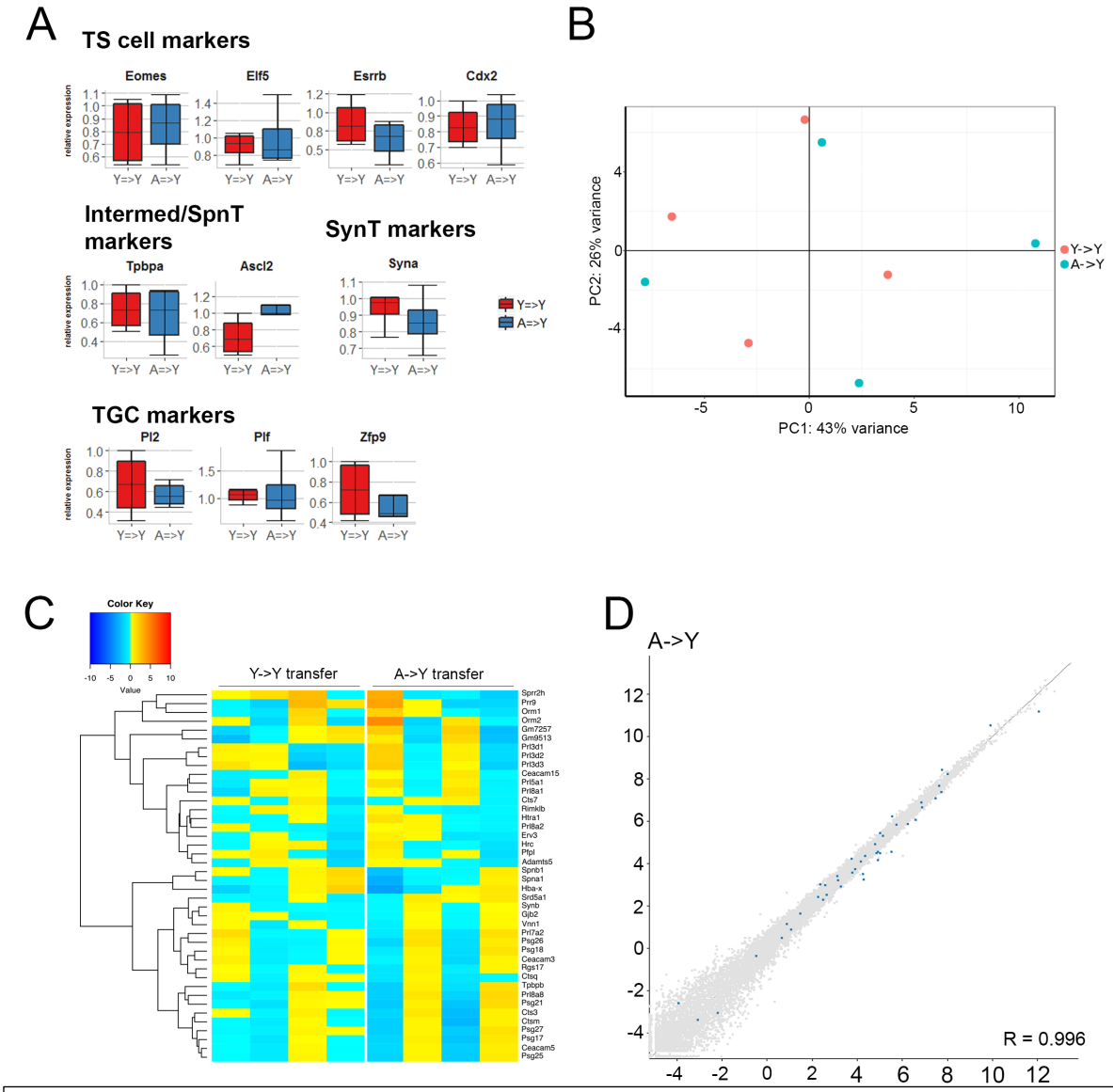

Figure 3.5 - Trophoblast differentiation defects are rescued in placentas from A->Y transfer pregnancies.

a) Boxplots showing relative expression of trophoblast lineage markers in trophoblast from Y->Y (n=4) and A->Y (n=4) transfer pregnancies. Statistical analysis is by two-tailed t-test ($p<0.05$).

b) PCA analysis of RNA-seq data from Y->Y and A->Y trophoblast at E10.5.

c) Heatmap showing expression of 42 genes differentially expressed between young and Aa trophoblast, in Y->Y and A->Y transfer trophoblast.

d) Scatter plot showing the expression of all genes in Y->Y and A->Y trophoblast. 42 genes differentially expressed between young and Aa trophoblast are highlighted in blue. R = Pearson correlation coefficient

In addition, no genes were identified as differentially expressed between trophoblast from Y->Y and A->Y transfer pregnancies by DESeq2. These results show that blastocysts from aged mothers are able to develop into grossly normal conceptuses, with transcriptomically normal placentas when allowed to develop in a young maternal environment. Therefore, the aged oocyte is not the main cause of gross embryonic and placental defects and developmental variability in the offspring of aged female mice. Instead, these data suggest that the abnormalities in embryonic and placental development in aged murine pregnancies are due to age-related changes in the maternal uterine environment.

3.2.4 Characterisation of aged decidua

Embryo transfer experiments showed that maternal age-related abnormalities in embryonic and placental development are not due to the oocyte, but are instead related to the quality of the maternal uterine environment. This prompted me to investigate gene expression in the decidua, the maternal portion of the placenta which is derived from the pregnant uterus. The decidua lies at the feto-maternal interface and is in direct contact with the trophoblast, with which it communicates extensively. Therefore, maternal age-related defects in trophoblast development may be a result of abnormal decidual function. In order to investigate this on a transcriptomic level, RNA-seq libraries were generated from the decidua of the same conceptuses analysed by RNA-seq in section 3.2.2. This includes deciduas from young mothers (n=6; 3 from the same conceptuses analysed in section 3.2.2 plus 3 additional controls), and from aged mothers where the accompanying embryo was grossly normal (An, n = 5), or abnormal (Aa, n=5). PCA analysis separated deciduas from aged pregnancies away from young along PC1, suggesting that they are transcriptomically distinct from each other (Fig 3.6a). Some aged samples, however, were more similar to young along PC1. These corresponded to deciduas from grossly normal conceptuses developed in aged mothers that were 43 weeks of age as opposed to 45 weeks or greater, suggesting that gene

expression in the decidua becomes considerably more dys-regulated as the mother gets older, similar to observations on the trophoblast side (Fig 3.6a).

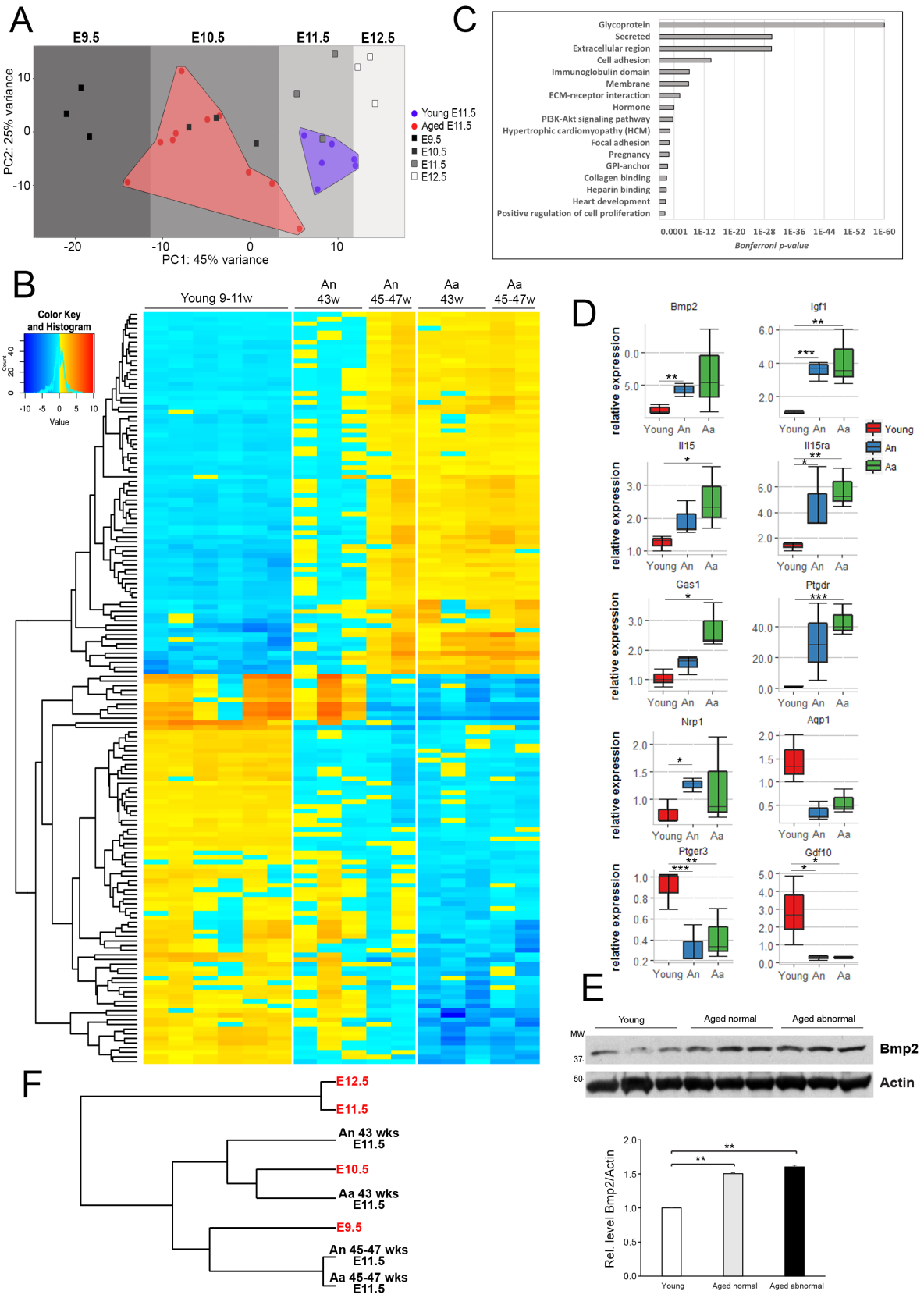

Figure 3.6 - Gene expression abnormalities in the decidua during pregnancy in aged females.

a) PCA analysis of RNA-seq data from deciduas from young and aged pregnancies at E11.5, and deciduas in a time-course of development from E9.5-E12.5.

b) Heatmap showing expression of 162 genes differentially expressed between young and Aa deciduas at E11.5. An = aged normal, Aa = aged normal. Young mothers were aged between 9-11 weeks, and aged mothers between 43-47 weeks. Differentially expressed genes were identified by both DESeq ($p>0.05$), and intensity difference ($p<0.05$).

c) Gene ontology annotations enriched in genes differentially expressed between young and Aa decidua. Differentially expressed genes were identified by either DESeq2 ($p<0.05$) and intensity difference ($p<0.05$).

d) Independent validation of differential expression of key decidualization genes in deciduas from young (n=6), An (n=5), and Aa (n=5) pregnancies. Statistical analysis is by one way ANOVA followed by Tukey's post-hoc test. *$p<0.05$, **$p<0.01$, ***$p<0.001$, error bars are S.E.M.

e) Confirmation of higher Bmp2 levels in deciduas from aged females. Protein levels of Bmp2 in 3 independent replicates of E11.5 deciduas from young, An, and Aa pregnancies by western blot. Level of Bmp2 was quantified relative to actin. Statistical analysis was by ANOVA with Holm-Bonferroni's post-hoc test, **$p<0.01$. (Western blot performed by V P-G, statistics performed by A S-P)

f) Closest neighbour analysis of global transcriptomes generated by RNA-seq, from E11.5 deciduas from An, and Aa pregnancies from mothers aged 43 weeks, or 45-47 weeks, and deciduas from young control females in a time-course of development from E9.5-E12.5 (red).

This is supported by differential expression (DE) analysis, which identified 162 genes that were differentially expressed between young and Aa deciduas (Fig 3.6b) (Appendix, Supplementary table 2). 78 genes were up-regulated, and 84 genes down-regulated in deciduas from older mothers. Gene ontology analysis showed that these genes are related to pregnancy and hormones, and are involved in processes important during decidualization such as cell proliferation, cell adhesion, collagen binding, heparin binding, and PI3K-Akt signalling (Fig 3.6c) (Covarrubias et al., 2015; Fabi et al., 2017; Fluhr et al., 2010; Wang et al., 2013). Interestingly, dys-regulated genes were also significantly enriched for the terms heart development and hypertrophic cardiomyopathy, suggesting that pathways involved in cardiac development are shared with decidual genes and may form an underlying basis for the link with heart defects in embryos from aged pregnancies. This pattern of gene expression was confirmed by RT-qPCR for genes known to be involved in

decidualization and/or expressed in the decidua (Fig 3.6d), such as *Bmp2* (Lee et al., 2007; Li et al., 2007; Paria et al., 2001), which was also confirmed at the protein level (Fig 3.6e).

In a similar way to the trophoblast, all deciduas from aged pregnancies that were tested exhibited an altered gene expression profile to some extent, even when the associated embryo was grossly normal (Fig 3.6a-b). Interestingly, and also similar to the picture in trophoblast, An embryos from 43 week old mothers had a less severely abnormal transcriptional signature, which lies in between that of young and An 45-47 week/Aa deciduas (Fig 3.6b). This suggests that the extent of decidual dysfunction varies between implantation sites from the same pregnancy, mirroring the variability that is observed in embryo development and trophoblast gene expression. The observation that the transcriptomes of decidua and trophoblast associated with normal embryos from 43 week old mothers were more similar to young controls, whereas those from 45-47 week old mothers were far more abnormal, is interesting. This observation raises the question of when in maternal ageing the decline in uterine function begins, and whether it progresses gradually or drops off suddenly between 43-45 weeks of age.

On closer inspection, the transcriptional signature of deciduas from aged pregnancies appeared to be reminiscent of an earlier stage of development. For example, in normal placentation, *Bmp2* expression peaks before mid-gestation and subsequently decreases, however its expression is increased in aged decidua compared to that in young samples (Fig 3.6d-e). A number of genes follow a similar pattern, suggesting that decidual development may be delayed in aged females. To explore this further, RNA-seq libraries were generated from normal, young deciduas in a time course of development from E9.5-E12.5. The expression profiles from E11.5 deciduas developed in young females correlate highly with the E11.5 time-course samples by PCA analysis, hierarchical clustering, and in their expression of the 162 age-related genes, whereas E11.5 deciduas from aged females corresponded more closely to E9.5 and E10.5 time-course samples (Fig 3.6a, f) (Appendix, Supplementary figure 1). This suggests that developmental progression of the decidua is delayed with advanced maternal age, causing deciduas from aged females to be developmentally up to 2 days behind those from young females at E11.5 of pregnancy.

Interestingly, a number of genes which were differentially expressed with age are involved in implantation and endometrial decidualization, processes required for development to proceed normally. For example, *Bmp2*, a critical regulator of decidualization

(Lee et al., 2007; Li et al., 2007), was up-regulated in aged deciduas (Fig 3.6d-e). In addition, expression of *Il15* and its receptor *Il15ra* which are recruitment factors for uterine natural killer (uNK) cells (Ashkar et al., 2003; Barber and Pollard, 2003; Croy et al., 2003) was significantly increased (Fig 3.6d), while expression of *Csf1*, a marker and recruitment factor of dendritic cells in the uterus, was decreased (Tagliani et al., 2011) (Fig 3.8d).

The maternal immune system is thought to play a significant role at the feto-maternal interface, and the perturbation of decidual immune cells can affect pregnancy. uNK cells are particularly important during mouse pregnancy, although their precise function is controversial as knockout models show variable phenotypes (Croy et al., 2003). Most consistently, uNK deficient models show that their absence leads to a deficit in the decidual bed characterized by hypocellularity and edema, and deficient spiral artery remodelling (Ashkar et al., 2000; Guimond et al., 1997). When analysed by *Dolichos Biflorus Agglutinin* (DBA) staining which marks uNK cells, there was no appreciable difference in the number and distribution of uNK cells in the young and aged decidua (Appendix, Supplementary figure 2).

To investigate this specialized immune cell type further, we utilised flow cytometry as a more sensitive and quantitative method to measure the composition of the immune cell population in the decidua at E10.5. Gating strategies separated decidual immune cells into the myeloid and lymphoid lineages, followed by further delineation into macrophages and dendritic cells, and into conventional CD49- and tissue resident CD49+ uNK cell subsets respectively (Fig 3.7 a, e). The absolute number of leukocytes per implantation site was significantly decreased in aged pregnancies, due to a decrease in the numbers of dendritic cells and macrophages, accompanied by decreased expression of the dendritic cell recruitment factor *Csf1* in aged deciduas (Fig 3.7b-d). In line with previous reports, the absolute number of NK cells, and the proportion of mature CD11b+ NK cells in the spleen of aged pregnant females was significantly decreased (Fig 3.7g) (Guo et al., 2014). However, this effect was not present in the uterus where the absolute number of uNK cells per implantation site was not significantly different between young and aged pregnancies (Fig 3.7f). The maturation of uNK cells was similarly unaffected, as was the proportion of uNK cells falling into the tissue-resident CD49a+ and conventional CD49a- subsets (Fig 3.7f).

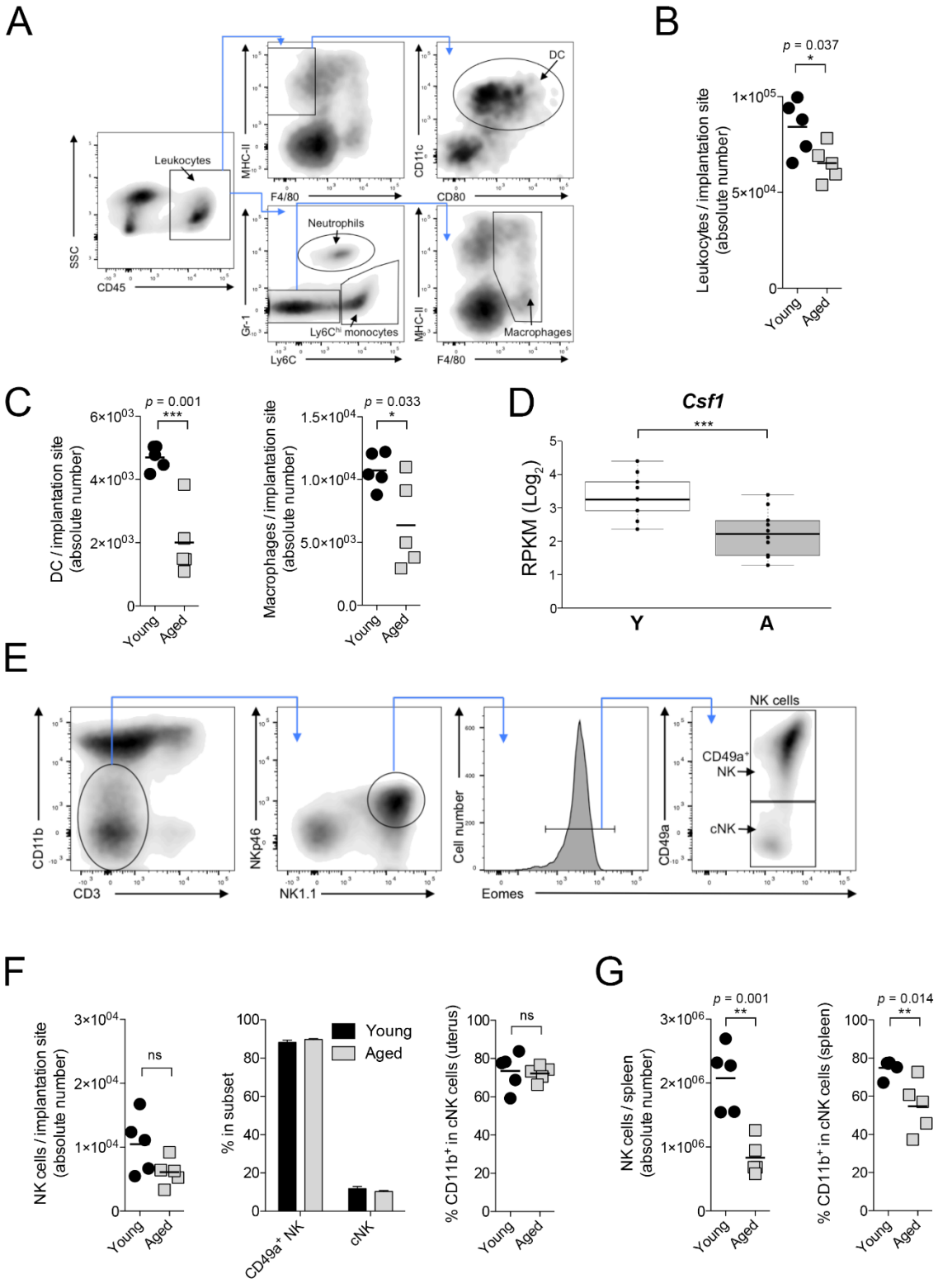
A
Leukocytes
SSC
CD45
MHC-II
F4/80
DC
CD11c
CD80
Neutrophils
Gr-1
Ly6C^hi monocytes
Ly6C
MHC-II
F4/80
Macrophages
B
p = 0.037
*
Leukocytes / implantation site (absolute number)
1×10^05
5×10^04
0
Young
Aged
C
p = 0.001
***
DC / implantation site (absolute number)
6×10^03
4×10^03
2×10^03
0
Young
Aged
p = 0.033
*
Macrophages / implantation site (absolute number)
1.5×10^04
1.0×10^04
5.0×10^03
0.0
Young
Aged
D
Csf1
***
RPKM (Log2)
5
4
3
2
1
0
Y
A
E
CD11b
CD3
NKp46
NK1.1
Cell number
Eomes
NK cells
CD49a
CD49a+ NK
cNK
F
NK cells / implantation site (absolute number)
3×10^04
2×10^04
1×10^04
0
ns
Young
Aged
% in subset
100
80
60
40
20
0
Young
Aged
CD49a+ NK
cNK
% CD11b+ in cNK cells (uterus)
100
80
60
40
20
0
ns
Young
Aged
G
p = 0.001
**
NK cells / spleen (absolute number)
3×10^06
2×10^06
1×10^06
0
Young
Aged
p = 0.014
**
% CD11b+ in cNK cells (spleen)
100
80
60
40
20
0
Young
Aged

Figure 3.7 - Altered leukocyte composition in the aged decidua at mid-gestation.

Flow cytometry and analysis performed by JK (Colucci lab, Cambridge)

a) Flow cytometry analysis of decidual leukocytes: gating strategy showing delineation of decidual cells into macrophages and dendritic cells. DC, dendritic cells.
b) Absolute number of leukocytes measured per implantation site.
c) Absolute numbers of DCs and macrophages per implantation site.
d) Expression levels of C*sf1,* a cytokine involved in DC maturation, determined by RNA-seq. Displayed by normalised read counts of young (Y, n = 9) and aged (A, n = 10) independent replicates.
e) Gating strategy used to delineate uNK (uterine natural killer) cells into resident CD49a+ and conventional CD49a- subsets.
f) Absolute number of uNK cells per implantation site, and relative abundance of tissue-resident and conventional subsets, as well as frequency of mature CD11b+ uNK cells.
g) Numbers and maturation of peripheral splenic NK cells in pregnant females. Each data point in b, c, f, and g represents an entire litter of one pregnant mouse, values in f) are means +/- SEM.

These results showed that uNK cells, the largest immune cell population in the decidua, were unaffected by advanced maternal age, whereas, dendritic cells and macrophages were decreased in number

3.3 Discussion

In this chapter, I have characterised the defects that occur during pregnancy in aged B6 females, and show that the majority of these defects arise as a result of abnormal placentation, mediated by an aged maternal uterine environment. A previous study by Lopes et al reported that advanced age in B6 females correlates with the development of gross morphological abnormalities of the embryo and placenta (Lopes et al., 2009), although this study lacked in-depth characterisation of placental defects. The data I have presented corroborate the observation that advanced maternal age is accompanied by defective embryonic and placental development, and for the first time characterized age-related abnormalities in the placenta in detail, at the transcriptomic level.

While maternal age dramatically affected gross embryonic and placental development, I found that there was no clear impact of paternal age in matings between young females and 12 month old males. This is in line with previous reports that advanced paternal age in rodents does not contribute to congenital malformations in the offspring (Parkening et al., 1988; Serre and Robaire, 1998). However, these studies found that paternal age of 24 months was associated with poor semen and sperm quality in C57BL/6 males, and pre-implantation loss, decreased fetal weight, and neonatal death in litters sired by male Brown Norway rats, suggesting that while 12 month old fathers do not adversely affect embryo development, there may be an effect when even older males are used.

In line with Lopes and colleagues, I found that embryonic defects were associated with abnormal placental development in pregnancies from aged females, as shown by the co-occurrence of embryonic and placental abnormalities. The observation that the severity of embryonic defects is paralleled by the severity in placental abnormalities also supports this idea, i.e. the most severe embryonic phenotypes were accompanied by very abnormal placentas. Less severely abnormal embryos had mild placental defects, and normal embryos were accompanied by grossly normal placentas. The main placental abnormality observed was a restriction of the labyrinth trophoblast compartment, and an relative overabundance of TGCs, as suggested previously by Lopes et al., 2009. I have confirmed this observation on the transcriptional level by both RT-qPCR and RNA-seq, showing that differentiation to the various trophoblast lineages is altered in placentas from aged pregnancies. This analysis shows that key TS cell markers *Esrrb*, *Eomes*, and *Elf5* are up-regulated in aged placentas at E11.5. Expression of these markers rapidly decreases on TS cell differentiation *in vitro*. Therefore, their persistence in aged placentas may reflect the continued presence of a population of trophoblast progenitor cells, although they are unlikely to be true TS cells at this stage of pregnancy (Tanaka et al., 1998; Uy et al., 2002). Maintenance of TS marker expression in aged trophoblast suggests a failure to properly exit the stem cell state and specify the various trophoblast lineages. Indeed, trophoblast from aged females expressed low levels of SynT and SpT markers at mid-gestation, indicating poor differentiation to these cell types. This is accompanied by over-representation of TGC lineage markers, and relative overabundance of TGCs themselves in the trophoblast compartment.

Trophoblast developing from the aged blastocyst is intrinsically normal, and indistinguishable from young counterparts when allowed to develop in a young maternal environment. It would be interesting to confirm this by derivation of TS cells from the aged

blastocyst to establish whether any changes that originate in the older oocyte, either genetic or epigenetic, have some minor impact on trophoblast proliferation or differentiation. It is also interesting to note that I detected gene expression changes in all aged samples including those in which the placenta and the embryo were seemingly normal, albeit these changes were much less pronounced in the An compared to the Aa group. This finding may be explained by (a) minor abnormalities that were not obvious by assessment of gross morphology and histology, (b) the possibility that sub-threshold mRNA expression changes have no overt effect on protein levels and/or on instructing trophoblast differentiation, or (c) that these placentas are prone to more obvious failure later on during development. This latter point is indeed supported by a recent study which shows that late fetal death up to E17.5 occurs more commonly in aged pregnancies, although this does not occur in every case as a number of fetuses remain viable at E17.5 (Lean et al., 2017).

One of the most interesting observations originating from this work is the striking developmental variability that exists within aged litters. Within a single litter the entire range of developmental outcomes was present, from normality, through mild to severe growth restriction, brain defects, and cardiac malformations, to complete embryo resorption. How is it that within a single litter, this entire range of abnormalities can be found? As I have shown, aged blastocysts are able to develop normally when transferred to a young surrogate mother, and therefore these defects must occur from a deficiency of the maternal environment during pregnancy. It does not seem likely that circulating steroid hormone levels are to blame - although ageing is accompanied by altered hormone levels - as they would be similar across all implantation sites, and a previous study found no correlation between plasma progesterone and the number of viable fetuses in litters from aged females (Holinka et al., 1979). It is possible that there are positional variations in the quality of the aged endometrium which may affect placentation at those sites, and this will be further investigated in Chapter 4. Another possibility is that some embryos are better able to adapt to age-related changes in decidual function than others, allowing the most adaptable to flourish whilst those that cannot adapt are resorbed, or develop abnormalities due to impaired placental development. If this was the case, then An trophoblast may exhibit beneficial adaptations in gene expression, which may be attributed to genes which are differentially expressed between An and Aa trophoblast and not between young and An. I could find no evidence of this in my RNA-seq data, however this hypothesis could be tested by co-culturing individual blastocysts *in vitro* with uterine stromal cells isolated from aged

females to measure the variation in their response to the aged uterine environment, as described by Teklenburg et al., in the context of recurrent pregnancy loss (Teklenburg et al., 2010).

However, the key data presented in this chapter highlight that the core failure in reproductive success in older female B6 mice resides with the mother, not the oocyte. This observation is strongly supported by several previous studies even if they did not investigate at the time how this comes to pass. Studies in the 1960s and '70s showed that the development of uterine deciduoma in response to mechanical stimulation of the endometrium is impaired in aged mice. This was one of the first suggestions that ageing of the uterus contributes to reproductive decline with advanced maternal age (Finn, 1966; Holinka and Finch, 1977; Shapiro and Talbert, 1974). Building on this, embryo transfer experiments showed that whilst the young uterus is able to support development of embryos from old donors (which my data confirm), transplants of young embryos to old recipient mothers are less successful (Talbert and Krohn, 1966). This study did not take into account the effect of parity on reproductive ageing, and both primiparous and multiparous mothers were used, potentially confounding the effect of maternal age (Baser et al., 2013; Gosden, 1979; Kalogiannidis et al., 2011). Although these studies highlighted the role of the uterus in reproductive ageing, no effort has since been made to fully characterise, and mechanistically unravel the basis of uterine ageing.

My data show that maternal ageing leads to major disturbances in the decidual compartment, which derives from the maternal endometrium and is instrumental in supporting normal placental development. Hence, I hypothesise that maternal age-related defects in placentation stem from a deficiency in the decidua, affecting cell communication at the feto-maternal interface. I have shown that development of the trophoblast is abnormal in the context of an aged maternal system, and, given the extensive communication at the feto-maternal interface, it is likely that ageing disrupts signalling between the maternal decidua and fetal trophoblast. This may lead to the disruption of appropriate trophoblast differentiation in aged pregnancies. It would be desirable to delineate the precise mechanisms by which the aged maternal environment perturbs the normal development of the trophoblast, as this may highlight pathways which could be modulated pharmacologically to improve trophoblast differentiation in aged pregnancies. This will be investigated further in Chapter 4.

My data show major disturbances in the decidual compartment, which is instrumental in supporting normal placental development (Bilinski et al., 1998; Mori et al., 2016). These findings lead me to hypothesise that the placental abnormalities stem from a defect in the maternal decidual compartment, without major contributions by uNK cell differentiation which remains largely unaltered in aged females. Hence, I focused on studying decidualization, the process by which the endometrium differentiates and develops into the decidua, in more detail in Chapter 4.

Chapter IV
Advanced maternal age perturbs the progression of early pregnancy

4.1 Introduction

In the previous chapter, I showed that placental development is abnormal in older B6 mothers as a result of as yet undefined age-related changes in the uterus. The developmental delay that was obvious in the decidual compartment may result in defective trophoblast differentiation, and consequentially abnormal development of the embryo.

At the RNA level, development of the maternal E11.5 decidua in aged females was delayed by up to 2 days when compared to those of young females, and was characterised by de-regulation of genes known to be important in decidualization. Decidualization is the process by which the stromal cells that make up much of the uterine bed undergo proliferation and differentiation in response to steroid hormones. This process facilitates implantation of the blastocyst into the uterine wall, and is critical for the formation of the decidual portion of the placenta. As this transformation of uterine stromal cells is initiated in the peri-implantation window, abnormalities in the decidual compartment in aged mothers are likely to be rooted in defects of the uterus at an earlier stage of pregnancy (Cha et al., 2012).

The detrimental effects of imbalances in the tightly orchestrated timing of decidualization events have been shown by the study of uterine-specific mouse gene knockouts. For example, uterine deletion of the muscle segment homeobox gene *Msx1* causes implantation to be delayed until after the normal window of implantation, and severely reduces the decidualization response. This leads to abnormal embryo spacing and increased rates of resorption (Daikoku et al., 2011). Similarly, a study from Zhang et al in 2014 showed that uterine expression of *Rbpj,* a transducer of Notch signalling, is required for proper orientation of the embryo during implantation and remodelling of the decidua during post-implantation development (Zhang et al., 2014). Perturbation of these events by deletion of *Rbpj* in the uterus leads to embryo resorption at mid-gestation. These, and other studies (Peng et al., 2015; Plaks et al., 2013) show that function of the uterus during pregnancy is vital for proper development of the embryo and placenta. Hence, in this chapter, I will investigate in detail the effect of advanced maternal age on uterine function during early pregnancy.

The literature suggests that uterine ageing is a determinant of fertility in advanced maternal age (Nelson et al., 2013), however the biology underlying this association remains

largely unexplored. Previous studies have reported age-related changes in uterine histology, including increased collagen deposition reminiscent of fibrosis (Blaha and Leavitt, 1974; Gosden, 1979; Ohta, 1987), lipofuscin deposits in the cytoplasm of USCs, and reduced numbers of microvilli present on LE cells (Craig, 1981). However, these histological defects have so far not been related to any functional disturbance in aged pregnancies. Most significantly, the artificial decidualization response is severely impaired in older mice (Finn, 1966; Holinka and Finch, 1977; Shapiro and Talbert, 1974). This could reflect either a deficiency in the levels of maternal steroid hormones - mainly progesterone (P4) and estrogen (E2) - or a decline in the ability of aged tissues to respond to hormonal cues. Indeed, P4 levels do vary between young and aged mothers during early pregnancy (Holinka et al., 1979), however even after P4 supplementation age-related differences in uterine weight and decidualization still persist (Finch and Holinka, 1982; Holinka and Finch, 1977). Additionally, P4 levels in older mice during pregnancy do not correlate with embryo viability or resorption (Holinka et al., 1979), which - as I have shown in Chapter 1 - are the major consequences of advanced maternal age. Also, the artificial decidualization response is routinely triggered in ovariectomized females after timed injections with E2 and P4, thus arguing against systemic age-related changes in hormone levels as the cause of these defects. Hence, I here specifically assessed the capacity of USCs from aged females, compared to young controls, to initiate the decidualization response.

4.2 Results

4.2.1 Decidualization is impaired in aged uteri

To investigate uterine function during early pregnancy, I performed RNA-seq analysis on uterus fragments of about 5mm in length from young (8-22 weeks) and aged (41-49 weeks) pseudo-pregnant females at E3.5. From each mouse, two fragments were taken that were located adjacent to the ovary and distal from it, close to the joining point of the uterine horns. There were no significant differences in gene expression between these proximal and distal uterine segments, and therefore sequencing reads from both samples were pooled

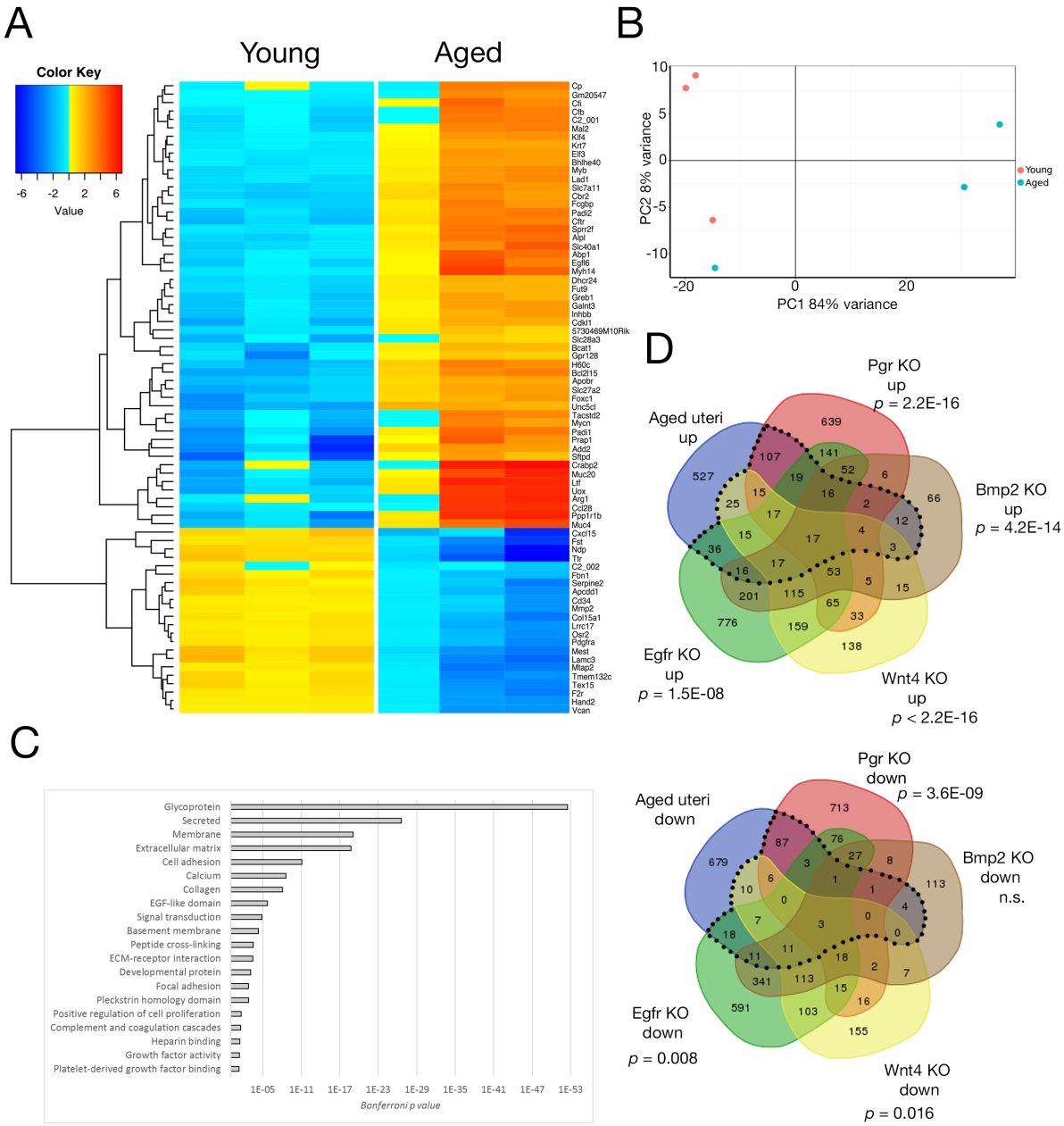

Figure 4.1 - Abnormal expression of decidualization genes in the pre-receptive uterus.

a) Heatmap showing 75 genes significantly differentially expressed between E3.5 uteri from young (8-22 weeks) and aged (41-49 weeks) females after mating with vasectomised males. Two independent samples of uterus were dissected from corresponding regions per uterus, which were pooled after sequencing resulting in a total of 3 independent replicates in each group. Differentially expressed genes were identified by both DESeq (p>0.05), and intensity difference (p<0.05).

b) Principal component analysis on RNA-seq data from E3.5 uteri from young (8-22 weeks) and aged (41-49 weeks) females.
c) Gene ontology annotations enriched in genes differentially expressed between young and aged uteri (*Bonferroni p<0.05)*. Differentially expressed genes were identified by either DESeq2 (p<0.05) and intensity difference (p<0.05).
d) Venn diagrams showing genes which were commonly differentially expressed in aged uteri, and in the E3.5 uteri of gene knockout (KO) mice. Differentially expressed genes were split into those which were up-regulated and down-regulated. Dotted line indicates groups overlapping with aged uteri. P values indicate the significance of the overlap (Fischer's exact test) between genes differentially expressed in the indicated gene KO, and in aged uteri.

prior to analysis. Analysis with DESeq2 and the intensity difference filter identified 75 genes which were significantly differentially expressed between young (n=3) and aged (n=3) uteri, with 53 genes up-regulated and 22 down-regulated (Fig 4.1a) Appendix, Supplementary table 3). This was at E3.5, during the period of hormonal priming, suggesting that priming of the endometrium is delayed, or incomplete in aged females. One out of the three aged samples showed a milder defect, with a gene expression pattern in between that of uteri from young females, and the remaining aged samples (Fig 4.1a, b). This did not correlate with the age of the female within this group, indicating that there is interindividual variability in the effect of maternal ageing on gene expression in the uterus during early pregnancy. It would be desirable to investigate this further with a larger number of samples at multiple ages to investigate the interindividual variability in, and age of onset of uterine deterioration with maternal ageing.

Gene ontology analysis of differentially expressed genes shows enrichment for annotations relevant to early pregnancy and decidualization, such as cell adhesion, extracellular matrix and collagen, developmental protein, growth factor activity, and heparin and platelet-derived growth factor binding (Fig 4.1c). Enrichment of the term glycoprotein may reflect the secretory function of USCs and uterine glands during decidualization, as secreted proteins such as growth factors and extracellular matrix components are often glycosylated.

A number of genes dys-regulated in uteri from aged females play important roles during early pregnancy, including *Follistatin* (*Fst*) which is required for the acquisition of

uterine receptivity and subsequent decidualization (Fullerton 2017), and *Hoxa10* and *Hand2*

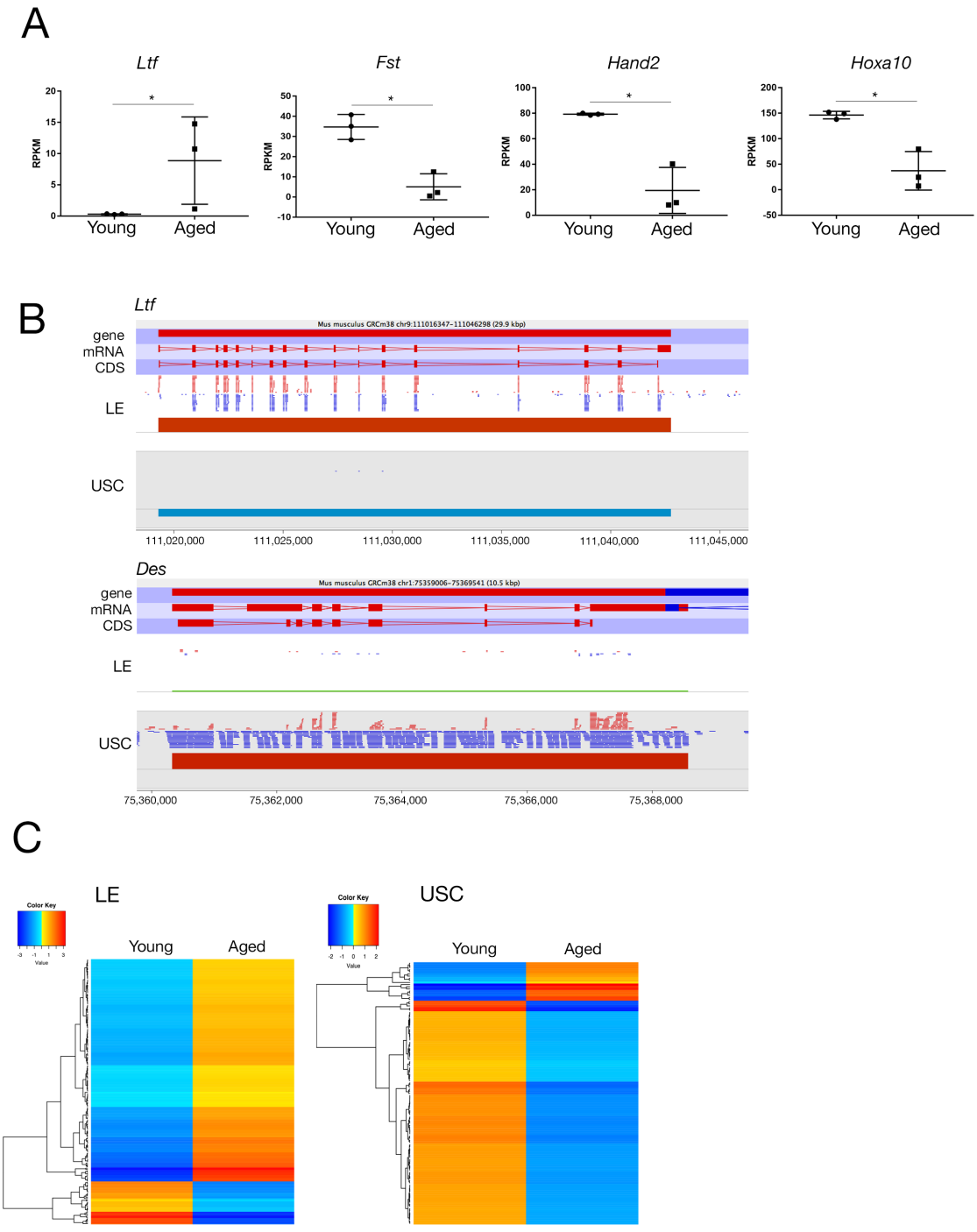

Figure 4.2 – Abnormal expression of LE and USC markers in aged E3.5 uteri.

a) Expression levels of genes specific to the luminal epithelium (*Ltf, Fst*) and uterine stroma (*Hand2, Hoxa10*) E3.5 uteri from young (n=3) and aged (n=3) females as determined by RNA-seq. Genes were identified as differentially expressed by DESeq2 ($p<0.05$) or intensity difference ($p<0.05$) in RNA-seq data.

b) Examples of aligned sequencing reads from RNA-seq datasets of luminal epithelial (LE), and uterine stromal cells (USC), at LE specific gene *Ltf*, and USC specific gene *Des,* in seqmonk. Very few reads align to *Ltf* in the USC dataset, and to *Des* in the LE dataset, as expected. USC data is opposing strand specific, whilst LE data from GSE57680 is non-strand specific.

c) Heatmaps showing expression of genes specific to LE cells or USCs in E3.5 uteri from young and aged females, determined by RNA-seq.

which are necessary for USC proliferation and differentiation (Benson et al., 1996; Lim et al., 1999; Mestre-Citrinovitz et al., 2015; Yu et al., 2017) (Fig 4.1a). Decidualization is driven by key signalling pathways, most notably these are regulated by the progesterone receptor (*Pgr*), which activates the *Egfr, Bmp2*, and *Wnt4* pathways (Large et al., 2014; Lee et al., 2007; Li et al., 2007; Lydon et al., 1995). I investigated the perturbation of these pathways in aged pregnancies using microarray data generated by our collaborators (Professor F. DeMayo's lab, USA), which identified targets of these signalling pathways in a uterine context, using uterus-specific knockout mice. I found that genes up-regulated in aged uteri were significantly enriched for genes up-regulated in the uterus of *Bmp2, Pgr, Egfr, and Wnt4* KO mice, and vice versa, suggesting that these key pathways of decidualization and early pregnancy are disturbed in aged uteri (Fig 4.1d) (Appendix, Supplementary table 4).

The uterus is a heterogeneous tissue comprised of multiple cells types, including USCs, LE, and GE, as well as immune cells such as uNK cells. uNK cells were not taken into account any further, as no differences were observed in their number or maturation state (Chapter 3, Fig 3.8f). During early pregnancy, the LE becomes receptive for implantation on the evening of day 4, in response to *Lif* secreted by the uterine glands (Pawar et al., 2015). The receptive LE enables blastocyst attachment and invasion into the uterine stroma, which stimulates decidualization of the stromal cell compartment. RNA-seq analysis of E3.5 uteri suggested that both the LE and USC compartments are affected by maternal ageing, revealing age-related changes in the expression of genes involved in both, epithelial receptivity (e.g., *Ltf, Fst*) and stromal cell decidualization (e.g. *Hand2, Hoxa10*) (Fig 4.2a). In order to elucidate which cell type in the uterus is most affected by maternal ageing, I bioinformatically defined gene expression profiles specific to USCs and LE in the uterus. I generated RNA-seq data from young USCs isolated from the uterus at E3.5 and used RNA-

seq data available in the GEO repository from LE obtained by laser capture micro-dissection (GSE57680). Each signature was generated by first identifying all genes expressed in the cell type of interest, and then excluding genes also expressed in the other cell type. This produced a signature of 666 and 811 genes representing the USC and LE respectively. The LE signature included the well-known LE marker *Lactotransferrin* (*Ltf*) and excluded *Desmin (Des)* which is specific to the uterine stroma, whilst the USC signature included *Des* and excluded *Ltf*, suggesting the signatures are representative of each individual cell type (Fig 4.2b).

I used these cell type specific signatures to interrogate the RNA-seq data from E3.5 uteri, to determine which compartment is most affected by maternal ageing. Both USC and LE specific genes were abnormally expressed in aged uteri. USC specific genes were mostly down-regulated, whereas LE genes were mainly up-regulated (Fig 4.2c), which may reflect the disruption of hormone responses in aged uteri. In the first 2 days of pregnancy, signalling is dominated by estrogen (E2) which stimulates proliferation of the LE. This signal is then antagonised from E2.5 by the action of progesterone (P4), which causes the LE to cease proliferation in preparation of embryo attachment and implantation. Meanwhile, progesterone stimulates USCs to proliferate and differentiate into decidual cells (Kurihara et al., 2007). It may be that the aged LE fails to down-regulate E2 controlled genes in response to P4, leading to increased expression of LE specific genes. Similarly, aged USCs may be unable to adequately activate decidualization genes in response to P4, leading to decreased expression of USC marker genes compared with young cells. These results suggest that both the LE and stroma are defective in the aged endometrium, and may exhibit resistance to the action of P4. However, as the number of implantation sites was not significantly different between young and aged mothers (Chapter 3, Fig 3.1a), as has been noted in previous studies (Lopes et al., 2009), implantation success *per se* does not appear to be affected by maternal age. This suggests that the major failure leading to embryo and placenta abnormalities lies within the stromal compartment. Therefore, I focused my attention on age-related changes in the function of USCs during early pregnancy.

The data shown above led me to hypothesise that defects in steroid hormone signalling, primarily through P4, may be responsible for the age-associated transcriptional defects observed in E3.5 uteri. It is possible that aged females fail to mount an adequate uterine response during early pregnancy either due to fluctuations in plasma levels of P4, or

because of an inability to adequately respond to pregnancy hormones. Although aged females do exhibit fluctuations in P4 levels during early pregnancy, this does not appear to be linked with embryo viability or resorption (Holinka et al., 1979), suggesting that the defect lies in hormone responsiveness rather than in maternal hormone levels. The ability of the aged endometrium to respond to a decidualization stimulus was studied by performing a deciduoma assay on hormonally primed ovariectomized (OVX) mice. This work was performed by our collaborators Dr Xiaoqiu Wang and Professor Francesco DeMayo (DeMayo lab, USA). The deciduoma assay allows us to study the extent and progression of decidualization in controlled hormone conditions, and in the absence of an implanting embryo. In confirmation of previous reports (Finn, 1966; Holinka and Finch, 1977), whilst young OVX females produced large deciduoma swellings in the stimulated uterine horn, aged OVX females exhibited much smaller swellings (Fig 4.3a), showing that decidualization was impaired in aged females. This suggests that a cell-intrinsic defect renders aged females unable to respond adequately to decidualization stimuli, as opposed to age-related changes in levels of maternal hormones.

Failure to mount a deciduoma response, coupled with the dysregulation of numerous genes involved in decidualization at E3.5 and E11.5, suggests a failure in the decidualization response of USCs from aged females. This hypothesis was investigated *in vitro* using USCs isolated at E3.5 of pregnancy. USCs were cultured in the presence of a decidualization cocktail comprised of E2, P4, and cyclic AMP (cAMP) to induce decidualization. USCs from young females responded to hormone treatment by up-regulating the expression of decidualization markers, as expected. However, aged USCs failed to upregulate the key marker *Dtprp* (*Prl8a2*) to the same extent as young USCs, and entirely failed to upregulate other important markers such as *Bmp2* and *Hoxa10* (Fig 4.3b). Taken together, these results suggest an intrinsic failure of USCs from aged females to undergo decidualization in response to hormonal stimulation.

To investigate the defective decidualization response of aged USCs in further detail, I generated RNA-seq libraries from USCs derived from one young and one aged female prior to, and after 4 days of *in vitro* decidualization. USCs from aged females were transcriptomically distinct from their young counterparts, both prior to and post decidualization (Fig 4.3c). PCA analysis defines 2 main clusters consisting of young and aged

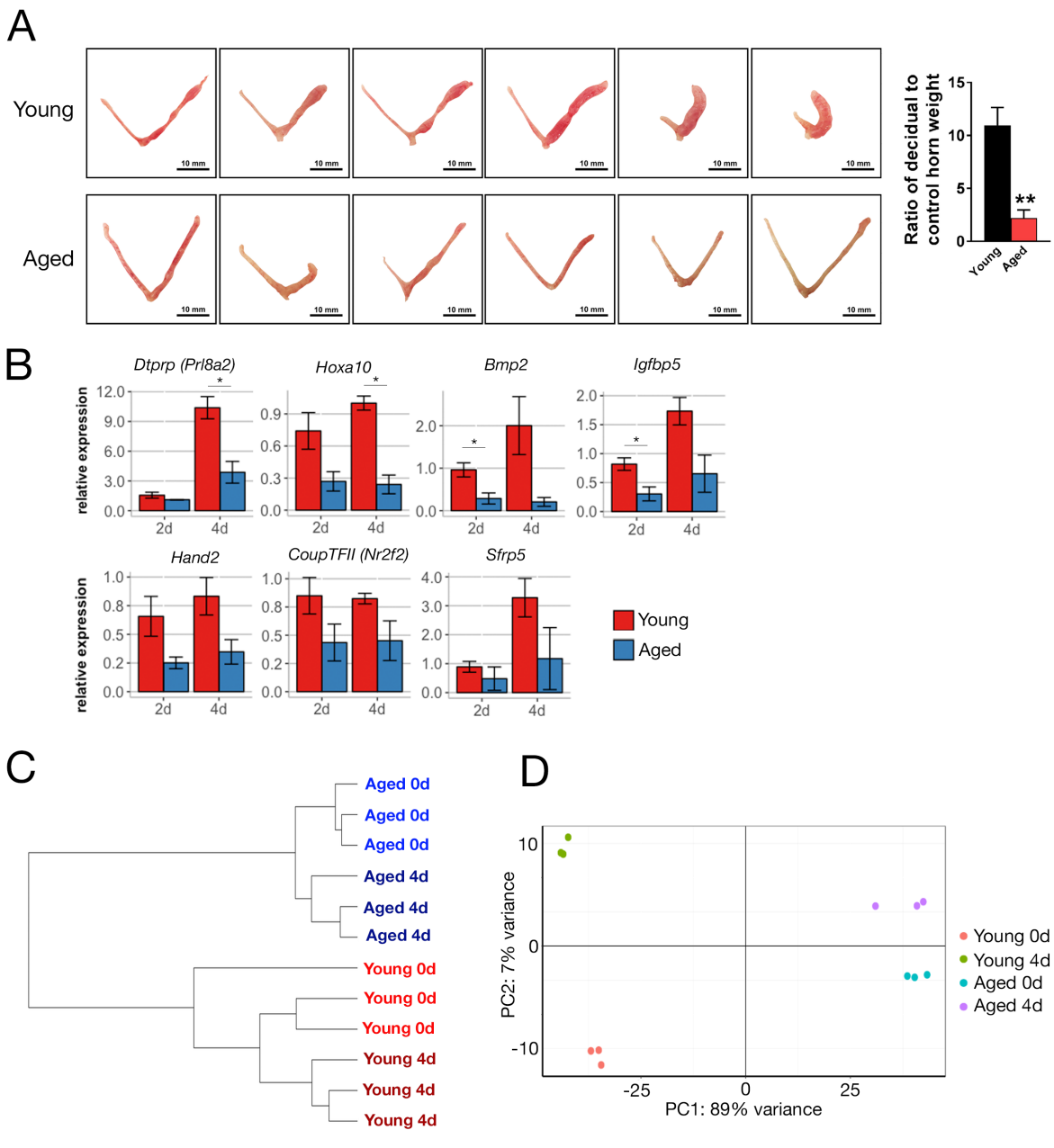

Figure 4.3 - The decidualization response is blunted in aged females.

a) Deciduoma assay showing the extent of the decidualization reaction in response to mechanical stimulation in hormonally primed young and aged mice. The ratio of weight of the stimulated horn (right) compared to the control (left) is also displayed. Statistical analysis is by two-tailed t-test, ** p<0.01. Deciduoma assay performed by XW (DeMayo lab, USA).

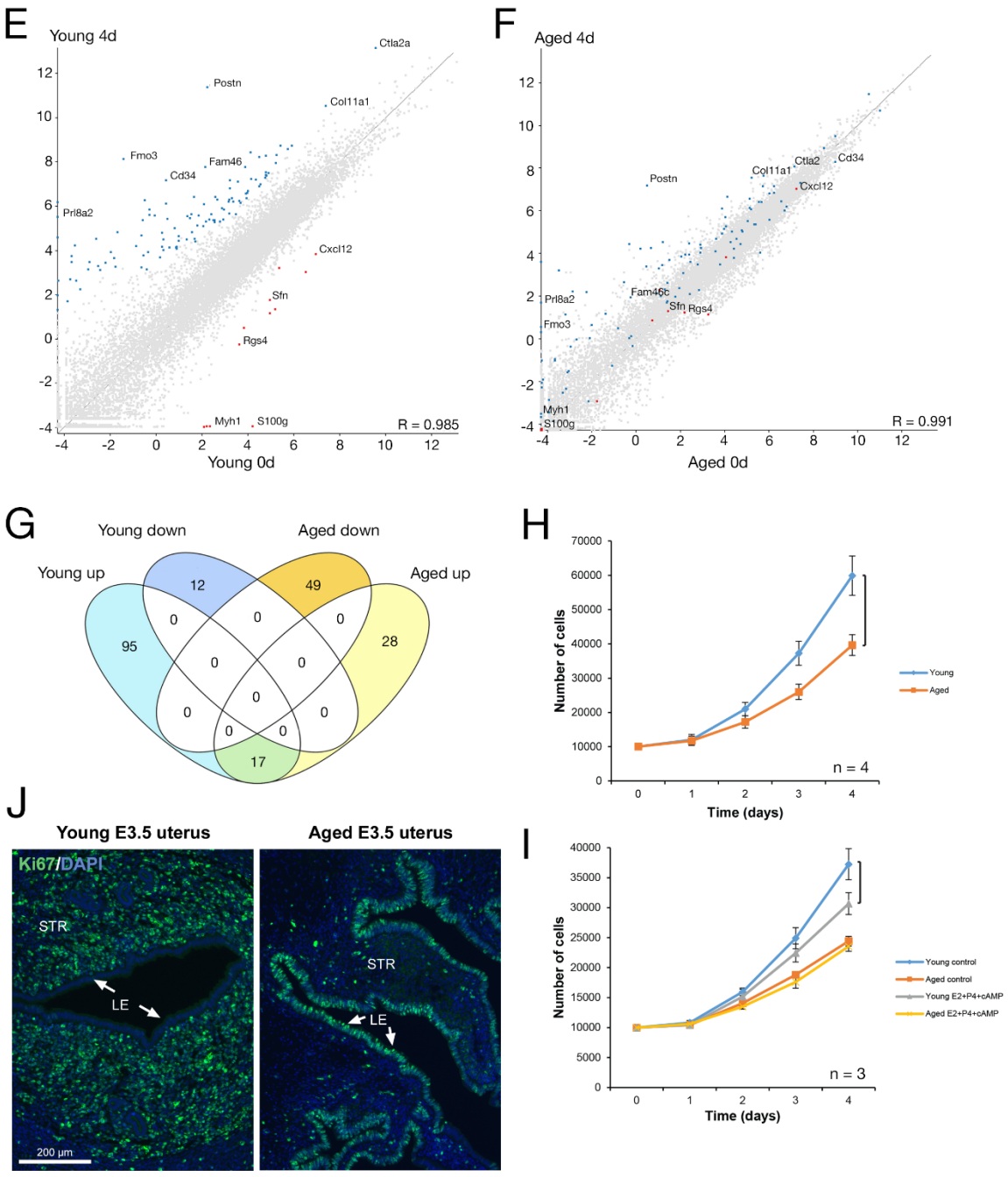

b) RT-qPCR analysis of decidualization markers in USCs stimulated for 2 and 4 days (mean +/- S.E.M., n=3). *p<0.05 two-tailed t-test. (USC isolation and *in vitro* decidualization performed jointly by LW and V P-G).

c) Closest neighbour analysis of RNA-seq datasets from USCs isolated from young, or aged females prior to *in vitro* decidualization, or after 4 days of treatment. Each group consisted of one independent biological sample, on which three technical replicates were performed.

d) Principal component analysis of the samples shown in c).

e) Scatter plot showing the expression (RPKM) of all genes in young USCs after 0 days and 4 days of *in vitro* decidualization. Genes which were significantly differentially expressed (DESeq2 $p<0.05$ and Intensity difference $p<0.05$) between 0d and 4d of treatment. Genes significantly upregulated at 4d are highlighted in blue, those downregulated are highlighted in red. A selection of genes are labelled for reference to f).

f) Scatter plot showing the expression (RPKM) of all genes in aged USCs after 0 days and 4 days of decidualization. Highlighted genes indicate those differentially expressed in young USCs between 0d and 4d of stimulation f) to compare the expression change in decidualization response genes between young and aged cells. A selection of genes are labelled for reference to e).

g) Venn diagram showing the genes which change in response to *in vitro* decidualization, which are common between young and aged USCs (DESeq2 $p<0.05$ and Intensity difference $p<0.05$). i.e. the which change significantly between young 0d vs 4d AND aged 0d vs 4d.

h) Proliferation curve of uterine stromal cells *in vitro*. Cells were isolated and counted on 4 consecutive days after plating. Cells from aged females display significant defects in proliferation (mean +/- S.E.M.). Statistical analysis by two-way ANOVA with Holm-Sidak's multiple comparisons test. (Proliferation assay performed by V P-G, statistics performed by A S-P).

i) Proliferation curve of uterine stromal cells *in vitro* from young and aged females. Cells were either unstimulated, or subjected to *in vitro* decidualization. Two-way ANOVA with Holm-Sidak's multiple comparisons test. (Proliferation assay performed by V. P-G, statistics performed by A. S-P).

j) Ki67 staining of uteri from young and aged pseudopregnant females at E3.5. Arrows indicate luminal epithelium. STR, stromal compartment. LE, luminal epithelium. Scale bar: 200µm.

samples which separate along PC1. Each group is sub- divided along PC2 into 2 groups representing USCs pre- and post-decidualization (Fig 4.3d).

Initially, I characterised the decidualization response of young USCs by identifying genes which were differentially expressed between pre- and post-decidualization. 124 genes were differentially expressed in response to the decidualization cocktail, 112 of which were up-regulated, and only 12 down-regulated (Fig 4.3e) (Appendix, Supplementary table 5). Genes that were up-regulated after 4 days of *in vitro* decidualization included well known decidualization markers including *Dtprp* (*Prl8a2*). Also up-regulated were the genes encoding nuclear receptor coactivator 4 (*Ncoa4*) which acts as a co-receptor for a number of steroid hormone receptors including *Esr1* and *Pgr (Kollara and Brown, 2012)*, and *Hsd11b1* which is induced by P4 in decidualizing human endometrial stromal cells (Kuroda et al., 2013) (Appendix, Supplementary table 5). The small group of only 12 genes that were significantly down-regulated by decidualization included regulators of G protein signalling *Rgs4* and *Rgs5*, and gap junction component *Connexin 26* (*Gjb2*) (Appendix, Supplementary table 5).

Analysis of USCs from aged females undergoing *in vitro* decidualization revealed that, as expected, they did not respond to hormonal stimulation as strongly as young USCs (Fig 4.3f). Only 17 of the 124 young decidualization response genes were differentially expressed in aged USCs after 4 days of *in vitro* decidualization (Fig 4.3g). These all fell into the up-regulated group. For example, decidualization marker *Prl8a2* was significantly up-regulated in aged USCs, but to a lesser extent than in young counterparts, as was the *Wnt3* regulated cell adhesion molecule *Periostin* (*Postn*) (Haertel-Wiesmann et al., 2000) (Fig 3e-f). No significantly down-regulated genes were shared between young and aged USCs. This further corroborates my previous data that USCs from aged females are less able to respond to decidualization cues than their young counterparts. Even those genes that do respond do so to a reduced extent. These findings lend further support to the hypothesis that maternal ageing leads to cell intrinsic changes in USCs, attenuating the hormonal responsiveness of the stromal compartment, which may perturb the early stages of extra-embryonic development and placentation in aged pregnancies. As these experiments were performed using only one independent biological replicate for each group, they should be replicated in the future to confirm the reproducibility of these results.

Endometrial decidualization is characterised by extensive proliferation and differentiation of USCs, which are vital for the establishment and maintenance of pregnancy (Lee et al., 2007; Wang et al., 2013). The regulation of USC proliferation during decidualization is not well understood, however the Wnt signalling pathway, and in

particular *Wnt4*, is a key player (Franco et al., 2011). As expression of *Wnt4* targets was perturbed in the uteri of aged females (Fig 4.1d) and GO analysis of E3.5 uteri showed that age-related genes were enriched for positive regulators of proliferation (Fig 4.1c), we next investigated the proliferative capacity of aged USCs. USCs isolated from aged females exhibited significantly reduced proliferation *in vitro* (Fig 4.3h). Aged USCs were also unable to modulate their rate of proliferation in response to the decidualization cocktail, whereas this led to a reduction in proliferation in young USCs (Fig 4.3i).

Corroborating the reduced proliferative capacity of aged USCs *in* vitro, the spatial distribution of proliferative cells was also clearly perturbed *in vivo*. At E3.5, the action of P4 on an E2 primed uterus normally inhibits the proliferation of the LE and stimulates proliferation in the stroma (Kurihara et al., 2007). On examination of uteri from young females by Ki67 staining we found that very few LE cells were positive for Ki67, whereas large numbers of USCs in the stromal compartment were actively dividing, as expected at this time-point (Fig 4.3j). In the majority of uteri from aged females however, the LE was still undergoing extensive proliferation, with minimal proliferation in the stroma (Fig 4.3j). This suggests that the switch from LE to stromal cell proliferation, brought about by the action of P4 on an E2 primed uterus, either does not occur adequately, or is delayed in uteri from aged females. This is likely to be another reflection of the impaired hormonal responsiveness, and specifically the P4-resistant phenotype that appears to interfere with the normal progression of pregnancy in aged females.

4.2.2 Effectors of progesterone signalling in the uterus are affected by maternal ageing

As uteri from aged females displayed a blunted response to decidualization hormones, I went on to investigate the expression and distribution of the steroid hormone receptors in the aged uterus. Immunohistochemical (IHC) staining at E3.5 showed that Esr1 levels were increased in some areas of the LE in aged females compared to young, with pEsr1 staining indicating it is in the transcriptionally active state (Fig 4.4a). However, the most striking differences were observed for Pgr distribution. In young females Pgr was strongly and homogeneously expressed in all cells of the LE, with some expression in the underlying stroma. By contrast, in aged females Pgr expression was patchy and highly variable in the LE. Some regions expressed reduced levels or completely lacked Pgr staining, whereas others showed largely normal expression at E3.5 (Fig 4.4b). At the RNA level, *Pgr* and *Esr1* were not

appreciably abnormal in whole uteri from aged females at E3.5, however both were significantly down-regulated in aged USCs both prior to and after 4d of decidualization (Fig 4.4c). At E6.5, Pgr expression has progressed from the primary decidual zone (PDZ) to the secondary decidual zone (SDZ) in young pregnancies, whereas in aged pregnancies it is still restricted to the PDZ at this time (Fig 4.4b). These differences in distribution are indicative of a slower progression of the decidualization wave across the stromal cell compartment (Tan et al., 1999). Pgr expression is still perturbed at E11.5, when protein levels of Pgr isoforms Pgr-A and Pgr-B are significantly decreased in An decidua (Fig 4.4d). Aa deciduas also displayed altered levels of Pgr-A and -B, however this did not reach statistical significance as Pgr levels were more variable within this group. Taken together, these data lend further support to the idea that the progression of decidualization is delayed in aged pregnancies. This may be due to the development of P4 resistance related to reduced expression of Pgr, likely causing a "ripple effect" interfering with the progression of placentation and embryo development that manifests as developmental delay and other abnormalities at later time points (Cha et al., 2012). Interestingly, one aged female displayed normal Pgr staining at E3.5 and was also transcriptomically more normal by RNA-seq (Fig 4.1a), showing that there is considerable inter-individual variability to the rate/onset of age-related reproductive decline. It is also tempting to speculate that the variability in Pgr expression observed in aged uteri may underlie the variability in embryo development at E11.5, perhaps with normal embryos implanting in regions expressing Pgr, and abnormal embryos implanting at regions depleted for Pgr (Fig 4.4b).

In the pregnant uterus Pgr interacts directly with phosphorylated Stat3 (pStat3), which acts as a Pgr co-activator. Ablation of *Stat3* in *Pgr* expressing cells of the uterus leads to defective decidualization and implantation (Liu and Ogle, 2002; Proietti et al., 2011), and diminishes the ability of Pgr to induce the expression of target genes (Lee et al., 2013). Thus, in addition to reduced Pgr expression, disturbances in pStat3 availability could contribute to the impaired P4 responsiveness. We therefore investigated the expression and localisation of pStat3 in aged pregnancies. pStat3 levels were significantly decreased in aged compared to young USCs undergoing *in vitro* decidualization (Fig 4.5a). Furthermore, IHC analysis showed that levels of pStat3 were also drastically reduced *in vivo* in the LE and GE of aged females at E3.5, and pStat3 was restricted to the cytoplasm and appeared to be conspicuously excluded from the nucleus (Fig 4.5b).

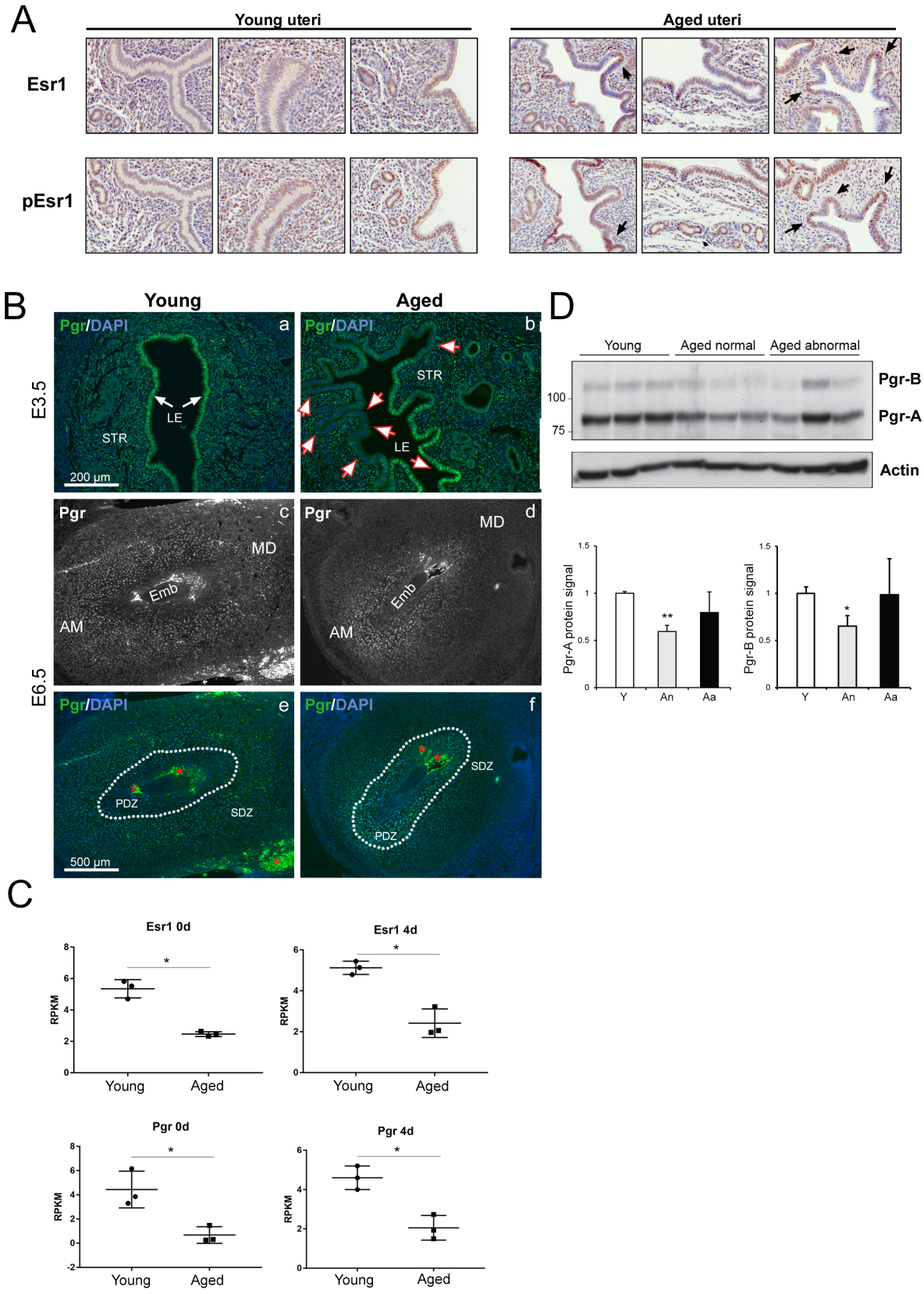

Figure 4.4 - Steroid hormone receptors are abnormally expressed in uteri from aged females.

a) E3.5 uteri from young and aged females, stained for Estrogen receptor (Esr1) and pEsr1 (brown). Arrows highlight intense patches of staining in the luminal epithelium of aged uteri.

(Stainings performed by XW in the FD lab).

b) E3.5 uteri (a-b) and E6.5 implantation sites (c-f) from young and aged females, stained for Progesterone receptor (Pgr). a-b) White arrows point to uniform staining in the luminal epithelium, red lined arrows highlight the mosaic staining of Pgr in the age luminal epithelium. LE, luminal epithelium. STR, stromal compartment. c-f) Dotted lines demarcate the boundary between the primary (PDZ) and secondary (SDZ) decidual zones. Red asterisks indicate autofluorescence from red blood cells. MD, mesometrial decidua. AM, anti-mesometrial decidua. Scale bar: 500µm.

c) Differential expression of *Esr1* and *Pgr* in uterine stromal cells from young and aged females before (0d) and after 4d (4d) of *in vitro* decidualization, determined by RNA-seq. DESeq2 $p<0.05$.

d) Expression levels of Progesterone receptor isoform -A and -B in deciduas isolated from young and aged pregnant females at E11.5. Aged samples were either associated to a grossly normal embryo (Aged normal), or an abnormal one (Aged abnormal). Graphs show Pgr protein levels normalised to actin, and relative to young mice (mean +/- S.E.M, n=3). (Western blot performed by V P-G).

This defect persisted at E6.5 (Fig 4.5c). These data suggest, that *in vivo*, the ability of pStat3 to localise to the nucleus where it interacts with Pgr is severely reduced, thereby preventing its function as a Pgr co-activator. Prevention of this vital interaction may interfere with the transcriptional responses of Pgr target genes, which could underlie the dampened response of Pgr target genes to P4 treatment in the aged uterus. Therefore, abnormal expression of Pgr in the aged uterus, combined with reduced expression and mis-localisation of pStat3, may explain the attenuation of uterine responses to P4, and the blunted decidualization reaction that is observed in aged females. Stat3 is phosphorylated as a result of Lif signalling. Lif is secreted from the uterine glands at E3.5 in response to E2 (Bhatt et al., 1991), and is required to initiate embryo implantation (Stewart et al., 1992); it also plays a role in stromal cell decidualization (Fouladi-Nashta et al., 2005; Shuya et al., 2011). As I found no implantation defect *per se* in aged pregnancies, and *Lif* expression was comparable in E3.5 uteri from young and aged pregnancies, I hypothesised that Lif deficiency was not the cause of reduced Stat3 phosphorylation. I confirmed this by Lif supplementation of USCs during *in vitro* decidualization, which failed to rescue the decidualization response of USCs from aged females (Fig 4.5d).

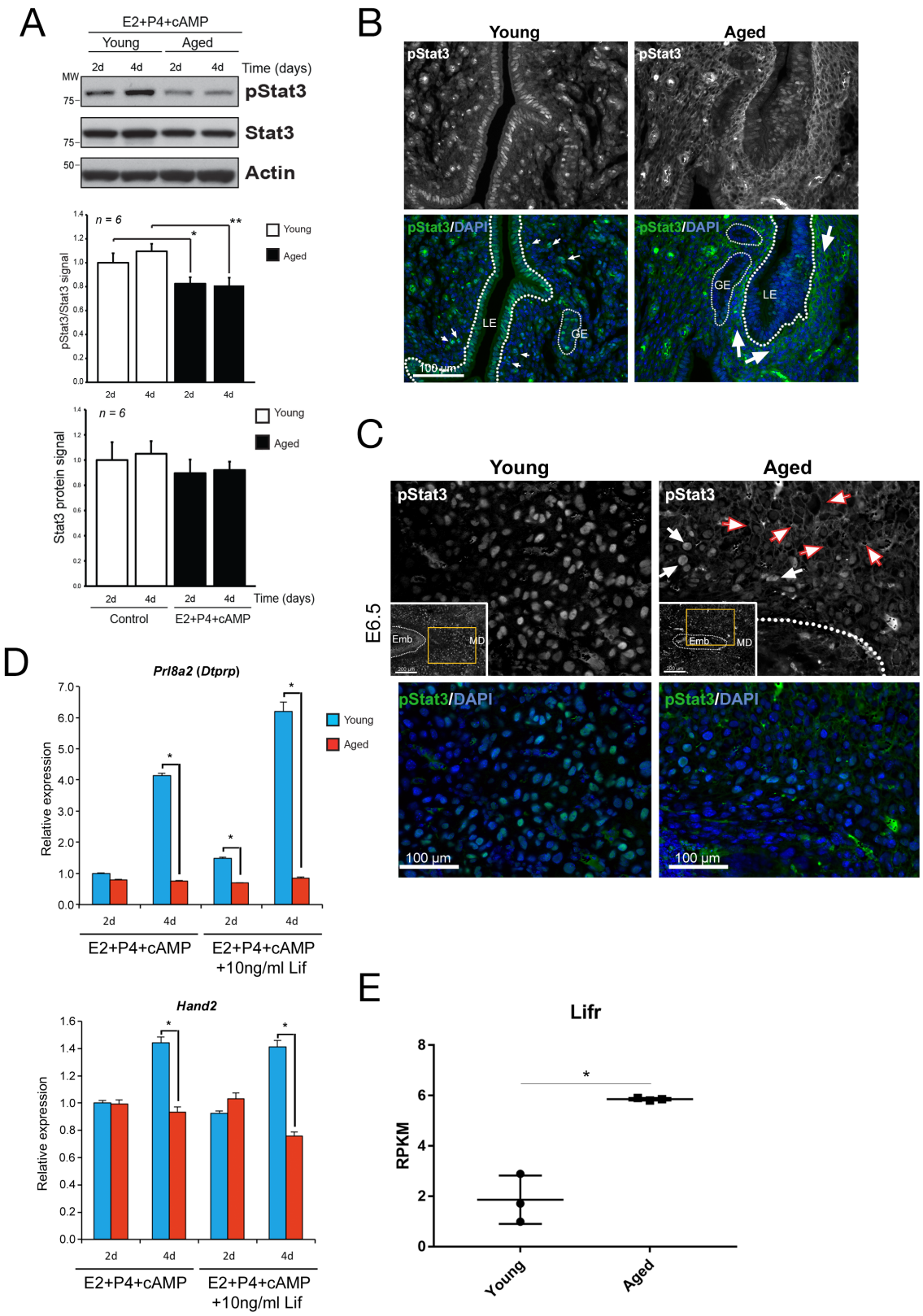

Figure 4.5 - Expression and activation of Stat3 is abnormal in aged pregnancies.

a) Western blot showing protein levels of Stat3 and pStat3 in uterine stromal cells from young and aged females, undergoing *in vitro* decidualization for 2-4 days. Graph shows the ratio of

pStat3/Stat3, normalised to 2 day young cells (mean +/- S.E.M., n=6). *p<0.05, **p<0.01 (ANOVA with Holm-Bonferroni's post-hoc test). (Western blot performed by V P-G).

b) IHC for pStat3 in E3.5 uteri from young and aged females. Dotted line demarcates the boundary between the luminal epithelium and uterine stroma. Small arrows indicate nuclear localisation of pStat3 in the stroma of young uteri, large arrows indicate the cytoplasmic localisation of pStat3 in the stroma of aged uteri. LE, luminal epithelium. GE, glandular epithelium. Scale bar: 100µm.

c) pStat3 staining in E6.5 implantation sites from young and aged females. Insets show an overview of the implantation site and yellow rectangles the location of the magnified image. In young females pStat3 is localised to the nucleus of uterine stromal cells (USCs), wheres in aged females only a few USCs show nuclear localisation (white arrows), and many show exclusion of pStat3 from the nucleus (red outlines arrows). Scale bar: 100µm.

d) Expression of decidualization markers *Prl8a2* and *Hand2* in uterine stromal cells undergoing *in vitro* decidualization in response to a decidualization cocktail of estrogen (E2), progesterone (P4), and cAMP, or the decidualization cocktail supplemented with 10ng/ml Lif for 2 days and 4 days (mean +/- S.E.M, n=3). Two-tailed t-test *p<0.05.

e) Expression of *Lifr* in E3.5 uteri from young and aged females, from RNA-seq data. Mean +/- S.E.M., DESeq2 *p<0.05

Interestingly, expression of the Lif receptor (*Lifr*) was increased in aged USCs (Fig 4.5e), despite a reduction in Stat3 phosphorylation in aged cells. Upregulation of *Lifr* may reflect an attempt to compensate for impaired Stat3 activation in aged USCs. This adds to the mounting evidence that an intrinsic defect in USCs from aged females, and not altered levels of maternal hormones and growth factor signals *per se*, prevents proper responses to P4, and underlies the decidualization and placentation defects.

4.2.3 Altered USC secretome in aged females impacts trophoblast differentiation

In Chapter 3 I showed that aged pregnancies exhibit abnormal differentiation of the trophoblast compartment, characterised by increased expression of TS cell markers, increased differentiation to the TGC lineage, and decreased differentiation to a labyrinth fate. A distinctive characteristic of USCs is that they acquire a unique secretory phenotype during decidualization. Gene ontology analysis of E3.5 uteri from young and aged females

shows that many secreted factors are differentially expressed as a function of age (Fig 4.1c). Many previous studies have highlighted the importance of highly orchestrated paracrine signalling between the LE, GE, uterine stroma, and trophoblast (Bany and Cross, 2006; Hess et al., 2007; Lee et al., 2006; Paria et al., 2002; Pawar et al., 2015). In 2017 Menkhorst and colleagues showed that invasive trophoblast cells signal to USCs to promote their decidualization (Menkhorst et al., 2017). In turn, the main function of the decidua is to limit trophoblast invasion; when placed at ectopic sites, trophoblast invades in an unrestricted manner. Decidual components such as tissue inhibitors of metalloproteases (TIMPs) function as a barrier to provide a "safe" environment for trophoblast invasion to occur. Thus, trophoblast invasion and likely trophoblast differentiation are also affected by the decidua. as a barrier to provide a "safe" environment for trophoblast invasion to occur.

I hypothesised that paracrine factors secreted by USCs during decidualization may direct trophoblast differentiation, and that age-related changes in the secretome of USCs would affect this process. To investigate this, I generated conditioned medium from decidualizing young USCs (yUSC-CM) and aged USCs (aUSC-CM), and analysed the stem cell capacity and differentiation dynamics of TS cells *in vitro* in the presence of these conditioned media (Fig 4.6a). Commonly, the stem cell potential of TS cells *in vitro* is maintained by supplementing the medium with mouse embryonic fibroblast conditioned medium (MEF-CM), Fgf, and Heparin. Differentiation is promoted by the withdrawal of MEF-CM, Fgf, and Heparin (Tanaka, 2006). As I wanted to investigate the effect of young- and aged-CM on differentiation, I promoted TS differentiation in the presence of USC-CM by withdrawal of only Fgf and Heparin for 3 and 5 days (Fig 4.6a). Despite the continued presence of CM, Fgf/Heparin withdrawal caused a rapid downregulation of TS cell markers at 3d, and upregulation of SpT, SynT, and TGC markers by 3d and 5d (Fig 4.6b), as expected from the dominant role of Fgf in maintaining the TS cell state. Therefore, differentiation in the presence of USC-CM would allow me to investigate the effect of the aged USC secretome on trophoblast differentiation. The first observation from these experiments is that USC-CM (irrespective of young versus aged) affects the TS cell state differently than MEF-CM. This was evident from the globally elevated levels of TS cell and TGC marker gene expression, and in particular a reduction of *Gcm1*. Whether or not these effects are due to USC-secreted factors, or instead due to the presence of E2, P4 and cAMP in the USC-CM but not the MEF-CM remains to be explored in the future.

A

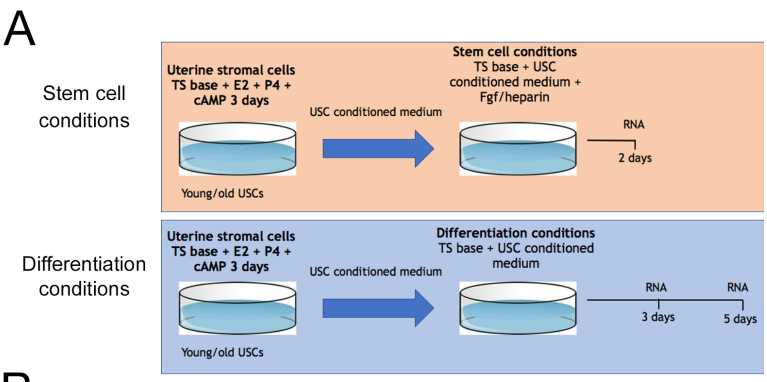
Stem cell conditions
Uterine stromal cells
TS base + E2 + P4 +
cAMP 3 days
USC conditioned medium
Stem cell conditions
TS base + USC
conditioned medium +
Fgf/heparin
RNA
2 days
Young/old USCs
Differentiation conditions
Uterine stromal cells
TS base + E2 + P4 +
cAMP 3 days
USC conditioned medium
Differentiation conditions
TS base + USC conditioned
medium
RNA
3 days
RNA
5 days
Young/old USCs

B

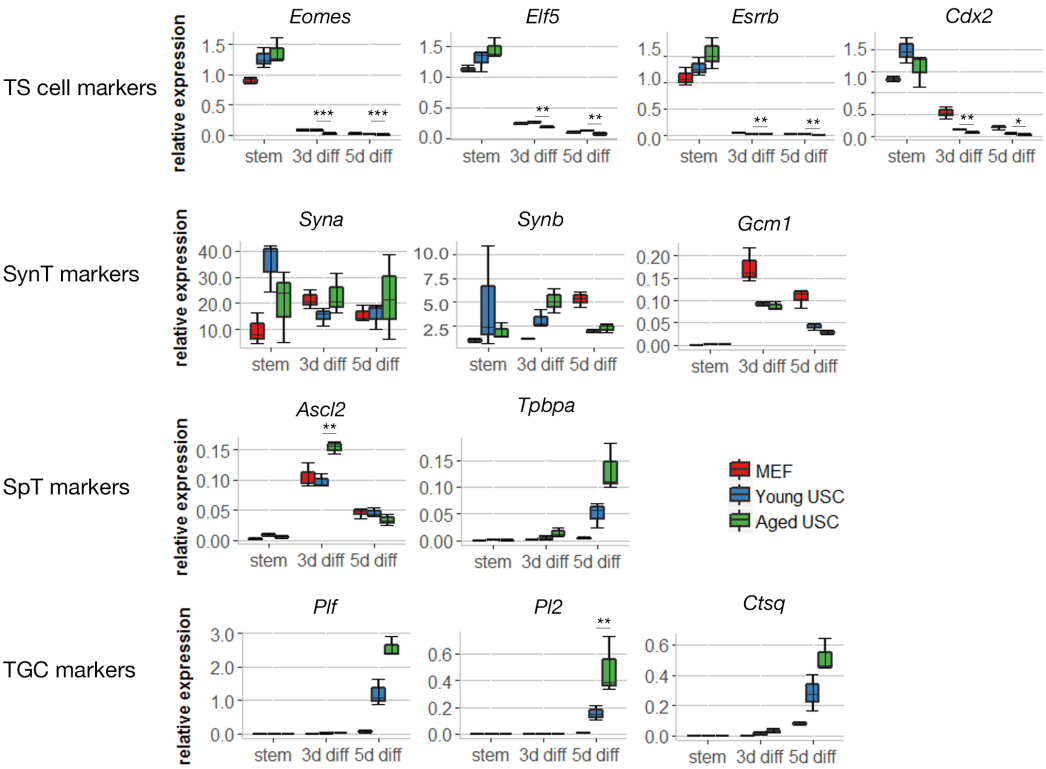
TS cell markers
SynT markers
SpT markers
TGC markers
relative expression
Eomes
Elf5
Esrrb
Cdx2
Syna
Synb
Gcm1
Ascl2
Tpbpa
Plf
Pl2
Ctsq
stem
3d diff
5d diff
MEF
Young USC
Aged USC

C

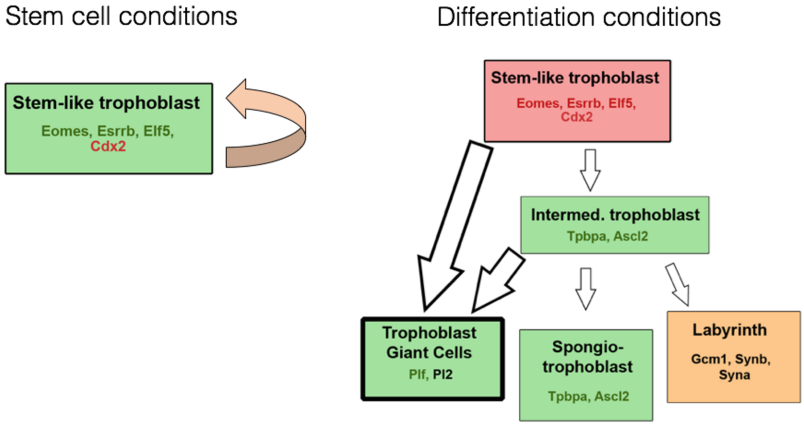
Stem cell conditions
Differentiation conditions
Stem-like trophoblast
Eomes, Esrrb, Elf5,
Cdx2
Stem-like trophoblast
Eomes, Esrrb, Elf5,
Cdx2
Intermed. trophoblast
Tpbpa, Ascl2
Trophoblast
Giant Cells
Plf, Pl2
Spongio-
trophoblast
Tpbpa, Ascl2
Labyrinth
Gcm1, Synb,
Syna

Figure 4.6 - Factors secreted by aged uterine stromal cells affect the differentiation of trophoblast stem cells.

a) Uterine stromal cells were cultured in TS base medium with the decidualization cocktail for 3 days to generate young- and aged-conditioned medium (CM). Trophoblast stem (TS) cells were either maintained undifferentiated in culture for 2 days in the presence on young- or aged-CM plus Fgf and Heparin, or differentiated in the presence of young- or aged-CM by withdrawal of Fgf and Hepain for 3 days and 5 days.
b) Expression of trophoblast lineage markers in trophoblast stem cells either under stem cell conditions (stem), and after 3 days (3d diff) or 5 days (5d diff) of differentiation. TS cells were cultured either in the presence of MEF conditioned medium, young-CM (Young USC), or aged-CM (aged USCs) as described in Fig 4.6a. Mean +/- S.E.M., n=3. Statistical analysis was by two-tailed t-test *p<0.05, **p<0.01, ***p<0.001.
c) Schematic showing suggested model of trophoblast differentiation in the presence of conditioned medium from aged uterine stromal cells, compared to young-CM. Intermed. trophoblast, intermediate trophoblast.

More importantly in the context of my project, I focussed on the differences between yUSC-CM and aUSC-CM. In the presence of aUSC-CM, TS cells under stem cell conditions exhibited slight increases in the expression of the TS markers *Eomes*, *Elf5*, and *Esrrb*, and decreased expression of *Cdx2* compared to yUSC-CM, although these differences did not reach statistical significance (Fig 4.6b). Under differentiation conditions, TS cell markers were significantly more rapidly down-regulated in the presence of aUSC-CM than yUSC-CM. Expression of the intermediate/SpT markers *Ascl2* and *Tpbpa* was increased with aUSC-CM, at 3d and 5d respectively, although only the difference in *Ascl2* expression was significant (Fig 4.6b). Differentiation in the presence of aUSC-CM also resulted in significantly increased expression of the TGC marker *Plf* and increased expression of *Pl2* and *Ctsq* after 5d of differentiation. The SynT markers *Syna* and *Synb* were not significantly affected, however expression of the labyrinth progenitor marker *Gcm1* was slightly decreased in aged cells at 3d and 5d of differentiation (Fig 4.6b).

These results suggest that CM from aged USCs promotes the expression of TS cell factors under stem cell conditions, and causes differentiation to progress more rapidly on

withdrawal of Fgf and Heparin. Differentiation with aUSC-CM was characterised by promotion of the TGC and SpT fates (Fig 4.6b-c). These *in vitro* findings partially recapitulate the phenotype observed in the trophoblast compartment in aged pregnancies. *In vivo,* expression of TS cell markers is aberrantly maintained at mid-gestation, accompanied by over-expression of TGC markers. These results show that factors secreted by young and aged USCs differentially affect the trophoblast differentiation programme. Aged UCSs interfere with this differentiation programme, either because they produce more and/or different factors than young USCs, or because they secrete reduced amounts of critical factors. The precise nature of these secretions will need to be determined in future experiments. However, these conditioned media experiments provide further striking evidence for my reasoning that declining uterine function with maternal ageing impacts on development of the fetal trophoblast compartment, thereby causing developmental abnormalities in the placenta and embryo.

4.3 Discussion

The successful establishment of pregnancy requires a highly orchestrated series of events which render the endometrium receptive to a blastocyst, synchronised with the presence of a competent blastocyst which subsequently implants into the uterine wall. Thus, gene expression in the uterus must be tightly controlled at this time. I have found that maternal ageing leads to a decline in the ability of the uterine stromal compartment to respond to P4, which plays a role in regulating gene expression in the endometrium during early pregnancy. Reduced hormonal responsiveness affects the expression of key genes, including *Bmp2*, *Hoxa10,* and *Hand2* which are indispensable for decidualization (Benson et al., 1996; Godbole and Modi, 2010; Lee et al., 2007; Li et al., 2007; Yu et al., 2017). Abnormalities in the progression of decidualization can lead to a "ripple effect", leading to abnormal trophoblast differentiation and resulting in the abnormal placental and embryonic development observed at mid-gestation in aged pregnancies.

In mice, USC decidualization is triggered by the presence of an implanting blastocyst in a hormonally primed endometrium. Hormonal priming takes place in the preimplantation stage of pregnancy, under the influence of E2 on days 0-2, and P4 from E2.5 onwards. This priming is necessary for successful implantation and decidualization, and for the induction of artificial decidualization. My results suggest that hormonal priming is delayed, or incomplete in the uteri of pseudo-pregnant aged females at E3.5. This leads to altered expression of *Pgr*

target genes such as *Hand2*, and downstream signalling pathways including the *Egfr*, *Bmp2*, and *Wnt4* pathways in aged females, even in the absence of an implanting blastocyst. Estrogen responsiveness appears to be less severely affected, as *Ltf*, a gene regulated by E2 in the uterine epithelium (Jefferson et al., 2000) is highly expressed in aged females, and E2-directed proliferation of the LE occurs robustly. Interestingly, expression *Ihh,* which acts as a paracrine signal from the LE to the stroma is reduced in E3.5 uteri from aged females (Appendix, Supplementary figure 3), suggesting that the ability or timing of communication between the LE and USCs is affected by maternal ageing.

The most severe defect appears to be in the progesterone responsiveness of uteri from aged females. This is supported by the persistence of proliferating cells in the LE, and robust expression of E2 response genes in aged E3.5 uteri, which suggests a failure of P4 to antagonise the E2-directed epithelial proliferation and gene expression. This may be a result of insufficient expression of the P4 regulated gene *Hand2*. *Hand2* expression in the uterine stroma promotes production of members of the Fgf family, which mediate the mitogenic effect of E2 on the LE (Li et al., 2011). Indeed, the expression of *Hand2*, and multiple members of the Fgf family including *Fgf2*, *Fgf5*, and *Fgf10* are decreased in USCs isolated from aged females (Appendix, Supplementary figure 3). The absence of proliferating cells in the uterine stroma, the reduced expression of P4 target genes and the severely reduced decidualization response in aged females provides further evidence of a defect in P4 responsiveness.

Impaired uterine responses to P4 in aged USCs may be a result of reduced expression of Pgr itself. The variability in Pgr expression between cells of the same type, i.e. within the LE compartment and also within the stromal cell compartment, was intriguing. As I alluded to above, these differences may explain why some embryos develop seemingly normally – perhaps because they implanted at sites of largely adequate Pgr expression – while others fail to thrive, possibly because they implanted at sites of low/absent Pgr expression. The cause of this variability needs to be addressed in future studies that should include single cell approaches, to elucidate the full extent of this cellular heterogeneity. It is possible that regional variations in uterine blood flow or levels of hormones or metabolites causes this variability. RNA-seq analysis of upper and lower portions of the uterus did not show any gene expression differences, however microenvironmental variations may be present which would be not be detected by this analysis. Additionally, inter-individual variations may

explain why some of the age-associated defects I described exhibit a substantial amount of variability between samples, expressed as sometimes rather large standard deviations/error (e.g. Pgr levels in E11.5 decidua).

The effect of decreased Pgr expression is likely to be compounded by the blunted expression, activation, and aberrant subcellular localisation of the Pgr co-activator Stat3 in aged USCs. Once ligand bound, Pgr translocates to the nucleus where the Pgr-A isoform physically interacts with activated, nuclear pStat3 (Lee et al., 2013). However, the impaired activation and unusual subcellular localisation of pStat3 in aged females suggests that this interaction may be severely impaired in the aged endometrium. These results could be verified in co-IP experiments from nuclear extracts in the future. Deletion of *Stat3* in the LE leads to implantation failure (Pawar et al., 2013), a defect which is not apparent in aged pregnancies. However, mice with a stromal cell-specific *Stat3* deletion exhibit a reproductive phenotype remarkably similar to that seen in aged pregnancies (Robker et al., 2014). The *Stat3* stromal cell-specific conditional KO has no effect on the total number of implantation sites, but results in reduced embryo viability at E18, placentation defects, and a significantly increased incidence of resorption. In Chapter 3 I showed that conceptuses from pregnancies in aged mothers show a strikingly similar phenotype. This strongly suggests that age-related disturbances in Stat3 expression, phosphorylation, and localisation in USCs contributes to impaired P4 responsiveness, leading to placental defects with detrimental downstream effects on embryo development. This should be studied in more detail to increase our understanding of Stat3 regulation during decidualization, and the intricacies of its interaction with Pgr. Future studies should also survey the effect of Pgr-pStat3 interaction on the repertoire and transcriptional activation of Pgr target genes.

Also of importance is the mechanism by which pStat3 is excluded from the nucleus in the uterine stroma of aged pregnancies. Studies suggest that Lif mediated phosphorylation of Stat3 occurs via the Jak/Stat pathway, where ligand bound Lifr induces Stat3 phosphorylation at the plasma membrane, mediated by Janus tyrosine kinases. Activated pStat3 is internalised by receptor-mediated endocytosis, and transits to the perinuclear region where it can translocate to the nucleus. Disruption of the endocytic machinery blocks the translocation of pStat3 to the perinuclear region, resulting in its retention at the plasma membrane in a pattern similar to that in the stromal compartment of aged females (Bild et al., 2002). Elucidation of the mechanism underlying pStat3 nuclear exclusion may allow us to

improve pStat3 activation and translocation, and thereby improve decidualization in aged females.

In the previous chapter, I showed that advanced maternal age perturbs development of the trophoblast compartment, with alterations in the normal differentiation programme from a trophoblast stem/progenitor cell to the various differentiated cell types. Maternal age-related defects in trophoblast differentiation are not due to intrinsic defects inherited from the oocyte of aged mothers, and instead ageing of the maternal uterine environment induces developmental defects in the trophoblast compartment. In this chapter, I have shown that USCs isolated from aged females exhibit a blunted decidualization response, which appears to be accompanied by alterations in the expression of secreted factors during decidualization. Culture and differentiation of TS cells in the presence of conditioned medium from aged USCs alters their differentiation programme, seemingly by increasing the rate of differentiation allowing more rapid downregulation of stem cell factors, and promoting differentiation to the TGC fate. This remarkably closely resembles abnormal differentiation of the trophoblast compartment which is associated with maternal ageing *in vivo,* suggesting that paracrine signals from the uterine stroma to the fetal trophoblast play a role in directing trophoblast differentiation *in vivo,* and this is perturbed in advanced maternal age.

These results prompt the question of what are the paracrine factors produced by USCs which modulate TS cell differentiation, and out of these which are the key mediators of abnormal TS differentiation in older females? In 2014 Ohinata and Tsukiyama derived TS cells from the mouse blastocyst under defined culture conditions, which included Fgf2, Activin A, and inhibitors of p160ROCK and Wnt signalling (Ohinata and Tsukiyama, 2014). A number of Fgf and Wnt family signalling molecules including *Fgf2, Fgf10, Wnt4*, and *Wnt9a* are significantly down-regulated in decidualizing USCs from aged females (Appendix, Supplementary figure 3), which may influence maintenance of the TS cell state in aged pregnancies. Another possible explanation lies in the ability of USCs to promote sequestration of Fgf and heparin, which would promote the maintenance of TS cell identity through the continued supply of these factors. Expression of *Heparin binding epidermal growth factor* (*Hbegf*) and glypicans which are able to sequester heparin and Fgfs, respectively, are de-regulated in *in vitro* decidualizing aged USCs (Appendix, Supplementary

figure 3). This may affect the availability of growth factors in the culture medium and thus alter the dynamics of TS cell differentiation.

Excitingly, this experiment could equally be performed on human TS cells which were successfully derived for the first time by Okae and colleagues in January 2018 (Okae et al., 2018). The identification of paracrine factors affecting trophoblast differentiation in human pregnancy could lead a to deeper understanding of the mechanisms underlying various placental pathologies, and may facilitate the development of treatments to combat them.

Chapter V
Epigenetic mechanisms of uterine ageing

5.1 Introduction

Traditionally, epigenetics has been defined as the study of heritable modifications to the genome which occur without any change to the underlying DNA sequence. Epigenetic modifications are responsible for the regulation of genetic material in terms of its functional use and stability, such that they represent the link between genotype and phenotype. The epigenetic landscape changes measurably with advancing age, with global changes to DNA methylation and histone modifications observed in ageing organisms and tissues (Pal and Tyler, 2016). As age increases chromatin becomes globally more open and accessible, a phenomenon known as the heterochromatin loss model of ageing which is conserved in all eukaryotes from yeast to humans (Tsurumi and Li, 2012; Villeponteau, 1997). This model suggests that loss of heterochromatin due to age-related changes in the epigenetic landscape alters global nuclear architecture, resulting in aberrant expression of genes in affected regions.

As well as global changes in chromatin structure, ageing is also associated with epigenetic drift at specific loci. Over the lifespan of an organism epigenetic modifications are imperfectly maintained, leading to stochastic changes mainly in DNA methylation which reflects a gradual drift away from the baseline (Issa, 2014). Although many studies looking into epigenetic mechanisms of ageing have yielded contradictory results, it is clear that ageing is accompanied by changes to DNA methylation and histone modifications which may be associated with the functional changes that can be observed during the ageing process. DNA methylation is subject to epigenetic drift, where environmental factors and stochastic errors leads to gradual divergence of the DNA methylation landscape. DNA methylation also exhibits specific, directional changes with ageing including hypermethylation of some promoter-associated CpG islands (Issa, 2014; Pal and Tyler, 2016), and hypomethylation at CpG-poor promoters, intergenic regions and gene bodies (Issa, 2014; Winnefeld and Lyko, 2012).

Epigenetic changes during ageing have not been thoroughly studied in a reproductive context, and most studies that have been published focus on age-related changes in oocytes. One study showed that the expression of DNA methyltransferases (DNMTs) is reduced in oocytes from aged females, accompanied by decreased levels of DNA methylation (Yue et al., 2012), and suggested that this could be the mechanism underlying the maternal-age-associated increase in fetal malformations. However, in Chapter 3 I showed through embryo

transfer experiments that the effect of ageing on the maternal reproductive tract underlies developmental abnormalities in the conceptus, with little effect from the ageing oocyte.

Age-related epigenetic changes have not previously been studied in the mouse uterus. However, maintenance of proper epigenetic regulation in mouse reproductive tissues is functionally important, as highlighted by one study which showed that the CBA/J x DBA/2 mouse model of pregnancy failure is characterised by disturbance of DNA methylation in the decidua (Brown et al., 2013), whilst methylation in the trophoblast portion remained normal. It is likely that DNA methylation in the endometrium is dynamic. Specifically, steroid hormone responsive gene promoters appear to rapidly methylate and demethylate at promoter CpG sites to regulate the transcription of target genes (Métivier et al., 2008), and could thereby cyclically regulate the transcriptome through the estrous/menstrual cycle. Indeed, in humans DNA methylation changes have been linked to reproductive disease states including endometriosis and endometrial cancers (Dyson et al., 2014; Ji et al., 2017; Jones et al., 2013; Tao and Freudenheim, 2010), and it has been suggested that DNMT expression is regulated throughout the menstrual cycle and correlates with cycle stage specific fluctuations in DNA methylation (Ghabreau et al., 2004; Houshdaran et al., 2014; Yamagata et al., 2009).

Decidualization itself may be regulated epigenetically through the action of steroid hormones on USCs. Research in this area is in its infancy. One study found that expression of *Dnmt1* and *Dnmt3a* is up-regulated during murine decidualization *in vivo*, and inhibition of DNA methylation with 5-azacytidine perturbs the decidualization response (Gao et al., 2012), thus demonstrating that DNA methylation is required for normal decidualization. Research into decidualization of human endometrial stromal cells similarly shows that the expression of DNMTs is regulated in response to *in vitro* decidualization (Grimaldi et al., 2012; Logan et al., 2013; Vincent et al., 2011; Yamagata et al., 2009), suggesting that the importance of DNA methylation in decidualization is conserved in humans.

In the previous chapter, I showed that aged mice have an altered uterine transcriptome during early pregnancy. This is characterised by a blunted response to P4, and dys-regulation of key genes involved in decidualization. As the epigenome changes as a function of age, and this can lead to age-related changes in gene expression and tissue function, this brought about the hypothesis that alterations in the uterine epigenetic landscape may underlie, or at least contribute to, the defects observed during pregnancy in aged females, which I will investigate in this chapter.

5.2 Results

5.2.1 Histone modifications in uterine stromal cells

In Chapter 4, I showed that in aged females the uterine stromal compartment is unable to mount a robust decidualization response, due to reduced hormone responsiveness associated with abnormal expression of Pgr and its co-activator pStat3. Hence, I proceeded to investigate the epigenetic regulation of transcription in aged USCs to shed light on the potential underlying mechanism. I focused on USCs as they appeared the cellular compartment exhibiting the most profound and physiologically relevant defects. To investigate the distribution of histone modifications in USCs from young and aged females, I performed chromatin immunoprecipitation sequencing (ChIP-seq) for the activating mark histone 3 lysine 4 trimethylation (H3K4me3). Peaks were called on each sample (n=3) using the Macs2 package (Feng et al., 2012; Zhang et al., 2008), and a consensus peak list was generated using the R package DiffBind (Stark and Brown, 2011) to find peaks present in young and/or aged samples. For H3K4me3, Macs2 peaks defined 2 groups containing young and aged samples respectively (Fig 5.1a). 19,419 peaks were called in young samples, and 13,178 in aged, with 12,426 peaks present in both young and aged (Fig 5.1b). H3K4me3 peaks were mainly located in promoter regions as expected, with similar proportions of peaks called in young and aged falling in promoters (Fig 5.1c) (Appendix, Supplementary figure 5). After correction for library size, the data showed higher enrichment under peaks in young USCs than aged, suggesting there may be a global decrease in H3K4me3 with ageing (Fig 5.1d), as has been shown in studies on *Drosophila* (Wood et al., 2010). To address this possibility, I measured total levels of H3K4me3 by western blot, which showed there was no difference in total H3K4me3 between young and aged USCs (Fig 5.1e). This led me to conclude that the differential enrichment intensity must have been due to technical variability in the efficiency of the IP between different samples, not absolute differences in H3K4me3 levels. Therefore, I normalised the ChIP-seq data using enrichment normalization quantitation at the 20^{th} and 90^{th} percentiles in Seqmonk to correct for the variability in enrichment. I then applied DESeq2 ($p<0.05$) to test for differential enrichment of H3K4me3 at consensus peaks in USCs from young and aged females. This resulted in 3318 differential peaks, 1963 of which were enriched and 1355 depleted for H3K4me3 in aged USCs (Fig 5.1f).

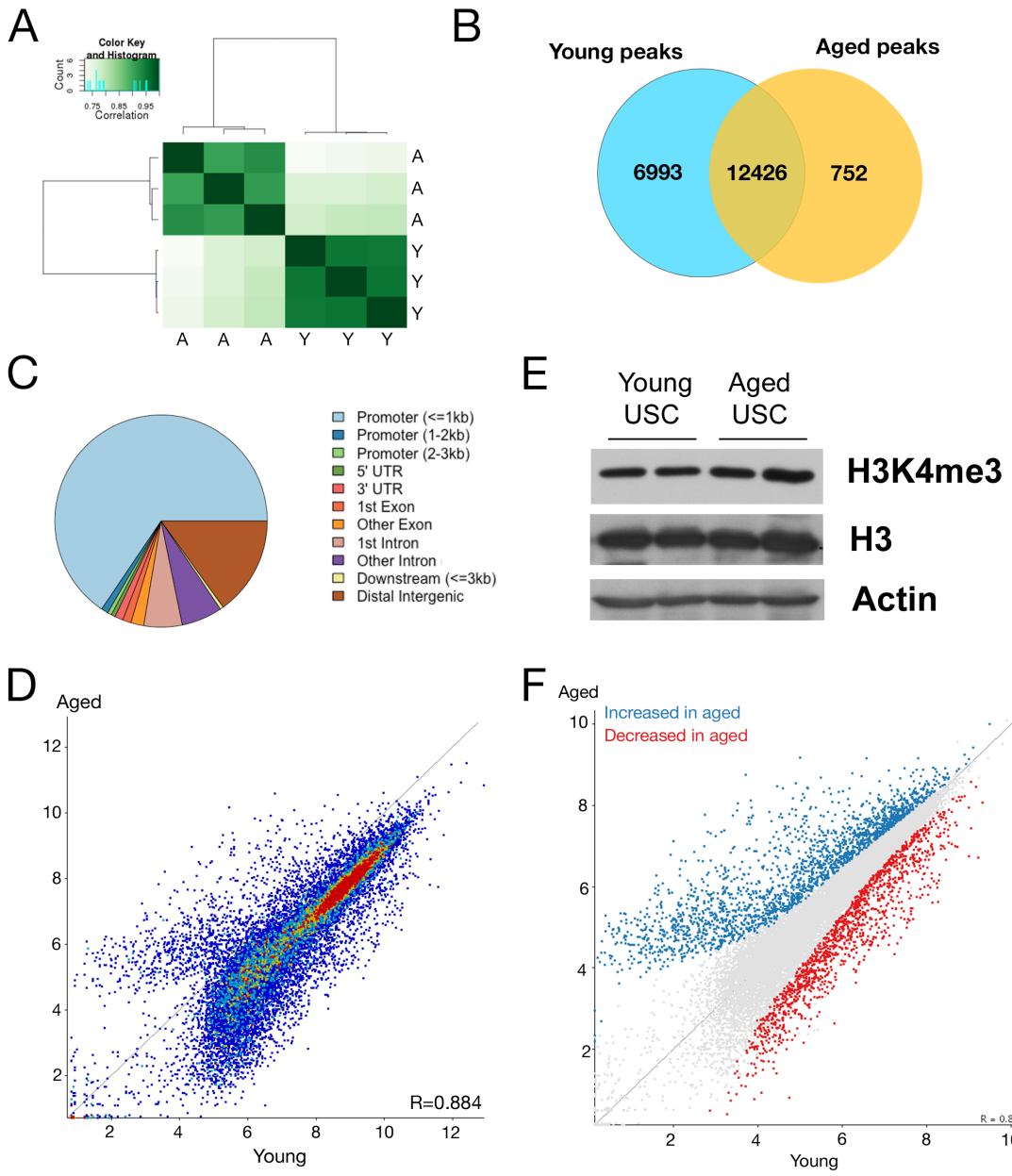

Figure 5.1 - The pattern of H3K4me3 is altered in aged USCs.

a) Correlation heatmap showing the correlation in H3K4me3 in young (Y) and aged (A) uterine stromal cells (n=3). Correlation is based on the read count under consensus peaks from ChIP-seq data. Plot was generated using the R package DiffBind.

b) Venn diagram showing the overlap between H3K4me3 peaks called in young and aged USCs.

c) Pie chart showing the distribution of H3K4me3 consensus peaks in genomic features.

d) Scatter plot showing the amount of H3K4me3 (RPKM) under consensus peaks in young and aged USCs (n=3), from ChIP-seq data, before normalisation in Seqmonk.

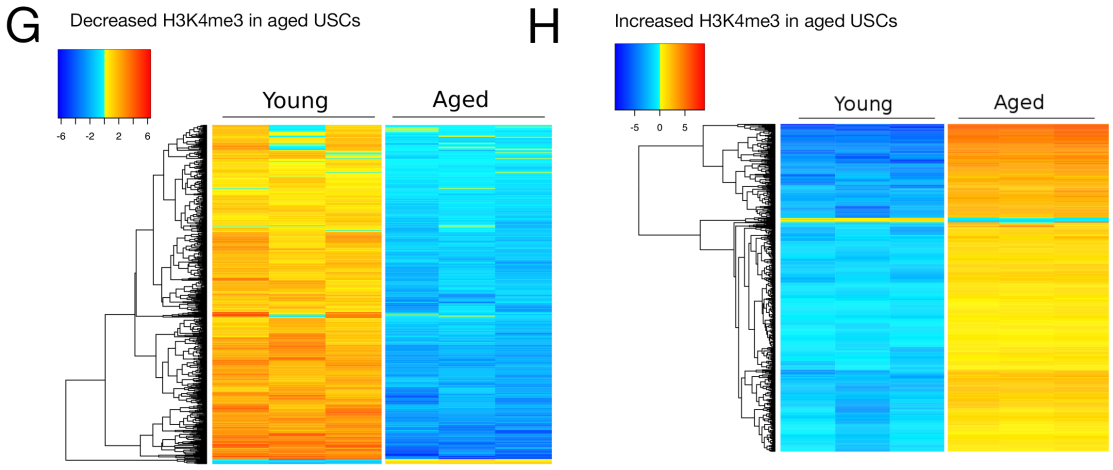

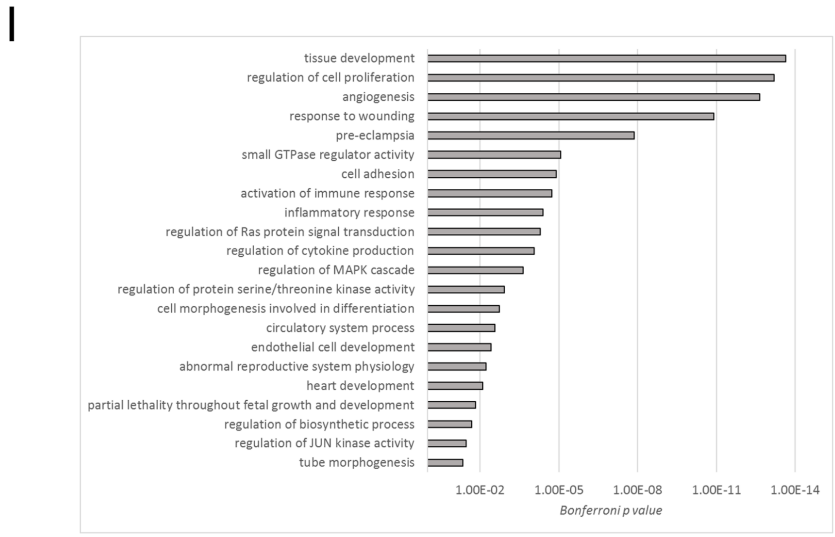

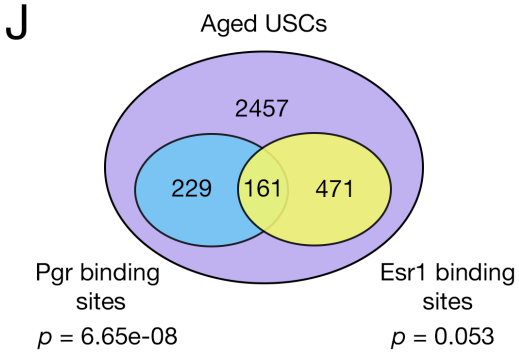

e) Western blot showing protein levels of H3K4me3 and H3 in uterine stromal cells (USC, n=2) from young and aged females.

f) Scatter plot showing the amount of H3K4me3 (RPKM) under consensus peaks in young and aged USCs (n=3), from ChIP-seq data, after normalisation to the 20th and 90th percentile in Seqmonk. Peaks with significantly increased levels of H3K4me3 in aged USCs are highlighted in blue, those with significantly decreased levels are highlighted in red (DESeq2 p<0.05).

g) Heatmap showing the expression (RPKM, RNA-seq data) of genes in young and aged USCs (n=3), which are within 2kb of a peak with significantly decreased levels of H3K4me3 in aged USCs, after normalisation of ChIP-seq data.
h) Heatmap showing the expression (RPKM, RNA-seq data) of genes in young and aged USCs (n=3), within 2kb of a peak with significantly increased levels of H3K4me3 in aged USCs, after normalisation of ChIP-seq data.
i) Gene ontology annotations which are significantly enriched in genes within 2kb of a peak with significantly increased/decreased levels of H3K4me3 in aged USCs. *Bonferroni p*<0.05
j) Venn diagram showing the number of H3K4me3 peaks with significantly increased/decreased levels of H3K4me3 in aged USCs which are within 2kb of a Progesterone receptor (Pgr), or Estrogen receptor (Esr1) binding site. Statistical analysis by Fischer's exact test.

Expression of genes with significantly different levels of H3K4me3 peak enrichment in their promoter shows that those with increased H3K4me3 in aged samples generally exhibited increased expression, and those with decreased H3K4me3 showed decreased expression (Fig 5.1g-h). This is in line with current knowledge on the function of H3K4me3, indicating that the normalisation yielded reliable results that accurately reflected the true biological situation.

Functional annotation of differentially modified regions using GREAT (McLean et al., 2010) showed their relevance to USCs, with significant enrichment of terms such as regulation of cell proliferation, angiogenesis, and cell adhesion, all of which were also enriched in RNA-seq data from aged USCs (Fig 5.1i) (Appendix, Supplementary figure 4). Interestingly, differentially modified peaks were also associated with pre-eclampsia, a condition of pregnancy characterised by shallow trophoblast invasion of the decidual bed (Kanasaki and Kalluri, 2009), and mouse phenotypes such as abnormal reproductive system morphology, partial lethality throughout fetal growth and development, and heart development (Fig 5.1i).

A significant proportion of peaks with differential enrichment of H3K4me3 in aged USCs overlapped with Pgr binding sites in the uterus (Fig 5.1j). As I showed in Chapter 4, transcriptional regulation of Pgr target genes is abnormal in aged uteri. Taken together,

these results suggest that Pgr fails to correctly modulate the expression of its target genes in aged uteri, and therefore H3K4me3 is not deposited and/or erased at these genes, in line with their transcriptional de-regulation.

This could be a result of reduced interaction between *Pgr* and its target genes, reduced competence of the *Pgr* to regulate its targets due to abnormal expression of Pgr coactivators, or an abnormal response of the histone methylation machinery. The enrichment of *Esr1* binding sites in H3K4me3 peaks perturbed by ageing did not reach significance (Fig 5.1j). This may reflect the greater importance of *Pgr* signalling in USCs, compared to *Esr1* signalling as suggested in the previous chapter. As this experiment was performed on USCs isolated at E3.5 of pregnancy during the period of hormonal priming, my results suggest that the remodelling of H3K4me3 at *Pgr* target genes in this priming period is incomplete or perturbed in aged females. This may contribute to the impaired decidualization response which I have shown occurs in aged females in both deciduoma assays and *in vitro* decidualization.

Interestingly, besides age-related differences in H3K4me3 peak location and intensity, H3K4me3 peaks also tended to be significantly shorter in aged USCs (Fig 5.2a-b). Most strikingly, in particular regions exhibiting the broadest peaks in young USCs of up to 50kb in length, were marked by much shorter stretches of H3K4me3 in USCs from aged females. For example, the Hox gene cluster containing *Hoxa10*, a gene necessary for stromal cell decidualization, is marked by a broad domain of H3K4me3 spanning 48.3kb in USCs from young females. This peak spans only 32.1kb in USCs from aged females, and the peak intensity is also reduced in magnitude (Fig 5.2c). The *Pgr* promoter is overlapped by a peak of 10.2kb in young USCs, however this was drastically reduced in both breadth and intensity in aged USCs (Fig 5.2d). In some cases, e.g. at *Hand2,* a very broad peak of 18kb spanned the entire gene in young USCs, but this was completely absent in aged USCs. This pattern of reduced peak breadth and the absence of very broad peaks in aged USCs is conserved over a number of genes that are of pivotal importance for decidualization. In general, these data are in line with a previous observation that genes essential for cell identity and cell type-specific function are marked by very broad regions of H3K4me3 (Benayoun et al., 2014). Benayoun et al., showed that genes in such regions are characterised by enhanced chromatin accessibility and increased occupancy of paused PolII at their promoters. Importantly, these broad H3K4me3 domains have been associated with enhanced transcriptional stability at the single cell level.

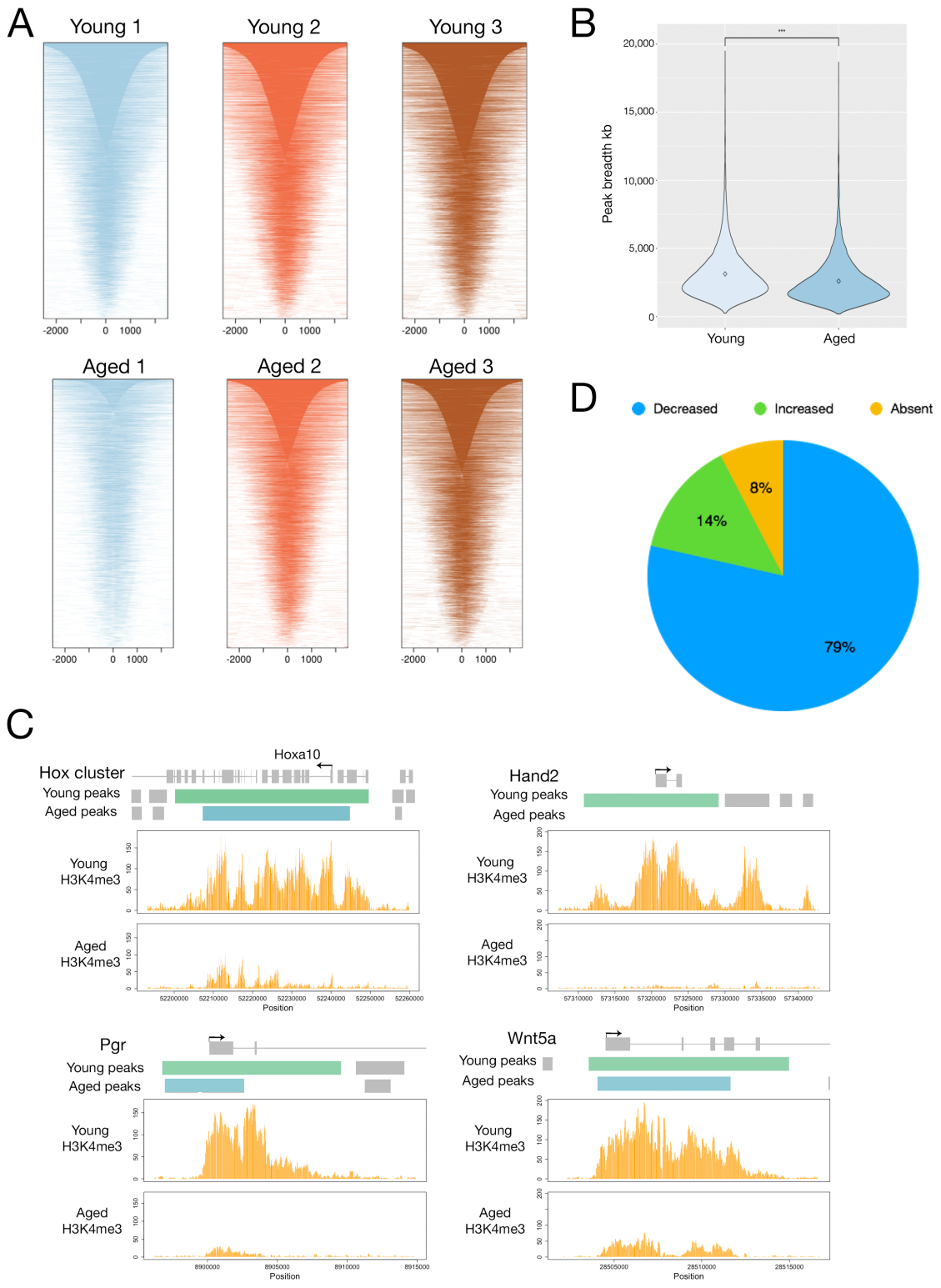

Figure 5.2 - The breadth of H3K4me3 peaks is decreased in aged USCs.

a) Heatmap showing the position and breadth of H3K4me3 peaks relative to the transcription start site. Peaks were called individually on 3 independent biological replicates of USCs from young and aged females.

b) Violin plot showing the difference in breadth of H3K4me3 peaks called independently in young and aged USCs (n=3). Plot has been cut-off at 20,000kb to better show the difference in mean. Black diamond indicates the mean of each group, two-tailed t-test ***p<0.001.

c) Plots showing the breadth of H3K4me3 peaks called independently on young (green bars) and aged (blue bars) USCs and their associated gene (arrow indicates the direction of transcription). Wiggle plots below indicate the read count of H3K4me3 ChIP-seq datasets (normalised to largest dataset) in young and aged USCs. Peaks within 2kb were merged.

d) Pie chart showing the direction of change when comparing the breadth of H3K4me3 peaks overlapping promoters in both young and aged USCs. Direction of change is relative to young USCs.

The authors suggested that broad H3K4me3 domains confer precise transcriptional regulation at key cell identity genes. In young USCs, genes marked by the top 5% broadest peaks included the P4 and E2 nuclear receptors *Pgr* and *Esr1*, and a number of genes associated with decidualization such as *Hand2* and *Wnt5a* (Fig 5.2d). Gene ontology analysis confirms that the affected genes are involved in decidualization, with terms such as differentiation, regulation of proliferation, PI3K signalling, and Wnt signalling (Appendix, supplementary figure 6). The breadth of these peaks was reduced in aged USCs in 79% of cases, by 2.7kb on average, and in 8% of cases the peak was completely absent in aged USCs (Fig 5.2d). These results suggest that changes in the pattern of H3K4me3 in USCs from aged females may affect the reinforcement of cell identity and function, potentially by reduced chromatin accessibility and paused PolII occupancy of key hormone responsive genes, although this would require further investigation.

Although my data suggest that H3K4me3 peak breadth at key decidualization genes is decreased in aged USCs, it is technically possible that this is due to a reduced ability to isolate chromatin, or immunoprecipitate H3K4me3 from aged cells, although the reasons for that would be difficult to explain. An inefficient H3K4me3 enrichment would result in increased background levels in the sequencing data, which may affect peak calling by Macs2. The fact that peak breadth is shorter overall, even at loci that have no obvious association with decidualization suggests this may indeed be a potential issue that has to be addressed in future experiments. However, the observation that very broad H3K4me3 domains at some

key decidualization genes including *Hand2* are not only shorter but in some cases absent in aged USCs, is likely to be a true biological age-related change that may reflect the impaired decidualization response of aged USCs. Reduced breadth of H3K27me3 domains has been previously described in ageing muscle stem cells (Liu et al., 2013). These changes may constitute either a cause, or a consequence, of the failing gene activation.

5.2.2 DNA methylation in young and aged E3.5 uteri

I next went on to study the DNA methylation landscape of the uterus during pregnancy in aged females. DNA methylation is perturbed in multiple ageing tissues, and such perturbations can lead to functional alterations and disease (Johnson et al., 2012).

I performed methylated DNA immunoprecipitation sequencing (MeDIP-seq) on DNA extracted from the same samples of pseudo-pregnant uteri as those analysed by RNA-seq in Chapter 4, to reveal any correlations between DNA methylation and gene expression. MeDIP-seq analysis shows that the young and aged uteri are overall highly similar in their pattern of 5-methylcytosine (5mC) deposition (Fig 5.3a). However, analysis of the enrichment of 5mC in various genomic features shows that there is a small, but significant increase in 5mC enrichment in CpG islands (CGIs) and at promoters – the latter probably reflecting the presence of CGIs in a subset of gene promoters (Fig 5.3b). This is in line with previous reports that promoter associated CGIs become hypermethylated with age in a tissue specific manner (Zampieri et al., 2015).

Closer interrogation of CGIs suggests that whilst globally they become slightly hypermethylated in aged uteri (Fig 5.3b), only 3 individual CGIs showed a significant change in 5mC when analysed using the MEDIPS package (Lienhard et al., 2014) (Fig 5.3c). The CGI spanning exon 2 of *C2 calcium dependent domain containing 4d* (*C2cd4d)* was significantly hypermethylated in aged uteri, however RNA-seq data shows this gene is not expressed in the maternal uterus at E3.5, nor in the decidua at E11.5 of pregnancy, and the *C2cd4d* knockout mouse displays no reproductive phenotype (Omori et al., 2016). Therefore, it is unlikely that this gene plays an important role in aged pregnancies. The remaining two differentially methylated CpG islands were located intergenically, one of which became hypermethylated with age, and the other hypomethylated (Fig 5.3c). I then scanned the genome in an unbiased manner to identify specific loci which were differentially methylated

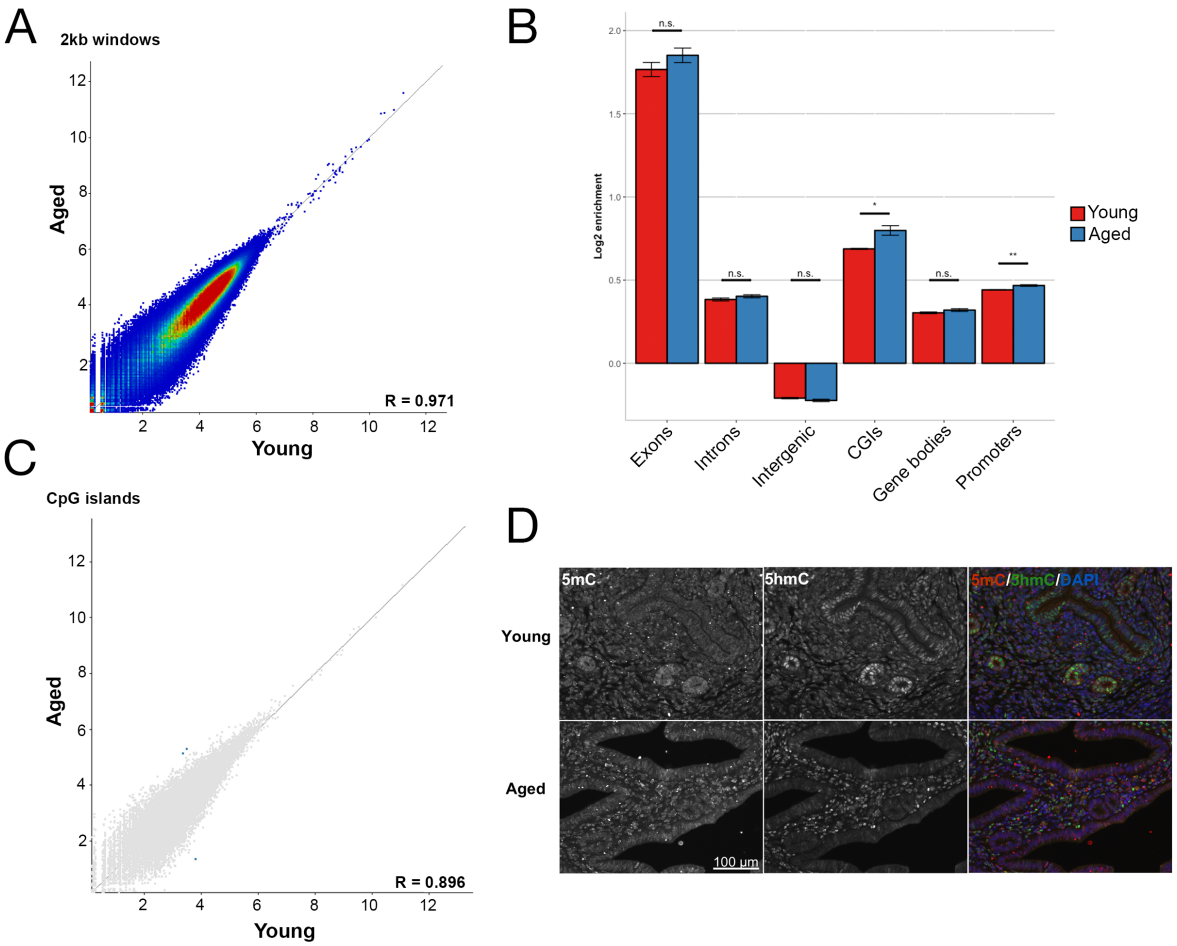

Figure 5.3 - DNA methylation in E3.5 uteri from aged females.

a) Scatter plot showing similar levels of 5-methylcytosine (5mC) (RPKM) as measured by MeDIP-seq, in E3.5 uteri from young (n=3) and aged (n=5) females, in 2kb windows running consecutively along the genome.

b) The relative enrichment (log2 transformed) of 5mC in different genomic features in E3.5 uteri from young (n=3) and aged (n=5) females, as measured by MeDIP-seq. Two-tailed t-test *p<0.05, **p<0.01.

c) Scatter plot showing the levels of 5mC at CpG islands in E3.5 uteri from young (n=3) and aged (n=5) females, as measured by MeDIP-seq. Three CpG islands with significantly different levels of 5mC as detected by MEDIPS analysis (p<0.05) in r are highlighted in blue.

d) IHC staining for 5-methylcytosine (5mC) and 5-hydroxymethylcytosine (5hmC) in E3.5 uteri from young and aged females. Arrows indicate higher levels of 5hmC in the glandular epithelium of young uteri. Scale bar: 100µm.

between young and aged uteri, using MEDIPS with a window size of 200bp. This identified only 1 region, located on chromosome 11 at *Sfi1 homolog, spindle assembly associated (yeast)* (*Sfi1*), however, this region was excluded from further analysis, as multiple loci in this

gene have been identified as 'blacklist' regions (http://mitra.stanford.edu/kundaje/akundaje/release/blacklists/). In addition, since RNA-seq data show that *Sfi1* is not expressed in E3.5 uteri it is unlikely to play a role in uterine function either.

These data suggest that ageing in the mouse uterus follows the generally accepted patterns of DNA methylation changes in terms of the acquisition of 5mC at CGIs. No changes were seen in gene body methylation. The age-related differences in DNA methylation that I have shown are of relatively small magnitude, and do not appear to affect gene expression at this stage of pregnancy. It is therefore unlikely that changes in DNA methylation are the primary mechanism underlying abnormal uterine function in advanced maternal age.

Immunohistochemical (IHC) staining suggests there are small cell-type specific differences in 5mC in the uterus, with enrichment of 5mC in the GE of uteri from young females which is not apparent in those from aged mice (Fig 5.3d). Interestingly, differences in the levels of 5-hydroxymethylcytosine (5hmC) are also apparent, showing a similar pattern of GE enrichment in young females. This would be interesting to investigate in detail in future studies, as 5hmC has been implicated in ageing in other tissues such as the cerebellum (Chen et al., 2012). So far 5hmC remains largely unstudied in the context of uterine function, however this topic was outside of the scope of my PhD thesis work.

5.2.3 DNA methylation in young and aged E11.5 decidual tissue

Although I observed only slight changes in 5mC in the uteri of aged females at E3.5, a study by Gao and colleagues in 2012 showed that in normal pregnancy the DNA methyltransferases *Dnmt1* and *Dnmt3a* are up-regulated at implantation sites from day 7, and were induced by artificial decidualization. Inhibition of DNA methylation by 5-azacytidine exposure strongly inhibited decidualization, affecting USC proliferation and expression of decidualization markers (Gao et al., 2012). This is similar to the age-related perturbation in decidualization I showed in Chapter 4, suggesting that DNA methylation may have a role in decidualization after the priming period, i.e. after E3.5. Hence, I went on to investigate DNA methylation in the E11.5 decidual samples that I had previously analysed by RNA-seq in Chapter 3. Analysis with MEDIPS identified 214 differentially methylated regions (DMRs) between E11.5 deciduas from young and aged females. Intriguingly, all these sites exhibited lower DNA methylation levels with age (Fig 5.4a). Differential methylation was

confirmed at base pair resolution for the promoter region of *Pou2f1*, by amplicon sequencing of bisulphite-treated DNA. This showed that DNA methylation was decreased in aged samples at some CpGs, although total DNA methylation was low at these regions even in young samples (Fig 5.4b).

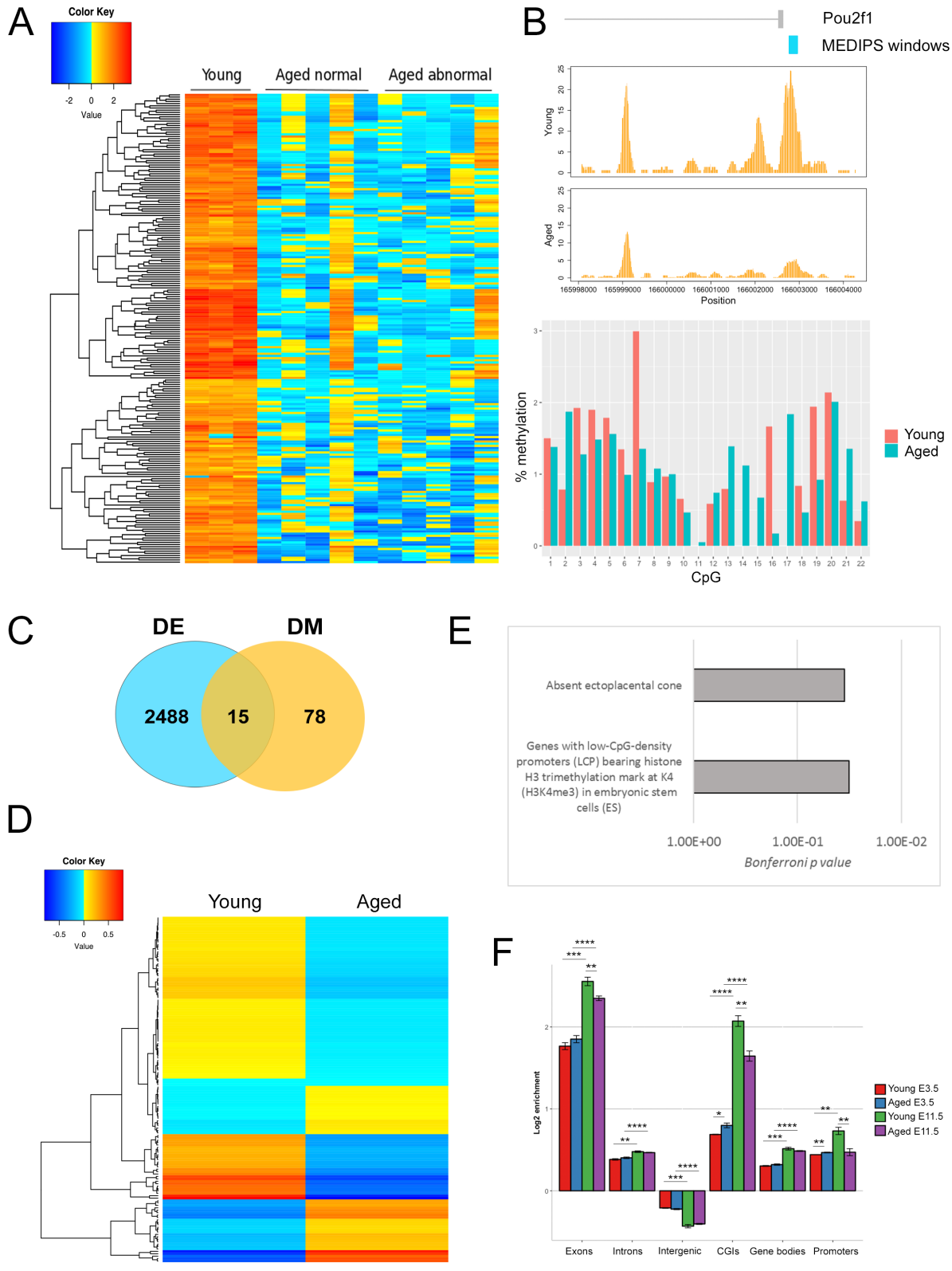

Figure 5.4 - DNA methylation is abnormal in E11.5 deciduas from aged females.

a) Heatmap showing significantly reduced DNA methylation at 214 differentially methylated regions (DMRs, identified by MEDIPS p>0.05) in E11.5 deciduas from aged females. DNA methylation is affected both in deciduas associated with grossly normal, and abnormal embryos.

b) Wiggle plot showing the relative amount of 5-methylcytosine near the promoter of the *Pou2f1* gene, which was identified as having significantly decreased 5mC in aged deciduas. Grey bars indicate location of *Pou2f1* gene. Blue rectangle indicates the location of the MEDIPS window identified as being differentially methylated in MeDIP-seq data. The bar plot below shows the %DNA methylation at CpGs within the MEDIPS window as measured by amplicon sequencing of bisulphite converted DNA from young and aged E11.5 deciduas.

c) Venn diagram showing the overlap between genes that were differentially expressed (DE, RNA-seq data), and regions that were differentially methylated (DM, MeDIP-seq data) in E11.5 deciduas from aged pregnancies.

d) Heatmap showing the relative expression (RNA-seq data) of genes associated with a DMR in aged E11.5 decidua. Gene expression changes are relatively small and inconsistent in direction.

e) Enrichment of biological annotations by Genomic regions enrichment of annotations tool (GREAT) analysis in the 214 DMRs in E11.5 deciduas from aged pregnancies.

f) The relative enrichment (log2 transformed) of 5-methylcytosine in genomic features in E3.5 uteri and E11.5 deciduas from young and aged pregnancies, as determined by MeDIP-seq. Statistical analysis by two-tailed t-test *p<0.05, **p<0.01, ***p<0.001, ****p<0.0001.

Overall, the majority of the 214 decidua DMRs were confined to intergenic and intronic regions, but a substantial proportion (~18%) were also located at promoters defined as immediately upstream (≤3kb) of the transcriptional start site (Appendix, Supplementary figure 7). 38 of the 214 DMRs overlapped CGIs, 16 of which were within the promoter group (Appendix, Supplementary figure 8). I hypothesised that loss of methylation may result in increased expression of the associated gene, and analysed the expression of genes associated with decidua DMRs in the corresponding RNA-seq datasets (Chapter 3). 93 DMRs were associated with a gene (i.e. within 2kb), and only 15/93 were significantly differentially expressed (Fig 5.4c). Moreover, similar fractions of these genes were up- as well as down-regulated, i.e. there was no consistent effect of differential methylation on the direction of gene expression changes (Fig 5.4d). However, when I used the 214 decidual DMRs for analysis with the Gene Regions Enrichment of Annotations tool (GREAT) (McLean et al.,

2010), two terms were significantly associated with these sites, notably the term "absent ectoplacental cone" (Fig 5.4e). This *per se* was surprising as the DMRs were identified in decidual tissue. However, these findings suggested that the genes regulated by these sites may be involved in placental development, and/or that these same genes have a function in trophoblast as well as decidual development, but that the latter is less well annotated. I performed motif analysis of the 214 DMRs, using the Analysis of Motif Enrichment (AME) tool in the MEME Suite package (McLeay and Bailey, 2010) to find known transcription factor binding motifs which were enriched in decidua DMRs. The only significantly enriched motif identified was specific to the binding site for the transcription factor *Ets2* (adjusted *p*-value = 1.28e-02) (Appendix, Supplementary table 6), which has been postulated to play an important role in decidualization as well as placentation (Georgiades et al., 2002; Salamonsen et al., 2003).

As region-specific alterations in DNA methylation were not detected in the uterus at E3.5, but had developed by E11.5, I hypothesised that 5mC is either lost, or fails to be deposited, at specific genomic regions during pregnancy in aged females. Globally, I found significantly reduced methylation at exons, CGIs, and promoters in E11.5 deciduas from aged versus young mothers (Fig 5.4f), suggesting this may indeed be the case. Interestingly, this is the opposite pattern to that observed at E3.5 of pregnancy. Focussing on young females, my data shows that the enrichment of 5mC at genomic features changes significantly between E3.5-E11.5. 5mC becomes more enriched at all features studied, apart from introns where it was depleted at E11.5 compared to E3.5 (Fig 5.4f). Most strikingly, 5mC was dramatically increased at exons, CGIs, and promoters at E11.5.

5.2.4 DNA methylation in the uterus is remodelled during pregnancy

This data, combined with the findings from Gao et al., 2012 that DNMT expression increases in the decidua at E7, suggest that DNA methylation may be remodelled as pregnancy progresses. Focussing on the young control samples only, a chromosome wide view of DNA methylation at E3.5 and E11.5 clearly shows that 5mC is globally altered between the two time-points, with significantly higher enrichment of 5mC across a large number of sites at E11.5 compared to E3.5 (Fig. 5.5a). This global pattern of 5mC acquisition with gestational progression is conserved in aged females.

To further investigate the behaviour of these dynamically changing 5mC sites, I analysed the MeDIP data for differential methylation, comparing uteri from young mothers at E3.5 with "young" decidua at E11.5. This identified 89,685 regions which were differentially methylated between the two stages, the bulk of which exhibited increased 5mC at E11.5 (Fig 5.5b). The majority of changes occurred at intergenic regions, approximately 10% were at promoter regions, 15% in exons, and 29% at introns (Appendix, Supplementary figure 7). 5356 differentially methylated windows overlapped with CGIs, with 1463 of these at promoter CGIs. The methylome dynamics in uteri and deciduas from aged females showed that these DNA methylation changes were globally similar to those observed in young females, when interrogated at the same loci (Fig 5.5c). This suggested that the acquisition of DNA methylation across these features occurs largely normally in aged pregnancies.

However, when assessing the DNA methylation dynamics between gestational stages between young and aged females, exons, CGIs, and promoter regions exhibited a significantly less pronounced enrichment of 5mC at E11.5 (Fig 5.5f). Strikingly, whilst 5mC became enriched at promoter regions in young females, there was no change at promoters in aged samples. These data suggest that DNA methylation remodelling at exons, CGIs, and promoters during decidual development is abnormal with advanced maternal age. Adding to this, on closer inspection of the 89,685 regions that gained DNA methylation between E3.5-E11.5 in young deciduas, I found that a subset of them remained hypomethylated in aged females compared to young. Using a differential methylation cut-off of 2 RPKM, I identified 331 regions which gained 5mC in deciduas from young mothers but failed to do so in deciduas from aged females (Fig 5.5d-e, g). This suggests that during pregnancy in aged females, although uterine methylome remodelling is largely successful, a small number of regions are resistant to methylation gain. I termed these sites "refractory DMRs".

The genomic distribution of these refractory DMRs was vastly different from the previously analysed sets of differentially methylated sites, with almost 50% located in promoters (Fig 5.5h), and a large proportion in CGIs (Appendix, Supplementary figure 7-8), in line with the genomic feature enrichment analysis (Fig 5.5f). This in itself suggested a potentially important role of these sites in uterine function and decidualization. However, enrichment analysis of refractory DMRs with GREAT did not reveal any terms relevant and specific to placentation (Fig 5.5i). Expression of genes overlapping refractory DMRs was altered in "aged" deciduas, with approximately half up-regulated and half down-regulated in

aged samples (Fig 5.5j). This suggests that the failure of refractory DMRs to gain methylation

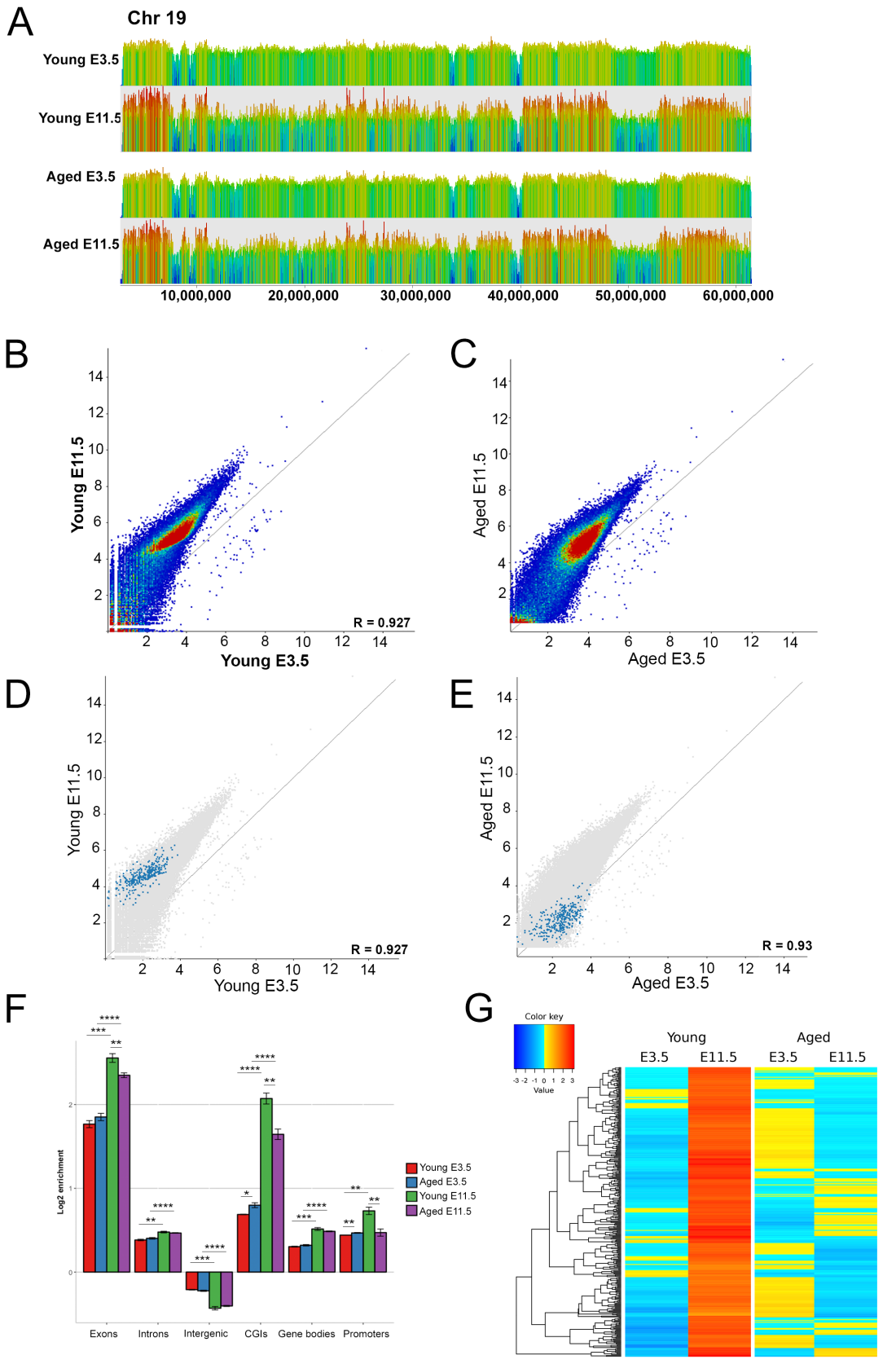

Figure 5.5 – DNA methylation remodelling in the decidua is incomplete in aged pregnancies.

a) Overview of the relative levels of 5-methylcytosine across the entirety of chromosome 19 in E3.5 uteri and E11.5 deciduas from young and aged females, as measured by MeDIP-seq.

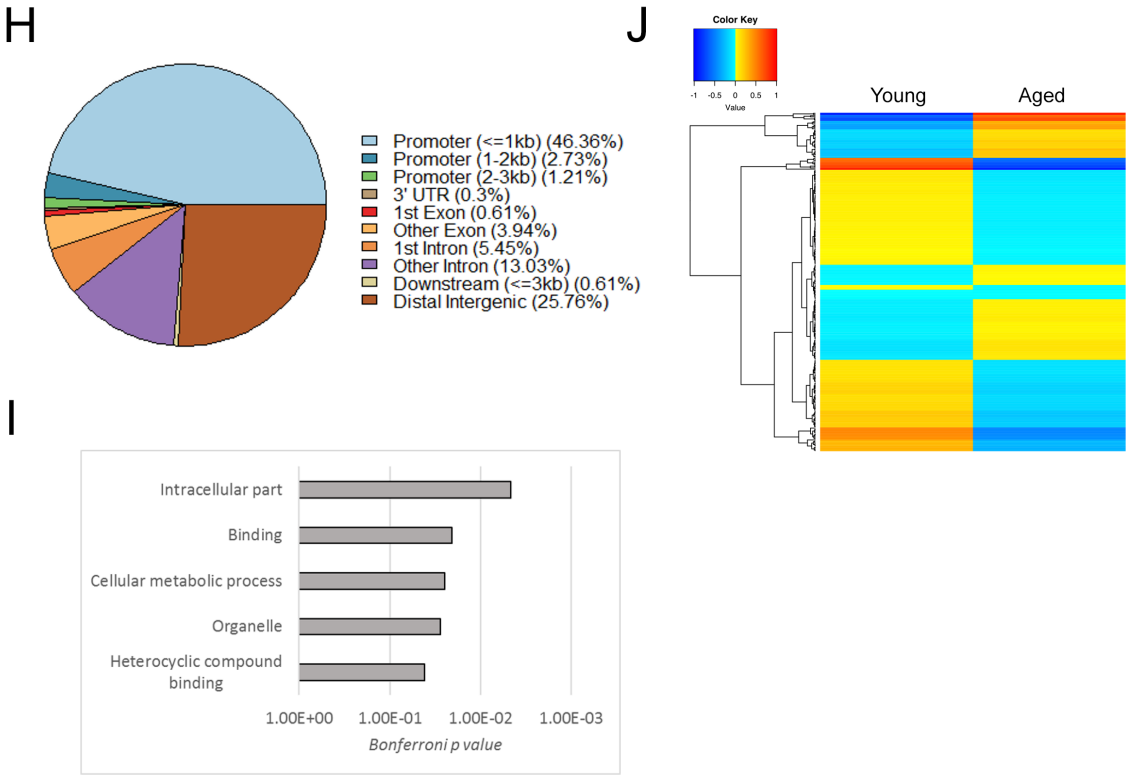

b) DNA methylation changes in young pregnancies. Scatterplot showing the relative levels (RPKM) of 5mC in regions found to be differentially methylated between young E3.5 uteri and E11.5 deciduas, by MEDIPS analysis of MeDIP-seq data. The overwhelming majority of regions gain methylation between E3.5-E11.5.

c) DNA methylation changes in aged pregnancies. Scatterplot showing the relative levels of DNA methylation in aged E3.5 uteri and E11.5 deciduas, at regions which are differentially methylated during pregnancy in young deciduas (Fig5.5b).

d) Repeat of scatterplot in Fig 5.5b, with refractory DMRs highlighted in blue. These regions gain methylation in young pregnancies between E3.5-E115.

e) Repeat of scatterplot in Fig5.5c, with refractory DMRs highlighted in blue. These regions do not change in terms of methylation level in aged deciduas between E3.5-E11.5.

f) The relative enrichment (log2 transformed) of 5-methylcytosine in genomic features in E3.5 uteri and E11.5 deciduas from young and aged pregnancies, as determined by MeDIP-seq. Statistical analysis by two-tailed t-test*p<0.05, **p<0.01, ***p<0.001, ****p<0.0001. Repeat of plot shown in Fig 5.4f.

g) Heatmap showing the relative levels of DNA methylation at refractory DMRs in young and aged pregnancies, between E3.5-E11.5. Refractory DMRs gain methylation in young pregnancies,but fail to do so in aged pregnancies.

h) Pie chart showing the distribution of refractory DMRs in genomic features. 3' UTR, 3'

in aged pregnancies does not systematically affect gene expression and decidual function at

untranslated region.

i) GREAT analysis of refractory DMRs, showing the enrichment of biological functional annotations at these regions.

j) Heatmap showing the expression of genes within 2kb of a refractory DMR in young and aged deciduas at E11.5. Note that gene expression changes are relatively small in magnitude and inconsistent in direction.

E11.5 of pregnancy, however this does not rule out the possibility that gene expression could be affected at earlier or later stages.

The 331 refractory DMRs did not overlap with DMRs found by directly comparing deciduas from young and aged females (Appendix, Supplementary figure 9), however decidual DMRs showed the same characteristics as refractory DMRs, gaining methylation during young pregnancies, and failing to gain methylation in aged pregnancies (Appendix, Supplementary figure 10). As mentioned earlier, decidual DMRs were enriched for the *Ets2* transcription factor binding motif. Interestingly, refractory DMRs were also enriched for the *Ets2* motif, as well as for a number of binding motifs specific for other TFs (Appendix, Supplementary table 6). These include members of the *Klf* family which are implicated in endometrial receptivity and female reproductive system pathologies (Simmen et al., 2015; Sun et al., 2012). These observations suggest that altered activity or availability of these TFs may prevent the acquisition of DNA methylation at refractory DMRs. Previous studies have found that TF binding to DNA can prevent DNA methylation (Marchal and Miotto, 2015), potentially by excluding the DNA methylation machinery. This suggests that increased DNA occupancy of *Ets2* and *Klf* TFs in aged pregnancies may block the acquisition of DNA methylation at refractory DMRs. While this possibility will require further investigation to confirm, it is strongly corroborated by the fact that expression levels of *Ets2* and some Klf family members are indeed increased in aged deciduas (Appendix, Supplementary figure 3).

5.2.5 DNA methylation in aged E11.5 trophoblast

DNA methylation plays a critical role during intra-uterine development, including in the development of extra embryonic tissues such as the trophoblast (Branco et al., 2016; Li et al., 1992; Okano et al., 1999; Tanaka et al., 2014), and is an important regulator of cell lineage decisions in the early embryo. Therefore, I analysed DNA methylation in trophoblast

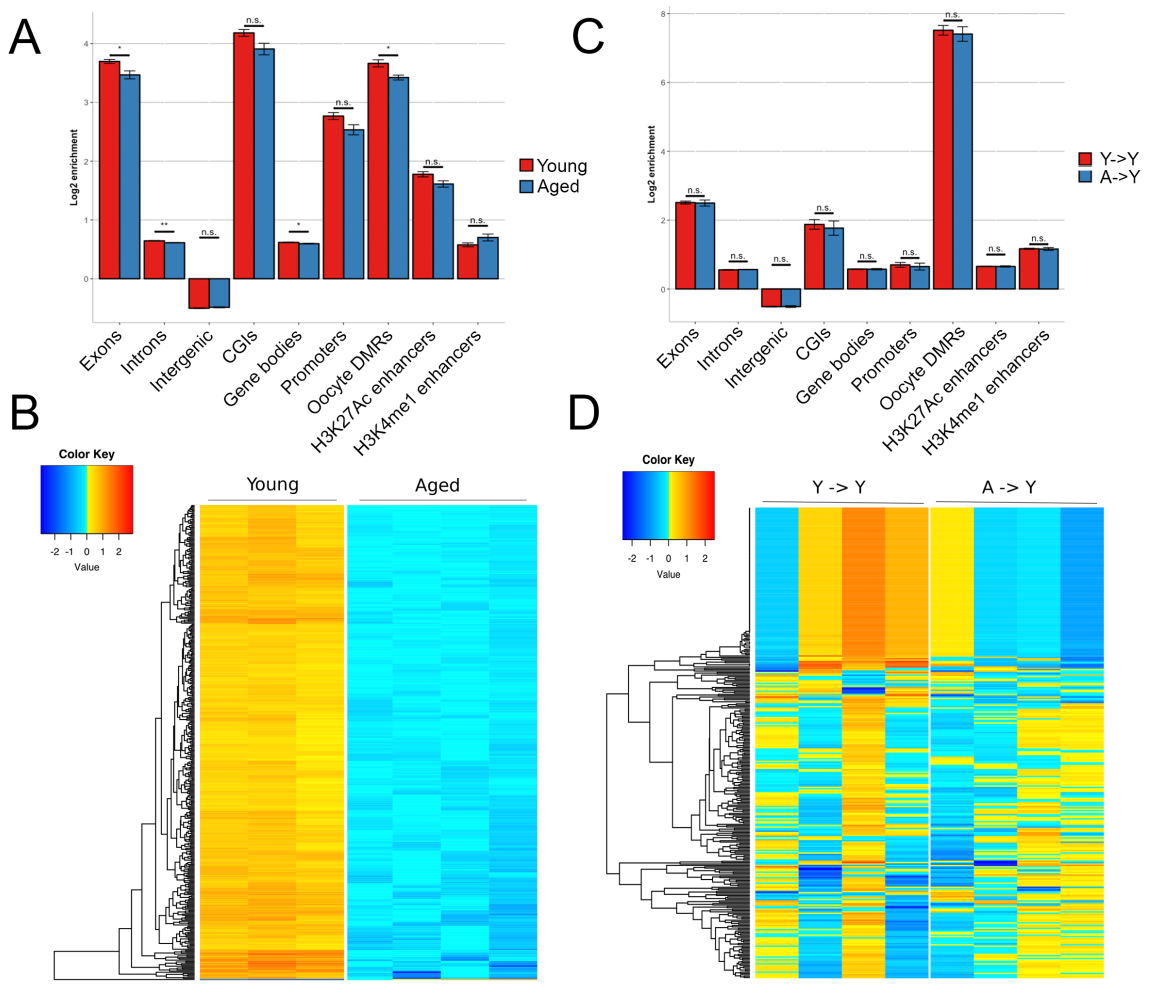

Figure 5.6 – Trophoblast from aged pregnancies loses DNA methylation at specific loci.

a) The relative enrichment (log2 transformed) of 5-methylcytosine in genomic features in E11.5 trophoblast from young (n=3) and aged (n=4) pregnancies, as determined by MeDIP-seq. Statistical analysis by one-way ANOVA followed by Tukey's post-hoc test *p<0.05, **p<0.01, ***p<0.001, ****p<0.0001.

b) Heatmap showing the relative levels of 5mC in trophoblast from young (n=3) and aged (n=5) pregnancies at E11.5.

c) The relative enrichment (log2 transformed) of 5-methylcytosine in genomic features in trophoblast from Y->Y (n=4) and A->Y (n=4) transfers, as determined by MeDIP-seq. Statistical analysis by two-tailed t-test *p<0.05, **p<0.01, ***p<0.001, ****p<0.0001.

d) Heatmap showing the relative levels of 5mC in trophoblast from Y->Y (n=4) and A->Y (n=4) transfers.

from young and aged pregnancies at E11.5 by MeDIP-seq, using DNA isolated from the same samples on which RNA-seq was performed in Chapter 3. This analysis showed that although the distribution of methylation across the genome was overall very similar between young and aged trophoblast, there was a small but significant decrease in enrichment of 5mC at

gene bodies, and in both introns and exons (Fig 5.6a). Trophoblast from aged females was also significantly depleted for 5mC in a set of differentially methylated regions (DMRs) inherited from the oocyte (Smallwood et al., 2011) (Fig 5.6a). Using MEDIPS, I identified 344 DMRs in trophoblast from aged mothers (excluding sex chromosomes), almost all of which showed depletion of 5mC in aged samples (Fig 5.6b). These DMRs should be confirmed by amplicon sequencing of bisulphite treated DNA. Trophoblast DMRs were enriched for genes with relevance to trophoblast development, including regulation of biosynthetic processes, genes based on mouse models with female fertility defects and negative regulation of stem cell differentiation (Appendix, Supplementary figure 13), suggesting these loci may be involved in abnormal trophoblast development in aged females. In a similar way to that described for genes associated with refractory DMRs, genes associated with trophoblast DMRs were not robustly or consistently differentially expressed in aged trophoblast (Appendix, supplementary figure 11).

As I showed in Chapter 3, transfer of embryos from aged females to young surrogate mothers rescued placental development on a gross morphological and transcriptional level. To investigate the effect of A->Y embryo transfer - compared to Y->Y transfer - on the DNA methylation landscape, I performed MeDIP-seq on DNA isolated from the same trophoblast samples which were analysed by RNA-seq. The methylomes of trophoblast from Y->Y and A->Y transfers were indistinguishable, both in terms of enrichment of 5mC in genomic features, and at the 344 trophoblast DMRs (Fig 5.6d-e). This lends further support to the hypothesis I put forward in Chapter 3, that the trophoblast compartment of embryos from aged mothers is intrinsically normal but develops abnormally when exposed to an aged maternal environment due to age-related defects in uterine function.

Trophoblast DMRs did not overlap with the DMRs identified in decidua from aged females, or “refractory DMRs” (Appendix, Supplementary figure 9), confirming there is no confounding effect of contamination with the other placental compartment. Intriguingly, however, the *Ets2* TF binding motif was also significantly enriched in trophoblast DMRs (adjusted *p* value = 4.70e-02) (Appendix, Supplementary table 6), similar to its enrichment in refractory DMRs in the decidua (Fig 5.5k). This suggests that there may be a common mechanism underlying the failing acquisition of DNA methylation at these DMRs in the trophoblast and decidua in aged pregnancies.

5.3 Discussion

In this chapter I have shown that advanced maternal age is associated with robust changes in the epigenetic landscape of uterine and placental tissues, with disturbances in both DNA methylation, and H3K4me3 histone modification. As ageing is clearly accompanied by changes to the epigenetic landscape in many contexts, impacting on cellular function, I hypothesised that age-related epigenetic changes may contribute to the decidualisation defects observed in aged uteri.

In Chapter 4 I showed that USCs from aged females were unable to adequately undergo *in vitro* decidualization, partially due to impaired up-regulation of the progesterone receptor. As activating histone modifications such as H3K4me3 mark promoters of actively transcribed genes (Gu and Lee, 2013; Santos-Rosa et al., 2002), I hypothesised that alterations in H3K4me3 deposition may disrupt the regulation of gene expression in aged USCs. H3K4me3 was indeed perturbed in aged USCs, with significant enrichment and depletion of H3K4me3 in aged cells at a large number of promoters associated with decidualization, such as *Hand2* and the *Hoxa10/11* cluster. In line with my findings that genes regulated by *Pgr* are abnormally expressed in uteri from aged females, I found that genes associated with a *Pgr* binding site in the aged uterus are also associated with abnormal levels of H3K4me3 (and show differences in gene expression). There are a number of possibilities for the mechanism behind this observation. Firstly, abnormal levels of H3K4me3 in aged USCs may alter the accessibility of the chromatin, thereby preventing *Pgr* binding at its target genes, or allowing binding at ectopic sites. Consequently, this may perturb transcriptional regulation by *Pgr*. Alternatively, perturbation of *Pgr* target gene regulation – possibly due to its reduced expression and/or impaired interaction with co-activators – may affect the deposition of H3K4me3, resulting in the abnormal H3K4me3 and transcriptional landscapes I have shown in aged USCs. It is unclear whether the abnormal distribution of H3K4me3 leads to the abnormal gene expression profile in aged USCs, or if H3K4me3 is a readout of expression. This is an area of active discussion in the field of epigenetics, and efforts to tease apart the relationship between H3K4me3 and transcription are ongoing (Cano-Rodriguez et al., 2016; Howe et al., 2017). It is also possible that the histone methyltransferase machinery is perturbed by ageing. For example, expression of the H3K9 methyltransferase *Suv39h1* decreases with age in mouse and human hematopoietic stem cells (HSCs), with a concomitant global decrease in H3K9me3 and altered HSC

differentiation (Djeghloul et al., 2016). This explanation is less likely in the case of ageing USCs, as global levels of H3K4me3 are unchanged, and expression of the H3K4me3 methyltransferases *Prdm9, Kmt2a, Kmt2b,* and *Kdm5b*, and demethylase *Jarid1b* is not altered in aged USCs (Appendix, Supplementary figure 12).

However, the most striking finding was the discovery of very broad regions of H3K4me3 marking USC identity genes, as observed in a variety of other cell types where they are associated with cell identity and transcriptional consistency with increased paused PolII occupancy (Benayoun et al., 2014). Interestingly, in aged USCs H3K4me3 peaks were significantly less broad at these regions, suggesting that the maintenance of open chromatin and transcriptional consistency at key USC identity genes is disrupted with advanced maternal age. I could not show this directly with the data available, but this could easily be investigated by ATAC-seq and single-cell RNA-seq as a measure of chromatin accessibility and transcriptional consistency, respectively.

The DNA methylome of uterine tissues during pregnancy has remained largely unstudied. Hence, I focused on DNA methylation in the uterus and decidua through the progression of pregnancy, to gain some insight into the role of DNA methylation in normal pregnancy, before attempting to delineate the effects of ageing. Through MeDIP-seq analysis, I observed a dramatic remodelling of the DNA methylome in the uterus/decidua between E3.5-E11.5 of pregnancy. This is characterised by enrichment of 5mC throughout the genome, especially at CGIs, with the exception of intergenic regions at which 5mC is depleted. From my data I cannot show whether global 5mC levels are altered during pregnancy, however my findings suggest that DNA methylation levels may increase in the decidua as pregnancy progresses. This should be investigated in the future by mass spectrometry. A previous study by Gao et al., 2012 supports these observations, showing that expression of both *Dnmt1* and *Dnmt3a* is induced in the uterus during decidualization. Inhibition of DNA methylation disrupts the decidualization response of uterine stromal cells, leading to embryonic demise. Taken together, this suggests that the deposition of DNA methylation in the uterus is of major importance during pregnancy, and disruption of this can affect decidualization, placentation, and embryo development.

Although my data suggest that uterine DNA methylation remodelling does take place during pregnancy, the MeDIP libraries were sequenced in 2 batches separating E3.5 and E11.5 samples. Therefore, these results may be confounded by batch effects during sequencing and the libraries should be re-sequenced in a single lane to control for this

effect. However, the pregnancy-stage related changes that are observed are robust and consistent across all replicates, suggesting they reflect true biological changes. This finding should be followed by analysis of uterine/decidual DNA methylation at multiple stages of pregnancy to more intricately assess the timing and effects of DNA methylome remodelling during pregnancy. Although previous studies have suggested a role for dynamic DNA methylation in the uterus across the estrous cycle in mice and menstrual cycle in humans (Guo, 2012; Houshdaran et al., 2014), this is the first direct evidence that DNA methylation in the pregnant uterus is highly dynamic. DNA methylation remodelling may be regulated through the activity of pregnancy hormones (Ghabreau et al., 2004; Logan et al., 2013; Yamagata et al., 2009), and could reflect the need for tightly regulated transcriptional responses that are required for successful decidualization and placentation.

After characterising the dynamic changes in DNA methylation during early pregnancy, I was able to investigate the effect of advanced maternal age on this process. As mentioned earlier, a previous study showed that inhibition of DNA methyltransferase activity during early pregnancy disrupted the decidualization response of USCs (Gao et al., 2012), leading to a remarkably similar phenotype to that seen in pregnancies from aged females. This suggested that aberrant DNA methylation may play a role in reproductive decline with advanced maternal age, and warrants further investigation. Prior to decidualization, uterine tissues from aged females exhibited very few perturbations in 5mC at specific loci, suggesting they are largely normal in terms of DNA methylation. Aged pregnancies displayed DNA methylome remodelling similar to that observed in young pregnancies, however a small number of regions remained refractory to this gain in methylation. This suggests that the acquisition of DNA methylation remains incomplete at specific sites in aged pregnancies, leading to the emergence of refractory decidual DMRs in aged pregnancies. Although I could not equate differential methylation at refractory DMRs with consistent changes in gene expression, reduced DNA methylation levels may render these sites permissive for transcriptional activation. Indeed, E11.5 decidua DMRs were associated with pregnancy related genes, suggesting they may have functional consequences at earlier or later time points during gestation.

Refractory DMRs in the deciduas of aged females may represent a delay in the acquisition of 5mC, similar to the delayed transcriptomic signature shown in Chapter 4. Alternatively, they may reflect a context specific inability to methylate these regions in aged pregnancies. It may be that refractory DMRs are rendered inaccessible to the DNA

methylation machinery, potentially by abnormal transcription factor binding activity as has been suggested in other contexts (Blattler and Farnham, 2013; Hervouet et al., 2010; Marchal and Miotto, 2015). Indeed, refractory DMRs are enriched for transcription factor binding motifs specific to a number of *Klf* family TFs, as well as *Ets2.* These TFs have known roles in decidualization (Salamonsen et al., 2003; Simmen et al., 2015; Sun et al., 2012), and are also more highly expressed in aged E3.5 uteri. Thus, it is likely that increased TF abundance leads to stronger or temporally prolonged genomic occupancy of their target sites, preventing these sites from becoming methylated in a timely manner. Alternatively, physical interactions between these TFs and the DNA methyltransferase machinery may alter DNMT catalytic activity. This is less likely, as DNA methylation was globally largely as normal in aged pregnancies, and the DNMTs were expressed at comparable levels in young and aged tissues (Appendix, Supplementary figure 12). Another possibility is that physical interaction between TFs and DNMTs could alter the targeting of DNMTs to genomic sites. This is possible, as *Ets2* has indeed been shown to interact with *Dnmt1 (Hervouet et al., 2010)*, however *Ets2* expression is increased in uteri from aged females (Appendix, Supplementary figure 3) which would be expected to promote DNA methylation targeting to its binding sites.

The importance of DNA methylation in the trophoblast compartment is well known, with most studies focusing on the maintenance of monoallelic expression at imprinted regions, where one parental allele is expressed and the other repressed, often by DNA methylation. I did not see any clear impact of advanced maternal age on DNA methylation in classical imprinted regions, however 5mC was significantly depleted in trophoblast from aged females at a set of DMRs carried over from the oocyte, as identified by Smallwood et al., 2011. MeDIP-seq analysis also revealed the presence of age-related hypomethylated DMRs in the trophoblast compartment at other sites, unrelated to oocyte-inherited DNA methylation.

Interestingly, the presence of trophoblast DMRs was similar to the situation observed in decidua from aged females where 5mC was reduced at a number of specific loci. Both E11.5 decidua and trophoblast DMRs were enriched for the *Ets2* TF binding motif, suggesting there may be a common mechanism involved in the emergence of maternal-age-associated DMRs in the trophoblast and decidua. Hypothetically, dys-regulation of a paracrine signal originating from the aged uterus/decidua may affect the activity of *Ets2* and other TFs in

both the decidua and trophoblast. This could lead to the loss of, or failure to gain 5mC at specific regions by a number of potential mechanisms, as discussed above.

Perhaps one of the most compelling observations of this analysis was that this site-specific depletion of DNA methylation was not evident in trophoblast from A->Y transfer conceptuses, i.e. upon development of embryos from aged mothers in a young maternal environment. Thus, these DMRs do not originate from epigenetic changes in the ageing oocyte or from defects in the protection of maternal methylation marks during preimplantation development. Instead, these findings demonstrate that the embryo's epigenome can be affected by the uterine environment. In the future this should be confirmed by direct analysis of the identified DMRs by pyrosequencing, and ideally the putative paracrine signals identified, for example by comparative mass spectrometric analysis of the secretomes of young and aged decidual tissues.

Chapter VI
Discussion

6.1 Age-associated developmental defects in the embryo and placenta

Maternal age is a significant risk factor for obstetric complications, and fetal developmental abnormalities in pregnancy. A significant proportion of pregnancy failure in older mothers can be attributed to aneuploidy and other age-related changes in the oocyte. However, some clinical studies have recognised that euploid pregnancies also fare significantly worse in older mothers, with increased risk of developing the "Great Obstetrical Syndromes". The ageing oocyte is unlikely to be the source of these particular pregnancy complications. Instead, this spectrum of complications is most frequently attributable to abnormal function of the placenta in pregnancies uncomplicated by advanced maternal age (Brosens et al., 2011). Development of the placenta is reliant on proper implantation of the conceptus into the uterine wall, and remodelling of the endometrium and maternal vasculature to support growth and development of the placenta and embryo. Thus, this implicates ageing of the uterus in the genesis of such developmental defects and obstetric complications in advanced maternal age.

Analysis of the gross morphology of conceptuses from B6 females between 48-52 weeks of age showed that the offspring of aged female mice are significantly more developmentally variable than those from young mothers. They are also affected by fetal growth restriction ranging from mild to severe, an increased resorption rate, and heart and brain defects, confirming and building on findings from previous studies (Lopes et al., 2009; Talbert and Krohn, 1966). These outcomes closely resemble the developmental abnormalities that are part of the "Great Obstetrical Syndromes" which are prevalent in older women, including fetal growth restriction, miscarriage, and pre-eclampsia. The similarities in maternal age-associated complications of pregnancy suggest that the B6 mouse can be used as model to mechanistically study uterine ageing, which may be conserved in humans. Aside from the morbidity directly associated with fetal growth restriction, offspring affected by low birth weight are subject to the long-lasting consequences of the pre-natal environment throughout their adult life. Fetuses affected by growth restriction due to an adverse *in utero* environment are thought to develop adaptations to cope with the pre-natal milieu, adapting them also to a thrifty, deprived environment after birth. This becomes deleterious in adult life if nutritional supply is plentiful, i.e. if there is a drastic imbalance between resource supply during pre- and

postnatal environment. For this reason, low birth weight and 'catch-up growth' postnatally are associated with an increased risk of hypertension, ischemic heart disease, diabetes, and kidney disease in adults (Barker, 1990, 1992; Ojeda et al., 2008). This hypothesis of fetal programming was first put forward by Dr David Barker, who suggested that the genesis of adult disease was programmed during gestation, with poor nutrition in prenatal life increasing susceptibility to the effects of an affluent diet during adulthood (Barker, 1990, 1992). Maternal age has been shown to increase the susceptibility of offspring from older females to cardiovascular disease as adults (Cooke et al., 2018). This highlights the importance of my work to not only address the immediate maternal and fetal morbidity and mortality associated with pregnancy in advanced maternal age, but also the effects of fetal programming on the offspring of older mothers into the future.

The embryonic defects which I have shown to commonly occur in older mice (growth restriction, resorption, and heart and brain defects), can be causally linked with abnormal development of the placenta (Linask, 2013; Perez-Garcia et al., 2018). In line with this, and previous gross histological findings from Lopes et al 2009., I found that although morphologically normal embryos exhibited largely normal placental development, abnormal embryos were accompanied by abnormal placentas. Abnormal placentas were characterised by underdevelopment of the labyrinth compartment and overabundance of TGCs. I performed in depth transcriptomic analysis which showed that the trophoblast differentiation program was perturbed by advanced maternal age, with increased expression of TS cell and TGC markers at the expense of SpT and SynT. Interestingly, a subset of placentas from older pregnancies exhibited trophoblast defects on the transcriptomic level, even when the placenta and embryo appeared grossly normal at E11.5. This suggests that all offspring of aged mothers may be subject to an adverse *in utero* environment. It is possible that grossly normal placentas (and embryos) exhibit more subtle developmental defects that were not detected, or that some defects will only manifest, or become more severe, later in gestation. Indeed, a recent study by the group of Rebecca Jones (Lean et al., 2017) – in a design very similar to ours – analysed the placentas of conceptuses developed in aged B6 females at E18.5, and found that they exhibit a diminished nutrient transport capacity. They further link this placental dysfunction to fetal growth restriction and stillbirth in women of advanced maternal age. This study showed there are similarities in placental phenotype with increased placental weight and decreased efficiency, as well as altered uteroplacental vascular function, although the phenotype is more severe in the mouse than in humans.

These findings strongly corroborate my own – my data focuses on the effects of maternal age in early pregnancy up to mid-gestation, whereas theirs focuses on late pregnancy events which would affect conceptuses that appear normal at E11.5.

My data indicate that the extent of maternal ageing has an effect on the severity of trophoblast abnormalities. The gene expression profiles of E11.5 deciduas associated with grossly normal embryos from 43-week old females were globally more similar to those from young mothers compared to those from 45-47 week old females. This prompts the question of when in maternal ageing these transcriptomic changes associated with reproductive decline begin to appear, if their onset is abrupt or gradual, and how rapidly they progress. My results suggest that there is a surprisingly rapid decline in placental development between 43 and 45 weeks of age in B6 mice. These questions should be further investigated by analysis of decidual and trophoblast development in females across a wider range of ages.

6.2 Uterine ageing is the dominant cause of reproductive decline in mice

Developmental defects in the offspring of older females may occur due to either deterioration in the quality of oocytes, or due to a decreasing ability of the uterus to support pregnancy (Kong et al., 2012; Nelson et al., 2013). In a study from 1966, Talbert and Krohn performed reciprocal embryo transfer between young and old mice. This showed that whilst the young uterus is able to support development of embryos from aged females, embryos from young females transferred to an older surrogate mother did not survive to term (Talbert and Krohn, 1966). Similarly, Schulkey et al 2015 showed that ovarian transplantation from young to aged females did not reduce the incidence of cardiac defects in the offspring of aged females, and vice versa transplants of aged ovarian tissue into young females did not affect fetal cardiac development. If assuming that these cardiac defects are caused by placental abnormalities, this study further supports the data from Talbert and Krohn, as well as my own. My findings confirm these results, as embryonic development was rescued by transfer of embryos from aged donors to young females. Furthermore, I found that placental development was also rescued by embryo transfer both at the gross morphological and transcriptional level, providing strong evidence that embryonic and placental defects in

advanced maternal age occur as a result of age-related changes in the uterus, and not the oocyte. This does not rule out the possibility that embryos are programmed during transit through the fallopian tubes in the aged donor as noted by Talbert and Krohn in 1966, however we saw no clear effect of donor age on the outcome of the transfer process.

During my studies, we did not perform the reciprocal transfer of embryos from young females into aged recipients, to follow up the Talbert and Krohn data on the molecular level. This was because it is very difficult to synchronise aged females and obtain vaginal plugs at a reasonable rate, in concert with having 'young' embryos ready for transfer on a given day. The inefficiency of plug rates of aged females, and the presumptive lower pregnancy rates one would obtain, prohibited this experiment from being feasible within the constraints of mouse numbers, expert technical help available (i.e. limited time availability of the technician performing embryo transfers for these experiments) and last but not least, cost.

Having shown that the source of embryonic and placental defects resides with the mother, I went on to perform the first in depth characterisation of the maternal decidua at mid-gestation in aged females. I identified a number of genes which are affected by maternal age in the E11.5 decidua, some of which were confirmed by RT-qPCR and western blot. A number of genes involved in decidualization, including *Bmp2, Il15ra, Gdf10*, and *Itgb8,* as well as placenta specific genes such as Pregnancy-specific Glycoproteins and members of the Prolactin family were expressed abnormally in aged deciduas. This suggested that decidualization and subsequent development of the decidua proceeds abnormally in aged females. Dys-regulated genes were also enriched for gene annotations such as hormone, secreted, and ECM-receptor interaction, suggesting that communication between the maternal decidua and fetal trophoblast is disrupted in aged pregnancies.

Comparison of E11.5 deciduas from aged females with a time course of decidual development from E9.5-E12.5 indicated that development of the decidua in aged pregnancies was delayed by up to 2 days. On the strength of my data I therefore suggest that the delay in the progression of decidualization is the root cause of the placental defects that ensue. Abnormal development of the decidua can indeed lead to failure in placental and embryonic development. One study found that maternal deletion of *Il11rα* allows implantation and decidualization to occur, but causes the decidua to subsequently degenerate. This leads to embryonic death and an abnormal placenta with reduced SpT and SynT, and large numbers of TGCs (Bilinski et al., 1998), a strikingly similar phenotype to aged

pregnancies. Other studies have similarly found that defects in decidualization disturb development of the placenta, with deleterious effects on the embryo (Gehin et al., 2002; Hirota et al., 2010; Jeong et al., 2007). Taken together, this suggests that developmental delay of the decidua in aged pregnancies may disturb communication at the feto-maternal interface, thus perturbing trophoblast differentiation and function with a knock-on effect on embryo development.

6.3 Immune cell ageing is likely not involved in the etiology of placentation defects of aged females

The maternal immune system has been proposed to play an important role in development of the decidua during pregnancy. Immune cells are abundant in the pregnant decidua, a large proportion of which are uNK cells, with smaller numbers of DCs and macrophages. Their role in the decidua is not well understood, however uNK cells and DCs may interact with each other and play a role in mediating trophoblast invasion, spiral artery remodelling, and decidual angiogenesis (Ashkar et al., 2000; Blois et al., 2008; Croy et al., 2003; Guimond et al., 1997). Despite a reduction in the numbers of peripheral NK that we saw in aged females and that are in line with previous reports (Guo et al., 2014), my results show that the abundance and maturation of uNK cells in the decidua is unaffected. Aged pregnancies do show slight reductions in the number of DCs and macrophages in the decidua. DC cells have been shown to be important in decidualization, although these results have remained controversial (Plaks et al., 2008). Thus, decreased DC numbers may possibly contribute to the retardation of decidual development, but is unlikely to be the primary cause as the changes are minimal. I hence focused in more detail on effects of maternal ageing unrelated to immune cells.

6.4 Trophoblast differentiation defects can be recapitulated in vitro using conditioned medium from aged decidual stromal cells

The decidua plays a key role in regulating invasion and differentiation of the trophoblast to form a functional placenta (King and Loke, 1994). It is thought the decidua acts to limit the

invasive properties of the trophoblast, as trophoblast tissue appears to invade unimpeded when decidual tissue is absent, as in ectopic pregnancies. Conversely, in pre-eclampsia, trophoblast invasion into the uterine wall is too shallow and remodelling of the maternal spiral arteries remains inadequate. This results in placental under-perfusion, and fetal growth restriction (Bibeau et al., 2016; Cartwright et al., 2010; Krishna and Bhalerao, 2011; Mandala and Osol, 2012).

The decidua produces large quantities of signalling molecules including cytokines, which provide cues to the trophoblast regulating its invasion and differentiation (Menkhorst et al., 2012). Notable examples of stromal cell-produced cytokines that affect trophoblast development and/or invasion are prolactin-related factors such as Prl8a2 in the mouse (Alam et al., 2007) and LIF, PRL, and IGFBP1 in human pregnancy (Garrido-Gomez et al., 2017; Kojima et al., 1995). The cross-talk between decidual stromal and trophoblast cells works in both directions with multiple feedback mechanisms. For example, proinflammatory cytokines and chemokines, as well as angiogenic/static factors are induced in decidualized endometrial stromal cells in response to trophoblast-secreted products (Hess et al., 2007). These decidual functions constitute a mechanism of how the decidua can impact on development of the trophoblast. This prompted me to investigate the effect of maternal age on paracrine signals from the uterine stroma to the trophoblast. I found that differentiation of TS cells, in the presence of conditioned media from aged USCs promoted rapid downregulation of TS cell markers *in vitro.* Trophoblast differentiation was skewed towards the TGC lineage, at the expense of other lineages. This recapitulated some of the characteristics of trophoblast differentiation in aged pregnancies *in vivo* remarkably closely. Differentiation to SynT was however, unaffected. This is unsurprising as it is difficult to differentiate TS cells to SynT *in vitro,* perhaps suggesting the absence of an important factor such as physical contact with maternal cells*,* or reciprocal communication between the decidua and trophoblast.

Overall, my data suggest that retarded decidual development disrupts communication at the feto-maternal interface. What precisely constitutes the change in the secretome of aged versus young uterine stromal cells remains to be determined in the future, for example by SILAC (Stable Isotope Labelling using Amino acids in Cell culture) experiments in which the proteins produced by the two cell populations are labelled by different isotopes followed by mass spectrometric identification of significant differences in

proteome composition. What seems to be the case, however, is that an altered communication signal that originates from aged uterine stromal cells impacts on trophoblast differentiation and disturbs the formation of a functionally normal placenta.

6.5 Endometrial decidualization is perturbed in aged females due to cell intrinsic defects

Embryos derived from aged females are able to develop into normal conceptuses when provided with a young uterine environment during gestation. This suggests that blastocysts derived from aged females are competent and able to give rise to a normal embryo and placenta. As I have shown, this implicates abnormal function of the maternal uterus during aged pregnancies as the root cause of embryo and placenta developmental defects in older mothers. Therefore, I next focused on studying maternal age-related changes in the endometrium during pregnancy.

In the mouse, the first physical contact between embryo and uterus occurs during implantation, beginning on the morning of day 4 when the uterus acquires receptivity. The success of this interaction relies on steroid hormone induced priming of the uterus in the preceding days. Days 1-2 of pregnancy are dominated by E2 signalling, which strongly stimulates proliferation of the LE. Corpora lutea form from the post-ovulation follicles, and begin to produce large quantities of P4 at E2.5 which antagonises the E2 mediated proliferation of the LE, and stimulates proliferation of the underlying stroma in a process referred to as endometrial priming. My data from RNA-seq and IHC analyses of the uterus at E3.5 provide evidence which suggests that this priming process is abnormal in uteri from aged females. In the majority of cases, proliferating cells can still be seen in the LE of aged uteri at E3.5, whereas there are many fewer proliferating cells in the stroma. Additionally, epithelial specific genes such as *Ltf* and *Areg* (Campbell et al., 2006) are up-regulated in uteri from aged females at E3.5, whereas markers of the uterine stroma such as *Des* and *Hand2* are less highly expressed. This suggests that hormonal priming of the uterus and the acquisition of uterine receptivity is abnormal or delayed in aged females. Data from a recent study indicates that implantation may also be delayed in aged females, as Chicago blue staining which indicates vascular permeability at implantation sites is severely reduced in aged uteri on E5 of pregnancy, suggesting that implantation has not yet occurred in aged

females at this time (Li et al., 2017). This priming defect may be a result of the progesterone resistance I have demonstrated in the age endometrium, as well as insufficient luteal support as has been suggested previously in aged females (Harman and Talbert, 1970).

Advanced maternal age does not appear to affect the ability of the endometrium to become receptive, or facilitate implantation *per se,* as there is no significant reduction in the total number of implantation sites in aged pregnancies. However, implantation may be delayed until uterine receptivity is acquired, potentially causing a shift in timing of the window of implantation in aged females. Mice and many other mammals are able to physiologically delay implantation to avoid pregnancy in times of stress, in a process known as diapause (Fenelon et al., 2014). However delayed implantation in other contexts can lead to developmental defects later in pregnancy in both the mouse and human (Cha and Dey, 2014; Macklon et al., 2002; Song et al., 2002; Wang and Dey, 2006). This may occur due to disruption of the synchronised communication between the blastocyst and uterus that is required for successful pregnancy.

A number of studies in the 1950s and '60s showed that aged ovariectomized (OVX) females undergo a severely reduced decidualization reaction when subjected to artificial decidualization involving treatment with exogenous hormones and physical stimulation of the endometrium (Holinka and Finch, 1977; Ohta, 1987; Shapiro and Talbert, 1974). In this thesis I have also found that aged females fail to mount a robust response to artificial decidualization. Additionally, I have shown that USCs isolated from aged mice at E3.5 of pregnancy are unable to upregulate markers of decidualization upon *in vitro* decidualization, despite supplementation with steroid hormones. In fact, USCs from aged females undergoing *in vitro* decidualization show very few transcriptional changes in response to hormonal treatment, and those changes in gene expression that do occur are severely reduced in magnitude compared to USCs from young females. These results indicate that the decidualization defect in aged females is due to an intrinsic defect in aged USCs, and not simply the effect - for example - of reduced maternal hormone levels.

Furthermore, I have shown that levels of pStat3, a critical mediator of Pgr transcriptional activation, are significantly reduced in aged USCs. Importantly, the *in vitro* decidualization defect could not be rescued by supplementation with Lif during *in vitro* decidualization, showing this is not a result of reduced Lif production by the uterine glands. There is some evidence that pStat3 in the stroma is regulated by *Hbegf,* which acts via the

Egfr/Erk axis to phosphorylate Stat3 (Zhang et al., 2013). However, my data show that pStat3 levels are decreased, despite increased expression of *Hbegf* in aged pregnancies. This further supports the idea of a cell intrinsic defect in the ability of aged USCs to respond to hormones and growth factor signals.

These results led me to conclude that the endometrium becomes resistant to the action of steroid hormones during female ageing, leading to an attenuation and/or delay of the decidualization response in early pregnancy. The effects of this delay can still be detected in aged pregnancies at E11.5, when the decidua exhibits a transcriptomic signature very similar to that of earlier stages of pregnancy at E9.5-E10.5, indicating that its development is delayed by up to 2 days. This delay in differentiation of the endometrium and development of the decidual compartment is likely to disrupt the highly orchestrated and synchronised signalling between the maternal and fetal tissues at the feto-maternal interface. This is critical for successful pregnancy, and thus may lead to the abnormal placental development that I have shown is prevalent in pregnancies in aged females.

It is however unclear how closely the decidualization response induced experimentally *in vitro* and *in vivo* reflects the physiological situation during pregnancy. Specifically, the decidualization failure observed *in vitro* and in deciduomas may be more pronounced than that *in vivo.* Decidualization during pregnancy in aged females clearly occurs to an extent which can support adequate implantation of the embryo, and to some extent placental development, and it is also noteworthy that some pups within litters of aged females develop entirely normally. A number of previous studies have found that decidual swellings during pregnancy are of a similar size in pregnancies from young and aged mice (Blaha and Leavitt, 1974; Finch and Holinka, 1982; Holinka et al., 1979; Maibenco and Krehbiel, 1973), whereas deciduoma swellings are severely impaired in aged females (Holinka and Finch, 1977; Shapiro and Talbert, 1974). This may be due to differences in the response of the uterus to artificial decidualization and physiological pregnancy. The deciduoma assay induces a decidualization response that reflects decidualization *in vivo* in terms of induction of stromal proliferation and differentiation. However, the artificial decidualization response occurs throughout the entirety of the uterine horn and the overall size of deciduomas is far greater than that of a localized decidual reaction, and also entails differences in gene expression (Herington et al., 2009). Pregnancy occurs in the presence of paracrine signals produced by the embryo, which affect, but are not required for normal

decidualization (Herington et al., 2009). Therefore, embryo derived signals during early pregnancy may improve the decidualization response in aged females compared to artificial decidualization. However, the presence of developmental abnormalities in the embryo and placenta at mid-gestation show that a placentation defect does occur which may be a result of abnormal endometrial decidualization, caused by a cell intrinsic defect as I have described.

6.6 Progesterone responsiveness in the uterus declines with age

As discussed above, events during early pregnancy, including hormonal priming of the endometrium, and the decidualization reaction are abnormal and/or delayed in aged females. These events are regulated mainly by the steroid hormones E2 and P4. The serum concentration of E2 and P4 has been shown to fluctuate in the estrous cycle and during pregnancy in aged females (Holinka et al., 1979; Lu et al., 1979), suggesting that reproductive decline could be a by-product of declining hormone levels with age. However, in this thesis I have shown evidence of an intrinsic defect in the responsiveness of the uterus - and USCs in particular - to steroid hormones, as discussed in the previous section. Decreased hormone responses may be mediated by reduced levels or activity of the estrogen and progesterone receptors, *Esr1* and *Pgr*. Studies in other contexts have indeed found that tissue responses to hormones are decreased during ageing, accompanied by reduced expression of hormone receptors (Roth, 1995; Thakur, 1988).

In the ageing reproductive system, *Esr1/2* expression in the rodent uterus declines with age (Hsueh et al., 1979; Saiduddin and Zassenhaus, 1979), and interaction between E2 and *Esr1/2* in the nucleus is diminished (Belisle et al., 1985; Gesell and Roth, 1981). Declining expression of *Esr1/2* could itself be a result of decreased E2 levels, as *Esr1/2* expression is regulated by binding to its own promoter (Clark et al., 1974; Mester et al., 1974; Pavlik and Coulson, 1976). However, one study found that whilst supplementation with E2 induced expression of *Esr1/2* in the uterus of young females, this did not occur to the same extent in aged mice (Belisle et al., 1985). Impaired uterine responsiveness to P4 in advanced maternal age has not been widely reported in rodents, however one study found that administration of P4 failed to downregulate the expression of *Esr1/2* in the LE of aged rats (Saiduddin and Zassenhaus, 1979) that occurs on day 3 of pregnancy. My IHC data also suggests that the

attenuation of *Esr1* signalling by *Pgr* may disrupted with age, as E2 mediated proliferation of the LE persisted at E3.5 in aged females. These data suggest that the ability of the LE to respond to P4 declines with age.

My results show that the expression and distribution of both *Esr1* and *Pgr* are abnormal in the LE of aged females during early pregnancy. Their expression is also reduced in USCs isolated from the E3.5 uterus, suggesting impaired hormone responsiveness may be linked to reduced expression of the steroid hormone receptors. Uterine responses to E2 are not dramatically affected by maternal ageing as E2 mediated stimulation of proliferation in the LE occurs robustly in aged females. However, P4 responses are severely affected, as shown by the sustained proliferation and expression of E2 response genes observed in the LE at E3.5, and failure to stimulate the proliferation and decidualization of USCs both *in vitro* and *in vivo*. The effects of this P4 resistance persist throughout pregnancy leading to developmental delay in the decidua, as can be seen at E6.5 when the wave of decidualization and *Pgr* expression expands to the secondary decidual zone in young pregnancies, but is restricted to the primary decidual zone in aged pregnancies. Decidual angiogenesis may also be affected in aged pregnancies, as *Pgr* expressing USCs secrete large quantities of angiogenic factors in response to P4 (Kim et al., 2013). This may impair blood flow to the uterus thus reducing perfusion of the placenta and the supply of nutrient rich blood to the fetus.

As well as decreased expression of the progesterone receptor, the expression and activation of Pgr co-activators are also affected in aged pregnancies. Expression of *Ncoa4*, a Pgr coactivator, fails to be induced in USCs on *in vitro* decidualization, which may affect the ability of Pgr to effect transcriptional responses (Kollara and Brown, 2012). Most strikingly, the expression, activation and localisation of pStat3 is abnormal in aged pregnancies. pStat3 is an important coactivator of Pgr in the uterus and is essential for implantation and decidualization (Lee et al., 2013; Sun et al., 2013). I have shown pStat3 levels are decreased in the LE and USCs of aged females during early pregnancy, and that pStat3 appears to be confined to the cytoplasm in the uterine stroma of aged pregnant females. Reduced expression of pStat3 in the LE at E3.5 as can be seen by IHC may contribute to the failure/delay in counteracting E2 stimulated proliferation and gene expression in the LE, which is mediated by Pgr. The exclusion of pStat3 from the nucleus in the stromal compartment suggests that the interaction between Pgr and pStat3 in USCs is reduced. This

may contribute to the impaired P4 responses observed in aged pregnancies, due to reduced transcriptional activation of Pgr target genes. The interaction between Pgr and its co-activators in aged USCs should be investigated in more detail in future studies to confirm the disruption of this interaction, and to study the effect on Pgr target genes.

The unusual subcellular localisation of pStat3 in the uterine stroma of aged females is intriguing. After Stat3 phosphorylation by JAK at the plasma membrane, pStat3 is translocated to the nucleus in a process that requires receptor-mediated endocytosis (Bild et al., 2002). The abnormal localisation of pStat3 in the uterine stroma in aged pregnancies is reminiscent of that observed when receptor-mediated endocytosis is inhibited (Bild et al., 2002), suggesting that this process may be reduced or blocked in aged pregnancies. As abnormalities in receptor-mediated endocytosis have been implicated in ageing in the context of liver sinusoidal epithelial cells in the rat (Simon-Santamaria et al., 2010), it would be interesting to explore this mechanism in detail in future studies.

6.7 Acquisition of a P4-resistant phenotype is reminiscent of human endometrial pathologies that increase with age

Intriguingly, the finding that the diminished and delayed decidualization response in aged female mice exhibits key features of a blunted P4 responsiveness is remarkably similar to the P4-resistant phenotype seen in a spectrum of endometrial pathologies in women. Intriguingly, many if not most of these, notably fibroids, adenomyosis and endometriosis, become markedly more prevalent with age and are also associated with fertility and pregnancy problems in the affected women (Benagiano et al., 2012; Bulletti et al., 2010; Zimmermann et al., 2012). Uterine fibroids (leiomyoma) are benign tumours of the myometrium. They are common, and by the age of 50 around 70% of Caucasian women and more than 80% of women of Afro-Caribbean descent will have at least one fibroid (Baird et al., 2003; Stewart et al., 2017). Adenomyosis is a condition where endometrial cells are found in the myometrium, causing pain and heavy menstrual bleeding. Endometriosis is a condition where endometrial cells are found outside the uterine cavity, which is also associated with severe pain and discomfort. All these pathologies have an underlying aetiology linked to a reduced endometrial responsiveness to P4, and predispose to a similar spectrum of pregnancy complications as those associated with advanced maternal age,

including infertility, miscarriage, preterm birth and fetal growth restriction (Al-Sabbagh et al., 2012; Li et al., 2014; Vannuccini et al., 2016). These correlations make it very likely that women of advanced age also exhibit at least some decidualization problems. My studies prompt for an in-depth investigation of the decidualization response of USCs from young and older women, as the age-related decline in hormone responsiveness may be conserved in humans. One recent study showed that USCs isolated from older women are able to mount an *in vitro* decidualization response (Gibson et al., 2018), however this was not compared to USCs from young women and therefore did not address the question of whether hormone responsiveness declines in advanced maternal age. It will be important to control for uterine pathologies when studying these ageing effects, to be able to account for potential confounding factors of any deficiency observed. Since older IVF patients do still become pregnant it is also possible that perhaps the age-associated decidualization defects are not as pronounced in women as they are in mice. However, given the above-mentioned correlations in particular with regard to the shared P4-resistant phenotype, and the hugely under-appreciated impact of age on uterine function, this is definitely an area that deserves careful and comprehensive investigations in the future.

6.8 Potential impact of ageing physiology on the reproductive ageing phenotype

Ageing is accompanied by physiological changes which may contribute to the reproductive ageing phenotype which I have described in this thesis. Ageing is associated with a shift in body composition, including loss of lean muscle mass and increased visceral fat and hepatic lipid deposits. The reason for these alterations in body composition aren't fully understood, but may relate to a decline in resting metabolic rate of 1-2% per decade, increasing respiratory quotient, and reduced physical activity (Johannsen and Ravussin, 2010). Most adults gradually gain weight throughout their lives at a rate of about 0.5kg/year (Lumsden and Hor, 2015), and as such being overweight or obese becomes more prevalent with increasing age. Data from the UK office of national statistics indicates that population obesity increases with age up to the age of 55-64, however there is a relatively small increase in obesity from the 25-34 to the 35-54 age brackets (statistics, 2017) – the age group at the highest risk of obstetric complications. Maternal overweight and obesity is an independent risk factor for pregnancy complications including pre-eclampsia, gestational

diabetes, miscarriage, stillbirth, fetal overgrowth and growth restriction, and congenital heart defects (Leddy et al., 2008). The impact of advanced maternal age on perinatal outcomes overlaps with these, with increased risk of pre-eclampsia, miscarriage, stillbirth, and fetal growth restriction as mentioned previously. It is likely that maternal age interacts with obesity in the pathogenesis of these complications, indeed one study found that being overweight at any age increases the risk of obstetric complications, however the combined effect of maternal age $\geq$35 and overweight/obesity was particularly high risk for stillbirth and preterm delivery (Lamminpaa et al., 2016).

Similar to the human the body composition of the C57BL/6 mouse changes with age, with increased fat mass and a decrease in lean mass (Houtkooper et al., 2011). As maternal obesity is associated with similar obstetric complication as advanced maternal age, it is possible that maternal obesity may impact on the reproductive ageing phenotype I have described here. Mouse models of diet induced obesity during pregnancy commonly lead to fetal and placental overgrowth with increased placental transport (Kim et al., 2014; Nam et al., 2017; Rosario et al., 2015). A similar phenotype has been described in human pregnancies affected by maternal obesity, with the most striking outcomes being fetal macrosomia and placental overgrowth (Altmae et al., 2017; Stang and Huffman, 2016; Vinturache et al., 2015). Importantly, I have shown that advanced maternal age in mice is associated with developmental variability and fetal growth restriction with no indication of the fetal overgrowth that is commonly reported with maternal obesity. This suggests that the maternal ageing phenotype is unlikely to be a result of age-related increases in adiposity. However, in some cases, maternal obesity is instead associated with fetal growth restriction in humans and some mouse models of diet induced obesity (Higgins et al., 2011; Howell and Powell, 2017; Luzzo et al., 2012; Radulescu et al., 2013). Fetal growth restriction in pregnancies complicated by maternal obesity may result from hypertensive disorders of pregnancy such as pre-eclampsia which are more prevalent in obese pregnancies, and are associated with fetal growth restriction. Therefore, it is possible that my results are affected by obesity-induced hypertension in aged females, which may contribute the restricted fetal growth commonly observed in the offspring of aged females.

Ageing is also associated with increased insulin resistance and a decrease in glucose tolerance. This means that older individuals become progressively hyperinsulinemic and glucose intolerant with age, and are significantly more likely to be affected by type 2

diabetes prior to pregnancy, or to develop gestational diabetes mellitus (GDM) during pregnancy (Anna et al., 2008; Jolly et al., 2000; Lao et al., 2006). This may be a result of the increased deposition of visceral fat and obesity which occurs with ageing (Hardy et al., 2012). Indeed, maternal obesity is a risk factor for GDM (Chu et al., 2007; Leddy et al., 2008), and both conditions are associated with increased risk for overlapping adverse perinatal outcomes, including macrosomia, pre-eclampsia, and congenital heart malformations (Billionnet et al., 2017; Leddy et al., 2008; Wendland et al., 2012). Mouse models of maternal obesity fed a high fat and/or high sugar diet exhibit characteristics of gestational diabetes including glucose intolerance and hyperinsulinemia, with impacts on fetal growth and development (Jones et al., 2009; Liang et al., 2010; Rosario et al., 2015).

Maternal obesity and diabetes impact on placental development and function (Howell and Powell, 2017; Vambergue and Fajardy, 2011). This raises the question of whether the fetal and placental defects associated with advanced maternal age are in fact a result of the accompanying adiposity and insulin resistance. Most relevant to maternal ageing, one study found that high fat diet induced obesity in female mice was associated with decreased size of the labyrinth compartment (Kim et al., 2014), similar to that seen in placentas from aged females. Placentas from diet induced diabetic mouse models also show signs of cellular necrosis and haemorrhage which was not observed in aged pregnancies (Liang et al., 2010). Therefore, while it is possible that the reduction in labyrinth size observed in placentas from aged females could be a result of maternal-age associated obesity or diabetes, placentas from obese/diabetic pregnancies exhibit additional defects that are not present in aged, suggesting that age-related placental defects are either not driven by maternal obesity/diabetes, or represent a milder phenotype caused by minor age-associated body composition and metabolic changes compared to the severe changes caused by a high fat/high sugar diet.

A key aspect of the reproductive ageing phenotype I have described is a severely reduced decidualization response in aged females. A mouse model of maternal obesity induced by a high fat/high sugar diet has been shown to exhibit an impaired decidualization response similar to that of aged mice, however, this was again associated with fetal and placental overgrowth rather than growth restriction (Rhee et al., 2016), suggesting that distinct mechanisms underlie the reproductive defects occurring as a result of maternal obesity and advanced maternal age.

In the future, it would be useful to directly compare the morphology and transcriptome of placentas, and the decidualization response from young, aged, obese, and diabetic females to delineate the individual contributions of age, obesity, and insulin resistance to the reproductive ageing phenotype. It would also be desirable to characterise the age-related physiological changes in female mice to attempt to attribute age-related defects to cellular ageing, adiposity, or metabolic defects. This question could also be addressed by examining the impact of advanced maternal age on endometrial decidualization and placental development in a mouse model which is not affected by age-related adiposity or insulin resistance.

6.9 Ageing leads to changes in the epigenetic landscape of the placenta

In most tissues, ageing is accompanied by changes in the epigenetic landscape, with altered patterns of DNA methylation and histone modifications leading to an abnormal chromatin state in aged organisms (Pal and Tyler, 2016). This can impact on cellular function and lead to age-related diseases (Calvanese et al., 2009).

Having already shown that USCs derived from aged females exhibit profound differences in their gene expression, I found that these transcriptional differences were accompanied by changes in the abundance of H3K4me3 at the promoter regions of genes which exhibit differential expression. In line with current knowledge, genes which were more highly expressed in aged USCs had more H3K4me3 at their promoter, and vice versa. Affected genes included those with relevance to decidualization, such as *Hand2* and the *Hoxa10/11* cluster, suggesting that abnormal distribution of H3K4me3 in aged females affects the function of the uterine stroma. In addition, I found that the breadth of H3K4me3 peaks was significantly reduced in USCs from aged females, at key genes involved in decidualization such as *Hoxa10* and *Hoxa11.* Very broad regions of H3K4me3 are associated with cell identity genes, and promote the maintenance of open chromatin, transcriptional consistency, and occupancy of paused PolII (Benayoun et al., 2014). This may allow these key genes to be rapidly and robustly induced when necessary - in this case on initiation of decidualization - suggesting that perturbation of broad H3K4me3 domains in aged USCs may contribute to the failure/delay of decidualization responses in the aged female.

Studies in humans have suggested that DNA methylation changes in the endometrium occur throughout the menstrual cycle, regulating gene expression (Kukushkina et al., 2017). In addition, DNA methylation in the human endometrium changes with advancing age allowing biological age to be accurately estimated using Horvath's epigenetic clock (Horvath, 2013; Olesen et al., 2018). This suggests that DNA methylation in the endometrium may be altered during ageing, with potential effects on uterine function during early pregnancy. My results show that uteri from aged mice at E3.5 of pregnancy do not exhibit DNA methylation changes at specific loci that could be detected by MeDIP-seq analysis, however they do show an overall increase in 5mC enrichment at CpG islands as has been commonly described in ageing tissues (Pal and Tyler, 2016). There may be smaller changes in DNA methylation which could not be identified by MeDIP-seq, but could potentially be detected when measured at single base pair resolution by sequencing of bisulphite converted DNA.

Although I could not detect age-related changes in DNA methylation in the uterus at E3.5, my results showed a significant reduction in 5mC at specific DMRs in the deciduas from aged mothers at E11.5. I also found significant global reductions in 5mC in exons, CGIs, and promoters in aged decidua at E11.5. This suggested that the deposition of 5mC is perturbed in advanced maternal age and was particularly interesting as disruption of the DNA methylation landscape in the decidua has been linked with a mouse model of pregnancy failure (Brown et al., 2013). DMRs in the E11.5 decidua were enriched for regions associated with the mouse phenotype "absent ectoplacental cone". Although this was surprising as these DMRs were present in the maternal decidua, it may suggest that these sites are involved in placental development or have a role in the decidua which has not yet been established.

Noteworthy in this context is also that this reduced DNA methylation was not associated with notably changes in the expression levels of DNMTs (*Dnmt1*, *Dnmt3a/b*) or TET (*Tet1*, *Tet2*, *Tet3*) enzymes, at least not at the mRNA level. Protein amounts should be measured in future experiments. Since globally DNA methylation levels and distribution were not vastly dramatically altered, however, failures in much more specific targeting or protection mechanisms, rather than global changes in DNA methylation levels, seem to be at play.

Changes in the global distribution of 5mC between E3.5 and E11.5 in young pregnancies, and the emergence of decidual DMRs in aged pregnancies at E11.5 suggested that DNA methylation is dynamic and may be remodelled in the uterus/decidua between E3.5-E11.5. Through differential methylation analysis with MEDIPS I showed that a large number of genomic regions gained methylation between E3.5-E11.5. As DNA methylation has been shown to be important for decidualization (Gao et al., 2012), I suggest that DNA methylation remodelling may be an important process during decidualization and placentation. My results show that this DNA methylation remodelling occurs largely as normal in aged pregnancies, however a small number of regions, mainly located at promoters, fail to gain methylation. I termed these regions "refractory DMRs". Overall, my results lead me to suggest that DNA methylation in the aged uterus is largely normal during early pregnancy and does not contribute to altered function of the endometrium. However, in aged pregnancies, the decidua fails to gain DNA methylation at refractory DMRs which may affect development of the placenta, or may be a readout of abnormal decidual development in aged pregnancies.

Although the expression of genes associated with refractory DMRs was not significantly affected - in terms of the magnitude of gene expression differences, and consistency of direction - refractory DMRs were enriched for binding motifs specific to a small number of transcription factors including *Ets2* and members of the *Klf* family, which play a role in decidualization at earlier stages of pregnancy (Salamonsen et al., 2003; Simmen et al., 2015; Sun et al., 2012). This suggests that abnormal function of *Ets2* and other TFs, or their regulators, perturbs the deposition of DNA methylation at some TF binding sites. This could occur by a number of possible mechanisms. TF binding sites may be blocked, potentially by increased occupancy by TF binding to the DNA, or histone modifications that promote closed chromatin, thus precluding access of the DNA methyltransferase machinery to these binding sites as has been proposed before (Blattler and Farnham, 2013; Hervouet et al., 2010; Marchal and Miotto, 2015). This is an attractive possibility, in particular since *Ets2* expression levels seem indeed higher in aged deciduas, implying that increased Ets2 levels lead to longer or tighter occupancy at target sites and may prevent the required acquisition of DNA methylation at these sites in a timely manner. Alternatively, interaction between DNMTs and TFs such as *Ets2* could affect the targeting of DNA methylation or may affect the catalytic activity of the DNMTs. Ets2 has been reported to physically interact with *Dnmt1* and to affect its catalytic activity, although the direction of

dys-regulation (increase in *Ets2* expression) is opposite to what would be expected in the context of decidualization. In any case, these are attractive possibilities to explore in future work aimed at understanding why these specific DMRs are refractory to the acquisition of DNA methylation.

I found a similar pattern of DNA methylation defects in the trophoblast compartment in aged pregnancies, with a set of DMRs that showed decreased methylation in aged trophoblast. Trophoblast DMRs were enriched for annotations relating to female infertility, stem cell differentiation, and the regulation of biosynthetic processes. This suggests that they may be involved in differentiation and development of the trophoblast, and reduced methylation at these DMRs in aged placentas may contribute to the abnormal development of the trophoblast compartment that is clear in aged pregnancies. Interestingly, like refractory DMRs in the decidua, trophoblast DMRs were also significantly enriched for the *Ets2* binding motif. The enrichment of *Ets2* binding motifs in both refractory DMRs and trophoblast DMRs suggests they may form in response to a common mechanism, although at this time the identity of the factors involved is unknown. These data also corroborate that the de-regulated cross-talk between endometrium and trophoblast does indeed affect trophoblast differentiation and the trophoblast epigenome, with a paracrine factor affecting these processes. As I have shown that trophoblast DMRs are abolished in the placentas of embryos transferred from an aged mother to a young surrogate, they must ultimately arise as a result of an age-related defect in the maternal uterus.

6.10 Implications of endometrial ageing for human health

The trend of delaying childbirth till later in life clearly has important implications on the health of the mother during pregnancy, and development of the baby. It is now well established that older mothers are at higher risk of adverse pregnancy outcomes such as miscarriage, stillbirth, pre-eclampsia, and fetal growth restriction. As such, women who are pregnant or planning to become pregnant beyond the age of 35 should be counselled of their increased risk of such adverse outcomes and monitored closely during pregnancy.

The data I have presented here suggest that abnormal development of the placenta mediates abnormal development of the embryo, most commonly leading to fetal growth restriction which is known to commonly occur as a result of placental insufficiency (Burton

and Jauniaux, 2018). An adverse environment during gestation such as that in growth restricted pregnancies can have lifelong effects on the health of the offspring. Growth restricted babies are more likely to develop cardiovascular, metabolic, and endocrine disease in later life due to the imbalance between the undernourished environment in utero, and the plentiful nutrition experienced by most in post-natal life (Kwon and Kim, 2017). This presents a significant burden to those affected and to healthcare services, and as such is may be beneficial to inform prospective parents of the potential long-term implications of reproducing in later life to enable informed decisions to be made.

The findings I have presented here suggest that reduced hormone responsiveness of the aged endometrium may underlie the abnormal placental development and adverse pregnancy outcomes observed in aged pregnancies – at least in mice. This mechanism may be conserved in human pregnancies, indeed the common fetal outcomes of aged pregnancy in mice – growth restriction, resorption, congenital heart defects – are mirrored when studying human populations (Carolan and Frankowska, 2011; Hollier et al., 2000; Huang et al., 2008; Mills and Lavender, 2011), although as discussed earlier there are significant differences in the reproductive physiology of mice and humans. My results suggest that ageing of the uterus is the most important factor in the mouse with relatively little contribution of oocyte ageing to embryo and placental development in aged females – the vast majority of embryo resorptions and congenital malformations are rescued by transfer to a young foster mother. However, the relative contribution of uterine and oocyte ageing in humans may be slightly different, with a relatively smaller impact from the ageing uterus and larger from the oocyte. It is well known that human ageing is associated with an exponential increase in chromosomal aberrations and aneuploidies, leading to miscarriage and aneuploid syndromes in the offspring, whereas the increased prevalence of obstetric complications unrelated to the oocyte have been more difficult to tease out in human populations, possibly due to variations between different populations and the interaction with other age-related physiological changes as described above. Nevertheless, endometrial ageing is likely to have a substantial impact on reproductive health and pregnancy in later life, and greater understanding of the progesterone resistance that develops with age may lead to the development of interventions to improve reproductive performance in older pregnancies, and treat conditions such as endometriosis and adenomyosis which are associated with progesterone resistance and become increasingly prevalent with age (Benagiano et al., 2012; Bulletti et al., 2010; Zimmermann et al., 2012).

The importance that is currently bestowed on maternal-age related changes in the oocyte has led to an increase in the practice of egg freezing to preserve fertility, as well as older women using young donor oocytes. While these interventions may stop the ticking of the oocyte ageing clock, they will do nothing to prevent endometrial ageing, and therefore will not guarantee a successful, healthy pregnancy. There is currently little evidence-based advice or treatment to slow endometrial ageing, however one study suggested that suppression of estrous cyclicity in mice by ovariectomy or long-term progesterone treatment prevents age-related changes to the transcriptional profile of the myometrium in aged females (Chong et al., 2016). The effect of estrous suppression on endometrial ageing is yet to be seen, but if this was found to be effective in preventing endometrial decline would be a simple and widely available intervention in the form of progesterone-based contraceptives.

6.11 Conclusion

The increase in women delaying childbearing till later in life is set to continue for the foreseeable future, and so the impact of the increased risk of obstetric complications and congenital abnormalities in this group is an important consideration.

It is well known that pregnancy in advanced maternal age carries an increased risk of chromosomal abnormalities and mitochondrial dysfunction that occur as a result of age-related changes in the oocyte. However, the contribution of uterine ageing to development of the “Great Obstetrical Syndromes” and congenital malformations that are unrelated to karyotypic abnormalities in pregnancies in older women is less well understood.

In this work I have shown that the ageing uterus is the source of a large proportion of the embryonic and placental defects which are common during pregnancy in aged mice. This is related to a decline in uterine function during early pregnancy, characterised by a reduction in the ability of the endometrium to respond to hormone and growth factor signals and undergo decidualization. A blunted decidualization response in aged females is likely to perturb the highly orchestrated signalling programme at the feto-maternal interface. This has a knock-on effect on development of the placenta, contributing to abnormal differentiation of the trophoblast compartment and affecting placental function and embryo development.

Abnormal decidualization and development of the placenta with advanced maternal age is accompanied by changes in the epigenetic landscape, and abnormal patterns of H3K4me3 and DNA methylation, which may contribute to the developmental defects that are prevalent in aged pregnancies.

In this thesis I have explored and highlighted the issue of declining endometrial function with advanced maternal age, and hope that these findings will prompt further mechanistic investigation into this area in the mouse, and also fundamentally in humans. Increasing our understanding of the effects of advanced maternal age on uterine function during pregnancy may allow us to minimise the risk to mother and baby during, and improve pregnancy outcomes in older mothers.

6.12 Future directions

In this thesis I have shown that female B6 mice aged 43 weeks and over exhibit a delay in placental development, with a transcriptional signature showing retardation by up to 2 days. Surprisingly, females aged 43 weeks show much milder transcriptional abnormalities than those aged just 2 weeks older. This prompts the question of when in maternal ageing do these abnormalities arise, and how rapidly does uterine function decline? It would be interesting to analyse placental development in mice at a variety of ages between 8-47 weeks to answer these questions.

From my RNA-seq data of pseudo-pregnant uteri and USCs I have identified a number of novel candidate genes which are dys-regulated during decidualization in aged pregnancies. In the future these candidates could be further investigated to elucidate their precise role in decidualization by over-expression and/or CRISPR knockout in USCs. In this work I have focussed on age-related defects in USCs, however the luminal epithelium and uterine glands display histological changes in aged females (Craig, 1981; Lejeune et al., 1981; Maibenco and Krehbiel, 1973; Martin et al., 1970). My results show that some LE markers are differentially expressed with age, and that LE proliferation persists in aged females at E3.5, suggesting they may also be resistant to the action of P4. This warrants further investigation into the function of the luminal and glandular epithelia in advanced maternal age. This could be done by isolation of individual cell types by laser capture microdissection

followed by genome-wide sequencing, or generation of endometrial epithelial organoids derived from young and aged uteri (Boretto et al., 2017; Turco et al., 2017).

I have also shown that factors secreted by aged USCs during *in vitro* decidualization affect the differentiation of TS cells. This work could be built on by characterising the factors which are absent/produced at abnormal levels in USCs from aged females, and studying their impact on trophoblast differentiation *in vitro.* This approach could be expanded by co-culturing USCs in direct contact with trophoblast cells or explants to more closely recapitulate the feto-maternal interface and the effect of USC ageing trophoblast function. Recently, it was reported that human TS cells can be derived from human blastocysts and trophoblast (Okae et al., 2018). Therefore, this experiment could also be performed using human TS cells and USCs to study the communication between the uterine stroma and trophoblast in older women.

My results showed that maternal ageing is accompanied by a decline in the ability of the endometrium to respond to hormonal and growth factor signals. This appears to be due to decreased expression of steroid hormone receptors and coactivators, particularly Pgr and pStat3, however the precise mechanism has not yet been elucidated. My results suggest that physical interactions between Pgr and pStat3 in the nucleus are perturbed with age, as *pStat3* is not able to translocate to the nucleus *in vivo.* Future studies should confirm the absence/reduction of Pgr/pStat3 interaction in aged USCs by co-immunoprecipitation, and investigate the effect of abolishing Pgr/pStat3 interactions on the robustness of transcriptional activation by Pgr, and the repertoire of target genes with which it interacts. The exclusion of pStat3 from the nucleus in the uterine stroma of aged females is likely to contribute to the impaired Pgr response, as it interacts with Pgr in the nucleus to facilitate transcriptional responses. The mechanism behind this abnormal localisation should be studied further, as promoting translocation of pStat3 to the nucleus could improve the activation of Pgr target genes, and therefore also the decidualization response.

Finally, some of the experiments I have performed could easily be performed using cells derived from human endometrial biopsies to determine whether uterine ageing occurs in a similar way in humans. For example, USCs can be isolated from endometrial biopsies and cultured and decidualized *in vitro.* These experiments will need to be carefully controlled for, in particular with regard to confounding factors such as other uterine

pathologies that increase with age. A thorough investigation in this area is much warranted on the basis of my findings.

References

ABS (2008). 3301.0 - Births. Canberra.. A.B.o. Statistics, ed.

Achache, H., and Revel, A. (2006). Endometrial receptivity markers, the journey to successful embryo implantation. Hum Reprod Update *12*, 731-746.

Adams, R.H., Porras, A., Alonso, G., Jones, M., Vintersten, K., Panelli, S., Valladares, A., Perez, L., Klein, R., and Nebreda, A.R. (2000). Essential role of p38alpha MAP kinase in placental but not embryonic cardiovascular development. Mol Cell *6*, 109-116.

Afonso, S., Tovar, C., Romagnano, L., and Babiarz, B. (2002). Control and expression of cystatin C by mouse decidual cultures. Mol Reprod Dev *61*, 155-163.

Al-Sabbagh, M., Lam, E.W., and Brosens, J.J. (2012). Mechanisms of endometrial progesterone resistance. Mol Cell Endocrinol *358*, 208-215.

Alam, S.M., Konno, T., Dai, G., Lu, L., Wang, D., Dunmore, J.H., Godwin, A.R., and Soares, M.J. (2007). A uterine decidual cell cytokine ensures pregnancy-dependent adaptations to a physiological stressor. Development *134*, 407-415.

Alam, S.M., Konno, T., Sahgal, N., Lu, L., and Soares, M.J. (2008). Decidual cells produce a heparin-binding prolactin family cytokine with putative intrauterine regulatory actions. J Biol Chem *283*, 18957-18968.

Altmae, S., Segura, M.T., Esteban, F.J., Bartel, S., Brandi, P., Irmler, M., Beckers, J., Demmelmair, H., Lopez-Sabater, C., Koletzko, B*., et al.* (2017). Maternal Pre-Pregnancy Obesity Is Associated with Altered Placental Transcriptome. PLoS One *12*, e0169223.

Anna, V., van der Ploeg, H.P., Cheung, N.W., Huxley, R.R., and Bauman, A.E. (2008). Sociodemographic correlates of the increasing trend in prevalence of gestational diabetes mellitus in a large population of women between 1995 and 2005. Diabetes care *31*, 2288-2293.

Anson-Cartwright, L., Dawson, K., Holmyard, D., Fisher, S.J., Lazzarini, R.A., and Cross, J.C. (2000). The glial cells missing-1 protein is essential for branching morphogenesis in the chorioallantoic placenta. Nat Genet *25*, 311-314.

Ashkar, A.A., Black, G.P., Wei, Q., He, H., Liang, L., Head, J.R., and Croy, B.A. (2003). Assessment of requirements for IL-15 and IFN regulatory factors in uterine NK cell differentiation and function during pregnancy. J Immunol *171*, 2937-2944.

Ashkar, A.A., Di Santo, J.P., and Croy, B.A. (2000). Interferon gamma contributes to initiation of uterine vascular modification, decidual integrity, and uterine natural killer cell maturation during normal murine pregnancy. J Exp Med *192*, 259-270.

B. Anne Croy, A.T.Y., Francseco J. DeMayo, S. Lee Adamson (2013). The guide to investigation of mouse pregnancy (Academic Press).

Baird, D.D., Dunson, D.B., Hill, M.C., Cousins, D., and Schectman, J.M. (2003). High cumulative incidence of uterine leiomyoma in black and white women: ultrasound evidence. Am J Obstet Gynecol *188*, 100-107.

Baird, D.T., Collins, J., Egozcue, J., Evers, L.H., Gianaroli, L., Leridon, H., Sunde, A., Templeton, A., Van Steirteghem, A., Cohen, J*., et al.* (2005). Fertility and ageing. Hum Reprod Update *11*, 261-276.

Baker, T.G. (1963). A QUANTITATIVE AND CYTOLOGICAL STUDY OF GERM CELLS IN HUMAN OVARIES. Proceedings of the Royal Society of London Series B, Biological sciences *158*, 417-433.

Bany, B.M., and Cross, J.C. (2006). Post-implantation mouse conceptuses produce paracrine signals that regulate the uterine endometrium undergoing decidualization. Dev Biol *294*, 445-456.

Barak, Y., Nelson, M.C., Ong, E.S., Jones, Y.Z., Ruiz-Lozano, P., Chien, K.R., Koder, A., and Evans, R.M. (1999). PPAR gamma is required for placental, cardiac, and adipose tissue development. Mol Cell *4*, 585-595.

Barber, E.M., and Pollard, J.W. (2003). The uterine NK cell population requires IL-15 but these cells are not required for pregnancy nor the resolution of a Listeria monocytogenes infection. J Immunol *171*, 37-46.

Barker, D.J. (1990). The fetal and infant origins of adult disease. BMJ (Clinical research ed) *301*, 1111.

Barker, D.J. (1992). Fetal growth and adult disease. British journal of obstetrics and gynaecology *99*, 275-276.

Baser, E., Seckin, K.D., Erkilinc, S., Karsli, M.F., Yeral, I.M., Kaymak, O., Caglar, T., and Danisman, N. (2013). The impact of parity on perinatal outcomes in pregnancies complicated by advanced maternal age. Journal of the Turkish German Gynecological Association *14*, 205-209.

Battaglia, D.E., Goodwin, P., Klein, N.A., and Soules, M.R. (1996). Influence of maternal age on meiotic spindle assembly in oocytes from naturally cycling women. Hum Reprod *11*, 2217-2222.

Beckman, D.A., and Brent, R.L. (1984). Mechanisms of teratogenesis. Annual review of pharmacology and toxicology *24*, 483-500.

Belisle, S., Bellabarba, D., and Lehoux, J.G. (1985). On the presence of nonfunctional uterine estrogen receptors in middle-aged and old C57BL/6J mice. Endocrinology *116*, 148-153.

Ben-Meir, A., Burstein, E., Borrego-Alvarez, A., Chong, J., Wong, E., Yavorska, T., Naranian, T., Chi, M., Wang, Y., Bentov, Y*., et al.* (2015). Coenzyme Q10 restores oocyte mitochondrial function and fertility during reproductive aging. Aging Cell *14*, 887-895.

Benagiano, G., Habiba, M., and Brosens, I. (2012). The pathophysiology of uterine adenomyosis: an update. Fertil Steril *98*, 572-579.

Benayoun, B.A., Pollina, E.A., Ucar, D., Mahmoudi, S., Karra, K., Wong, E.D., Devarajan, K., Daugherty, A.C., Kundaje, A.B., Mancini, E.*, et al.* (2014). H3K4me3 breadth is linked to cell identity and transcriptional consistency. Cell *158*, 673-688.

Benson, G.V., Lim, H., Paria, B.C., Satokata, I., Dey, S.K., and Maas, R.L. (1996). Mechanisms of reduced fertility in Hoxa-10 mutant mice: uterine homeosis and loss of maternal Hoxa-10 expression. Development *122*, 2687-2696.

Bhatt, H., Brunet, L.J., and Stewart, C.L. (1991). Uterine expression of leukemia inhibitory factor coincides with the onset of blastocyst implantation. Proceedings of the National Academy of Sciences of the United States of America *88*, 11408-11412.

Bibeau, K., Sicotte, B., Beland, M., Bhat, M., Gaboury, L., Couture, R., St-Louis, J., and Brochu, M. (2016). Placental Underperfusion in a Rat Model of Intrauterine Growth Restriction Induced by a Reduced Plasma Volume Expansion. PLoS One *11*, e0145982.

Bild, A.H., Turkson, J., and Jove, R. (2002). Cytoplasmic transport of Stat3 by receptor-mediated endocytosis. EMBO J *21*, 3255-3263.

Bilinski, P., Roopenian, D., and Gossler, A. (1998). Maternal IL-11Ralpha function is required for normal decidua and fetoplacental development in mice. Genes Dev *12*, 2234-2243.

Billionnet, C., Mitanchez, D., Weill, A., Nizard, J., Alla, F., Hartemann, A., and Jacqueminet, S. (2017). Gestational diabetes and adverse perinatal outcomes from 716,152 births in France in 2012. Diabetologia *60*, 636-644.

Blaha, G.C., and Leavitt, W.W. (1974). Ovarian steroid dehydrogenase histochemistry and circulating progesterone in aged golden hamsters during the estrous cycle and pregnancy. Biol Reprod *11*, 153-161.

Blattler, A., and Farnham, P.J. (2013). Cross-talk between site-specific transcription factors and DNA methylation states. J Biol Chem *288*, 34287-34294.

Block, E. (1952). Quantitative morphological investigations of the follicular system in women; variations at different ages. Acta anatomica *14*, 108-123.

Blois, S.M., Barrientos, G., Garcia, M.G., Orsal, A.S., Tometten, M., Cordo-Russo, R.I., Klapp, B.F., Santoni, A., Fernández, N., Terness, P.*, et al.* (2008). Interaction between dendritic cells and natural killer cells during pregnancy in mice. J Mol Med (Berl) *86*, 837-852.

Boretto, M., Cox, B., Noben, M., Hendriks, N., Fassbender, A., Roose, H., Amant, F., Timmerman, D., Tomassetti, C., Vanhie, A.*, et al.* (2017). Development of organoids from mouse and human endometrium showing endometrial epithelium physiology and long-term expandability. Development *144*, 1775-1786.

Borum, K. (1961). Oogenesis in the mouse. A study of the meiotic prophase. Experimental cell research *24*, 495-507.

Branco, M.R., King, M., Perez-Garcia, V., Bogutz, A.B., Caley, M., Fineberg, E., Lefebvre, L., Cook, S.J., Dean, W., Hemberger, M.*, et al.* (2016). Maternal DNA Methylation Regulates Early Trophoblast Development. Dev Cell *36*, 152-163.

Bratic, A., and Larsson, N.G. (2013). The role of mitochondria in aging. J Clin Invest *123*, 951-957.

Breart, G., Barros, H., Wagener, Y., and Prati, S. (2003). Characteristics of the childbearing population in Europe. Eur J Obstet Gynecol Reprod Biol *111 Suppl 1*, S45-52.

Brighton, P.J., Maruyama, Y., Fishwick, K., Vrljicak, P., Tewary, S., Fujihara, R., Muter, J., Lucas, E.S., Yamada, T., Woods, L.*, et al.* (2017). Clearance of senescent decidual cells by uterine natural killer cells drives endometrial remodeling during the window of implantation. bioRxiv.

Broekmans, F.J., Knauff, E.A., te Velde, E.R., Macklon, N.S., and Fauser, B.C. (2007). Female reproductive ageing: current knowledge and future trends. Trends in endocrinology and metabolism: TEM *18*, 58-65.

Brosens, I., Pijnenborg, R., Vercruysse, L., and Romero, R. (2011). The "Great Obstetrical Syndromes" are associated with disorders of deep placentation. Am J Obstet Gynecol *204*, 193-201.

Brosens, J.J., Hayashi, N., and White, J.O. (1999). Progesterone receptor regulates decidual prolactin expression in differentiating human endometrial stromal cells. Endocrinology *140*, 4809-4820.

Brown, L.Y., Bonney, E.A., Raj, R.S., Nielsen, B., and Brown, S. (2013). Generalized disturbance of DNA methylation in the uterine decidua in the CBA/J x DBA/2 mouse model of pregnancy failure. Biol Reprod *89*, 120.

Bulletti, C., Coccia, M.E., Battistoni, S., and Borini, A. (2010). Endometriosis and infertility. Journal of Assisted Reproduction and Genetics *27*, 441-447.

Burton, G.J., and Jauniaux, E. (2018). Pathophysiology of placental-derived fetal growth restriction. Am J Obstet Gynecol *218*, S745-s761.

Calvanese, V., Lara, E., Kahn, A., and Fraga, M.F. (2009). The role of epigenetics in aging and age-related diseases. Ageing Res Rev *8*, 268-276.

Campbell, E.A., O'Hara, L., Catalano, R.D., Sharkey, A.M., Freeman, T.C., and Johnson, M.H. (2006). Temporal expression profiling of the uterine luminal epithelium of the pseudo-pregnant mouse suggests receptivity to the fertilized egg is associated with complex transcriptional changes. Hum Reprod *21*, 2495-2513.

Cano, F., Simon, C., Remohi, J., and Pellicer, A. (1995). Effect of aging on the female reproductive system: evidence for a role of uterine senescence in the decline in female fecundity. Fertil Steril *64*, 584-589.

Cano-Rodriguez, D., Gjaltema, R.A.F., Jilderda, L.J., Jellema, P., Dokter-Fokkens, J., Ruiters, M.H.J., and Rots, M.G. (2016). Writing of H3K4Me3 overcomes epigenetic silencing in a sustained but context-dependent manner. Nature communications *7*, 12284.

Carney, E.W., Prideaux, V., Lye, S.J., and Rossant, J. (1993). Progressive expression of trophoblast-specific genes during formation of mouse trophoblast giant cells in vitro. Mol Reprod Dev *34*, 357-368.

Carolan, M., and Frankowska, D. (2011). Advanced maternal age and adverse perinatal outcome: a review of the evidence. Midwifery *27*, 793-801.

Carranza-Lira, S., Blanquet, J., Tserotas, K., and Calzada, L. (2000). Endometrial progesterone and estradiol receptors in patients with recurrent early pregnancy loss of unknown etiology--preliminary report. Medical science monitor : international medical journal of experimental and clinical research *6*, 759-762.

Cartwright, J.E., Fraser, R., Leslie, K., Wallace, A.E., and James, J.L. (2010). Remodelling at the maternal-fetal interface: relevance to human pregnancy disorders. Reproduction *140*, 803-813.

Cha, J., and Dey, S.K. (2014). Cadence of procreation: orchestrating embryo-uterine interactions. Semin Cell Dev Biol *34*, 56-64.

Cha, J., Sun, X., and Dey, S.K. (2012). Mechanisms of implantation: strategies for successful pregnancy. Nature medicine *18*, 1754-1767.

Chen, H., Dzitoyeva, S., and Manev, H. (2012). Effect of aging on 5-hydroxymethylcytosine in the mouse hippocampus. Restor Neurol Neurosci *30*, 237-245.

Chong, H.P., Cordeaux, Y., Ranjan, Y.S., Richardson, S., Liquet, B., Smith, G.C., and Charnock-Jones, D.S. (2016). Age-related changes in murine myometrial transcript profile are mediated by exposure to the female sex hormones. Aging Cell *15*, 177-180.

Chu, S.Y., Callaghan, W.M., Kim, S.Y., Schmid, C.H., Lau, J., England, L.J., and Dietz, P.M. (2007). Maternal obesity and risk of gestational diabetes mellitus. Diabetes care *30*, 2070-2076.

Cierna, Z., Varga, I., Danihel, L., Kuracinova, K., and Janegova, A. (2016). Intermediate trophoblast--A distinctive, unique and often unrecognized population of trophoblastic cells. Ann Anat *204*, 45-50.

Clark, J.H., Peck, E.J., Jr., and Anderson, J.N. (1974). Oestrogen receptors and antagonism of steroid hormone action. Nature *251*, 446-448.

Cohen, M.A., Lindheim, S.R., and Sauer, M.V. (1999). Donor age is paramount to success in oocyte donation. Hum Reprod *14*, 2755-2758.

Conneely, O.M., Mulac-Jericevic, B., Lydon, J.P., and De Mayo, F.J. (2001). Reproductive functions of the progesterone receptor isoforms: lessons from knock-out mice. Mol Cell Endocrinol *179*, 97-103.

Cooke, C.M., Shah, A., Kirschenman, R.D., Quon, A.L., Morton, J.S., Care, A.S., and Davidge, S.T. (2018). Increased susceptibility to cardiovascular disease in offspring born from dams of advanced maternal age. J Physiol.

Corral-Debrinski, M., Shoffner, J.M., Lott, M.T., and Wallace, D.C. (1992). Association of mitochondrial DNA damage with aging and coronary atherosclerotic heart disease. Mutat Res *275*, 169-180.

Covarrubias, A.E., Barrence, F.C., and Zorn, T.M. (2015). The absence of the embryo in the pseudopregnant uterus alters the deposition of some ECM molecules during decidualization in mice. Connective tissue research *56*, 253-263.

Craig, S.S. (1981). Effect of age upon uterine response to deciduagenic stimulus. Acta anatomica *110*, 146-158.

Cross, J.C. (2000). Genetic insights into trophoblast differentiation and placental morphogenesis. Semin Cell Dev Biol *11*, 105-113.

Cross, J.C., Hemberger, M., Lu, Y., Nozaki, T., Whiteley, K., Masutani, M., and Adamson, S.L. (2002). Trophoblast functions, angiogenesis and remodeling of the maternal vasculature in the placenta. Mol Cell Endocrinol *187*, 207-212.

Croy, B.A., He, H., Esadeg, S., Wei, Q., McCartney, D., Zhang, J., Borzychowski, A., Ashkar, A.A., Black, G.P., Evans, S.S*., et al.* (2003). Uterine natural killer cells: insights into their cellular and molecular biology from mouse modelling. Reproduction *126*, 149-160.

Dai, R., Li, L., Zhu, H., Geng, D., Deng, S., and Liu, R. (2017). Effect of maternal age on spontaneous abortion during the first trimester in Northeast China. The journal of maternal-fetal & neonatal medicine : the official journal of the European Association of Perinatal Medicine, the Federation of Asia and Oceania Perinatal Societies, the International Society of Perinatal Obstet, 1-6.

Daikoku, T., Cha, J., Sun, X., Tranguch, S., Xie, H., Fujita, T., Hirota, Y., Lydon, J., DeMayo, F., Maxson, R*., et al.* (2011). Conditional Deletion of MSX Homeobox Genes in the Uterus Inhibits Blastocyst Implantation by Altering Uterine Receptivity. Developmental Cell *21*, 1014-1025.

Das, A., Mantena, S.R., Kannan, A., Evans, D.B., Bagchi, M.K., and Bagchi, I.C. (2009). De novo synthesis of estrogen in pregnant uterus is critical for stromal decidualization and angiogenesis. Proceedings of the National Academy of Sciences of the United States of America *106*, 12542-12547.

DaSilva-Arnold, S., James, J.L., Al-Khan, A., Zamudio, S., and Illsley, N.P. (2015). Differentiation of first trimester cytotrophoblast to extravillous trophoblast involves an epithelial-mesenchymal transition. Placenta *36*, 1412-1418.

de Ziegler, D., Bergeron, C., Cornel, C., Medalie, D.A., Massai, M.R., Milgrom, E., Frydman, R., and Bouchard, P. (1992). Effects of luteal estradiol on the secretory transformation of human endometrium and plasma gonadotropins. J Clin Endocrinol Metab *74*, 322-331.

Dey, S.K., Lim, H., Das, S.K., Reese, J., Paria, B.C., Daikoku, T., and Wang, H. (2004). Molecular cues to implantation. Endocr Rev *25*, 341-373.

Diez-Juan, A., Rubio, C., Marin, C., Martinez, S., Al-Asmar, N., Riboldi, M., Díaz-Gimeno, P., Valbuena, D., and Simón, C. (2015). Mitochondrial DNA content as a viability score in human euploid embryos: less is better. Fertil Steril *104*, 534-541.e531.

Djeghloul, D., Kuranda, K., Kuzniak, I., Barbieri, D., Naguibneva, I., Choisy, C., Bories, J.-C., Dosquet, C., Pla, M., Vanneaux, V*., et al.* (2016). Age-Associated Decrease of the Histone

Methyltransferase SUV39H1 in HSC Perturbs Heterochromatin and B Lymphoid Differentiation. Stem Cell Reports *6*, 970-984.

Downs, K.M. (2002). Early placental ontogeny in the mouse. Placenta *23*, 116-131.

Dudley, D.J., Trautman, M.S., Araneo, B.A., Edwin, S.S., and Mitchell, M.D. (1992). Decidual cell biosynthesis of interleukin-6: regulation by inflammatory cytokines. J Clin Endocrinol Metab *74*, 884-889.

Dupressoir, A., Vernochet, C., Bawa, O., Harper, F., Pierron, G., Opolon, P., and Heidmann, T. (2009). Syncytin-A knockout mice demonstrate the critical role in placentation of a fusogenic, endogenous retrovirus-derived, envelope gene. Proceedings of the National Academy of Sciences of the United States of America *106*, 12127-12132.

Dupressoir, A., Vernochet, C., Harper, F., Guegan, J., Dessen, P., Pierron, G., and Heidmann, T. (2011). A pair of co-opted retroviral envelope syncytin genes is required for formation of the two-layered murine placental syncytiotrophoblast. Proceedings of the National Academy of Sciences of the United States of America *108*, E1164-1173.

Dyson, M.T., Roqueiro, D., Monsivais, D., Ercan, C.M., Pavone, M.E., Brooks, D.C., Kakinuma, T., Ono, M., Jafari, N., Dai, Y.*, et al.* (2014). Genome-wide DNA methylation analysis predicts an epigenetic switch for GATA factor expression in endometriosis. PLoS Genet *10*, e1004158.

E. Davies, J., Pollheimer, J., Yong, H.E.J., Kokkinos, M.I., Kalionis, B., Knöfler, M., and Murthi, P. (2016). Epithelial-mesenchymal transition during extravillous trophoblast differentiation. Cell Adhesion & Migration *10*, 310-321.

Eichenlaub-Ritter, U. (1998). Genetics of oocyte ageing. Maturitas *30*, 143-169.

Eichenlaub-Ritter, U. (2012). Oocyte ageing and its cellular basis. Int J Dev Biol *56*, 841-852.

Enders, A.C.S., S. (1967). A morphological analysis of the early implantation stages in the rat. American Journal Of Anatomy *120*, 185-226.

Erlebacher, A., Price, K.A., and Glimcher, L.H. (2004). Maintenance of mouse trophoblast stem cell proliferation by TGF-beta/activin. Dev Biol *275*, 158-169.

Fabi, F., Grenier, K., Parent, S., Adam, P., Tardif, L., Leblanc, V., and Asselin, E. (2017). Regulation of the PI3K/Akt pathway during decidualization of endometrial stromal cells. PLoS One *12*, e0177387.

Faddy, M.J., Gosden, R.G., Gougeon, A., Richardson, S.J., and Nelson, J.F. (1992). Accelerated disappearance of ovarian follicles in mid-life: implications for forecasting menopause. Hum Reprod *7*, 1342-1346.

Farfalli, V.I., Magli, M.C., Ferraretti, A.P., and Gianaroli, L. (2007). Role of aneuploidy on embryo implantation. Gynecol Obstet Invest *64*, 161-165.

Fenelon, J.C., Banerjee, A., and Murphy, B.D. (2014). Embryonic diapause: development on hold. Int J Dev Biol *58*, 163-174.

Feng, J., Liu, T., Qin, B., Zhang, Y., and Liu, X.S. (2012). Identifying ChIP-seq enrichment using MACS. Nature protocols *7*, 10.1038/nprot.2012.1101.

Finch, C.E., and Holinka, C.F. (1982). Aging and uterine growth during implantation in C57BL/6J mice. Exp Gerontol *17*, 235-241.

Findlay, J.K., Hutt, K.J., Hickey, M., and Anderson, R.A. (2015). How Is the Number of Primordial Follicles in the Ovarian Reserve Established? Biol Reprod *93*, 111.

Finn, C.A. (1966). The initiation of the decidual cell reaction in the uterus of the aged mouse. J Reprod Fertil *11*, 423-428.

Fluhr, H., Spratte, J., Ehrhardt, J., Steinmuller, F., Licht, P., and Zygmunt, M. (2010). Heparin and low-molecular-weight heparins modulate the decidualization of human endometrial stromal cells. Fertil Steril *93*, 2581-2587.

Fouladi-Nashta, A.A., Jones, C.J., Nijjar, N., Mohamet, L., Smith, A., Chambers, I., and Kimber, S.J. (2005). Characterization of the uterine phenotype during the peri-implantation period for LIF-null, MF1 strain mice. Dev Biol *281*, 1-21.

Franco, H.L., Dai, D., Lee, K.Y., Rubel, C.A., Roop, D., Boerboom, D., Jeong, J.W., Lydon, J.P., Bagchi, I.C., Bagchi, M.K*., et al.* (2011). WNT4 is a key regulator of normal postnatal uterine development and progesterone signaling during embryo implantation and decidualization in the mouse. FASEB J *25*, 1176-1187.

Franco, H.L., Jeong, J.W., Tsai, S.Y., Lydon, J.P., and DeMayo, F.J. (2008). In vivo analysis of progesterone receptor action in the uterus during embryo implantation. Semin Cell Dev Biol *19*, 178-186.

Franco, H.L., Lee, K.Y., Broaddus, R.R., White, L.D., Lanske, B., Lydon, J.P., Jeong, J.W., and DeMayo, F.J. (2010). Ablation of Indian hedgehog in the murine uterus results in decreased cell cycle progression, aberrant epidermal growth factor signaling, and increased estrogen signaling. Biol Reprod *82*, 783-790.

Fretts, R.C., and Usher, R.H. (1997). Causes of fetal death in women of advanced maternal age. Obstet Gynecol *89*, 40-45.

Fulton, N., Martins da Silva, S.J., Bayne, R.A., and Anderson, R.A. (2005). Germ cell proliferation and apoptosis in the developing human ovary. J Clin Endocrinol Metab *90*, 4664-4670.

Gao, F., Ma, X., Rusie, A., Hemingway, J., Ostmann, A.B., Chung, D., and Das, S.K. (2012). Epigenetic changes through DNA methylation contribute to uterine stromal cell decidualization. Endocrinology *153*, 6078-6090.

Gardner, R.L., and Davies, T.J. (1993). Lack of coupling between onset of giant transformation and genome endoreduplication in the mural trophectoderm of the mouse blastocyst. J Exp Zool *265*, 54-60.

Garrido-Gomez, T., Dominguez, F., Quinonero, A., Diaz-Gimeno, P., Kapidzic, M., Gormley, M., Ona, K., Padilla-Iserte, P., McMaster, M., Genbacev, O*., et al.* (2017). Defective decidualization during and after severe preeclampsia reveals a possible maternal

contribution to the etiology. Proceedings of the National Academy of Sciences of the United States of America *114*, E8468-e8477.

Gehin, M., Mark, M., Dennefeld, C., Dierich, A., Gronemeyer, H., and Chambon, P. (2002). The function of TIF2/GRIP1 in mouse reproduction is distinct from those of SRC-1 and p/CIP. Mol Cell Biol *22*, 5923-5937.

Gellersen, B., and Brosens, J.J. (2014). Cyclic Decidualization of the Human Endometrium in Reproductive Health and Failure. Endocrine Reviews *35*, 851-905.

Georgiades, P., Ferguson-Smith, A.C., and Burton, G.J. (2002). Comparative developmental anatomy of the murine and human definitive placentae. Placenta *23*, 3-19.

Gesell, M.S., and Roth, G.S. (1981). Decrease in rat uterine estrogen receptors during aging: physio- and immunochemical properties. Endocrinology *109*, 1502-1508.

Ghabreau, L., Roux, J.P., Niveleau, A., Fontanière, B., Mahe, C., Mokni, M., and Frappart, L. (2004). Correlation between the DNA global methylation status and progesterone receptor expression in normal endometrium, endometrioid adenocarcinoma and precursors. Virchows Arch *445*, 129-134.

Gibson, D.A., Simitsidellis, I., Kelepouri, O., Critchley, H.O.D., and Saunders, P.T.K. (2018). Dehydroepiandrosterone enhances decidualization in women of advanced reproductive age. Fertility and Sterility.

Goad, J., Ko, Y.A., Kumar, M., Syed, S.M., and Tanwar, P.S. (2017). Differential Wnt signaling activity limits epithelial gland development to the anti-mesometrial side of the mouse uterus. Dev Biol *423*, 138-151.

Godbole, G., and Modi, D. (2010). Regulation of decidualization, interleukin-11 and interleukin-15 by homeobox A 10 in endometrial stromal cells. J Reprod Immunol *85*, 130-139.

Goldman-Wohl, D., and Yagel, S. (2002). Regulation of trophoblast invasion: from normal implantation to pre-eclampsia. Mol Cell Endocrinol *187*, 233-238.

Gosden, R.G. (1979). Effects of age and parity on the breeding potential of mice with one or two ovaries. J Reprod Fertil *57*, 477-487.

Grimaldi, G., Christian, M., Quenby, S., and Brosens, J.J. (2012). Expression of epigenetic effectors in decidualizing human endometrial stromal cells. Mol Hum Reprod *18*, 451-458.

Gu, B., and Lee, M. (2013). Histone H3 lysine 4 methyltransferases and demethylases in self-renewal and differentiation of stem cells, Vol 3.

Guillemot, F., Nagy, A., Auerbach, A., Rossant, J., and Joyner, A.L. (1994). Essential role of Mash-2 in extraembryonic development. Nature *371*, 333-336.

Guimond, M.J., Luross, J.A., Wang, B., Terhorst, C., Danial, S., and Croy, B.A. (1997). Absence of natural killer cells during murine pregnancy is associated with reproductive compromise in TgE26 mice. Biol Reprod *56*, 169-179.

Guo, S.W. (2012). The endometrial epigenome and its response to steroid hormones. Mol Cell Endocrinol *358*, 185-196.

Guo, Z., Tilburgs, T., Wong, B., and Strominger, J.L. (2014). Dysfunction of dendritic cells in aged C57BL/6 mice leads to failure of natural killer cell activation and of tumor eradication. Proceedings of the National Academy of Sciences of the United States of America *111*, 14199-14204.

Guzman-Ayala, M., Ben-Haim, N., Beck, S., and Constam, D.B. (2004). Nodal protein processing and fibroblast growth factor 4 synergize to maintain a trophoblast stem cell microenvironment. Proceedings of the National Academy of Sciences of the United States of America *101*, 15656-15660.

Haertel-Wiesmann, M., Liang, Y., Fantl, W.J., and Williams, L.T. (2000). Regulation of cyclooxygenase-2 and periostin by Wnt-3 in mouse mammary epithelial cells. J Biol Chem *275*, 32046-32051.

Hardy, K., and Hardy, P.J. (2015). 1(st) trimester miscarriage: four decades of study. Translational pediatrics *4*, 189-200.

Hardy, O.T., Czech, M.P., and Corvera, S. (2012). What causes the insulin resistance underlying obesity? Current opinion in endocrinology, diabetes, and obesity *19*, 81-87.

Harman, S.M., and Talbert, G.B. (1970). The effect of maternal age on ovulation, corpora lutea of pregnancy, and implantation failure in mice. J Reprod Fertil *23*, 33-39.

Harton, G.L., Munne, S., Surrey, M., Grifo, J., Kaplan, B., McCulloh, D.H., Griffin, D.K., and Wells, D. (2013). Diminished effect of maternal age on implantation after preimplantation genetic diagnosis with array comparative genomic hybridization. Fertil Steril *100*, 1695-1703.

Hassold, T., and Chiu, D. (1985). Maternal age-specific rates of numerical chromosome abnormalities with special reference to trisomy. Human genetics *70*, 11-17.

Hassold, T., and Hunt, P. (2001). To err (meiotically) is human: the genesis of human aneuploidy. Nat Rev Genet *2*, 280-291.

Heffner, L.J. (2004). Advanced maternal age--how old is too old? The New England journal of medicine *351*, 1927-1929.

Hemberger, M., Nozaki, T., Masutani, M., and Cross, J.C. (2003). Differential expression of angiogenic and vasodilatory factors by invasive trophoblast giant cells depending on depth of invasion. Dev Dyn *227*, 185-191.

Herbert, M., Kalleas, D., Cooney, D., Lamb, M., and Lister, L. (2015). Meiosis and maternal aging: insights from aneuploid oocytes and trisomy births. Cold Spring Harbor perspectives in biology *7*, a017970.

Herington, J.L., Underwood, T., McConaha, M., and Bany, B.M. (2009). Paracrine signals from the mouse conceptus are not required for the normal progression of decidualization. Endocrinology *150*, 4404-4413.

Hervouet, E., Vallette, F.M., and Cartron, P.F. (2010). Dnmt1/Transcription factor interactions: an alternative mechanism of DNA methylation inheritance. Genes & cancer *1*, 434-443.

Hess, A.P., Hamilton, A.E., Talbi, S., Dosiou, C., Nyegaard, M., Nayak, N., Genbecev-Krtolica, O., Mavrogianis, P., Ferrer, K., Kruessel, J.*, et al.* (2007). Decidual stromal cell response to paracrine signals from the trophoblast: amplification of immune and angiogenic modulators. Biol Reprod *76*, 102-117.

Hetherington, C.M. (1972). The effect of parity on decidual, placental and fetal weight in the mouse. J Reprod Fertil *28*, 125-129.

Higgins, L., Greenwood, S.L., Wareing, M., Sibley, C.P., and Mills, T.A. (2011). Obesity and the placenta: A consideration of nutrient exchange mechanisms in relation to aberrant fetal growth. Placenta *32*, 1-7.

Hirota, Y., Daikoku, T., Tranguch, S., Xie, H., Bradshaw, H.B., and Dey, S.K. (2010). Uterine-specific p53 deficiency confers premature uterine senescence and promotes preterm birth in mice. J Clin Invest *120*, 803-815.

Hitz, M.-P., and Andelfinger, G. (2015). Race for healthy hearts. Nature *520*, 160.

Holinka, C.F., and Finch, C.E. (1977). Age-related changes in the decidual response of the C57BL/6J mouse uterus. Biol Reprod *16*, 385-393.

Holinka, C.F., Tseng, Y.C., and Finch, C.E. (1979). Reproductive aging in C57BL/6J mice: plasma progesterone, viable embryos and resorption frequency throughout pregnancy. Biol Reprod *20*, 1201-1211.

Hollier, L.M., Leveno, K.J., Kelly, M.A., DD, M.C., and Cunningham, F.G. (2000). Maternal age and malformations in singleton births. Obstet Gynecol *96*, 701-706.

Horvath, S. (2013). DNA methylation age of human tissues and cell types. Genome Biol *14*, R115.

Houshdaran, S., Zelenko, Z., Irwin, J.C., and Giudice, L.C. (2014). Human endometrial DNA methylome is cycle-dependent and is associated with gene expression regulation. Mol Endocrinol *28*, 1118-1135.

Houtkooper, R.H., Argmann, C., Houten, S.M., Cantó, C., Jeninga, E.H., Andreux, P.A., Thomas, C., Doenlen, R., Schoonjans, K., and Auwerx, J. (2011). The metabolic footprint of aging in mice. Scientific Reports *1*, 134.

Howe, F.S., Fischl, H., Murray, S.C., and Mellor, J. (2017). Is H3K4me3 instructive for transcription activation? Bioessays *39*, 1-12.

Howell, K.R., and Powell, T.L. (2017). Effects of maternal obesity on placental function and fetal development. Reproduction *153*, R97-r108.

Hsueh, A.J., Erickson, G.F., and Lu, K.H. (1979). Changes in uterine estrogen receptor and morphology in aging female rats. Biol Reprod *21*, 793-800.

Hu, D., and Cross, J.C. (2010). Development and function of trophoblast giant cells in the rodent placenta. Int J Dev Biol *54*, 341-354.

Huang da, W., Sherman, B.T., and Lempicki, R.A. (2009). Systematic and integrative analysis of large gene lists using DAVID bioinformatics resources. Nature protocols *4*, 44-57.

Huang, L., Sauve, R., Birkett, N., Fergusson, D., and van Walraven, C. (2008). Maternal age and risk of stillbirth: a systematic review. Canadian Medical Association Journal *178*, 165-172.

Hughes, M., Dobric, N., Scott, I.C., Su, L., Starovic, M., St-Pierre, B., Egan, S.E., Kingdom, J.C., and Cross, J.C. (2004). The Hand1, Stra13 and Gcm1 transcription factors override FGF signaling to promote terminal differentiation of trophoblast stem cells. Dev Biol *271*, 26-37.

Ishikawa, H., Ishi, K., Serna, V.A., Kakazu, R., Bulun, S.E., and Kurita, T. (2010). Progesterone is essential for maintenance and growth of uterine leiomyoma. Endocrinology *151*, 2433-2442.

Issa, J.P. (2014). Aging and epigenetic drift: a vicious cycle. J Clin Invest *124*, 24-29.

Itsekson, A.M., Seidman, D.S., Zolti, M., Lazarov, A., and Carp, H.J. (2007). Recurrent pregnancy loss and inappropriate local immune response to sex hormones. Am J Reprod Immunol *57*, 160-165.

Iwatsuki, K., Shinozaki, M., Sun, W., Yagi, S., Tanaka, S., and Shiota, K. (2000). A novel secretory protein produced by rat spongiotrophoblast. Biol Reprod *62*, 1352-1359.

Jacobsson, B., Ladfors, L., and Milsom, I. (2004). Advanced maternal age and adverse perinatal outcome. Obstet Gynecol *104*, 727-733.

Jefferson, W.N., Padilla-Banks, E., and Newbold, R.R. (2000). Lactoferrin is an estrogen responsive protein in the uterus of mice and rats. Reproductive toxicology (Elmsford, NY) *14*, 103-110.

Jeong, J.W., Lee, K.Y., Han, S.J., Aronow, B.J., Lydon, J.P., O'Malley, B.W., and DeMayo, F.J. (2007). The p160 steroid receptor coactivator 2, SRC-2, regulates murine endometrial function and regulates progesterone-independent and -dependent gene expression. Endocrinology *148*, 4238-4250.

Ji, F., Yang, X., He, Y., Wang, H., Aili, A., and Ding, Y. (2017). Aberrant endometrial DNA methylome of homeobox A10 and catechol-O-methyltransferase in endometriosis. J Assist Reprod Genet *34*, 409-415.

Johannsen, D.L., and Ravussin, E. (2010). Obesity in the elderly: is faulty metabolism to blame? Aging health *6*, 159-167.

Johnson, A.A., Akman, K., Calimport, S.R., Wuttke, D., Stolzing, A., and de Magalhaes, J.P. (2012). The role of DNA methylation in aging, rejuvenation, and age-related disease. Rejuvenation research *15*, 483-494.

Jolly, M., Sebire, N., Harris, J., Robinson, S., and Regan, L. (2000). The risks associated with pregnancy in women aged 35 years or older. Hum Reprod *15*, 2433-2437.

Jones, A., Teschendorff, A.E., Li, Q., Hayward, J.D., Kannan, A., Mould, T., West, J., Zikan, M., Cibula, D., Fiegl, H.*, et al.* (2013). Role of DNA methylation and epigenetic silencing of HAND2 in endometrial cancer development. PLoS Med *10*, e1001551.

Jones, H.N., Woollett, L.A., Barbour, N., Prasad, P.D., Powell, T.L., and Jansson, T. (2009). High-fat diet before and during pregnancy causes marked up-regulation of placental nutrient transport and fetal overgrowth in C57/BL6 mice. Faseb j *23*, 271-278.

Joseph, K.S., Allen, A.C., Dodds, L., Turner, L.A., Scott, H., and Liston, R. (2005). The perinatal effects of delayed childbearing. Obstet Gynecol *105*, 1410-1418.

Kalogiannidis, I., Margioula-Siarkou, C., Petousis, S., Masoura, S., Goutzioulis, A., Traianos, A., Prapas, N., and Agorastos, T. (2011). Parity affects pregnancy outcomes in women 35 and older. Clin Exp Obstet Gynecol *38*, 146-149.

Kanasaki, K., and Kalluri, R. (2009). The biology of preeclampsia. Kidney Int *76*, 831-837.

Katz, S.G. (1995). Extracellular and intracellular degradation of collagen by trophoblast giant cells in acute fasted mice examined by electron microscopy. Tissue Cell *27*, 713-721.

Kaya Okur, H.S., Das, A., Taylor, R.N., Bagchi, I.C., and Bagchi, M.K. (2016). Roles of Estrogen Receptor-alpha and the Coactivator MED1 During Human Endometrial Decidualization. Mol Endocrinol *30*, 302-313.

Kerr, J.B., Myers, M., and Anderson, R.A. (2013). The dynamics of the primordial follicle reserve. Reproduction *146*, R205-215.

Khalil, A., Syngelaki, A., Maiz, N., Zinevich, Y., and Nicolaides, K.H. (2013). Maternal age and adverse pregnancy outcome: a cohort study. Ultrasound in obstetrics & gynecology : the official journal of the International Society of Ultrasound in Obstetrics and Gynecology *42*, 634-643.

Kidd, S.A., Lancaster, P.A., and McCredie, R.M. (1993). The incidence of congenital heart defects in the first year of life. Journal of paediatrics and child health *29*, 344-349.

Kim, D.W., Young, S.L., Grattan, D.R., and Jasoni, C.L. (2014). Obesity During Pregnancy Disrupts Placental Morphology, Cell Proliferation, and Inflammation in a Sex-Specific Manner Across Gestation in the Mouse1. Biology of Reproduction *90*, 130, 131-111-130, 131-111.

Kim, M., Park, H.J., Seol, J.W., Jang, J.Y., Cho, Y.S., Kim, K.R., Choi, Y., Lydon, J.P., Demayo, F.J., Shibuya, M.*, et al.* (2013). VEGF-A regulated by progesterone governs uterine angiogenesis and vascular remodelling during pregnancy. EMBO molecular medicine *5*, 1415-1430.

King, A., and Loke, Y.W. (1994). Unexplained fetal growth retardation: what is the cause? Arch Dis Child Fetal Neonatal Ed *70*, F225-227.

Kojima, K., Kanzaki, H., Iwai, M., Hatayama, H., Fujimoto, M., Narukawa, S., Higuchi, T., Kaneko, Y., Mori, T., and Fujita, J. (1995). Expression of leukaemia inhibitory factor (LIF) receptor in human placenta: a possible role for LIF in the growth and differentiation of trophoblasts. Hum Reprod *10*, 1907-1911.

Kollara, A., and Brown, T.J. (2012). Expression and function of nuclear receptor co-activator 4: evidence of a potential role independent of co-activator activity. Cell Mol Life Sci *69*, 3895-3909.

Kong, S., Zhang, S., Chen, Y., Wang, W., Wang, B., Chen, Q., Duan, E., and Wang, H. (2012). Determinants of uterine aging: lessons from rodent models. Sci China Life Sci *55*, 687-693.

Krishna, U., and Bhalerao, S. (2011). Placental Insufficiency and Fetal Growth Restriction. Journal of Obstetrics and Gynaecology of India *61*, 505-511.

Kroon, B., Harrison, K., Martin, N., Wong, B., and Yazdani, A. (2011). Miscarriage karyotype and its relationship with maternal body mass index, age, and mode of conception. Fertil Steril *95*, 1827-1829.

Kukushkina, V., Modhukur, V., Suhorutšenko, M., Peters, M., Mägi, R., Rahmioglu, N., Velthut-Meikas, A., Altmäe, S., Esteban, F.J., Vilo, J.*, et al.* (2017). DNA methylation changes in endometrium and correlation with gene expression during the transition from pre-receptive to receptive phase. Sci Rep *7*, 3916.

Kurihara, I., Lee, D.K., Petit, F.G., Jeong, J., Lee, K., Lydon, J.P., DeMayo, F.J., Tsai, M.J., and Tsai, S.Y. (2007). COUP-TFII mediates progesterone regulation of uterine implantation by controlling ER activity. PLoS Genet *3*, e102.

Kuroda, K., Venkatakrishnan, R., Salker, M.S., Lucas, E.S., Shaheen, F., Kuroda, M., Blanks, A., Christian, M., Quenby, S., and Brosens, J.J. (2013). Induction of 11β-HSD 1 and activation of distinct mineralocorticoid receptor- and glucocorticoid receptor-dependent gene networks in decidualizing human endometrial stromal cells. Mol Endocrinol *27*, 192-202.

Kushnir, V.A., Ludaway, T., Russ, R.B., Fields, E.J., Koczor, C., and Lewis, W. (2012). Reproductive aging is associated with decreased mitochondrial abundance and altered structure in murine oocytes. J Assist Reprod Genet *29*, 637-642.

Kwon, E.J., and Kim, Y.J. (2017). What is fetal programming?: a lifetime health is under the control of in utero health. Obstetrics & gynecology science *60*, 506-519.

Lamminpaa, R., Vehvilainen-Julkunen, K., Gissler, M., and Heinonen, S. (2012). Preeclampsia complicated by advanced maternal age: a registry-based study on primiparous women in Finland 1997-2008. BMC pregnancy and childbirth *12*, 47.

Lamminpaa, R., Vehvilainen-Julkunen, K., Gissler, M., Selander, T., and Heinonen, S. (2016). Pregnancy outcomes of overweight and obese women aged 35 years or older - A registry-based study in Finland. Obesity research & clinical practice *10*, 133-142.

Lao, T.T., Ho, L.-F., Chan, B.C.P., and Leung, W.-C. (2006). Maternal Age and Prevalence of Gestational Diabetes Mellitus. Diabetes care *29*, 948-949.

Large, M.J., and DeMayo, F.J. (2012). The regulation of embryo implantation and endometrial decidualization by progesterone receptor signaling. Mol Cell Endocrinol *358*, 155-165.

Large, M.J., Wetendorf, M., Lanz, R.B., Hartig, S.M., Creighton, C.J., Mancini, M.A., Kovanci, E., Lee, K.F., Threadgill, D.W., Lydon, J.P*., et al.* (2014). The epidermal growth factor receptor critically regulates endometrial function during early pregnancy. PLoS Genet *10*, e1004451.

Latos, P.A., Goncalves, A., Oxley, D., Mohammed, H., Turro, E., and Hemberger, M. (2015). Fgf and Esrrb integrate epigenetic and transcriptional networks that regulate self-renewal of trophoblast stem cells. Nature communications *6*, 7776.

Lean, S.C., Heazell, A.E.P., Dilworth, M.R., Mills, T.A., and Jones, R.L. (2017). Placental Dysfunction Underlies Increased Risk of Fetal Growth Restriction and Stillbirth in Advanced Maternal Age Women. Sci Rep *7*, 9677.

Leddy, M.A., Power, M.L., and Schulkin, J. (2008). The Impact of Maternal Obesity on Maternal and Fetal Health. Reviews in Obstetrics and Gynecology *1*, 170-178.

Lee, J.H., Kim, T.H., Oh, S.J., Yoo, J.Y., Akira, S., Ku, B.J., Lydon, J.P., and Jeong, J.W. (2013). Signal transducer and activator of transcription-3 (Stat3) plays a critical role in implantation via progesterone receptor in uterus. Faseb j *27*, 2553-2563.

Lee, K., Jeong, J., Kwak, I., Yu, C.T., Lanske, B., Soegiarto, D.W., Toftgard, R., Tsai, M.J., Tsai, S., Lydon, J.P*., et al.* (2006). Indian hedgehog is a major mediator of progesterone signaling in the mouse uterus. Nat Genet *38*, 1204-1209.

Lee, K.Y., and DeMayo, F.J. (2004). Animal models of implantation. Reproduction *128*, 679-695.

Lee, K.Y., Jeong, J.W., Wang, J., Ma, L., Martin, J.F., Tsai, S.Y., Lydon, J.P., and DeMayo, F.J. (2007). Bmp2 is critical for the murine uterine decidual response. Mol Cell Biol *27*, 5468-5478.

LeFevre, J., and McClintock, M.K. (1988). Reproductive senescence in female rats: a longitudinal study of individual differences in estrous cycles and behavior. Biol Reprod *38*, 780-789.

Lejeune, B., Van Hoeck, J., and Leroy, F. (1981). Transmitter role of the luminal uterine epithelium in the induction of decidualization in rats. J Reprod Fertil *61*, 235-240.

Li, E., Bestor, T.H., and Jaenisch, R. (1992). Targeted mutation of the DNA methyltransferase gene results in embryonic lethality. Cell *69*, 915-926.

Li, M.Q., Yao, M.N., Yan, J.Q., Li, Z.L., Gu, X.W., Lin, S., Hu, W., and Yang, Z.M. (2017). The decline of pregnancy rate and abnormal uterine responsiveness of steroid hormones in aging mice. Reproductive biology *17*, 305-311.

Li, Q., Kannan, A., DeMayo, F.J., Lydon, J.P., Cooke, P.S., Yamagishi, H., Srivastava, D., Bagchi, M.K., and Bagchi, I.C. (2011). The antiproliferative action of progesterone in uterine epithelium is mediated by Hand2. Science *331*, 912-916.

Li, Q., Kannan, A., Wang, W., Demayo, F.J., Taylor, R.N., Bagchi, M.K., and Bagchi, I.C. (2007). Bone morphogenetic protein 2 functions via a conserved signaling pathway involving Wnt4 to regulate uterine decidualization in the mouse and the human. J Biol Chem *282*, 31725-31732.

Li, X., Feng, Y., Lin, J.-F., Billig, H., and Shao, R. (2014). Endometrial progesterone resistance and PCOS. Journal of Biomedical Science *21*, 2-2.

Liang, C., DeCourcy, K., and Prater, M.R. (2010). High-saturated-fat diet induces gestational diabetes and placental vasculopathy in C57BL/6 mice. Metabolism: clinical and experimental *59*, 943-950.

Lienhard, M., Grimm, C., Morkel, M., Herwig, R., and Chavez, L. (2014). MEDIPS: genome-wide differential coverage analysis of sequencing data derived from DNA enrichment experiments. Bioinformatics *30*, 284-286.

Lim, H., Ma, L., Ma, W.G., Maas, R.L., and Dey, S.K. (1999). Hoxa-10 regulates uterine stromal cell responsiveness to progesterone during implantation and decidualization in the mouse. Mol Endocrinol *13*, 1005-1017.

Lima, P.D., Zhang, J., Dunk, C., Lye, S.J., and Croy, B.A. (2014). Leukocyte driven-decidual angiogenesis in early pregnancy. Cellular & molecular immunology *11*, 522-537.

Linask, K.K. (2013). The Heart-Placenta Axis in the First Month of Pregnancy: Induction and Prevention of Cardiovascular Birth Defects. Journal of Pregnancy *2013*, 11.

Liu, L., Cheung, T.H., Charville, G.W., Hurgo, B.M., Leavitt, T., Shih, J., Brunet, A., and Rando, T.A. (2013). Chromatin modifications as determinants of muscle stem cell quiescence and chronological aging. Cell Rep *4*, 189-204.

Liu, T., and Ogle, T.F. (2002). Signal transducer and activator of transcription 3 is expressed in the decidualized mesometrium of pregnancy and associates with the progesterone receptor through protein-protein interactions. Biol Reprod *67*, 114-118.

Llurba, E., Syngelaki, A., Sanchez, O., Carreras, E., Cabero, L., and Nicolaides, K.H. (2013). Maternal serum placental growth factor at 11-13 weeks' gestation and fetal cardiac defects. Ultrasound in obstetrics & gynecology : the official journal of the International Society of Ultrasound in Obstetrics and Gynecology *42*, 169-174.

Loeb, L., Suntzeff, V., and Burns, E.L. (1938). THE EFFECTS OF AGE AND ESTROGEN ON THE STROMA OF VAGINA, CERVIX AND UTERUS IN THE MOUSE. Science *88*, 432-433.

Logan, P.C., Ponnampalam, A.P., Steiner, M., and Mitchell, M.D. (2013). Effect of cyclic AMP and estrogen/progesterone on the transcription of DNA methyltransferases during the decidualization of human endometrial stromal cells. Mol Hum Reprod *19*, 302-312.

Lopes, F.L., Fortier, A.L., Darricarrere, N., Chan, D., Arnold, D.R., and Trasler, J.M. (2009). Reproductive and epigenetic outcomes associated with aging mouse oocytes. Hum Mol Genet *18*, 2032-2044.

Love, M.I., Huber, W., and Anders, S. (2014). Moderated estimation of fold change and dispersion for RNA-seq data with DESeq2. Genome Biol *15*, 550.

Lu, K.H., Hopper, B.R., Vargo, T.M., and Yen, S.S. (1979). Chronological changes in sex steroid, gonadotropin and prolactin secretions in aging female rats displaying different reproductive states. Biol Reprod *21*, 193-203.

Lubahn, D.B., Moyer, J.S., Golding, T.S., Couse, J.F., Korach, K.S., and Smithies, O. (1993). Alteration of reproductive function but not prenatal sexual development after insertional disruption of the mouse estrogen receptor gene. Proceedings of the National Academy of Sciences of the United States of America *90*, 11162-11166.

Lumsden, M.A., and Hor, K. (2015). Impact of obesity on the health of women in midlife. The Obstetrician & Gynaecologist *17*, 201-208.

Luzzo, K.M., Wang, Q., Purcell, S.H., Chi, M., Jimenez, P.T., Grindler, N., Schedl, T., and Moley, K.H. (2012). High fat diet induced developmental defects in the mouse: oocyte meiotic aneuploidy and fetal growth retardation/brain defects. PLoS One *7*, e49217.

Lydon, J.P., DeMayo, F.J., Funk, C.R., Mani, S.K., Hughes, A.R., Montgomery, C.A., Jr., Shyamala, G., Conneely, O.M., and O'Malley, B.W. (1995). Mice lacking progesterone receptor exhibit pleiotropic reproductive abnormalities. Genes Dev *9*, 2266-2278.

Ma, W., Tan, J., Matsumoto, H., Robert, B., Abrahamson, D.R., Das, S.K., and Dey, S.K. (2001). Adult tissue angiogenesis: evidence for negative regulation by estrogen in the uterus. Mol Endocrinol *15*, 1983-1992.

MacAuley, A., Cross, J.C., and Werb, Z. (1998). Reprogramming the cell cycle for endoreduplication in rodent trophoblast cells. Mol Biol Cell *9*, 795-807.

Macklon, N.S., Geraedts, J.P., and Fauser, B.C. (2002). Conception to ongoing pregnancy: the 'black box' of early pregnancy loss. Hum Reprod Update *8*, 333-343.

MacLennan, M., Crichton, J.H., Playfoot, C.J., and Adams, I.R. (2015). Oocyte development, meiosis and aneuploidy. Semin Cell Dev Biol *45*, 68-76.

Maibenco, H.C., and Krehbiel, R.H. (1973). Reproductive decline in aged female rats. J Reprod Fertil *32*, 121-123.

Main, D.M., Main, E.K., and Moore, D.H., 2nd (2000). The relationship between maternal age and uterine dysfunction: a continuous effect throughout reproductive life. Am J Obstet Gynecol *182*, 1312-1320.

Mandala, M., and Osol, G. (2012). Physiological remodelling of the maternal uterine circulation during pregnancy. Basic & clinical pharmacology & toxicology *110*, 12-18.

Marchal, C., and Miotto, B. (2015). Emerging concept in DNA methylation: role of transcription factors in shaping DNA methylation patterns. J Cell Physiol *230*, 743-751.

Martin, J.A., Hamilton, B.E., Sutton, P.D., Ventura, S.J., Mathews, T.J., Kirmeyer, S., and Osterman, M.J. (2010). Births: final data for 2007. National vital statistics reports : from the Centers for Disease Control and Prevention, National Center for Health Statistics, National Vital Statistics System *58*, 1-85.

Martin, L., Finn, C.A., and Carter, J. (1970). Effects of progesterone and oestradiol-17 beta on the luminal epithelium of the mouse uterus. J Reprod Fertil *21*, 461-469.

Matthiesen, N.B., Henriksen, T.B., Agergaard, P., Gaynor, J.W., Bach, C.C., Hjortdal, V.E., and Ostergaard, J.R. (2016). Congenital Heart Defects and Indices of Placental and Fetal Growth in a Nationwide Study of 924 422 Liveborn Infants. Circulation *134*, 1546-1556.

Maurer, M., Ebner, T., Puchner, M., Mayer, R.B., Shebl, O., Oppelt, P., and Duba, H.C. (2015). Chromosomal Aneuploidies and Early Embryonic Developmental Arrest. International journal of fertility & sterility *9*, 346-353.

May-Panloup, P., Boucret, L., Chao de la Barca, J.M., Desquiret-Dumas, V., Ferré-L'Hotellier, V., Morinière, C., Descamps, P., Procaccio, V., and Reynier, P. (2016). Ovarian ageing: the role of mitochondria in oocytes and follicles. Hum Reprod Update *22*, 725-743.

McCoy, R.C., Demko, Z.P., Ryan, A., Banjevic, M., Hill, M., Sigurjonsson, S., Rabinowitz, M., and Petrov, D.A. (2015). Evidence of Selection against Complex Mitotic-Origin Aneuploidy during Preimplantation Development. PLoS Genet *11*, e1005601.

McLean, C.Y., Bristor, D., Hiller, M., Clarke, S.L., Schaar, B.T., Lowe, C.B., Wenger, A.M., and Bejerano, G. (2010). GREAT improves functional interpretation of cis-regulatory regions. Nat Biotechnol *28*, 495-501.

McLeay, R.C., and Bailey, T.L. (2010). Motif Enrichment Analysis: a unified framework and an evaluation on ChIP data. BMC bioinformatics *11*, 165.

Menken, J., Trussell, J., and Larsen, U. (1986). Age and infertility. Science *233*, 1389-1394.

Menkhorst, E.M., Lane, N., Winship, A.L., Li, P., Yap, J., Meehan, K., Rainczuk, A., Stephens, A., and Dimitriadis, E. (2012). Decidual-secreted factors alter invasive trophoblast membrane and secreted proteins implying a role for decidual cell regulation of placentation. PLoS One *7*, e31418.

Menkhorst, E.M., Van Sinderen, M.L., Rainczuk, K., Cuman, C., Winship, A., and Dimitriadis, E. (2017). Invasive trophoblast promote stromal fibroblast decidualization via Profilin 1 and ALOX5. Sci Rep *7*, 8690.

Merriman, J.A., Jennings, P.C., McLaughlin, E.A., and Jones, K.T. (2012). Effect of aging on superovulation efficiency, aneuploidy rates, and sister chromatid cohesion in mice aged up to 15 months. Biol Reprod *86*, 49.

Mester, I., Martel, D., Psychoyos, A., and Baulieu, E.E. (1974). Hormonal control of oestrogen receptor in uterus and receptivity for ovoimplantation in the rat. Nature *250*, 776-778.

Mestre-Citrinovitz, A.C., Kleff, V., Vallejo, G., Winterhager, E., and Saragueta, P. (2015). A Suppressive Antagonism Evidences Progesterone and Estrogen Receptor Pathway Interaction with Concomitant Regulation of Hand2, Bmp2 and ERK during Early Decidualization. PLoS One *10*, e0124756.

Métivier, R., Gallais, R., Tiffoche, C., Le Péron, C., Jurkowska, R.Z., Carmouche, R.P., Ibberson, D., Barath, P., Demay, F., Reid, G.*, et al.* (2008). Cyclical DNA methylation of a transcriptionally active promoter. Nature *452*, 45-50.

Miller, A., Riehle-Colarusso, T., Siffel, C., Frias, J.L., and Correa, A. (2011). Maternal age and prevalence of isolated congenital heart defects in an urban area of the United States. American journal of medical genetics Part A *155a*, 2137-2145.

Mills, T.A., and Lavender, T. (2011). Advanced maternal age. Obstetrics, Gynaecology & Reproductive Medicine *21*, 107-111.

Mori, M., Bogdan, A., Balassa, T., Csabai, T., and Szekeres-Bartho, J. (2016). The decidua-the maternal bed embracing the embryo-maintains the pregnancy. Seminars in immunopathology *38*, 635-649.

Motta, P.M., Makabe, S., and Nottola, S.A. (1997). The ultrastructure of human reproduction. I. The natural history of the female germ cell: origin, migration and differentiation inside the developing ovary. Hum Reprod Update *3*, 281-295.

Mould, A., Morgan, M.A., Li, L., Bikoff, E.K., and Robertson, E.J. (2012). Blimp1/Prdm1 governs terminal differentiation of endovascular trophoblast giant cells and defines multipotent progenitors in the developing placenta. Genes Dev *26*, 2063-2074.

Munne, S. (2002). Preimplantation genetic diagnosis of numerical and structural chromosome abnormalities. Reprod Biomed Online *4*, 183-196.

Nagaoka, S.I., Hassold, T.J., and Hunt, P.A. (2012). Human aneuploidy: mechanisms and new insights into an age-old problem. Nat Rev Genet *13*, 493-504.

Nait-Oumesmar, B., Copperman, A.B., and Lazzarini, R.A. (2000). Placental expression and chromosomal localization of the human Gcm 1 gene. The journal of histochemistry and cytochemistry : official journal of the Histochemistry Society *48*, 915-922.

Nam, J., Greenwald, E., Jack-Roberts, C., Ajeeb, T.T., Malysheva, O.V., Caudill, M.A., Axen, K., Saxena, A., Semernina, E., Nanobashvili, K*., et al.* (2017). Choline prevents fetal overgrowth and normalizes placental fatty acid and glucose metabolism in a mouse model of maternal obesity. The Journal of nutritional biochemistry *49*, 80-88.

Nasmyth, K., and Haering, C.H. (2009). Cohesin: its roles and mechanisms. Annu Rev Genet *43*, 525-558.

Natale, B.V., Schweitzer, C., Hughes, M., Globisch, M.A., Kotadia, R., Tremblay, E., Vu, P., Cross, J.C., and Natale, D.R.C. (2017). Sca-1 identifies a trophoblast population with multipotent potential in the mid-gestation mouse placenta. Sci Rep *7*, 5575.

Nelson, J.F., Felicio, L.S., Randall, P.K., Sims, C., and Finch, C.E. (1982). A longitudinal study of estrous cyclicity in aging C57BL/6J mice: I. Cycle frequency, length and vaginal cytology. Biol Reprod *27*, 327-339.

Nelson, S.M., and Lawlor, D.A. (2011). Predicting live birth, preterm delivery, and low birth weight in infants born from in vitro fertilisation: a prospective study of 144,018 treatment cycles. PLoS Med *8*, e1000386.

Nelson, S.M., Telfer, E.E., and Anderson, R.A. (2013). The ageing ovary and uterus: new biological insights. Hum Reprod Update *19*, 67-83.

Norwitz, E.R., Edusa, V., and Park, J.S. (2005). Maternal physiology and complications of multiple pregnancy. Semin Perinatol *29*, 338-348.

Nybo Andersen, A.M., Wohlfahrt, J., Christens, P., Olsen, J., and Melbye, M. (2000). Maternal age and fetal loss: population based register linkage study. BMJ (Clinical research ed) *320*, 1708-1712.

Ogle, T.F., Dai, D., and George, P. (1999). Progesterone-regulated determinants of stromal cell survival and death in uterine decidua are linked to protein kinase C activity. Steroids *64*, 628-633.

Ogle, T.F., George, P., and Dai, D. (1998). Progesterone and estrogen regulation of rat decidual cell expression of proliferating cell nuclear antigen. Biol Reprod *59*, 444-450.

Ohinata, Y., and Tsukiyama, T. (2014). Establishment of trophoblast stem cells under defined culture conditions in mice. PLoS One *9*, e107308.

Ohta, Y. (1987). Age-related decline in deciduogenic ability of the rat uterus. Biology of Reproduction *37*, 779-785.

Ojeda, N.B., Grigore, D., and Alexander, B.T. (2008). Intrauterine growth restriction: fetal programming of hypertension and kidney disease. Adv Chronic Kidney Dis *15*, 101-106.

Okae, H., Toh, H., Sato, T., Hiura, H., Takahashi, S., Shirane, K., Kabayama, Y., Suyama, M., Sasaki, H., and Arima, T. (2018). Derivation of Human Trophoblast Stem Cells. Cell stem cell *22*, 50-63.e56.

Okano, M., Bell, D.W., Haber, D.A., and Li, E. (1999). DNA methyltransferases Dnmt3a and Dnmt3b are essential for de novo methylation and mammalian development. Cell *99*, 247-257.

Olesen, M.S., Starnawska, A., Bybjerg-Grauholm, J., Bielfeld, A.P., Agerholm, I., Forman, A., Overgaard, M.T., and Nyegaard, M. (2018). Biological age of the endometrium using DNA methylation. Reproduction *155*, 167-172.

Omori, H., Ogaki, S., Sakano, D., Sato, M., Umeda, K., Takeda, N., Nakagata, N., and Kume, S. (2016). Changes in expression of C2cd4c in pancreatic endocrine cells during pancreatic development. FEBS letters *590*, 2584-2593.

Oreshkova, T., Dimitrov, R., and Mourdjeva, M. (2012). A cross-talk of decidual stromal cells, trophoblast, and immune cells: a prerequisite for the success of pregnancy. Am J Reprod Immunol *68*, 366-373.

Ozalp, S., Tanir, H.M., Sener, T., Yazan, S., and Keskin, A.E. (2003). Health risks for early (< or =19) and late (> or =35) childbearing. Arch Gynecol Obstet *268*, 172-174.

Pal, S., and Tyler, J.K. (2016). Epigenetics and aging. Sci Adv *2*, e1600584.

Pan, H., Ma, P., Zhu, W., and Schultz, R.M. (2008). Age-associated increase in aneuploidy and changes in gene expression in mouse eggs. Dev Biol *316*, 397-407.

Parast, M.M., Aeder, S., and Sutherland, A.E. (2001). Trophoblast giant-cell differentiation involves changes in cytoskeleton and cell motility. Dev Biol *230*, 43-60.

Paria, B.C., Ma, W., Tan, J., Raja, S., Das, S.K., Dey, S.K., and Hogan, B.L. (2001). Cellular and molecular responses of the uterus to embryo implantation can be elicited by locally applied growth factors. Proceedings of the National Academy of Sciences of the United States of America *98*, 1047-1052.

Paria, B.C., Reese, J., Das, S.K., and Dey, S.K. (2002). Deciphering the cross-talk of implantation: advances and challenges. Science *296*, 2185-2188.

Parkening, T.A., Collins, T.J., and Au, W.W. (1988). Paternal age and its effects on reproduction in C57BL/6NNia mice. J Gerontol *43*, B79-84.

Patel, B., Elguero, S., Thakore, S., Dahoud, W., Bedaiwy, M., and Mesiano, S. (2015). Role of nuclear progesterone receptor isoforms in uterine pathophysiology. Hum Reprod Update *21*, 155-173.

Patel, R., Moffatt, J.D., Mourmoura, E., Demaison, L., Seed, P.T., Poston, L., and Tribe, R.M. (2017). Effect of reproductive ageing on pregnant mouse uterus and cervix. J Physiol *595*, 2065-2084.

Pavlik, E.J., and Coulson, P.B. (1976). Modulation of estrogen receptors in four different target tissues: differential effects of estrogen vs progesterone. Journal of steroid biochemistry *7*, 369-376.

Pawar, S., Laws, M.J., Bagchi, I.C., and Bagchi, M.K. (2015). Uterine Epithelial Estrogen Receptor-α Controls Decidualization via a Paracrine Mechanism. Mol Endocrinol *29*, 1362-1374.

Pawar, S., Starosvetsky, E., Orvis, G.D., Behringer, R.R., Bagchi, I.C., and Bagchi, M.K. (2013). STAT3 regulates uterine epithelial remodeling and epithelial-stromal crosstalk during implantation. Mol Endocrinol *27*, 1996-2012.

Peng, J., Monsivais, D., You, R., Zhong, H., Pangas, S.A., and Matzuk, M.M. (2015). Uterine activin receptor-like kinase 5 is crucial for blastocyst implantation and placental development. Proceedings of the National Academy of Sciences of the United States of America *112*, E5098-5107.

Pepling, M.E. (2012). Follicular assembly: mechanisms of action. Reproduction *143*, 139-149.

Perez-Garcia, V., Fineberg, E., Wilson, R., Murray, A., Mazzeo, C.I., Tudor, C., Sienerth, A., White, J.K., Tuck, E., Ryder, E.J.*, et al.* (2018). Placentation defects are highly prevalent in embryonic lethal mouse mutants. Nature *555*, 463-468.

Pijnenborg, R., Vercruysse, L., and Brosens, I. (2011). Deep placentation. Best practice & research Clinical obstetrics & gynaecology *25*, 273-285.

Plaks, V., Birnberg, T., Berkutzki, T., Sela, S., BenYashar, A., Kalchenko, V., Mor, G., Keshet, E., Dekel, N., Neeman, M.*, et al.* (2008). Uterine DCs are crucial for decidua formation during embryo implantation in mice. J Clin Invest *118*, 3954-3965.

Plaks, V., Rinkenberger, J., Dai, J., Flannery, M., Sund, M., Kanasaki, K., Ni, W., Kalluri, R., and Werb, Z. (2013). Matrix metalloproteinase-9 deficiency phenocopies features of preeclampsia and intrauterine growth restriction. Proceedings of the National Academy of Sciences of the United States of America *110*, 11109-11114.

Pratt, W.B., and Toft, D.O. (1997). Steroid receptor interactions with heat shock protein and immunophilin chaperones. Endocr Rev *18*, 306-360.

Prescott, M.J., and Lidster, K. (2017). Improving quality of science through better animal welfare: the NC3Rs strategy. Lab animal *46*, 152-156.

Proietti, C.J., Beguelin, W., Flaque, M.C., Cayrol, F., Rivas, M.A., Tkach, M., Charreau, E.H., Schillaci, R., and Elizalde, P.V. (2011). Novel role of signal transducer and activator of transcription 3 as a progesterone receptor coactivator in breast cancer. Steroids *76*, 381-392.

Psychoyos, A. (1973). Hormonal control of ovoimplantation. Vitam Horm *31*, 201-256.

Qi, Q.R., Xie, Q.Z., Liu, X.L., and Zhou, Y. (2014). Osteopontin is expressed in the mouse uterus during early pregnancy and promotes mouse blastocyst attachment and invasion in vitro. PLoS One *9*, e104955.

Qiao, J., Wang, Z.B., Feng, H.L., Miao, Y.L., Wang, Q., Yu, Y., Wei, Y.C., Yan, J., Wang, W.H., Shen, W.*, et al.* (2014). The root of reduced fertility in aged women and possible therapentic options: current status and future perspects. Molecular aspects of medicine *38*, 54-85.

Quinlan, A.R., and Hall, I.M. (2010). BEDTools: a flexible suite of utilities for comparing genomic features. Bioinformatics *26*, 841-842.

Radulescu, L., Munteanu, O., Popa, F., and Cirstoiu, M. (2013). The implications and consequences of maternal obesity on fetal intrauterine growth restriction. Journal of medicine and life *6*, 292-298.

Ramathal, C.Y., Bagchi, I.C., Taylor, R.N., and Bagchi, M.K. (2010). Endometrial decidualization: of mice and men. Semin Reprod Med *28*, 17-26.

Ratajczak, C.K., and Muglia, L.J. (2008). Insights into parturition biology from genetically altered mice. Pediatric research *64*, 581-589.

Renoir, J.M., Radanyi, C., Faber, L.E., and Baulieu, E.E. (1990). The non-DNA-binding heterooligomeric form of mammalian steroid hormone receptors contains a hsp90-bound 59-kilodalton protein. J Biol Chem *265*, 10740-10745.

Rhee, J.S., Saben, J.L., Mayer, A.L., Schulte, M.B., Asghar, Z., Stephens, C., Chi, M.M.Y., and Moley, K.H. (2016). Diet-induced obesity impairs endometrial stromal cell decidualization: a potential role for impaired autophagy. Human Reproduction (Oxford, England) *31*, 1315-1326.

Robker, R.L., Watson, L.N., Robertson, S.A., Dunning, K.R., McLaughlin, E.A., and Russell, D.L. (2014). Identification of sites of STAT3 action in the female reproductive tract through conditional gene deletion. PLoS One *9*, e101182.

Rosario, F.J., Kanai, Y., Powell, T.L., and Jansson, T. (2015). Increased placental nutrient transport in a novel mouse model of maternal obesity with fetal overgrowth. Obesity (Silver Spring, Md) *23*, 1663-1670.

Rossant, J., and Cross, J.C. (2001). Placental development: lessons from mouse mutants. Nat Rev Genet *2*, 538-548.

Roth, G.S. (1995). Changes in tissue responsiveness to hormones and neurotransmitters during aging. Exp Gerontol *30*, 361-368.

Saiduddin, S., and Zassenhaus, H.P. (1979). Estrous cycles, decidual cell response and uterine estrogen and progesterone receptor in Fischer 344 virgin aging rats. Proc Soc Exp Biol Med *161*, 119-122.

Salafia, C.M., Charles, A.K., and Maas, E.M. (2006). Placenta and fetal growth restriction. Clin Obstet Gynecol *49*, 236-256.

Salamonsen, L.A., Dimitriadis, E., Jones, R.L., and Nie, G. (2003). Complex regulation of decidualization: a role for cytokines and proteases--a review. Placenta *24 Suppl A*, S76-85.

Santos-Rosa, H., Schneider, R., Bannister, A.J., Sherriff, J., Bernstein, B.E., Emre, N.C., Schreiber, S.L., Mellor, J., and Kouzarides, T. (2002). Active genes are tri-methylated at K4 of histone H3. Nature *419*, 407-411.

Sato, M., and Sato, K. (2013). Maternal inheritance of mitochondrial DNA by diverse mechanisms to eliminate paternal mitochondrial DNA. Biochimica et biophysica acta *1833*, 1979-1984.

Schon, E.A., Kim, S.H., Ferreira, J.C., Magalhães, P., Grace, M., Warburton, D., and Gross, S.J. (2000). Chromosomal non-disjunction in human oocytes: is there a mitochondrial connection? Hum Reprod *15 Suppl 2*, 160-172.

Schulkey, C.E., Regmi, S.D., Magnan, R.A., Danzo, M.T., Luther, H., Hutchinson, A.K., Panzer, A.A., Grady, M.M., Wilson, D.B., and Jay, P.Y. (2015). The maternal-age-associated risk of congenital heart disease is modifiable. Nature *520*, 230-233.

Selesniemi, K., Lee, H.J., Muhlhauser, A., and Tilly, J.L. (2011). Prevention of maternal aging-associated oocyte aneuploidy and meiotic spindle defects in mice by dietary and genetic strategies. Proceedings of the National Academy of Sciences of the United States of America *108*, 12319-12324.

Senner, C.E., and Hemberger, M. (2010). Regulation of early trophoblast differentiation - lessons from the mouse. Placenta *31*, 944-950.

Serre, V., and Robaire, B. (1998). Paternal age affects fertility and progeny outcome in the Brown Norway rat. Fertil Steril *70*, 625-631.

Sever, R., and Glass, C.K. (2013). Signaling by nuclear receptors. Cold Spring Harbor perspectives in biology *5*, a016709.

Shapiro, M., and Talbert, G.B. (1974). The Effect of Maternal Age on Decidualization in the Mouse. Journal of Gerontology *29*, 145-148.

Sharma, S., Godbole, G., and Modi, D. (2016). Decidual Control of Trophoblast Invasion. Am J Reprod Immunol *75*, 341-350.

Shuya, L.L., Menkhorst, E.M., Yap, J., Li, P., Lane, N., and Dimitriadis, E. (2011). Leukemia inhibitory factor enhances endometrial stromal cell decidualization in humans and mice. PLoS One *6*, e25288.

Simmen, R.C., Heard, M.E., Simmen, A.M., Montales, M.T., Marji, M., Scanlon, S., and Pabona, J.M. (2015). The Krüppel-like factors in female reproductive system pathologies. J Mol Endocrinol *54*, R89-R101.

Simmons, D.G., and Cross, J.C. (2005). Determinants of trophoblast lineage and cell subtype specification in the mouse placenta. Dev Biol *284*, 12-24.

Simmons, D.G., Fortier, A.L., and Cross, J.C. (2007). Diverse subtypes and developmental origins of trophoblast giant cells in the mouse placenta. Dev Biol *304*, 567-578.

Simmons, D.G., Natale, D.R., Begay, V., Hughes, M., Leutz, A., and Cross, J.C. (2008). Early patterning of the chorion leads to the trilaminar trophoblast cell structure in the placental labyrinth. Development *135*, 2083-2091.

Simon-Santamaria, J., Malovic, I., Warren, A., Oteiza, A., Le Couteur, D., Smedsrød, B., McCourt, P., and Sørensen, K.K. (2010). Age-Related Changes in Scavenger Receptor–Mediated Endocytosis in Rat Liver Sinusoidal Endothelial Cells. The Journals of Gerontology Series A: Biological Sciences and Medical Sciences *65A*, 951-960.

Simsek-Duran, F., Li, F., Ford, W., Swanson, R.J., Jones, H.W., and Castora, F.J. (2013). Age-associated metabolic and morphologic changes in mitochondria of individual mouse and hamster oocytes. PLoS One *8*, e64955.

Singh, H., Endo, Y., and Nie, G. (2011). Decidual HtrA3 negatively regulates trophoblast invasion during human placentation. Hum Reprod *26*, 748-757.

Smallwood, S.A., Tomizawa, S., Krueger, F., Ruf, N., Carli, N., Segonds-Pichon, A., Sato, S., Hata, K., Andrews, S.R., and Kelsey, G. (2011). Dynamic CpG island methylation landscape in oocytes and preimplantation embryos. Nat Genet *43*, 811-814.

Soares, S.R., Troncoso, C., Bosch, E., Serra, V., Simon, C., Remohi, J., and Pellicer, A. (2005). Age and uterine receptiveness: predicting the outcome of oocyte donation cycles. J Clin Endocrinol Metab *90*, 4399-4404.

Sonderegger, S., Pollheimer, J., and Knöfler, M. (2010). Wnt Signalling in Implantation, Decidualisation and Placental Differentiation – Review. Placenta *31*, 839-847.

Song, H., Lim, H., Paria, B.C., Matsumoto, H., Swift, L.L., Morrow, J., Bonventre, J.V., and Dey, S.K. (2002). Cytosolic phospholipase A2alpha is crucial [correction of A2alpha deficiency is crucial] for 'on-time' embryo implantation that directs subsequent development. Development *129*, 2879-2889.

Speroff, L. (1994). The effect of aging on fertility. Curr Opin Obstet Gynecol *6*, 115-120.

Sroga, J.M., Ma, X., and Das, S.K. (2012). Developmental regulation of decidual cell polyploidy at the site of implantation. Frontiers in bioscience (Scholar edition) *4*, 1475-1486.

Staley, K., and Scharfman, H. (2005). A woman's prerogative. Nature Neuroscience *8*, 697.

Stang, J., and Huffman, L.G. (2016). Position of the Academy of Nutrition and Dietetics: Obesity, Reproduction, and Pregnancy Outcomes. Journal of the Academy of Nutrition and Dietetics *116*, 677-691.

Stark, R., and Brown, G. (2011). DiffBind differential binding analysis of ChIP-Seq peak data, Vol 100.

Statistics, O.f.N. (2014). Live Birth in England and Wales by Characteristics of Mother 1, 2013.

statistics, O.f.n. (2017). Statistics on Obesity, Physical Activity and Diet England: 2017.

Stewart, C.L., Kaspar, P., Brunet, L.J., Bhatt, H., Gadi, I., Köntgen, F., and Abbondanzo, S.J. (1992). Blastocyst implantation depends on maternal expression of leukaemia inhibitory factor. Nature *359*, 76-79.

Stewart, E.A., Cookson, C.L., Gandolfo, R.A., and Schulze-Rath, R. (2017). Epidemiology of uterine fibroids: a systematic review. BJOG : an international journal of obstetrics and gynaecology *124*, 1501-1512.

Stindl, R. (2011). Old Fathers and Long-Telomered Offspring: Elongation of Telomeres in the Testes of Older Men Versus Transgenerational Erosion of Germline Telomeres, Vol 5.

Strumpf, D., Mao, C.A., Yamanaka, Y., Ralston, A., Chawengsaksophak, K., Beck, F., and Rossant, J. (2005). Cdx2 is required for correct cell fate specification and differentiation of trophectoderm in the mouse blastocyst. Development *132*, 2093-2102.

Su, M.T., Lin, S.H., and Chen, Y.C. (2011). Association of sex hormone receptor gene polymorphisms with recurrent pregnancy loss: a systematic review and meta-analysis. Fertil Steril *96*, 1435-1444.e1431.

Sun, X., Bartos, A., Whitsett, J.A., and Dey, S.K. (2013). Uterine Deletion of Gp130 or Stat3 Shows Implantation Failure with Increased Estrogenic Responses. Molecular Endocrinology *27*, 1492-1501.

Sun, X., Zhang, L., Xie, H., Wan, H., Magella, B., Whitsett, J.A., and Dey, S.K. (2012). Kruppel-like factor 5 (KLF5) is critical for conferring uterine receptivity to implantation. Proceedings of the National Academy of Sciences of the United States of America *109*, 1145-1150.

Tagliani, E., Shi, C., Nancy, P., Tay, C.S., Pamer, E.G., and Erlebacher, A. (2011). Coordinate regulation of tissue macrophage and dendritic cell population dynamics by CSF-1. J Exp Med *208*, 1901-1916.

Talbert, G.B. (1971). Effect of maternal age on postimplantation reproductive failure in mice. J Reprod Fertil *24*, 449-452.

Talbert, G.B., and Krohn, P.L. (1966). Effect of maternal age on viability of ova and uterine support of pregnancy in mice. J Reprod Fertil *11*, 399-406.

Tan, J., Paria, B.C., Dey, S.K., and Das, S.K. (1999). Differential uterine expression of estrogen and progesterone receptors correlates with uterine preparation for implantation and decidualization in the mouse. Endocrinology *140*, 5310-5321.

Tanaka, S. (2006). Derivation and culture of mouse trophoblast stem cells in vitro. Methods in molecular biology (Clifton, NJ) *329*, 35-44.

Tanaka, S., Kunath, T., Hadjantonakis, A.K., Nagy, A., and Rossant, J. (1998). Promotion of trophoblast stem cell proliferation by FGF4. Science *282*, 2072-2075.

Tanaka, S., Nakanishi, M.O., and Shiota, K. (2014). DNA methylation and its role in the trophoblast cell lineage. Int J Dev Biol *58*, 231-238.

Tao, M.H., and Freudenheim, J.L. (2010). DNA methylation in endometrial cancer. Epigenetics *5*, 491-498.

te Velde, E.R., and Pearson, P.L. (2002). The variability of female reproductive ageing. Hum Reprod Update *8*, 141-154.

Teklenburg, G., Salker, M., Molokhia, M., Lavery, S., Trew, G., Aojanepong, T., Mardon, H.J., Lokugamage, A.U., Rai, R., Landles, C*., et al.* (2010). Natural selection of human embryos: decidualizing endometrial stromal cells serve as sensors of embryo quality upon implantation. PLoS One *5*, e10258.

Thakur, M.K. (1988). Molecular mechanism of steroid hormone action during aging. A review. Mech Ageing Dev *45*, 93-110.

Tilly, J.L., and Sinclair, D.A. (2013). Germline energetics, aging, and female infertility. Cell Metab *17*, 838-850.

Tranguch, S., Cheung-Flynn, J., Daikoku, T., Prapapanich, V., Cox, M.B., Xie, H., Wang, H., Das, S.K., Smith, D.F., and Dey, S.K. (2005). Cochaperone immunophilin FKBP52 is critical to uterine receptivity for embryo implantation. Proceedings of the National Academy of Sciences of the United States of America *102*, 14326-14331.

Tsurumi, A., and Li, W.X. (2012). Global heterochromatin loss: a unifying theory of aging? Epigenetics *7*, 680-688.

Turco, M.Y., Gardner, L., Hughes, J., Cindrova-Davies, T., Gomez, M.J., Farrell, L., Hollinshead, M., Marsh, S.G.E., Brosens, J.J., Critchley, H.O*., et al.* (2017). Long-term, hormone-responsive organoid cultures of human endometrium in a chemically defined medium. Nat Cell Biol *19*, 568-577.

Ueno, M., Lee, L.K., Chhabra, A., Kim, Y.J., Sasidharan, R., Van Handel, B., Wang, Y., Kamata, M., Kamran, P., Sereti, K.I*., et al.* (2013). c-Met-dependent multipotent labyrinth trophoblast progenitors establish placental exchange interface. Dev Cell *27*, 373-386.

Uy, G.D., Downs, K.M., and Gardner, R.L. (2002). Inhibition of trophoblast stem cell potential in chorionic ectoderm coincides with occlusion of the ectoplacental cavity in the mouse. Development *129*, 3913-3924.

Vambergue, A., and Fajardy, I. (2011). Consequences of gestational and pregestational diabetes on placental function and birth weight. World Journal of Diabetes *2*, 196-203.

van Echten-Arends, J., Mastenbroek, S., Sikkema-Raddatz, B., Korevaar, J.C., Heineman, M.J., van der Veen, F., and Repping, S. (2011). Chromosomal mosaicism in human preimplantation embryos: a systematic review. Hum Reprod Update *17*, 620-627.

Vannuccini, S., Clifton, V.L., Fraser, I.S., Taylor, H.S., Critchley, H., Giudice, L.C., and Petraglia, F. (2016). Infertility and reproductive disorders: impact of hormonal and inflammatory mechanisms on pregnancy outcome. Hum Reprod Update *22*, 104-115.

Ventura, S.J., Abma, J.C., Mosher, W.D., and Henshaw, S.K. (2009). Estimated pregnancy rates for the United States, 1990-2005: an update. National vital statistics reports : from the Centers for Disease Control and Prevention, National Center for Health Statistics, National Vital Statistics System *58*, 1-14.

Villeponteau, B. (1997). The heterochromatin loss model of aging. Exp Gerontol *32*, 383-394.

Vincent, Z.L., Farquhar, C.M., Mitchell, M.D., and Ponnampalam, A.P. (2011). Expression and regulation of DNA methyltransferases in human endometrium. Fertil Steril *95*, 1522-1525.e1521.

Vinturache, A.E., McDonald, S., Slater, D., and Tough, S. (2015). Perinatal outcomes of maternal overweight and obesity in term infants: a population-based cohort study in Canada. Scientific Reports *5*, 9334.

Volarcik, K., Sheean, L., Goldfarb, J., Woods, L., Abdul-Karim, F.W., and Hunt, P. (1998). The meiotic competence of in-vitro matured human oocytes is influenced by donor age: evidence that folliculogenesis is compromised in the reproductively aged ovary. Hum Reprod *13*, 154-160.

Wang, H., Critchley, H.O., Kelly, R.W., Shen, D., and Baird, D.T. (1998). Progesterone receptor subtype B is differentially regulated in human endometrial stroma. Mol Hum Reprod *4*, 407-412.

Wang, H., and Dey, S.K. (2006). Roadmap to embryo implantation: clues from mouse models. Nat Rev Genet *7*, 185-199.

Wang, Q., Lu, J., Zhang, S., Wang, S., Wang, W., Wang, B., Wang, F., Chen, Q., Duan, E., Leitges, M.*, et al.* (2013). Wnt6 is essential for stromal cell proliferation during decidualization in mice. Biol Reprod *88*, 5.

Wang, Y.A., Farquhar, C., and Sullivan, E.A. (2012). Donor age is a major determinant of success of oocyte donation/recipient programme. Hum Reprod *27*, 118-125.

Weissbein, U., Schachter, M., Egli, D., and Benvenisty, N. (2016). Analysis of chromosomal aberrations and recombination by allelic bias in RNA-Seq. Nature communications *7*, 12144.

Wells, D., Kaur, K., Grifo, J., Glassner, M., Taylor, J.C., Fragouli, E., and Munne, S. (2014). Clinical utilisation of a rapid low-pass whole genome sequencing technique for the diagnosis of aneuploidy in human embryos prior to implantation. J Med Genet *51*, 553-562.

Wendland, E.M., Torloni, M.R., Falavigna, M., Trujillo, J., Dode, M.A., Campos, M.A., Duncan, B.B., and Schmidt, M.I. (2012). Gestational diabetes and pregnancy outcomes - a systematic review of the World Health Organization (WHO) and the International Association of Diabetes in Pregnancy Study Groups (IADPSG) diagnostic criteria. BMC Pregnancy and Childbirth *12*, 23.

Winnefeld, M., and Lyko, F. (2012). The aging epigenome: DNA methylation from the cradle to the grave. Genome Biol *13*, 165.

Wood, J.G., Hillenmeyer, S., Lawrence, C., Chang, C., Hosier, S., Lightfoot, W., Mukherjee, E., Jiang, N., Schorl, C., Brodsky, A.S*., et al.* (2010). Chromatin remodeling in the aging genome of Drosophila. Aging Cell *9*, 971-978.

Wu, L., de Bruin, A., Saavedra, H.I., Starovic, M., Trimboli, A., Yang, Y., Opavska, J., Wilson, P., Thompson, J.C., Ostrowski, M.C*., et al.* (2003). Extra-embryonic function of Rb is essential for embryonic development and viability. Nature *421*, 942-947.

Yamagata, Y., Asada, H., Tamura, I., Lee, L., Maekawa, R., Taniguchi, K., Taketani, T., Matsuoka, A., Tamura, H., and Sugino, N. (2009). DNA methyltransferase expression in the human endometrium: down-regulation by progesterone and estrogen. Hum Reprod *24*, 1126-1132.

Yang, J., Boerm, M., McCarty, M., Bucana, C., Fidler, I.J., Zhuang, Y., and Su, B. (2000). Mekk3 is essential for early embryonic cardiovascular development. Nat Genet *24*, 309-313.

Yang, Z., Wolf, I.M., Chen, H., Periyasamy, S., Chen, Z., Yong, W., Shi, S., Zhao, W., Xu, J., Srivastava, A*., et al.* (2006). FK506-binding protein 52 is essential to uterine reproductive physiology controlled by the progesterone receptor A isoform. Mol Endocrinol *20*, 2682-2694.

Ying, Y., and Zhao, G.Q. (2000). Detection of multiple bone morphogenetic protein messenger ribonucleic acids and their signal transducer, Smad1, during mouse decidualization. Biol Reprod *63*, 1781-1786.

Yu, H.F., Yue, Z.P., Wang, K., Yang, Z.Q., Zhang, H.L., Geng, S., and Guo, B. (2017). Gja1 acts downstream of Acvr1 to regulate uterine decidualization via Hand2 in mice. The Journal of endocrinology *233*, 145-157.

Yue, M.X., Fu, X.W., Zhou, G.B., Hou, Y.P., Du, M., Wang, L., and Zhu, S.E. (2012). Abnormal DNA methylation in oocytes could be associated with a decrease in reproductive potential in old mice. J Assist Reprod Genet *29*, 643-650.

Zampieri, M., Ciccarone, F., Calabrese, R., Franceschi, C., Bürkle, A., and Caiafa, P. (2015). Reconfiguration of DNA methylation in aging. Mech Ageing Dev *151*, 60-70.

Zhang, S., Kong, S., Wang, B., Cheng, X., Chen, Y., Wu, W., Wang, Q., Shi, J., Zhang, Y., Wang, S*., et al.* (2014). Uterine Rbpj is required for embryonic-uterine orientation and decidual

remodeling via Notch pathway-independent and -dependent mechanisms. Cell Res *24*, 925-942.

Zhang, X., Wu, X.Q., Lu, S., Guo, Y.L., and Ma, X. (2006). Deficit of mitochondria-derived ATP during oxidative stress impairs mouse MII oocyte spindles. Cell Res *16*, 841-850.

Zhang, X.H., Liang, X., Wang, T.S., Liang, X.H., Zuo, R.J., Deng, W.B., Zhang, Z.R., Qin, F.N., Zhao, Z.A., and Yang, Z.M. (2013). Heparin-binding epidermal growth factor-like growth factor (HB-EGF) induction on Snail expression during mouse decidualization. Mol Cell Endocrinol *381*, 272-279.

Zhang, Y., Liu, T., Meyer, C.A., Eeckhoute, J., Johnson, D.S., Bernstein, B.E., Nusbaum, C., Myers, R.M., Brown, M., Li, W*., et al.* (2008). Model-based analysis of ChIP-Seq (MACS). Genome Biol *9*, R137.

Zhu, J.Y., Pang, Z.J., and Yu, Y.H. (2012). Regulation of trophoblast invasion: the role of matrix metalloproteinases. Reviews in obstetrics & gynecology *5*, e137-143.

Zimmermann, A., Bernuit, D., Gerlinger, C., Schaefers, M., and Geppert, K. (2012). Prevalence, symptoms and management of uterine fibroids: an international internet-based survey of 21,746 women. BMC Women's Health *12*, 6-6.

Appendix

Supplementary table 1 – List of 42 genes differentially expressed in RNA-seq data (DESeq2 p<0.05 and Intensity difference p<0.05) between trophoblast from implantation sites in young females, and implantation in aged females with a grossly abnormal embryo. Displayed as log2 fold change from young to aged.

Gene	Description	Log2 fold change
Sprr2h	small proline-rich protein 2H [Source:MGI Symbol;Acc:MGI:1330343]	6.04881159
Orm2	orosomucoid 2 [Source:MGI Symbol;Acc:MGI:97444]	5.721094281
Prr9	proline rich 9 [Source:MGI Symbol;Acc:MGI:1925680]	5.126459168
Gm7257	predicted gene 7257 [Source:MGI Symbol;Acc:MGI:3647831]	5.024863655
Hrc	histidine rich calcium binding protein [Source:MGI Symbol;Acc:MGI:96226]	4.404359793
Gm9513	predicted gene 9513 [Source:MGI Symbol;Acc:MGI:3779923]	4.205814487
Orm1	orosomucoid 1 [Source:MGI Symbol;Acc:MGI:97443]	4.083662161
Prl3d1	prolactin family 3, subfamily d, member 1 [Source:MGI Symbol;Acc:MGI:97606]	4.016602917
Prl3d3	prolactin family 3, subfamily d, member 3 [Source:MGI Symbol;Acc:MGI:2660938]	3.896496483
Ceacam15	carcinoembryonic antigen-related cell adhesion molecule 15 [Source:MGI Symbol;Acc:MGI:2141810]	3.55801466
Prl3d2	prolactin family 3, subfamily d, member 1 [Source:MGI Symbol;Acc:MGI:2660935]	3.532794993
Prl5a1	prolactin family 5, subfamily a, member 1 [Source:MGI Symbol;Acc:MGI:106332]	3.366017537
Cts7	cathepsin 7 [Source:MGI Symbol;Acc:MGI:1860262]	3.351687553
Pfpl	pore forming protein-like [Source:MGI Symbol;Acc:MGI:1860266]	3.092158355
Erv3	endogenous retroviral sequence 3 [Source:MGI Symbol;Acc:MGI:1919245]	2.855199307
Rimklb	ribosomal modification protein rimK-like family member B [Source:MGI Symbol;Acc:MGI:1918325]	2.818320493
Prl8a1	prolactin family 8, subfamily a, member 1 [Source:MGI Symbol;Acc:MGI:1920494]	2.807027443
Htra1	HtrA serine peptidase 1 [Source:MGI Symbol;Acc:MGI:1929076]	2.781584173
Srd5a1	steroid 5 alpha-reductase 1 [Source:MGI Symbol;Acc:MGI:98400]	2.655812037
Prl8a2	prolactin family 8, subfamily a, member 2 [Source:MGI Symbol;Acc:MGI:894281]	2.589404407
Adamts5	a disintegrin-like and metallopeptidase (reprolysin type) with thrombospondin type 1 motif, 5 (aggrecanase-2) [Source:MGI Symbol;Acc:MGI:1346321]	2.256366183
Gjb2	gap junction protein, beta 2 [Source:MGI Symbol;Acc:MGI:95720]	-1.82263817
Ctsq	cathepsin Q [Source:MGI Symbol;Acc:MGI:2137385]	-1.981924423
Ceacam3	carcinoembryonic antigen-related cell adhesion molecule 3 [Source:MGI Symbol;Acc:MGI:3646296]	-2.17745023
Vnn1	vanin 1 [Source:MGI Symbol;Acc:MGI:108395]	-2.222526406
Synb	syncytin b [Source:MGI Symbol;Acc:MGI:3045308]	-2.276715743
Rgs17	regulator of G-protein signaling 17 [Source:MGI Symbol;Acc:MGI:1927469]	-2.49523986
Prl7a2	prolactin family 7, subfamily a, member 2 [Source:MGI Symbol;Acc:MGI:1206571]	-2.58688511
Spna1	spectrin alpha 1 [Source:MGI Symbol;Acc:MGI:98385]	-2.854647365
Tpbpb	trophoblast specific protein beta [Source:MGI Symbol;Acc:MGI:2151721]	-3.08609485
Spnb1	spectrin beta 1 [Source:MGI Symbol;Acc:MGI:98387]	-3.212407375
Psg26	pregnancy-specific glycoprotein 26 [Source:MGI Symbol;Acc:MGI:1891358]	-3.336263763

Gene	Description	Log2 fold change
Hba-x	hemoglobin X, alpha-like embryonic chain in Hba complex [Source:MGI Symbol;Acc:MGI:96019]	-3.36435228
Psg17	pregnancy specific glycoprotein 17 [Source:MGI Symbol;Acc:MGI:1347250]	-3.480721067
Psg18	pregnancy specific glycoprotein 18 [Source:MGI Symbol;Acc:MGI:1347251]	-3.53887766
Psg27	pregnancy-specific glycoprotein 27 [Source:MGI Symbol;Acc:MGI:1891359]	-3.57915276
Psg21	pregnancy-specific glycoprotein 21 [Source:MGI Symbol;Acc:MGI:1891353]	-4.009178287
Psg25	pregnancy-specific glycoprotein 25 [Source:MGI Symbol;Acc:MGI:1891357]	-4.056768033
Ceacam5	carcinoembryonic antigen-related cell adhesion molecule 5 [Source:MGI Symbol;Acc:MGI:1920500]	-4.104822782
Cts3	cathepsin 3 [Source:MGI Symbol;Acc:MGI:2151929]	-5.17780764
Ctsm	cathepsin M [Source:MGI Symbol;Acc:MGI:1927229]	-5.34532527
Prl8a8	prolactin family 8, subfamily a, member 81 [Source:MGI Symbol;Acc:MGI:1921438]	-5.419780078

Supplementary table 2 – List of 162 genes differentially expressed in RNA-seq data (DESeq2 $p<0.05$ and Intensity difference $p<0.05$) between deciduas from implantation sites in young females, and implantation in aged females with a grossly abnormal embryo. Displayed as log2 fold change from young to aged.

Gene	Description	Log2 fold change
Gm14085	predicted gene 14085 [Source:MGI Symbol;Acc:MGI:3702173]	6.977279923
Gpr151	G protein-coupled receptor 151 [Source:MGI Symbol;Acc:MGI:2441887]	5.599317794
Ptgdr	prostaglandin D receptor [Source:MGI Symbol;Acc:MGI:102966]	5.022367813
Cyp2j11	cytochrome P450, family 2, subfamily j, polypeptide 11 [Source:MGI Symbol;Acc:MGI:2140224]	4.534497434
Col14a1	collagen, type XIV, alpha 1 [Source:MGI Symbol;Acc:MGI:1341272]	4.355903981
Hmgcs2	3-hydroxy-3-methylglutaryl-Coenzyme A synthase 2 [Source:MGI Symbol;Acc:MGI:101939]	4.086267072
Hsd17b1	hydroxysteroid (17-beta) dehydrogenase 1 [Source:MGI Symbol;Acc:MGI:105077]	3.556262188
A530099J19Rik	RIKEN cDNA A530099J19 gene [Source:MGI Symbol;Acc:MGI:2441809]	3.309328058
Klrb1c	killer cell lectin-like receptor subfamily B member 1C [Source:MGI Symbol;Acc:MGI:107538]	3.169925001
Apcdd1	adenomatosis polyposis coli down-regulated 1 [Source:MGI Symbol;Acc:MGI:3513977]	3.160920188
Pcolce	procollagen C-endopeptidase enhancer protein [Source:MGI Symbol;Acc:MGI:105099]	3.080805944
Cbln1	cerebellin 1 precursor protein [Source:MGI Symbol;Acc:MGI:88281]	3.045936284
Mmp1a	matrix metallopeptidase 1a (interstitial collagenase) [Source:MGI Symbol;Acc:MGI:1933846]	3.030145164
Odz3	odd Oz/ten-m homolog 3 (Drosophila) [Source:MGI Symbol;Acc:MGI:1345183]	2.908395232
Gzma	granzyme A [Source:MGI Symbol;Acc:MGI:109266]	2.902567051
Vcan	versican [Source:MGI Symbol;Acc:MGI:102889]	2.894225492
Hrc	histidine rich calcium binding protein [Source:MGI Symbol;Acc:MGI:96226]	2.88675295

Dio3	deiodinase, iodothyronine type III [Source:MGI Symbol;Acc:MGI:1306782]	2.833670864
Ceacam15	carcinoembryonic antigen-related cell adhesion molecule 15 [Source:MGI Symbol;Acc:MGI:2141810]	2.83359125
Pfpl	pore forming protein-like [Source:MGI Symbol;Acc:MGI:1860266]	2.749816513
Capn6	calpain 6 [Source:MGI Symbol;Acc:MGI:1100850]	2.690411799
Col6a1	collagen, type VI, alpha 1 [Source:MGI Symbol;Acc:MGI:88459]	2.475213014
Kcnk2	potassium channel, subfamily K, member 2 [Source:MGI Symbol;Acc:MGI:109366]	2.455201818
Lrp4	low density lipoprotein receptor-related protein 4 [Source:MGI Symbol;Acc:MGI:2442252]	2.450278883
Col15a1	collagen, type XV, alpha 1 [Source:MGI Symbol;Acc:MGI:88449]	2.440664072
Qrfpr	pyroglutamylated RFamide peptide receptor [Source:MGI Symbol;Acc:MGI:2677633]	2.395484702
Tac2	tachykinin 2 [Source:MGI Symbol;Acc:MGI:98476]	2.394534528
Col6a2	collagen, type VI, alpha 2 [Source:MGI Symbol;Acc:MGI:88460]	2.373667366
Tshr	thyroid stimulating hormone receptor [Source:MGI Symbol;Acc:MGI:98849]	2.331929487
Atp1a2	ATPase, Na+/K+ transporting, alpha 2 polypeptide [Source:MGI Symbol;Acc:MGI:88106]	2.298029827
Krt84	keratin 84 [Source:MGI Symbol;Acc:MGI:96700]	2.297680549
Frem1	Fras1 related extracellular matrix protein 1 [Source:MGI Symbol;Acc:MGI:2670972]	2.272083328
Prl3d1	prolactin family 3, subfamily d, member 1 [Source:MGI Symbol;Acc:MGI:97606]	2.252700536
Adamtsl1	ADAMTS-like 1 [Source:MGI Symbol;Acc:MGI:1924989]	2.237833852
Bmp2	bone morphogenetic protein 2 [Source:MGI Symbol;Acc:MGI:88177]	2.123774278
4930547N16Rik	RIKEN cDNA 4930547N16 gene [Source:MGI Symbol;Acc:MGI:1922567]	2.098223536
Kazald1	Kazal-type serine peptidase inhibitor domain 1 [Source:MGI Symbol;Acc:MGI:2147606]	2.061065663
Pcsk5	proprotein convertase subtilisin/kexin type 5 [Source:MGI Symbol;Acc:MGI:97515]	2.032910315
Ldhd	lactate dehydrogenase D [Source:MGI Symbol;Acc:MGI:106428]	2.01264665
Igf1	insulin-like growth factor 1 [Source:MGI Symbol;Acc:MGI:96432]	1.988569995
Abat	4-aminobutyrate aminotransferase [Source:MGI Symbol;Acc:MGI:2443582]	1.961148134
Rcn1	reticulocalbin 1 [Source:MGI Symbol;Acc:MGI:104559]	1.93078679
2810417H13Rik	RIKEN cDNA 2810417H13 gene [Source:MGI Symbol;Acc:MGI:1915276]	1.912848051
Dhcr24	24-dehydrocholesterol reductase [Source:MGI Symbol;Acc:MGI:1922004]	1.887649206
Ptn	pleiotrophin [Source:MGI Symbol;Acc:MGI:97804]	1.84521885
Bcmo1	beta-carotene 15,15'-monooxygenase [Source:MGI Symbol;Acc:MGI:1926923]	1.82237174
Penk	preproenkephalin [Source:MGI Symbol;Acc:MGI:104629]	1.816355897
Hephl1	hephaestin-like 1 [Source:MGI Symbol;Acc:MGI:2685355]	1.803722422
Kcnip3	Kv channel interacting protein 3, calsenilin [Source:MGI Symbol;Acc:MGI:1929258]	1.772814273
Prps2	phosphoribosyl pyrophosphate synthetase 2 [Source:MGI Symbol;Acc:MGI:97776]	1.737904321
Il15ra	interleukin 15 receptor, alpha chain [Source:MGI Symbol;Acc:MGI:104644]	1.737427183
Cdh11	cadherin 11 [Source:MGI Symbol;Acc:MGI:99217]	1.736965594
Fmo1	flavin containing monooxygenase 1 [Source:MGI Symbol;Acc:MGI:1310002]	1.6966471
Anln	anillin, actin binding protein [Source:MGI Symbol;Acc:MGI:1920174]	1.695924237

Prkg2	protein kinase, cGMP-dependent, type II [Source:MGI Symbol;Acc:MGI:108173]	1.685950701
S100a4	S100 calcium binding protein A4 [Source:MGI Symbol;Acc:MGI:1330282]	1.681200912
Adamts3	a disintegrin-like and metallopeptidase (reprolysin type) with thrombospondin type 1 motif, 3 [Source:MGI Symbol;Acc:MGI:3045353]	1.679123328
F13a1	coagulation factor XIII, A1 subunit [Source:MGI Symbol;Acc:MGI:1921395]	1.597473504
Cyp11b1	cytochrome P450, family 11, subfamily b, polypeptide 1 [Source:MGI Symbol;Acc:MGI:88583]	1.586736254
Pi15	peptidase inhibitor 15 [Source:MGI Symbol;Acc:MGI:1934659]	1.533531218
Nrcam	neuron-glia-CAM-related cell adhesion molecule [Source:MGI Symbol;Acc:MGI:104750]	1.530706186
S100g	S100 calcium binding protein G [Source:MGI Symbol;Acc:MGI:104528]	1.528006616
Acaa2	acetyl-Coenzyme A acyltransferase 2 (mitochondrial 3-oxoacyl-Coenzyme A thiolase) [Source:MGI Symbol;Acc:MGI:1098623]	1.515917432
Ccnd1	cyclin D1 [Source:MGI Symbol;Acc:MGI:88313]	1.503489885
Tdo2	tryptophan 2,3-dioxygenase [Source:MGI Symbol;Acc:MGI:1928486]	1.498164212
Col1a1	collagen, type I, alpha 1 [Source:MGI Symbol;Acc:MGI:88467]	1.47781787
Ccr2	chemokine (C-C motif) receptor 2 [Source:MGI Symbol;Acc:MGI:106185]	1.39959221
Serpina3n	serine (or cysteine) peptidase inhibitor, clade A, member 3N [Source:MGI Symbol;Acc:MGI:105045]	1.369320287
Magi1	membrane associated guanylate kinase, WW and PDZ domain containing 1 [Source:MGI Symbol;Acc:MGI:1203522]	1.322001794
Top2a	topoisomerase (DNA) II alpha [Source:MGI Symbol;Acc:MGI:98790]	1.286707235
Olfml3	olfactomedin-like 3 [Source:MGI Symbol;Acc:MGI:1914877]	1.276362051
Kcnd3	potassium voltage-gated channel, Shal-related family, member 3 [Source:MGI Symbol;Acc:MGI:1928743]	1.234420686
Ugt1a7c	UDP glucuronosyltransferase 1 family, polypeptide A7C [Source:MGI Symbol;Acc:MGI:3032636]	1.199774119
Tlr3	toll-like receptor 3 [Source:MGI Symbol;Acc:MGI:2156367]	1.176174004
Smad6	MAD homolog 6 (Drosophila) [Source:MGI Symbol;Acc:MGI:1336883]	1.141243912
Sulf1	sulfatase 1 [Source:MGI Symbol;Acc:MGI:2138563]	1.101518199
Nrp1	neuropilin 1 [Source:MGI Symbol;Acc:MGI:106206]	0.967663026
Gimap4	GTPase, IMAP family member 4 [Source:MGI Symbol;Acc:MGI:1349656]	0.939634696
Peg3	paternally expressed 3 [Source:MGI Symbol;Acc:MGI:104748]	-0.103516897
Prl8a9	prolactin family8, subfamily a, member 9 [Source:MGI Symbol;Acc:MGI:1914560]	-0.246265233
Dsg2	desmoglein 2 [Source:MGI Symbol;Acc:MGI:1196466]	-0.330759662
Gpr126	G protein-coupled receptor 126 [Source:MGI Symbol;Acc:MGI:1916151]	-0.344179743
Obsl1	obscurin-like 1 [Source:MGI Symbol;Acc:MGI:2138628]	-0.53652628
Nt5e	5' nucleotidase, ecto [Source:MGI Symbol;Acc:MGI:99782]	-0.536709606
Pcsk6	proprotein convertase subtilisin/kexin type 6 [Source:MGI Symbol;Acc:MGI:102897]	-0.612303906
Phactr1	phosphatase and actin regulator 1 [Source:MGI Symbol;Acc:MGI:2659021]	-0.627987432
Prl3b1	prolactin family 3, subfamily b, member 1 [Source:MGI Symbol;Acc:MGI:97607]	-0.662026097
1600014K23Rik	RIKEN cDNA 1600014K23 gene [Source:MGI Symbol;Acc:MGI:1919246]	-0.70824409
Serpinb9e	serine (or cysteine) peptidase inhibitor, clade B, member 9e [Source:MGI Symbol;Acc:MGI:894672]	-0.751020415
Fam43a	family with sequence similarity 43, member A [Source:MGI Symbol;Acc:MGI:2676309]	-0.768955708

Leprel1	leprecan-like 1 [Source:MGI Symbol;Acc:MGI:2146663]	-0.777240994
4933402E13Rik	RIKEN cDNA 4933402E13 gene [Source:MGI Symbol;Acc:MGI:1921687]	-0.786542213
Ildr2	immunoglobulin-like domain containing receptor 2 [Source:MGI Symbol;Acc:MGI:1196370]	-0.81325738
Kank3	KN motif and ankyrin repeat domains 3 [Source:MGI Symbol;Acc:MGI:1098615]	-0.856641737
Ak3	adenylate kinase 3 [Source:MGI Symbol;Acc:MGI:1860835]	-0.86628093
Fnd3c2	fibronectin type III domain containing 3C2 [Source:MGI Symbol;Acc:MGI:2685621]	-0.868882634
1600012P17Rik	RIKEN cDNA 1600012P17 gene [Source:MGI Symbol;Acc:MGI:1919275]	-0.876803307
Sele	selectin, endothelial cell [Source:MGI Symbol;Acc:MGI:98278]	-0.880598283
Lamb1	laminin B1 [Source:MGI Symbol;Acc:MGI:96743]	-0.914123125
Psg27	pregnancy-specific glycoprotein 27 [Source:MGI Symbol;Acc:MGI:1891359]	-0.943830623
Prl7d1	prolactin family 7, subfamily d, member 1 [Source:MGI Symbol;Acc:MGI:97619]	-1.00415618
Prl7a2	prolactin family 7, subfamily a, member 2 [Source:MGI Symbol;Acc:MGI:1206571]	-1.010262874
Taf7l	TAF7-like RNA polymerase II, TATA box binding protein (TBP)-associated factor [Source:MGI Symbol;Acc:MGI:1921719]	-1.015006045
Ceacam14	carcinoembryonic antigen-related cell adhesion molecule 14 [Source:MGI Symbol;Acc:MGI:1914334]	-1.024280997
AU015836	expressed sequence AU015836 [Source:MGI Symbol;Acc:MGI:2147954]	-1.071683929
Sct	secretin [Source:MGI Symbol;Acc:MGI:99466]	-1.087794373
Ceacam3	carcinoembryonic antigen-related cell adhesion molecule 3 [Source:MGI Symbol;Acc:MGI:3646296]	-1.088770952
4932442L08Rik	RIKEN cDNA 4932442L08 gene [Source:MGI Symbol;Acc:MGI:1921682]	-1.129283017
Pappa2	pappalysin 2 [Source:MGI Symbol;Acc:MGI:3051647]	-1.140217179
Steap4	STEAP family member 4 [Source:MGI Symbol;Acc:MGI:1923560]	-1.161497382
Sema3g	sema domain, immunoglobulin domain (Ig), short basic domain, secreted, (semaphorin) 3G [Source:MGI Symbol;Acc:MGI:3041242]	-1.161794253
Ctsm	cathepsin M [Source:MGI Symbol;Acc:MGI:1927229]	-1.177054466
Psg28	pregnancy-specific glycoprotein 28 [Source:MGI Symbol;Acc:MGI:1891360]	-1.189477799
Psg23	pregnancy-specific glycoprotein 23 [Source:MGI Symbol;Acc:MGI:1891355]	-1.194936889
Psg25	pregnancy-specific glycoprotein 25 [Source:MGI Symbol;Acc:MGI:1891357]	-1.199189123
Tpbpb	trophoblast specific protein beta [Source:MGI Symbol;Acc:MGI:2151721]	-1.211849766
Galnt6	No description	-1.228336315
Tpbpa	trophoblast specific protein alpha [Source:MGI Symbol;Acc:MGI:98795]	-1.253566028
Prl2c1	Prolactin family 2, subfamily c, member 1 [Source:MGI Symbol;Acc:MGI:3649927]	-1.269546215
Mmp11	matrix metallopeptidase 11 [Source:MGI Symbol;Acc:MGI:97008]	-1.281560053
Psg21	pregnancy-specific glycoprotein 21 [Source:MGI Symbol;Acc:MGI:1891353]	-1.291238891
Fabp3	fatty acid binding protein 3, muscle and heart [Source:MGI Symbol;Acc:MGI:95476]	-1.292617255
Edn1	endothelin 1 [Source:MGI Symbol;Acc:MGI:95283]	-1.298201319
Ntn4	netrin 4 [Source:MGI Symbol;Acc:MGI:1888978]	-1.347997195
Spna1	spectrin alpha 1 [Source:MGI Symbol;Acc:MGI:98385]	-1.349186302
Lama1	laminin, alpha 1 [Source:MGI Symbol;Acc:MGI:99892]	-1.359716243

Tmc5	transmembrane channel-like gene family 5 [Source:MGI Symbol;Acc:MGI:1921674]	-1.367731785
Crispld2	cysteine-rich secretory protein LCCL domain containing 2 [Source:MGI Symbol;Acc:MGI:1926142]	-1.372311474
Sfrp5	secreted frizzled-related sequence protein 5 [Source:MGI Symbol;Acc:MGI:1860298]	-1.375274024
Ptger3	prostaglandin E receptor 3 (subtype EP3) [Source:MGI Symbol;Acc:MGI:97795]	-1.414919781
Hbb-bh1	hemoglobin Z, beta-like embryonic chain [Source:MGI Symbol;Acc:MGI:96024]	-1.444363385
Cts3	cathepsin 3 [Source:MGI Symbol;Acc:MGI:2151929]	-1.445477447
Prl7b1	prolactin family 7, subfamily b, member 1 [Source:MGI Symbol;Acc:MGI:1922846]	-1.520928668
Nov	nephroblastoma overexpressed gene [Source:MGI Symbol;Acc:MGI:109185]	-1.532054713
Inhba	inhibin beta-A [Source:MGI Symbol;Acc:MGI:96570]	-1.534273709
Uchl1	ubiquitin carboxy-terminal hydrolase L1 [Source:MGI Symbol;Acc:MGI:103149]	-1.565041807
Tfpi2	tissue factor pathway inhibitor 2 [Source:MGI Symbol;Acc:MGI:108543]	-1.597300451
Krt14	keratin 14 [Source:MGI Symbol;Acc:MGI:96688]	-1.618321098
Tmem132e	transmembrane protein 132E [Source:MGI Symbol;Acc:MGI:2685490]	-1.623383418
Ednra	endothelin receptor type A [Source:MGI Symbol;Acc:MGI:105923]	-1.627956554
Fam46c	family with sequence similarity 46, member C [Source:MGI Symbol;Acc:MGI:1921895]	-1.648474189
Igfbp5	insulin-like growth factor binding protein 5 [Source:MGI Symbol;Acc:MGI:96440]	-1.700949518
Pamr1	peptidase domain containing associated with muscle regeneration 1 [Source:MGI Symbol;Acc:MGI:2445082]	-1.796883319
Ermap	erythroblast membrane-associated protein [Source:MGI Symbol;Acc:MGI:1349816]	-1.797560119
9530008L14Rik	RIKEN cDNA 9530008L14 gene [Source:MGI Symbol;Acc:MGI:1924596]	-1.806899885
Epb4.2	erythrocyte protein band 4.2 [Source:MGI Symbol;Acc:MGI:95402]	-1.843354939
Cldn11	claudin 11 [Source:MGI Symbol;Acc:MGI:106925]	-1.906305442
Pkhd1l1	polycystic kidney and hepatic disease 1-like 1 [Source:MGI Symbol;Acc:MGI:2183153]	-1.955605881
Mmrn1	multimerin 1 [Source:MGI Symbol;Acc:MGI:1918195]	-1.977462661
Pla2g4d	phospholipase A2, group IVD [Source:MGI Symbol;Acc:MGI:1925640]	-2.011328006
Itgb8	integrin beta 8 [Source:MGI Symbol;Acc:MGI:1338035]	-2.018378529
Hemgn	hemogen [Source:MGI Symbol;Acc:MGI:2136910]	-2.086156644
Gpm6a	glycoprotein m6a [Source:MGI Symbol;Acc:MGI:107671]	-2.090047346
Gdf10	growth differentiation factor 10 [Source:MGI Symbol;Acc:MGI:95684]	-2.185169957
Gm98	predicted gene 98 [Source:MGI Symbol;Acc:MGI:2684944]	-2.217397511
Slc4a1	solute carrier family 4 (anion exchanger), member 1 [Source:MGI Symbol;Acc:MGI:109393]	-2.313791045
Lum	lumican [Source:MGI Symbol;Acc:MGI:109347]	-2.380527903
Spnb1	spectrin beta 1 [Source:MGI Symbol;Acc:MGI:98387]	-2.41670632
Hba-x	hemoglobin X, alpha-like embryonic chain in Hba complex [Source:MGI Symbol;Acc:MGI:96019]	-2.435182932
Hbb-y	hemoglobin Y, beta-like embryonic chain [Source:MGI Symbol;Acc:MGI:96027]	-2.705944603
Igsf1	immunoglobulin superfamily, member 1 [Source:MGI Symbol;Acc:MGI:2147913]	-2.974004791
Klk1	kallikrein 1 [Source:MGI Symbol;Acc:MGI:102850]	-3.799975392

Supplementary table 3 – List of 75 genes differentially expressed in RNA-seq data (DESeq2 p<0.05 and Intensity difference p<0.05) between E3.5 uteri from young and aged pseudopregnant females. Displayed as log2 fold change from young to aged.

Gene	Description	Log2 fold change
Ppp1r1b	protein phosphatase 1, regulatory (inhibitor) subunit 1B [Source:MGI Symbol;Acc:MGI:94860]	6.00020252
Ltf	lactotransferrin [Source:MGI Symbol;Acc:MGI:96837]	5.594178933
Add2	adducin 2 (beta) [Source:MGI Symbol;Acc:MGI:87919]	5.37152698
Uox	urate oxidase [Source:MGI Symbol;Acc:MGI:98907]	5.294050013
Crabp2	cellular retinoic acid binding protein II [Source:MGI Symbol;Acc:MGI:88491]	5.232057922
Prap1	proline-rich acidic protein 1 [Source:MGI Symbol;Acc:MGI:893573]	5.029754367
Muc20	mucin 20 [Source:MGI Symbol;Acc:MGI:2385039]	4.9190818
Padi1	peptidyl arginine deiminase, type I [Source:MGI Symbol;Acc:MGI:1338893]	4.770014633
Muc4	mucin 4 [Source:MGI Symbol;Acc:MGI:2153525]	4.6953699
Unc5cl	unc-5 homolog C (C. elegans)-like [Source:MGI Symbol;Acc:MGI:1923839]	4.457631593
Sftpd	surfactant associated protein D [Source:MGI Symbol;Acc:MGI:109515]	4.417358457
Bcl2l15	BCLl2-like 15 [Source:MGI Symbol;Acc:MGI:2685412]	4.345126067
H60c	histocompatibility 60c [Source:MGI Symbol;Acc:MGI:3774845]	4.238539627
Ccl28	chemokine (C-C motif) ligand 28 [Source:MGI Symbol;Acc:MGI:1861731]	4.065596167
Padi2	peptidyl arginine deiminase, type II [Source:MGI Symbol;Acc:MGI:1338892]	3.9931634
Arg1	arginase, liver [Source:MGI Symbol;Acc:MGI:88070]	3.956521117
Slc27a2	solute carrier family 27 (fatty acid transporter), member 2 [Source:MGI Symbol;Acc:MGI:1347099]	3.711052267
Abp1	amiloride binding protein 1 (amine oxidase, copper-containing) [Source:MGI Symbol;Acc:MGI:1923757]	3.66670419
Sprr2f	small proline-rich protein 2F [Source:MGI Symbol;Acc:MGI:1330349]	3.6606205
5730469M10Rik	RIKEN cDNA 5730469M10 gene [Source:MGI Symbol;Acc:MGI:1917814]	3.647230167
Foxc1	forkhead box C1 [Source:MGI Symbol;Acc:MGI:1347466]	3.646881533
Egfl6	EGF-like-domain, multiple 6 [Source:MGI Symbol;Acc:MGI:1858599]	3.543155233
Cbr2	carbonyl reductase 2 [Source:MGI Symbol;Acc:MGI:107200]	3.505507333
Alpl	alkaline phosphatase, liver/bone/kidney [Source:MGI Symbol;Acc:MGI:87983]	3.497439167
Tacstd2	tumor-associated calcium signal transducer 2 [Source:MGI Symbol;Acc:MGI:1861606]	3.4060581
Slc40a1	solute carrier family 40 (iron-regulated transporter), member 1 [Source:MGI Symbol;Acc:MGI:1315204]	3.404302267
Mycn	v-myc myelocytomatosis viral related oncogene, neuroblastoma derived (avian) [Source:MGI Symbol;Acc:MGI:97357]	3.345628727
Slc7a11	solute carrier family 7 (cationic amino acid transporter, y+ system), member 11 [Source:MGI Symbol;Acc:MGI:1347355]	3.300270067
Cftr	cystic fibrosis transmembrane conductance regulator homolog [Source:MGI Symbol;Acc:MGI:88388]	3.2550155
Inhbb	inhibin beta-B [Source:MGI Symbol;Acc:MGI:96571]	3.2324636
C2	complement component 2 (within H-2S) [Source:MGI Symbol;Acc:MGI:88226]	3.163670367
Apobr	apolipoprotein B receptor [Source:MGI Symbol;Acc:MGI:2176230]	3.120002933

Gene	Description	Log2 fold change
Fcgbp	Fc fragment of IgG binding protein [Source:MGI Symbol;Acc:MGI:2444336]	3.088762733
Cfb	complement factor B [Source:MGI Symbol;Acc:MGI:105975]	3.0129261
Lad1	ladinin [Source:MGI Symbol;Acc:MGI:109343]	2.905850133
Greb1	gene regulated by estrogen in breast cancer protein [Source:MGI Symbol;Acc:MGI:2149712]	2.890090733
Mal2	mal, T cell differentiation protein 2 [Source:MGI Symbol;Acc:MGI:2146021]	2.8559284
Fut9	fucosyltransferase 9 [Source:MGI Symbol;Acc:MGI:1330859]	2.817215767
Galnt3	No description	2.775580567
Myb	myeloblastosis oncogene [Source:MGI Symbol;Acc:MGI:97249]	2.7695104
Cfi	complement component factor i [Source:MGI Symbol;Acc:MGI:105937]	2.7120536
Bcat1	branched chain aminotransferase 1, cytosolic [Source:MGI Symbol;Acc:MGI:104861]	2.640403533
Elf3	E74-like factor 3 [Source:MGI Symbol;Acc:MGI:1101781]	2.489441033
Bhlhe40	basic helix-loop-helix family, member e40 [Source:MGI Symbol;Acc:MGI:1097714]	2.373932933
Dhcr24	24-dehydrocholesterol reductase [Source:MGI Symbol;Acc:MGI:1922004]	2.361236067
Myh14	myosin, heavy polypeptide 14 [Source:MGI Symbol;Acc:MGI:1919210]	2.360458367
Gpr128	G protein-coupled receptor 128 [Source:MGI Symbol;Acc:MGI:2441732]	2.3417932
Klf4	Kruppel-like factor 4 (gut) [Source:MGI Symbol;Acc:MGI:1342287]	2.299556267
Cp	ceruloplasmin [Source:MGI Symbol;Acc:MGI:88476]	2.257516967
Slc28a3	solute carrier family 28 (sodium-coupled nucleoside transporter), member 3 [Source:MGI Symbol;Acc:MGI:2137361]	2.1462713
Krt7	keratin 7 [Source:MGI Symbol;Acc:MGI:96704]	2.090661667
Gm20547	predicted gene 20547 [Source:MGI Symbol;Acc:MGI:5142012]	2.046076167
Cdkl1	cyclin-dependent kinase-like 1 (CDC2-related kinase) [Source:MGI Symbol;Acc:MGI:1918341]	1.8998963
C2	complement component 2 (within H-2S) [Source:MGI Symbol;Acc:MGI:88226]	-0.895269833
Fbn1	fibrillin 1 [Source:MGI Symbol;Acc:MGI:95489]	-1.8841821
Cd34	CD34 antigen [Source:MGI Symbol;Acc:MGI:88329]	-1.905820367
Mmp2	matrix metallopeptidase 2 [Source:MGI Symbol;Acc:MGI:97009]	-1.976179633
Osr2	odd-skipped related 2 (Drosophila) [Source:MGI Symbol;Acc:MGI:1930813]	-2.2587181
Vcan	versican [Source:MGI Symbol;Acc:MGI:102889]	-2.3753268
Pdgfra	platelet derived growth factor receptor, alpha polypeptide [Source:MGI Symbol;Acc:MGI:97530]	-2.391184933
Lrrc17	leucine rich repeat containing 17 [Source:MGI Symbol;Acc:MGI:1921761]	-2.4015725
Hand2	heart and neural crest derivatives expressed transcript 2 [Source:MGI Symbol;Acc:MGI:103580]	-2.416261567
Serpine2	serine (or cysteine) peptidase inhibitor, clade E, member 2 [Source:MGI Symbol;Acc:MGI:101780]	-2.4604312
Apcdd1	adenomatosis polyposis coli down-regulated 1 [Source:MGI Symbol;Acc:MGI:3513977]	-2.531863367
Col15a1	collagen, type XV, alpha 1 [Source:MGI Symbol;Acc:MGI:88449]	-2.607754567
F2r	coagulation factor II (thrombin) receptor [Source:MGI Symbol;Acc:MGI:101802]	-2.784162867
Tmem132c	transmembrane protein 132C [Source:MGI Symbol;Acc:MGI:2443061]	-2.907442467
Tex15	testis expressed gene 15 [Source:MGI Symbol;Acc:MGI:1934816]	-3.042044533

Gene	Description	Log2 fold change
Mtap2	microtubule-associated protein 2 [Source:MGI Symbol;Acc:MGI:97175]	-3.0499195
Mest	mesoderm specific transcript [Source:MGI Symbol;Acc:MGI:96968]	-3.675537467
Fst	follistatin [Source:MGI Symbol;Acc:MGI:95586]	-3.811741367
Lamc3	laminin gamma 3 [Source:MGI Symbol;Acc:MGI:1344394]	-3.816011361
Cxcl15	chemokine (C-X-C motif) ligand 15 [Source:MGI Symbol;Acc:MGI:1339941]	-3.922341333
Ndp	Norrie disease (pseudoglioma) (human) [Source:MGI Symbol;Acc:MGI:102570]	-4.79584922
Ttr	transthyretin [Source:MGI Symbol;Acc:MGI:98865]	-5.350652667

Supplementary table 4 - Genes commonly up- or down-regulated in E3.5 uteri from aged females by RNA-seq (shown as Log2 fold change), and in E3.5 uteri from gene knockout mice by microarray analysis. Differential expression and direction of change in the associated KO mouse is indicated by green cells.

Probe	Log2 fold change	Pgr up	Pgr down	Bmp up	Bmp2 down	Wnt4 up	Wnt4 down	Egfr up	Egfr down
Ltf	5.594179								
Sftpd	4.41735855								
Gabrp	4.2301169								
Sprr2f	3.6606205								
5730469M10Rik	3.6472303								
Slc40a1	3.4043025								
Mycn	3.3456284								
Inhbb	3.2324638								
Lad1	2.9058498								
Mal2	2.8559285								
Tmem45b	2.646802								
Cp	2.2575174								
Muc1	2.2284354								
Krt7	2.0906615								
Nrtn	2.059478								
Epsti1	2.037082								
Myo5c	2.0169658								
Sgpp2	1.9916013								
Glis3	1.9185133								
0610040J01Rik	1.8765116								
Tspan8	1.857882								
5730559C18Rik	1.8522244								
Alcam	1.827052								
Rnf128	1.769124								
Tmem20	1.767132								

Probe	Log2 fold change	Pgr up	Pgr down	Bmp up	Bmp2 down	Wnt4 up	Wnt4 down	Egfr up	Egfr down
Krt19	1.765891								
Tmcc3	1.7321795								
Capn5	1.6746078								
F5	1.6656057								
Lrig1	1.6276775								
Six4	1.6119552								
Cndp2	1.483544								
Prom1	1.4701465								
Wnk2	1.4675837								
Mbp	1.4366543								
Dsp	1.422717								
Clu	1.4189513								
P2ry14	1.4127219								
Stxbp6	1.3413641								
Laptm5	1.3313734								
Slc15a2	1.3010027								
2810474O19Rik	1.2572924								
1600029D21Rik	1.2539195								
St14	1.2289347								
Dsg2	1.2095853								
Tmem30b	1.1833545								
Grb7	1.156587								
Hsd17b11	1.1517256								
Dlx5	1.1409769								
Ephx1	1.140866								
Mal	1.1389353								
Mapkapk3	1.1100836								
Krt8	1.0746023								
Car2	1.0716176								
Rab25	1.0503268								
Ifitm1	1.0389709								
Pdgfa	0.9433034								
Ehf	0.9285977								
Reln	0.9228894								
Kcnk1	0.9141556								
Ngfr	0.8837457								
Cldn7	0.875958								
1810019J16Rik	0.8567223								
Krt18	0.7616294								
Phactr1	0.7453968								
Cdh1	0.7437								
Vav3	0.7003964								
Camk2n1	0.6603548								
Meis1	0.6365033								
Casp1	0.5395123								

Probe	Log2 fold change	Pgr up	Pgr down	Bmp up	Bmp2 down	Wnt4 up	Wnt4 down	Egfr up	Egfr down
Epb4.1l5	0.4850833								
Adamts2	-1.1776839								
Limk1	-1.1843187								
Adam12	-1.6752146								
Apln	-1.68126636								
Fads3	-1.8989812								
Fscn1	-2.0768049								
Clic6	-2.11356427								
Daam2	-2.1295806								
Adora2b	-2.254475987								
Pcsk5	-2.321739								
Hand2	-2.4162614								
Dact1	-2.787129								
Tmod2	-3.0639783								
Slc2a3	-3.466418								
Fst	-3.8117418								

Supplementary table 5 – List of 112 genes differentially expressed in RNA-seq data (DESeq2 p<0.05 and Intensity difference p<0.05) in uterine stromal cells from young females prior to decidualization, and after 4 days of *in vitro* decidualization. Displayed as log2 fold change from 0d to 4d in young USCs, and aged USCs.

Probe	Description	Log2 fold change young	Log2 fold change aged
Zbtb16	zinc finger and BTB domain containing 16 [Source:MGI Symbol;Acc:MGI:103222]	10.48319223	7.8408429
Prl8a2	prolactin family 8, subfamily a, member 2 [Source:MGI Symbol;Acc:MGI:894281]	9.804755933	5.945765
Fmo3	flavin containing monooxygenase 3 [Source:MGI Symbol;Acc:MGI:1100496]	9.547525927	4.566104013
Postn	periostin, osteoblast specific factor [Source:MGI Symbol;Acc:MGI:1926321]	9.1631688	6.672819967
Lcn2	lipocalin 2 [Source:MGI Symbol;Acc:MGI:96757]	8.867341233	0.2168918
Art3	ADP-ribosyltransferase 3 [Source:MGI Symbol;Acc:MGI:1202729]	7.7539719	-0.7883424
Sult1a1	sulfotransferase family 1A, phenol-preferring, member 1 [Source:MGI Symbol;Acc:MGI:102896]	7.4135518	6.967767333
Folh1	folate hydrolase 1 [Source:MGI Symbol;Acc:MGI:1858193]	7.151643267	4.6980099
Hif3a	hypoxia inducible factor 3, alpha subunit [Source:MGI Symbol;Acc:MGI:1859778]	7.105283933	4.77025181
Myocd	myocardin [Source:MGI Symbol;Acc:MGI:2137495]	6.862529	4.275450473
Cd34	CD34 antigen [Source:MGI Symbol;Acc:MGI:88329]	6.751656063	-0.714828667
Gpr64	G protein-coupled receptor 64 [Source:MGI Symbol;Acc:MGI:2446854]	6.743909	-0.312738
Mme	membrane metallo endopeptidase [Source:MGI Symbol;Acc:MGI:97004]	6.507193567	0.7846721

Probe	Description	Log2 fold change young	Log2 fold change aged
A730046J19 Rik	RIKEN cDNA A730046J19 gene [Source:MGI Symbol;Acc:MGI:2442684]	6.4158691	0.0166699
Krt23	keratin 23 [Source:MGI Symbol;Acc:MGI:2148866]	6.373122567	0.0166699
Slc38a5	solute carrier family 38, member 5 [Source:MGI Symbol;Acc:MGI:2148066]	6.2688025	0.0166699
Serpina3n	serine (or cysteine) peptidase inhibitor, clade A, member 3N [Source:MGI Symbol;Acc:MGI:105045]	6.122508253	3.32612225
Stmn2	stathmin-like 2 [Source:MGI Symbol;Acc:MGI:98241]	6.1039385	0.34430151
Ly6c1	lymphocyte antigen 6 complex, locus C1 [Source:MGI Symbol;Acc:MGI:96882]	6.088597033	2.274099167
Chrdl1	chordin-like 1 [Source:MGI Symbol;Acc:MGI:1933172]	5.93420747	0.734004417
Itgbl1	integrin, beta-like 1 [Source:MGI Symbol;Acc:MGI:2443439]	5.892322333	2.174647067
Rapgef5	Rap guanine nucleotide exchange factor (GEF) 5 [Source:MGI Symbol;Acc:MGI:2444365]	5.865334333	1.5483278
Sult1e1	sulfotransferase family 1E, member 1 [Source:MGI Symbol;Acc:MGI:98431]	5.803165967	0.4513386
Tcf23	transcription factor 23 [Source:MGI Symbol;Acc:MGI:1934960]	5.661076457	3.206934377
Vat1l	vesicle amine transport protein 1 homolog-like (T. californica) [Source:MGI Symbol;Acc:MGI:2142534]	5.647358367	0.646326133
Aldh1a7	aldehyde dehydrogenase family 1, subfamily A7 [Source:MGI Symbol;Acc:MGI:1347050]	5.628256663	5.026000853
Fam46c	family with sequence similarity 46, member C [Source:MGI Symbol;Acc:MGI:1921895]	5.606365167	2.151824723
Bcmo1	beta-carotene 15,15'-monooxygenase [Source:MGI Symbol;Acc:MGI:1926923]	5.600545233	2.2722412
Cldn1	claudin 1 [Source:MGI Symbol;Acc:MGI:1276109]	5.573591523	2.706958757
Nrcam	neuron-glia-CAM-related cell adhesion molecule [Source:MGI Symbol;Acc:MGI:104750]	5.553652967	0.940865467
Hsd11b2	hydroxysteroid 11-beta dehydrogenase 2 [Source:MGI Symbol;Acc:MGI:104720]	5.534508033	1.604482767
Tgfa	transforming growth factor alpha [Source:MGI Symbol;Acc:MGI:98724]	5.472005367	-0.451506933
Nt5e	5' nucleotidase, ecto [Source:MGI Symbol;Acc:MGI:99782]	5.285162333	2.63875305
Ccdc88c	coiled-coil domain containing 88C [Source:MGI Symbol;Acc:MGI:1915589]	5.0575814	1.195681867
Fabp4	fatty acid binding protein 4, adipocyte [Source:MGI Symbol;Acc:MGI:88038]	5.0423107	0.772995233
Col15a1	collagen, type XV, alpha 1 [Source:MGI Symbol;Acc:MGI:88449]	4.91367749	2.5260314
Mt2	metallothionein 2 [Source:MGI Symbol;Acc:MGI:97172]	4.770019383	3.605217568
Ly6a	lymphocyte antigen 6 complex, locus A [Source:MGI Symbol;Acc:MGI:107527]	4.5385236	0.6830375
Aldh1a1	aldehyde dehydrogenase family 1, subfamily A1 [Source:MGI Symbol;Acc:MGI:1353450]	4.327248633	3.999938391
Lbp	lipopolysaccharide binding protein [Source:MGI Symbol;Acc:MGI:1098776]	4.299177473	0.9357202
Fam65b	family with sequence similarity 65, member B [Source:MGI Symbol;Acc:MGI:2444879]	4.263789309	-0.555210533
Rgs2	regulator of G-protein signaling 2 [Source:MGI Symbol;Acc:MGI:1098271]	4.19970341	1.167640267
Lama2	laminin, alpha 2 [Source:MGI Symbol;Acc:MGI:99912]	4.187990577	2.234587733

Probe	Description	Log2 fold change young	Log2 fold change aged
Podxl	podocalyxin-like [Source:MGI Symbol;Acc:MGI:1351317]	4.1814549	-0.2903301
Sez6l	seizure related 6 homolog like [Source:MGI Symbol;Acc:MGI:1935121]	4.084291047	2.574537821
Pdk4	pyruvate dehydrogenase kinase, isoenzyme 4 [Source:MGI Symbol;Acc:MGI:1351481]	3.990984933	1.032657733
Ccdc141	coiled-coil domain containing 141 [Source:MGI Symbol;Acc:MGI:1919735]	3.9611922	0.4562093
Thsd7a	thrombospondin, type I, domain containing 7A [Source:MGI Symbol;Acc:MGI:2685683]	3.95674784	1.422839867
Fkbp5	FK506 binding protein 5 [Source:MGI Symbol;Acc:MGI:104670]	3.908226467	0.897722867
Gpm6a	glycoprotein m6a [Source:MGI Symbol;Acc:MGI:107671]	3.897684433	0.033415467
Mest	mesoderm specific transcript [Source:MGI Symbol;Acc:MGI:96968]	3.866498949	-0.118829633
Gda	guanine deaminase [Source:MGI Symbol;Acc:MGI:95678]	3.852076333	1.230579467
Muc16	mucin 16 [Source:MGI Symbol;Acc:MGI:1920982]	3.73595034	0.451338633
Cfh	complement component factor h [Source:MGI Symbol;Acc:MGI:88385]	3.724656233	1.882306933
A2m	alpha-2-macroglobulin [Source:MGI Symbol;Acc:MGI:2449119]	3.684481813	-0.189722647
Ms4a4d	membrane-spanning 4-domains, subfamily A, member 4D [Source:MGI Symbol;Acc:MGI:1913857]	3.68159794	1.258300921
Cdkn1c	cyclin-dependent kinase inhibitor 1C (P57) [Source:MGI Symbol;Acc:MGI:104564]	3.66303451	0.874659067
Smpd3	sphingomyelin phosphodiesterase 3, neutral [Source:MGI Symbol;Acc:MGI:1927578]	3.6365646	-0.1955956
Tsc22d3	TSC22 domain family, member 3 [Source:MGI Symbol;Acc:MGI:1196284]	3.596432367	1.4796912
Ctla2a	cytotoxic T lymphocyte-associated protein 2 alpha [Source:MGI Symbol;Acc:MGI:88554]	3.576968667	0.953448667
Tmtc1	transmembrane and tetratricopeptide repeat containing 1 [Source:MGI Symbol;Acc:MGI:3039590]	3.5702268	1.674721567
Ncoa4	nuclear receptor coactivator 4 [Source:MGI Symbol;Acc:MGI:1350932]	3.560808367	0.1548964
Emcn	endomucin [Source:MGI Symbol;Acc:MGI:1891716]	3.558063423	-0.295343667
Ap1s2	adaptor-related protein complex 1, sigma 2 subunit [Source:MGI Symbol;Acc:MGI:1889383]	3.490244233	0.4652957
Gpr115	G protein-coupled receptor 115 [Source:MGI Symbol;Acc:MGI:1925499]	3.484537916	1.0537904
Rasd1	RAS, dexamethasone-induced 1 [Source:MGI Symbol;Acc:MGI:1270848]	3.4225667	2.541639687
Dlg2	discs, large homolog 2 (Drosophila) [Source:MGI Symbol;Acc:MGI:1344351]	3.315330133	2.09080088
Net1	neuroepithelial cell transforming gene 1 [Source:MGI Symbol;Acc:MGI:1927138]	3.3055887	-0.047524333
Gm6768	predicted gene 6768 [Source:MGI Symbol;Acc:MGI:3648259]	3.275000867	0.197589633
Actn3	actinin alpha 3 [Source:MGI Symbol;Acc:MGI:99678]	3.265299533	0.377490773
Itga10	integrin, alpha 10 [Source:MGI Symbol;Acc:MGI:2153482]	3.25660497	0.3097703
Itga2	integrin alpha 2 [Source:MGI Symbol;Acc:MGI:96600]	3.253656343	1.16884148
Megf6	multiple EGF-like-domains 6 [Source:MGI Symbol;Acc:MGI:1919351]	3.186586677	1.5268416

Probe	Description	Log2 fold change young	Log2 fold change aged
Capn6	calpain 6 [Source:MGI Symbol;Acc:MGI:1100850]	3.165517377	-0.12765
Krt19	keratin 19 [Source:MGI Symbol;Acc:MGI:96693]	3.138473717	-0.34604352
Col11a1	collagen, type XI, alpha 1 [Source:MGI Symbol;Acc:MGI:88446]	3.130930833	2.3257644
Clca1	chloride channel calcium activated 1 [Source:MGI Symbol;Acc:MGI:1316732]	3.1217567	0.483757
Ptprq	protein tyrosine phosphatase, receptor type, Q [Source:MGI Symbol;Acc:MGI:1096349]	3.087149867	0.684141967
Cdo1	cysteine dioxygenase 1, cytosolic [Source:MGI Symbol;Acc:MGI:105925]	3.069659067	4.347902767
Gabra3	gamma-aminobutyric acid (GABA) A receptor, subunit alpha 3 [Source:MGI Symbol;Acc:MGI:95615]	3.068406033	1.54982408
Mt1	metallothionein 1 [Source:MGI Symbol;Acc:MGI:97171]	3.062686233	2.1952893
Aldh6a1	aldehyde dehydrogenase family 6, subfamily A1 [Source:MGI Symbol;Acc:MGI:1915077]	3.057717067	0.523397567
Lum	lumican [Source:MGI Symbol;Acc:MGI:109347]	3.0385072	2.52277844
A730049H05Rik	RIKEN cDNA A730049H05 gene [Source:MGI Symbol;Acc:MGI:1921766]	3.0276826	0.544990767
Frem1	Fras1 related extracellular matrix protein 1 [Source:MGI Symbol;Acc:MGI:2670972]	2.880669767	2.483629793
Plxna4	plexin A4 [Source:MGI Symbol;Acc:MGI:2179061]	2.872199533	0.287972467
Fgl2	fibrinogen-like protein 2 [Source:MGI Symbol;Acc:MGI:103266]	2.855010167	2.905942323
Fibin	fin bud initiation factor homolog (zebrafish) [Source:MGI Symbol;Acc:MGI:1914856]	2.840006333	1.8275965
Gm20488	predicted gene 20488 [Source:MGI Symbol;Acc:MGI:5141953]	2.837578467	0.976945367
Olfml3	olfactomedin-like 3 [Source:MGI Symbol;Acc:MGI:1914877]	2.837482667	1.1953327
Errfi1	ERBB receptor feedback inhibitor 1 [Source:MGI Symbol;Acc:MGI:1921405]	2.826762167	0.618389867
Abcb1b	ATP-binding cassette, sub-family B (MDR/TAP), member 1B [Source:MGI Symbol;Acc:MGI:97568]	2.815717633	-1.563645033
Sgk1	serum/glucocorticoid regulated kinase 1 [Source:MGI Symbol;Acc:MGI:1340062]	2.766427367	0.446731333
Adamts1	a disintegrin-like and metallopeptidase (reprolysin type) with thrombospondin type 1 motif, 1 [Source:MGI Symbol;Acc:MGI:109249]	2.736711867	1.446210233
Shroom4	shroom family member 4 [Source:MGI Symbol;Acc:MGI:2685570]	2.701693967	-0.116016967
Fgf7	fibroblast growth factor 7 [Source:MGI Symbol;Acc:MGI:95521]	2.694014913	2.202090967
Parm1	prostate androgen-regulated mucin-like protein 1 [Source:MGI Symbol;Acc:MGI:2443349]	2.691764833	0.7215971
Rbbp8	retinoblastoma binding protein 8 [Source:MGI Symbol;Acc:MGI:2442995]	2.658159367	-0.635270933
Fmo2	flavin containing monooxygenase 2 [Source:MGI Symbol;Acc:MGI:1916776]	2.633288533	3.181531012
Itm2a	integral membrane protein 2A [Source:MGI Symbol;Acc:MGI:107706]	2.625492633	1.0449875
Itga1	integrin alpha 1 [Source:MGI Symbol;Acc:MGI:96599]	2.604744367	0.252555467
Olr1	oxidized low density lipoprotein (lectin-like) receptor 1 [Source:MGI Symbol;Acc:MGI:1261434]	2.590810167	1.724422267
Htra1	HtrA serine peptidase 1 [Source:MGI Symbol;Acc:MGI:1929076]	2.558684233	2.063658333

Probe	Description	Log2 fold change young	Log2 fold change aged
Ctla2b	cytotoxic T lymphocyte-associated protein 2 beta [Source:MGI Symbol;Acc:MGI:88555]	2.524623	0.924925167
Mertk	c-mer proto-oncogene tyrosine kinase [Source:MGI Symbol;Acc:MGI:96965]	2.515193567	-0.586141433
Prrg3	proline rich Gla (G-carboxyglutamic acid) 3 (transmembrane) [Source:MGI Symbol;Acc:MGI:2685214]	2.4875803	-0.205412127
Pdgfc	platelet-derived growth factor, C polypeptide [Source:MGI Symbol;Acc:MGI:1859631]	2.467168067	1.324884233
Usp53	ubiquitin specific peptidase 53 [Source:MGI Symbol;Acc:MGI:2139607]	2.4646975	1.1340332
Loxl3	lysyl oxidase-like 3 [Source:MGI Symbol;Acc:MGI:1337004]	2.457788033	0.851176167
Bicd1	bicaudal D homolog 1 (Drosophila) [Source:MGI Symbol;Acc:MGI:1101760]	2.430138467	0.308702833
Slco2a1	solute carrier organic anion transporter family, member 2a1 [Source:MGI Symbol;Acc:MGI:1346021]	2.3859458	-0.682518267
Gprc5b	G protein-coupled receptor, family C, group 5, member B [Source:MGI Symbol;Acc:MGI:1927596]	2.1485134	0.999197833
A330021E22Rik	RIKEN cDNA A330021E22 gene [Source:MGI Symbol;Acc:MGI:2443778]	-2.1501082	-0.231326433
Cxcl12	chemokine (C-X-C motif) ligand 12 [Source:MGI Symbol;Acc:MGI:103556]	-3.106840367	-0.201007267
Sfn	stratifin [Source:MGI Symbol;Acc:MGI:1891831]	-3.200778867	-0.150829967
Oxtr	oxytocin receptor [Source:MGI Symbol;Acc:MGI:109147]	-3.30073332	-1.2289851
Sprr1a	small proline-rich protein 1A [Source:MGI Symbol;Acc:MGI:106660]	-3.5106827	-2.124680833
Rgs5	regulator of G-protein signaling 5 [Source:MGI Symbol;Acc:MGI:1098434]	-3.795466717	1.2585441
Pcp4l1	Purkinje cell protein 4-like 1 [Source:MGI Symbol;Acc:MGI:1913675]	-3.8322291	0.15259964
Rgs4	regulator of G-protein signaling 4 [Source:MGI Symbol;Acc:MGI:108409]	-3.860807113	-0.977440967
Gjb2	gap junction protein, beta 2 [Source:MGI Symbol;Acc:MGI:95720]	-6.080767517	0.0166699
Myb	myeloblastosis oncogene [Source:MGI Symbol;Acc:MGI:97249]	-6.140042833	-0.033997633
Myh1	myosin, heavy polypeptide 1, skeletal muscle, adult [Source:MGI Symbol;Acc:MGI:1339711]	-6.291334433	0.0166699
S100g	S100 calcium binding protein G [Source:MGI Symbol;Acc:MGI:104528]	-8.149190433	-0.033997767

Supplementary table 6 – Motif enrichment analysis, showing transcription factors with significantly enriched motifs in a) decidua DMRs, b) refractory DMRs, c) trophoblast DMRs.

a)

Database	ID	*p*-value	Adjusted *p*-value
HOCOMOCOv11 core MOUSE mono meme format	ETS2_MOUSE.H11MO.0.A	3.61E-05	1.28E-02

b)

Database	ID	*p*-value	Adjusted *p*-value
HOCOMOCOv11 core MOUSE mono meme format	TAF1_MOUSE.H11MO.0.A	6.54E-06	2.34E-03
HOCOMOCOv11 core MOUSE mono meme format	KLF4_MOUSE.H11MO.0.A	1.91E-05	6.81E-03
HOCOMOCOv11 core MOUSE mono meme format	KLF5_MOUSE.H11MO.0.A	2.41E-05	8.58E-03
HOCOMOCOv11 core MOUSE mono meme format	SP5_MOUSE.H11MO.0.C	3.23E-05	1.15E-02
HOCOMOCOv11 core MOUSE mono meme format	KLF3_MOUSE.H11MO.0.A	3.52E-05	1.25E-02
HOCOMOCOv11 core MOUSE mono meme format	ETS2_MOUSE.H11MO.0.A	3.67E-05	1.31E-02
HOCOMOCOv11 core MOUSE mono meme format	SP4_MOUSE.H11MO.0.B	4.11E-05	1.46E-02
HOCOMOCOv11 core MOUSE mono meme format	E2F4_MOUSE.H11MO.0.A	8.01E-05	2.83E-02
HOCOMOCOv11 core MOUSE mono meme format	KLF1_MOUSE.H11MO.0.A	1.02E-04	3.58E-02
HOCOMOCOv11 core MOUSE mono meme format	ZN281_MOUSE.H11MO.0.A	1.09E-04	3.82E-02
HOCOMOCOv11 core MOUSE mono meme format	KLF15_MOUSE.H11MO.0.A	1.14E-04	3.99E-02

c)

Database	ID	*p*-value	Adjusted *p*-value
HOCOMOCOv11 core MOUSE mono meme format	ETS2_MOUSE.H11MO.0.A	1.34E-04	4.70E-02

Supplementary figure 1 – Heatmap showing the expression of 162 genes differentially expressed between young and Aa deciduas, in young deciduas, aged deciduas, and deciduas from young mothers in a time-course of development.

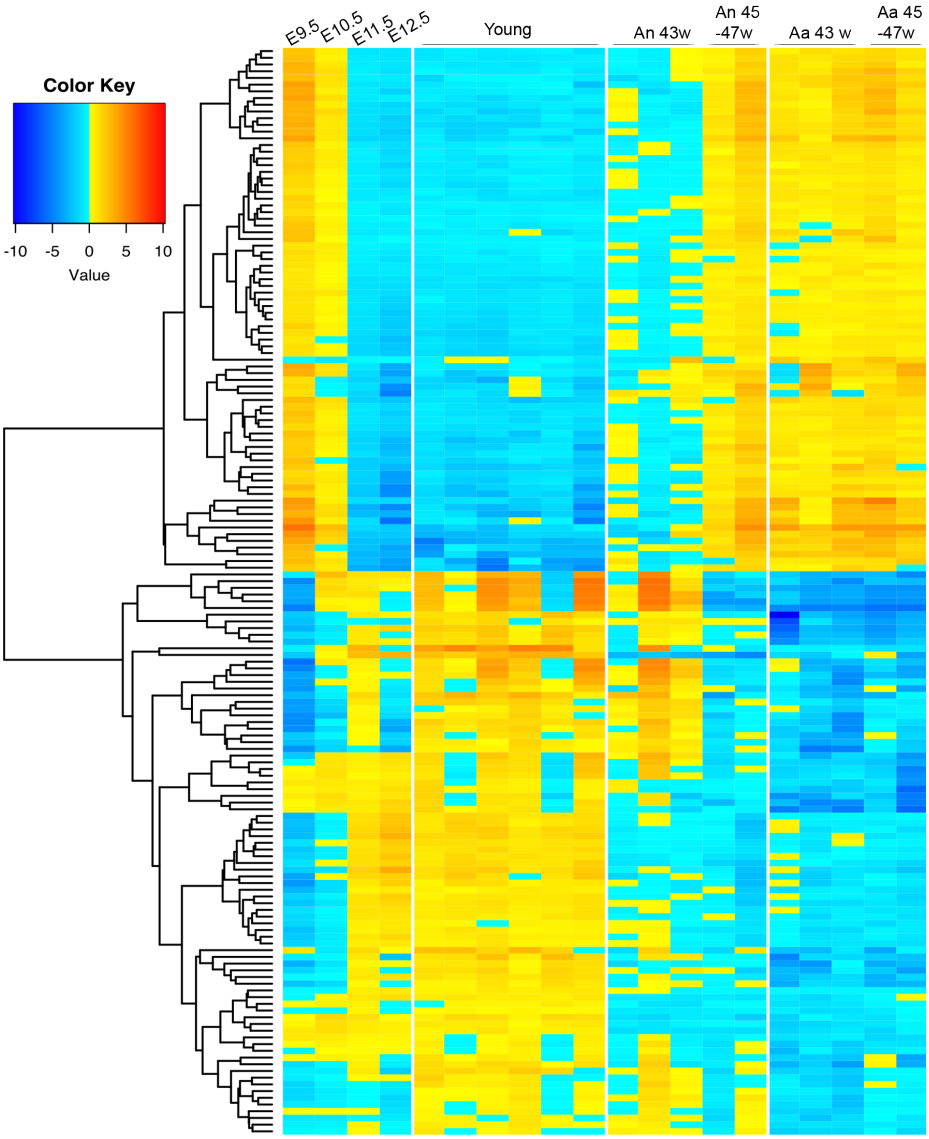

Supplementary figure 2 - Gross morphology of embryos and placentas at E11.5 from a litter from an aged female. Arrowhead indicates a forebrain defect. Placentas were stained with Haemotoxylin and Eosin, by IHC for *Prl2c2 (Plf)*, or by DBA staining to mark uterine natural killer cells (uNK cells). (Dissection and histology performed by MH and LW, DBA staining performed by LW).

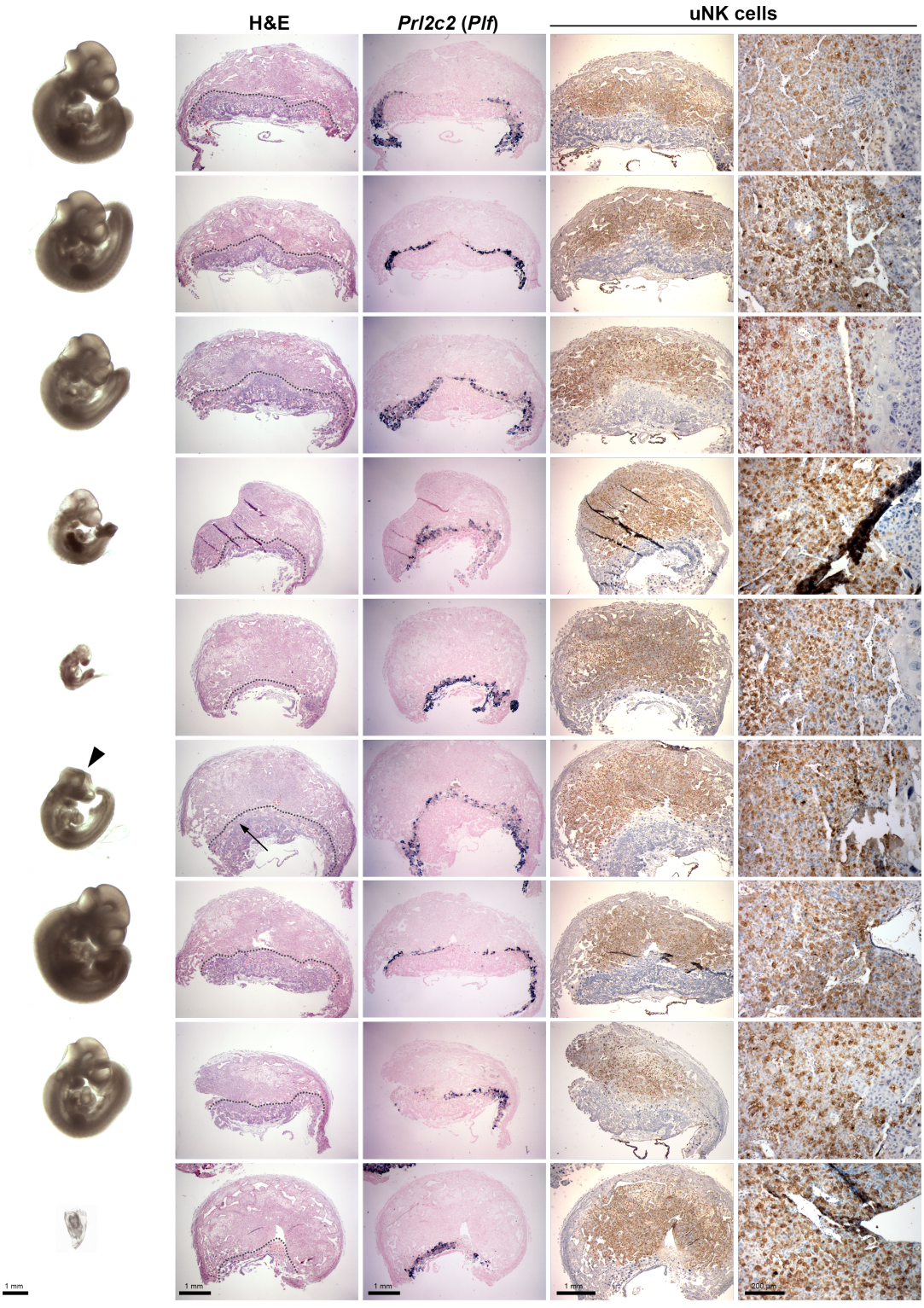

Supplementary figure 3 - Expression of genes involved in decidualization in USCs at 0d and/or 4d of *in vitro* decidualization. DESeq2 *p<0.05. Next page, Expression of genes involved in decidualization in E3.5 uteri DESeq2 *p<0.05.

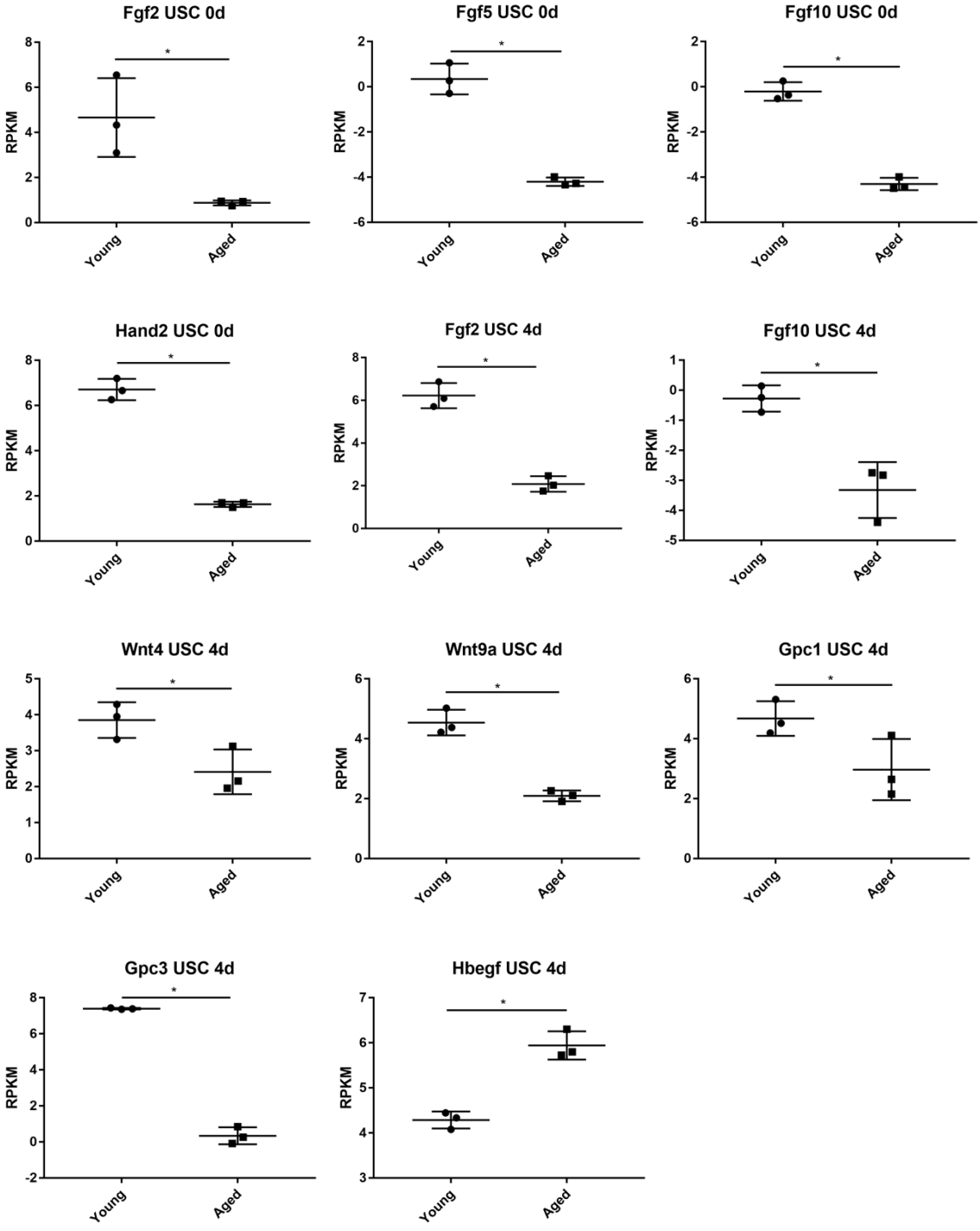

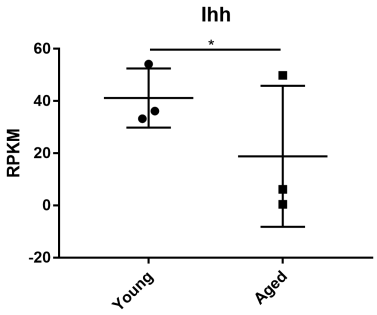
Ihh
RPKM
60
40
20
0
-20
*
Young
Aged

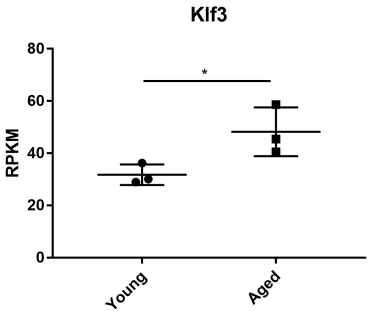
Klf3
RPKM
80
60
40
20
0
*
Young
Aged

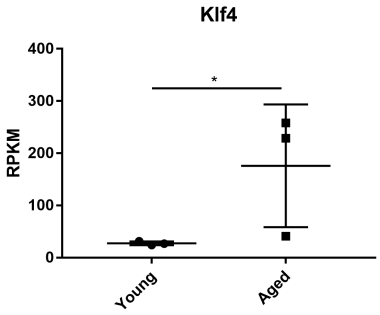
Klf4
RPKM
400
300
200
100
0
*
Young
Aged

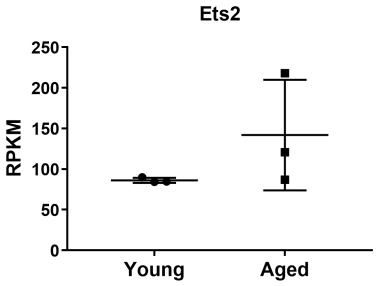
Ets2
RPKM
250
200
150
100
50
0
Young
Aged

Supplementary figure 4 – GO analysis of genes dys-regulated in USCs isolated at E3.5 from aged females, compared with those from aged females, from RNA-seq data. DESeq p<0.05 and/or intensity difference p<0.05.

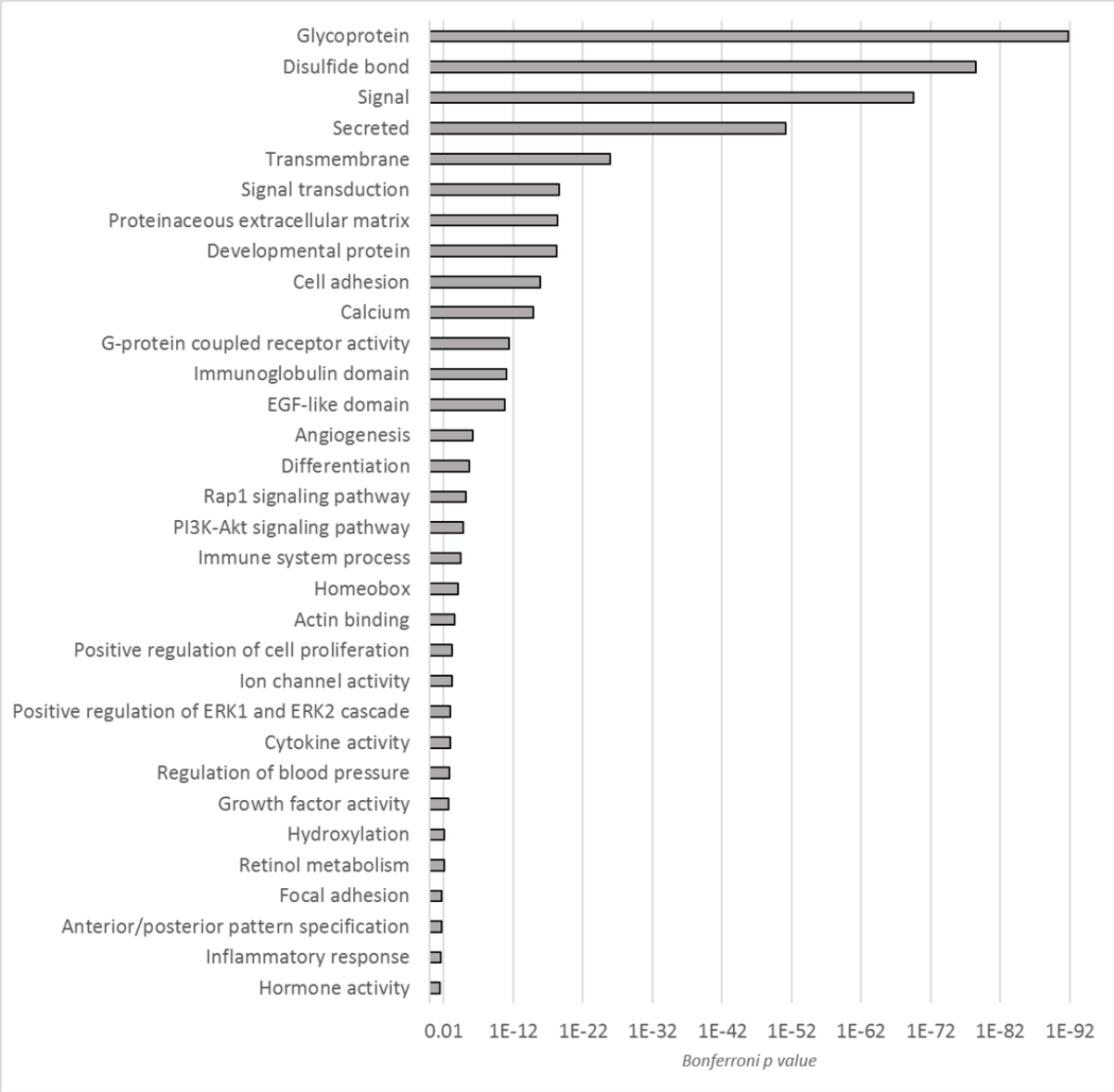

Supplementary figure 5 – Distribution of H3K4me3 peaks in genomic features: a) peaks called in young USCs, b) peaks called in aged USCs.

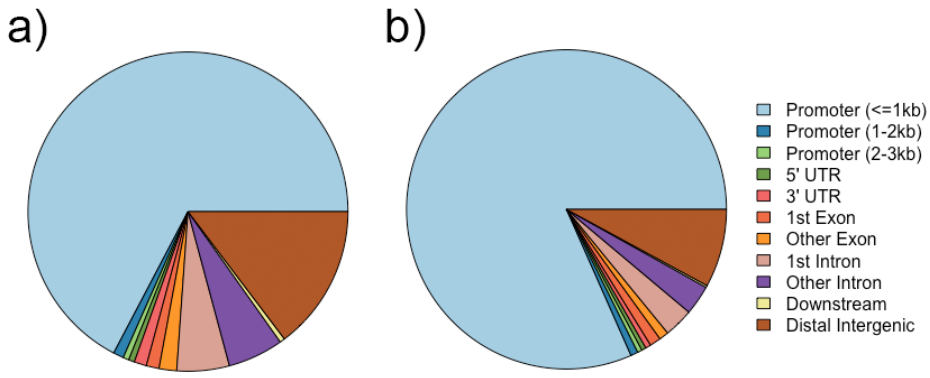

Supplementary figure 6 – Gene ontology analysis of genes associated with the top 5% broadest H3K4me3 peaks in uterine stromal cells.

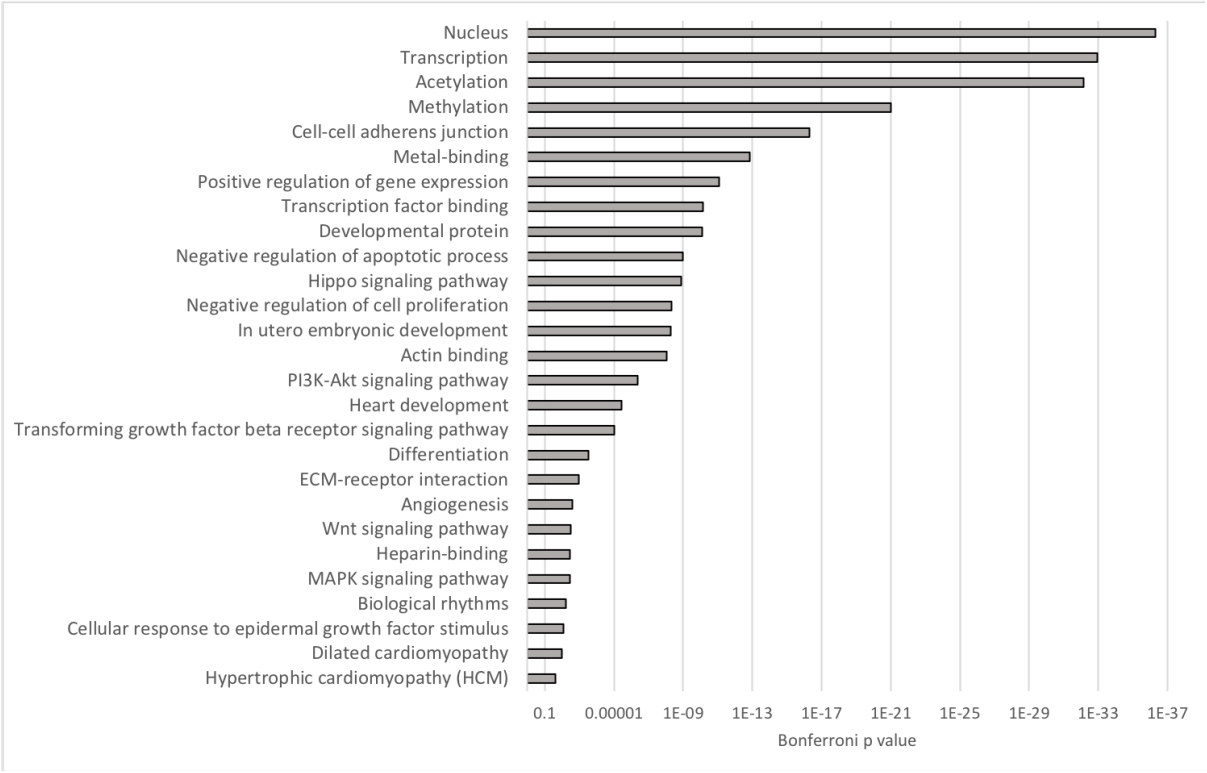

Supplementary figure 7 – Distribution of differentially methylated regions in genomic features: a) 214 DMRs in aged E11.5 deciduas b) 89,685 regions differentially methylated between young E3.5 uteri and E11.5 deciduas, c) 334 trophoblast DMRs.

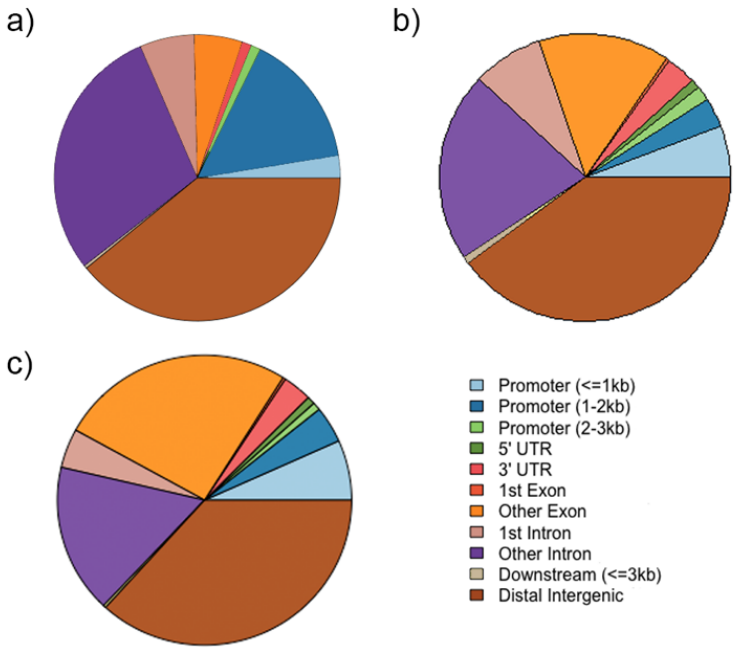

Supplementary figure 8 – Overlap between differentially methylated regions, CpG islands, and promoters.

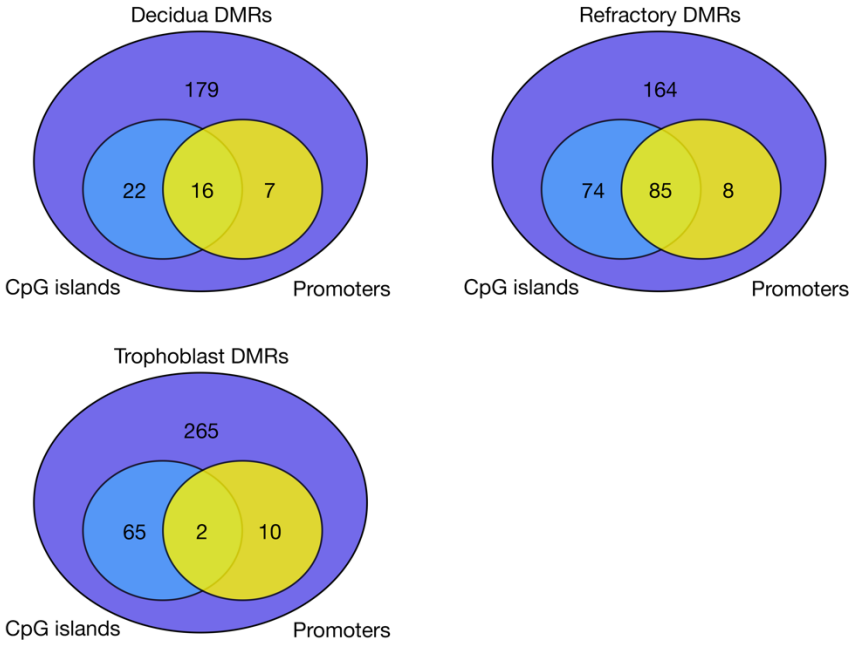

Supplementary figure 9 – Overlap between maternal-age-related DMRs identified in E11.5 decidua, E11.5 trophoblast, and refractory DMRs in decidua.

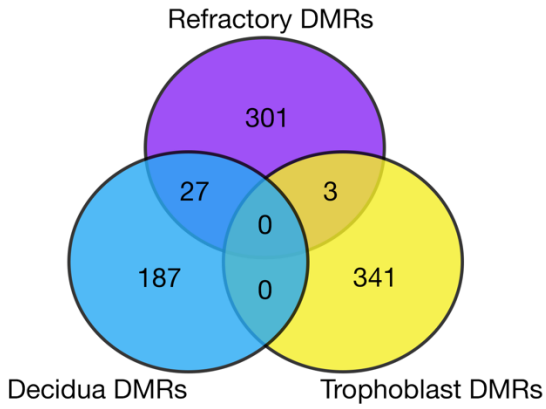

Supplementary figure 10 – Heatmap showing the change in 5mC enrichment between E3.5 uteri and E11.5 from deciduas from young and aged females, at 214 decidua DMRs.

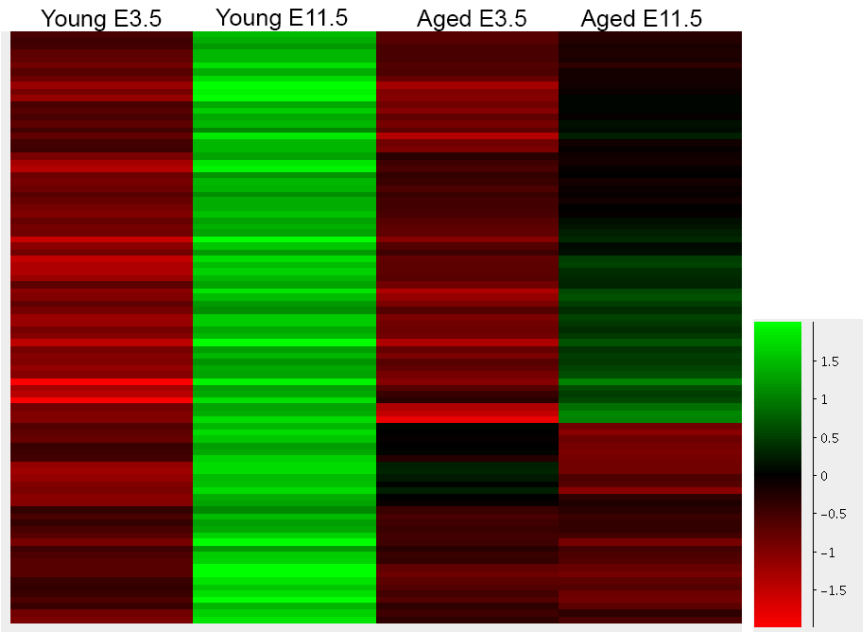

Supplementary figure 11 – Expression of genes within 2kb of a trophoblast DMR in a) E11.5 trophoblast from young and aged mice (RNA-seq) and b) transfer trophoblast (RNA-seq) from Y->Y transfer and A->Y transfer pregnancies.

a)

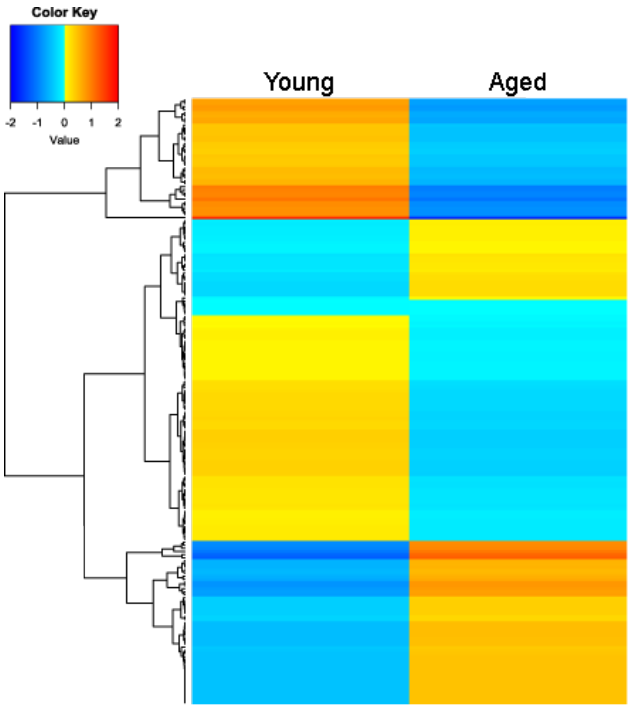

b)

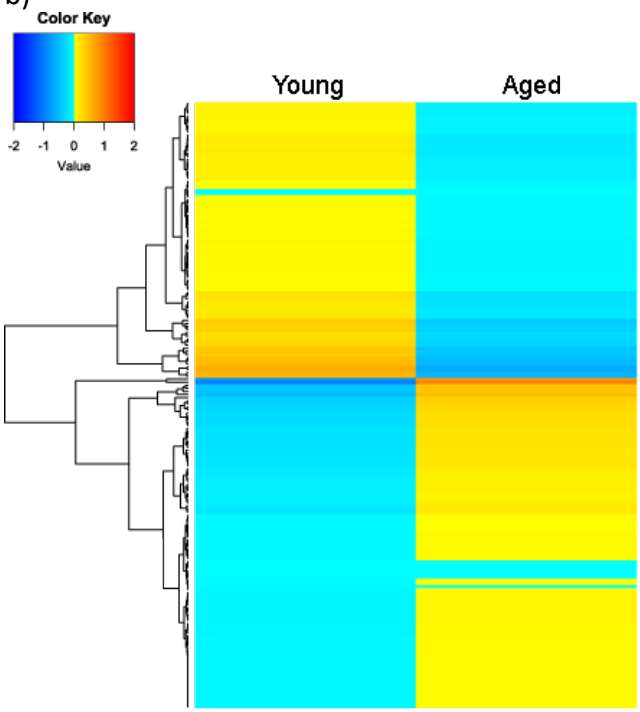

Supplementary figure 12 – Expression of components of the DNA methylation and histone lysine methylation machinery in deciduas from young and aged females at E11.5. DESeq2 *p<0.05

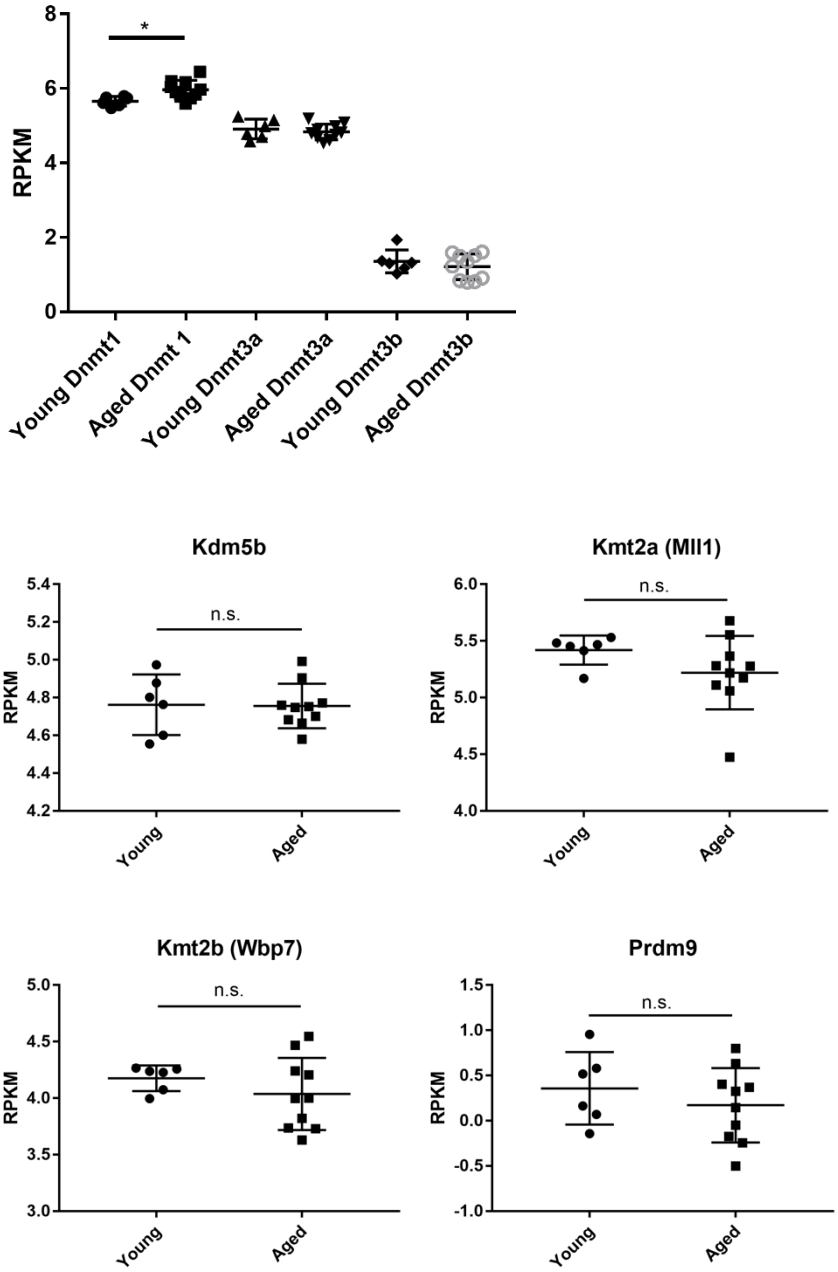

Supplementary figure 13 – Genomic annotation enrichment analysis of trophoblast DMRs with GREAT.